AD NUMBER

AD392715

CLASSIFICATION CHANGES

TO: unclassified

FROM: confidential

LIMITATION CHANGES

TO:

Approved for public release, distribution unlimited

FROM:

Distribution authorized to U.S. Gov't. agencies and their contractors; Administrative/Operational Use; Aug 1968. Other requests shall be referred to Air Force Rocket Propulsion Lab. [RPPR/STINFO], Edwards AFB, CA 93523.

AUTHORITY

31 Aug 1980 per Grp-4 document marking; Air Force Rocket Propulsion Lab ltr dtd 5 Feb 1986

(TITLE UNCLASSIFIED)

DEMONSTRATION OF ADVANCED POST-BOOST PROPULSION SUBSYSTEMS FINAL REPORT

Technical Report AFRPL-TR-68-126

August 1968

Prepared for

AIR FORCE ROCKET PROPULSION LABORATORY
Air Force Systems Command
Edwards, California

(1075)

When U.S. Government drawings, specifications, or other data are used for any purpose other than a definitely related Government procurement operation, the Government thereby incurs no responsibility nor any obligation whatsoever, and the fact that the Government may have formulated, furnished, or in any way supplied the said drawings, specifications, or other data, is not to be regarded by implication or otherwise, or in any manner licensing the holder or any other person or corporation, or conveying any rights or permission to manufacture, use, or sell any patented invention that may in any way be related thereto.

(TITLE UNCLASSIFIED)

DEMONSTRATION OF ADVANCED POST-BOOST PROPULSION SUBSYSTEMS FINAL REPORT

Technical Report AFRPL-TR-68-126

August 1968

Roy E. Jones
Donald E. Lemke
Owen D. Goodman

Aerojet-General Corporation
Liquid Rocket Operations
Propulsion Division

In addition to security requirements which must be met, this document is subject to special export controls and each transmittal to foreign governments or foreign nationals may be made only with prior approval of AFRPL (RPPR/STINFO), Edwards, California 93523.

GROUP 4
DOWNGRADED AT 3 YEAR INTERVALS DECLASSIFIED AFTER 12 YEARS

THIS MATERIAL CONTAINS INFORMATION AFFECTING THE NATIONAL DEFENSE OF THE UNITED STATES WITHIN THE MEANING OF THE ESPIONAGE LAWS, TITLE 18, U.S.C. SECTION 793 OR 794. THE TRANSMISSION OR REVELATION OF WHICH IN ANY MANNER TO AN UNAUTHORIZED PERSON IS PROHIBITED BY LAW.

1075

AEROJET-GENERAL CORPORATION
A SUBSIDIARY OF THE GENERAL TIRE & RUBBER COMPANY

This is the Final Technical Report for Contract AF 04(611)-11614, Demonstration of Advanced Post-Boost Propulsion Subsystems, which was under the cognizance of C. H. Allen, RPRPR, Project Engineer, AFFTC (FTMKR-2), Edwards Air Force Base, California 93523. It is submitted by the Aerojet-General Corporation (Liquid Rocket Operations, Sacramento, California 95813) in accordance with the requirements of Item 80, DD Form 1423, Exhibit B and in fulfillment of said contract. It encompasses the complete program period of 1 July 1966 through 30 April 1968 and the preliminary draft was submitted for approval during June 1968.

This technical report has been reviewed and is approved.

Charles H. Allen
Chief, Reentry Propulsion Office
Air Force Rocket Propulsion Laboratory

TABLE OF CONTENTS

TABLE OF CONTENTS (cont.)

LIST OF TABLES

LIST OF FIGURES

LIST OF FIGURES (cont.)

LIST OF FIGURES (cont.)

SECTION I

INTRODUCTION

(U) The Demonstration of Advanced Post-Boost Propulsion Subsystems Program, Contract AF 04(611)-11614, had as its objective the development of improved technology for advanced, post-boost liquid propulsion subsystems having a ten-year storage life and which would be maintenance-free, inherently reliable, and offer minimal production costs. The performance requirements for these subsystems, which are intended for application in the next generation ICBM weapon systems, are typical of those for a liquid bipropellant (nitrogen tetroxide/monomethyl hydrazine) propulsion system.

(U) Initially, this effort was directed toward the requirement of providing advanced system technology and demonstration of subsystems sized to satisfy the anticipated needs of the Minuteman III weapon system, then under development by the Air Force. Thus, the original program was intended to provide technological back-up for the PBPS weapon system of the Minuteman III development. However, during the preliminary design effort (Phase I), the advanced PBPS program requirements were modified to reflect the increased propulsion system size of the anticipated Advanced ICBM Weapon System. This change had a significant effect upon the existing program because both the pre-contract design and development accomplished were keyed to the original Minuteman III requirements. Greater development risk was incurred as well as increased program costs resulting from the considerably greater component sizes and the more severe duty cycle requirements.

(C) There are four primary subsystems which make up the Post-Boost Propulsion System; gas pressurization, propellant tank with positive expulsion, controls, and engines. The total system supplies propellant (N_2O_4/MMH) on demand to the attitude control engines for control of post-boost vehicle attitude. It also provides this on-demand propellant to the axial thrust engine(s) to permit changes in vehicle velocity to ensure proper vehicle re-entry position as well as over-all velocity control.

(U) The program reported herein was divided into two phases; a Preliminary Design effort (Phase I) and a Subsystem Development effort (Phase II). In Phase I, primary subsystem concepts were identified and evaluated for Phase II development. The latter effort was devoted to providing technological improvements in the primary subsystems selected which would permit their ready incorporation into an advanced PBPS for the next generation of ICBM weapon systems. The results of these efforts are fully detailed herein along with appropriate conclusions and recommendations. It should be noted that in connection with engine development that this was limited to workhorse hardware solely intended for use in testing the controls subsystem components.

SECTION II

SUMMARY

Contractual effort in the Demonstration of Advanced Post-Boost Propulsion Subsystems Program (originally designated the Advanced Post-Boost Propulsion Systems Program) was initiated on 1 July 1966. It was negotiated as a three-phase, 15-month program comprised of the following:

Phase I - Preliminary System Design
Phase II - Subsystem Development
Phase III - System Design

In Phase I, the primary subsystem concepts were to be identified and evaluated for development. In addition, appropriate subcontractors were to be selected for development of each subsystem. Further, a Post-Boost Propulsion System design incorporating the selected subsystems was to be provided; this design to be based upon the performance requirements, design criteria, and envelope limitations associated with the Minuteman III.

The selected subsystem concepts were to be developed and tested during Phase II.

Phase III was to provide a Post-Boost Propulsion System redesign based upon the Phase II development efforts as well as the most current data regarding the advanced ICBM configuration and performance requirements. This phase was not completed as a result of development problems encountered during Phase II.

A. PHASE I - PRELIMINARY DESIGN

This effort was completed on 30 Septebmer 1966 with the presentation of preliminary drawings and specifications to AFRPL for approval. The Post-Boost Propulsion System design utilized the selected subsystem concepts and was based upon the Advanced ICBM requirements. In addition, appropriate qualified subcontractors were selected for the development of the gas pressurization subsystem, the tank and positive expulsion subsystem, and the fluidic controls subsystem. As will be subsequently noted, there was a high degree of inter-dependence between the subsystems. Some aspects of individual subsystem development were predicated upon the requirements of the other subsystems which necessitated a close liaison with the subcontractors as well as appropriate analyses.

II, Summary (cont.)

B. PHASE II - SUBSYSTEM DEVELOPMENT

1. Gas Pressurization

The subcontractor engaged in this development was the Hamilton Standard Division of United Aircraft, Windsor Locks, Connecticut.

The size of the gas generator was significantly affected by the fluidic controls concept because the efficiency of the controls components exerts the major influence upon the gas requirements. With fluidic controls, the pressurization gas is the working fluid. Further, consideration of the controls configuration was necessary in ascertaining the distribution of monopropellant requirements between the two stages of the selected gas pressurization system.

A liquid monopropellant hydrazine gas generator system where the pressurant is stored at low vapor pressure during the entire "armed" life of the vehicle was successfully demonstrated. This concept offers advantages in weight and reliability over the current technology high-pressure gas supply systems. This satisfactory development and delivery of a first-stage gas generator assembly and a second-stage gas generator was a major milepost in advanced technology for PBPS application.

2. Tank and Positive Expulsion

Arde, Inc. of Paramus, New Jersey was selected as the subcontractor to develop this subsystem. The concept pursued is an all-welded steel tank with an integral ring-stabilized, controlled-collapse, steel diaphragm for positive expulsion. The propellant tank is cryogenically-stretched to achieve the high strength-to-weight ratios desired for flight vehicle application. Propellant is stored in two equal-volume, cono-spheroid tanks. This shape was selected for optimum vehicle packaging within the defined Advanced ICBM envelope. The tank and expulsion concept was demonstrated to be feasible for vehicle application.

The increase in vehicle size from that originally contemplated at the outset of the program had a major impact upon the development of the positive expulsion propellant tank subsystem. Expulsion diaphragm shell forming became an immediate development problem because the standard forming processes are size-limited. Only minor difficulties had been experienced in forming subscale expulsion shells of a size that would satisfy the Minuteman III requirements. The increased size requirements necessitated that a major fabrication development program be undertaken to successfully form the full-scale expulsion diaphragm shells. A combination of sequential deep-draw forming and

hydroforming was investigated with the initial result that the shell thickness produced was non-uniform and as a consequence, further development problems were encountered during reversal. However, subsequent electropolishing of the shells produced acceptable parts for the demonstration of the concept and the testing. The compatibility of the selected gas generator concept and the propellant tank concept was verified in a limited subsystem integration demonstration.

3. Fluidic Controls

(U) This effort was undertaken by the Bowles Engineering Corporation, Silver Spring, Maryland. The concept under development utilizes all-fluidic components for both the regulation of pressurization gas and the control of bipropellant engine flow.

(C) The fluidic concept offers a number of advantages in terms of inherent reliability as well as long-term storage because there are no moving parts. In addition, it probably offers advantages in connection with its ability to survive in a nuclear environment because of the minimal electrical components. However, this concept does impose a penalty upon vehicle performance because a continuous flow of gas through each control component is necessary for fluidic control.

(C) The development of the fluidic controls was not accomplished because of the inadequacy of existing technology for fluidic elements operating with hot gas at high pressure. The primary concept was demonstrated at the laboratory level utilizing low pressures with ambient air and the control of propellant through an engine vortex throttle with hot gas pressurization was accomplished. However, the flow stability and response characteristics were unfavorable for subsequent workhorse engine testing.

(U) The development problems associated with the fluidic regulator precluded any integration testing of the combined monopropellant gas generator, the fluidic gas regulator, and the propellant tank subsystems. Therefore, the first-stage gas generator was assembled with the prototype hydrazine bootstrap tank and the workhorse pressure-switch/solenoid-valve controls for subsequent hot gas expulsion of the propellant tank subsystem.

C. MAJOR CONCLUSIONS AND RECOMMENDATIONS

(U) The state-of-the-art of the major subsystems of liquid propellant Post-Boost Propulsion was substantially improved by the developmental achievements in the contracted effort. The performance and operational flexibility advantages of liquid propellant propulsion over solid propellant and hybrid

II, C, Major Conclusions and Recommendations (cont.)

propulsion is well known. However, liquid propellant system storeability, maintainability, and inherent reliability have been of concern for potential strategic weapon system application. This program demonstrated a gas generator subsystem and a positive expulsion propellant tank subsystem that inherently provide the desired propellant containment and simplified operational requirements. This demonstration was accomplished with components sized to encompass the expected weapon system application.

The gas generator subsystem was developed and demonstrated to be ready for final development into an optimum configuration to be applied in the vehicle. The design requirements of the fluidically-controlled PBPS dictated a two-stage monopropellant N_2H_4 decomposition gas generator subsystem. Satisfactory development of the first-stage bootstrap gas generator circuit provides a system which can be expected to meet the gas requirements of the next strategic missile application. The demonstration of the larger, second-stage gas generator provides the growth potential for the reactor. The areas reamining to be demonstrated are the N_2H_4 propellant isolation weld or shear area of the bootstrap tank and an analog throttling control for throttling control for the bootstrap circuit, which will provide a uniform gas output pressure for the variable demand requirements of a typical PBPS mission. Digital control, using a pressure switch/solenoid valve combination, was used successfully during this program because the fluidic regulator was not available.

The propellant tank expulsion concept was satisfactorily demonstrated. The ring-stabilized steel expulsion bladder showed a functional capability in the low acceleration PBPS vehicle environment. Structural integrity as well as the low weight of the cryogenically-stretched stainless steel tank were demonstrated with the flightweight, verification tank assembly. This tank concept proved to be relatively insensitive to fabrication tolerances as well as adaptable to low cost fabrication techniques. Further demonstration of this propellant tank concept through hot gas expulsion tests of flightweight tank assemblies will be provided under the Air Force Rocket Propulsion Laboratory, Contract F04611-67-C-0095 (PBPS Engine Development Program and System Design). Further improvements in expulsion diaphragm fabrication techniques will be required to provide a diaphragm shell of uniform thickness and to ensure a more consistent quality of product. The necessary fabrication improvements fall within the shell drawing or forming processes as well as the tack-welding and brazing of the reinforcing wires to the shell. These improvements will assure the fabrication of reliable, controlled collapse conospherical diaphragm assemblies.

The concept of an all-fluidic controls subsystem for advanced rocket propulsion systems remain appealing on the basis of reliability and other obvious potential advantages over the existing conventional control systems. However, the results of this program demonstrated an urgent need for extensive analytical and development efforts for high pressure fluidic controls in hot gas technology before an all-fluidic controls subsystem can become competitive with the existing control systems.

II, C, Major Conclusions and Recommendations (cont.)

Improvements in fluidic elements and the techniques for their integration into fluidic control circuits are continually being realized. The area requiring more understanding in fluidic control technology encompasses both high pressure and high temperature operation, which is similar to that experienced in a rocket propulsion control subsystem.

The work performed in this program yielded considerable data and knowledge of fluidic controls while outlining the serious problem areas. Areas for further research and development have become evident. Upon this basis, it is recommended that any efforts pursued in the near future in connection with the development of an all-fluidic controls subsystem be implemented in smaller increments or even at the individual component level. It is further recommended that pre-development of the various components, utilizing an analytical approach in several areas, should be undertaken to fully define performance characteristics before integrating the components into a complete system.

SECTION III

PHASE I - PRELIMINARY SYSTEM DESIGN

A. BASIC REQUIREMENTS

The basic program requirement was to provide an improved technology for advanced, post-boost liquid propulsion subsystems having a ten-year storage life and which would be maintenance-free as well as inherently reliable. Also, these subsystems, which are intended for application in future propulsion systems, must offer minimal production costs.

Consideration was given to the anticipated requirements of a liquid bipropellant system for future ICBM applications in establishing the basic design approach for an advanced PBPS. Special emphasis was placed upon inherent reliability and the long, maintenance-free storage period. In addition, the design of an advanced PBPS must provide for performance that will complement the achievement of maximum payload capability.

The performance requirements for these subsystems are typical of those for a liquid bipropellant (nitrogen tetroxide/monomethyl hydrazine) propulsion system. These design requirements are shown on Tables I and II.

B. PRELIMINARY SYSTEM DESIGN

The preliminary design of the advanced PBPS was established in Phase I, which started on 1 July 1966, for subsequent development during Phase II. The primary accomplishments in establishing this preliminary design follow in the sequence of their achievement.

1. The basic system design approach was identified.
2. Qualified subcontractors for each subsystem were solicited, evaluated, and selected.
3. Each subsystem configuration was evaluated.
4. The full PBPS system was evaluated and made optimum as regards subsystem compatibility.
5. The subsystem designs were identified and preliminary drawings as well as specifications were submitted to the Air Force for review and approval.

The PBPS subsystem designs satisfy the contractually-specified objectives. The design approach applied resulted in a minimum of moving parts as well as a storeability not previously attained with liquid systems. This

TABLE I

ADVANCED PBPS PERFORMANCE REQUIREMENTS (U)

Total impulse, lb-sec	684,000
Axial	632,000
ACS	52,000
Mission time, sec	800
Axial thrust time, sec	400
Total weight, lb	3,650
Maneuvers	≈ 35
Thrust	
Axial	4 engs at 600 to 300 lb
Pitch	4 engs at 75 lb
Yaw	4 engs at 75 lb
Roll	4 engs at 30 lb
Envelope Constraints	95 in. dia by 28.5 in. high*

Engine Design Goals

Engine	Thrust, lb	Response Rise	Response Decay	Isp, sec	Duration	Max External Temperature, °F	Mixture Ratio
Axial	600 ± 3% (3 σ)	50 msec to 90%	50 msec to 10%	300 ± 5 (3 σ)	400 sec during 800 sec mission	400	1.6 ± 3%
ACS	75 ± 3% (3 σ)	20 msec to 90%	20 msec to 10%	285 ± 5 (3 σ)	worst thermal duty cycle for 800-sec mission	400	1.6 ± 3%

*Small additional heights can be used provided that the PBPS propulsion system is sufficiently flexible to allow for packaging around the surrounding equipment.

TABLE II

ADVANCED PBPS ENVIRONMENTAL DESIGN CRITERIA

Environments	Design Point
System storage temperature, °F	+ 20 to + 150
System operating temperature, °F	+ 40 to + 120
Storage life goal, years	10
Shock	± 100 g at 100 cps decreasing linearly to 0 g at 0 cps
Acceleration (sustained)	14 g parallel to missile axis 3 g lateral to missile axis
Ambient pressure	Vacuum
Vibration	
Random, g^2/cps	0.0015 to 0.05 at 12 db/octave, 0 to 35 cps
	0.05, 35 to 200 cps
	0.05 to 0.16 at 12 db/octave, 200 to 300 cps
	0.16, 300 to 1500 cps
Sine, g-rms	1.4, 0 to 300 cps
	3.0, 300 to 1500 cps
Vibration (Transporation and Handling), g-rms	3.5, 5 to 50 cps
	1.5, 50 to 300 cps

III, B, Preliminary System Design (cont.)

storeability is achieved by using an all-welded design which isolates all liquid at vapor pressure and does not require stored, high-pressure gas. The liquid propellant combination, N_2O_4/MMH, selected provides maximum performance utilizing demonstrated propellant technology.

Figure No. 1 is a conceptual layout of the PBPS and Figure No. 2 is a partial schematic of the controls system. Table III is a listing of the symbols used in Figure No. 2 and Table IV, which is a pressure and flow rate s edule.

The pressurization subsystem was required to provide the pressurized gas needed to expel propellant from the tankage as well as the working fluid used to activate the engine controls. Its design had to provide a regulated pressure upon demand along with a capability for being stored in an inert condition.

The use of stored, high-pressure gas as a pressurization source was eliminated because of the 10-year storage capability requirement. Three primary configurations were considered: a bootstrap monopropellant gas generator; a staged, monopropellant gas generator; and a warm-gas, solid-propellant gas generator. The staged, monopropellant gas generator was selected because it allows greater component design flexibility to satisfy increased gas requirements.

Propellant tankage and associated isolation squib valves make up the tankage/propulsion subsystem. The propellant is isolated (at the propellant vapor pressure) in all-welded steel tankage during storage. During operation, the pressurization gas displaces a steel diaphragm within the tanks, which results in a positive displacement of the propellant.

The objectives of the tankage design were to provide high single-cycle reliability after 10-year storage, high propellant expulsion efficiency for maximum propellant utilization, and high volumetric efficiency for packaging considerations.

The primary designs considered for the tankage subsystem were the spherical and conospheroid concepts (using ring-stabilized reversing diaphragms) and the cylindrical concept (using a bonded rolling diaphragm). The conospheroid stainless-steel tankage with the ring-stabilized reversing diaphragm was selected because its shape provides the best packaging for the post-boost control system wafer-configuration bus.

The controls subsystem regulates the pressurization gas and provides propellant control for each engine. The design objective of the controls system was to provide inherent simplicity and reliability. Also,

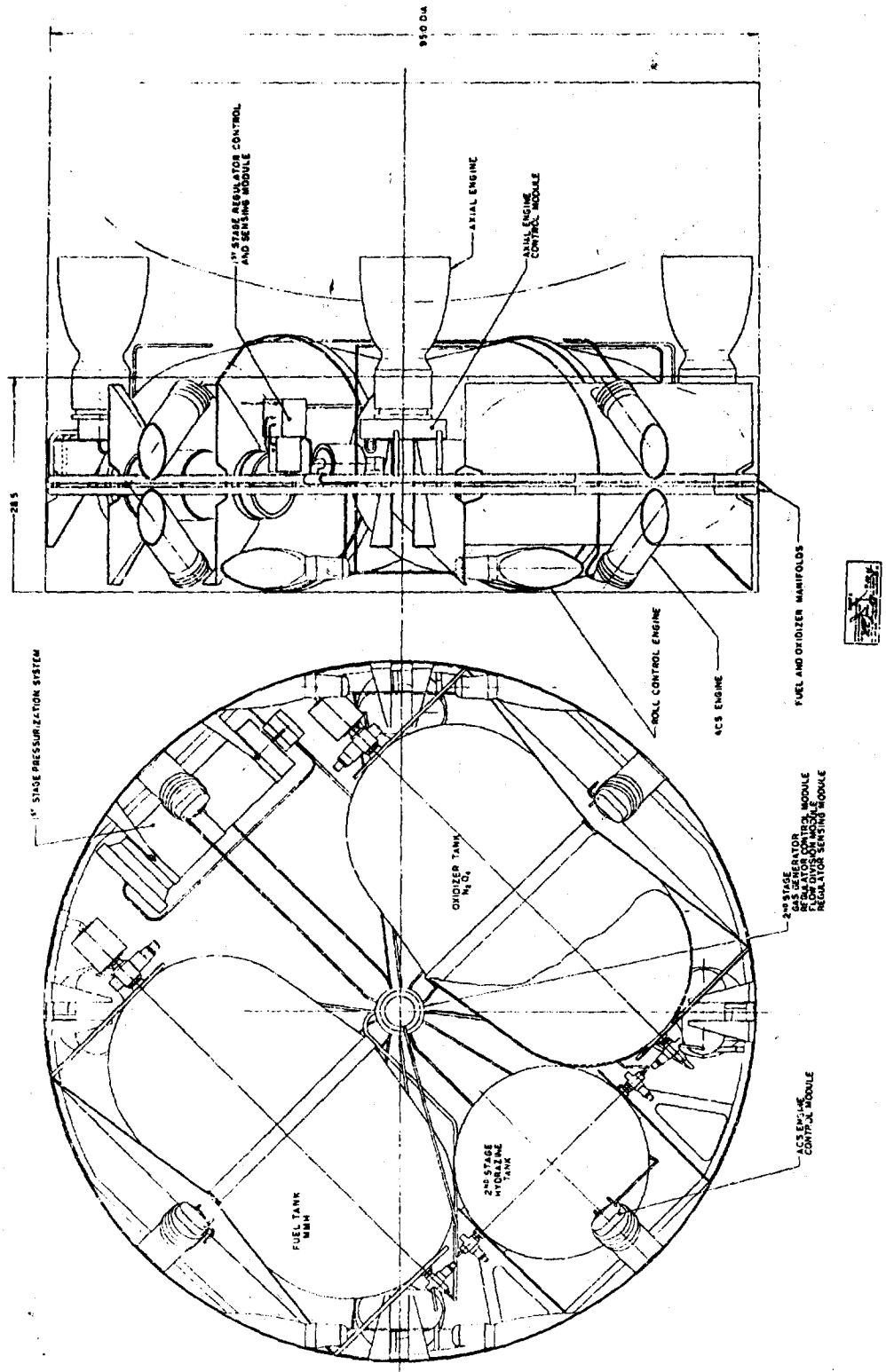

Figure 1. PBPS Conceptual Layout (u)

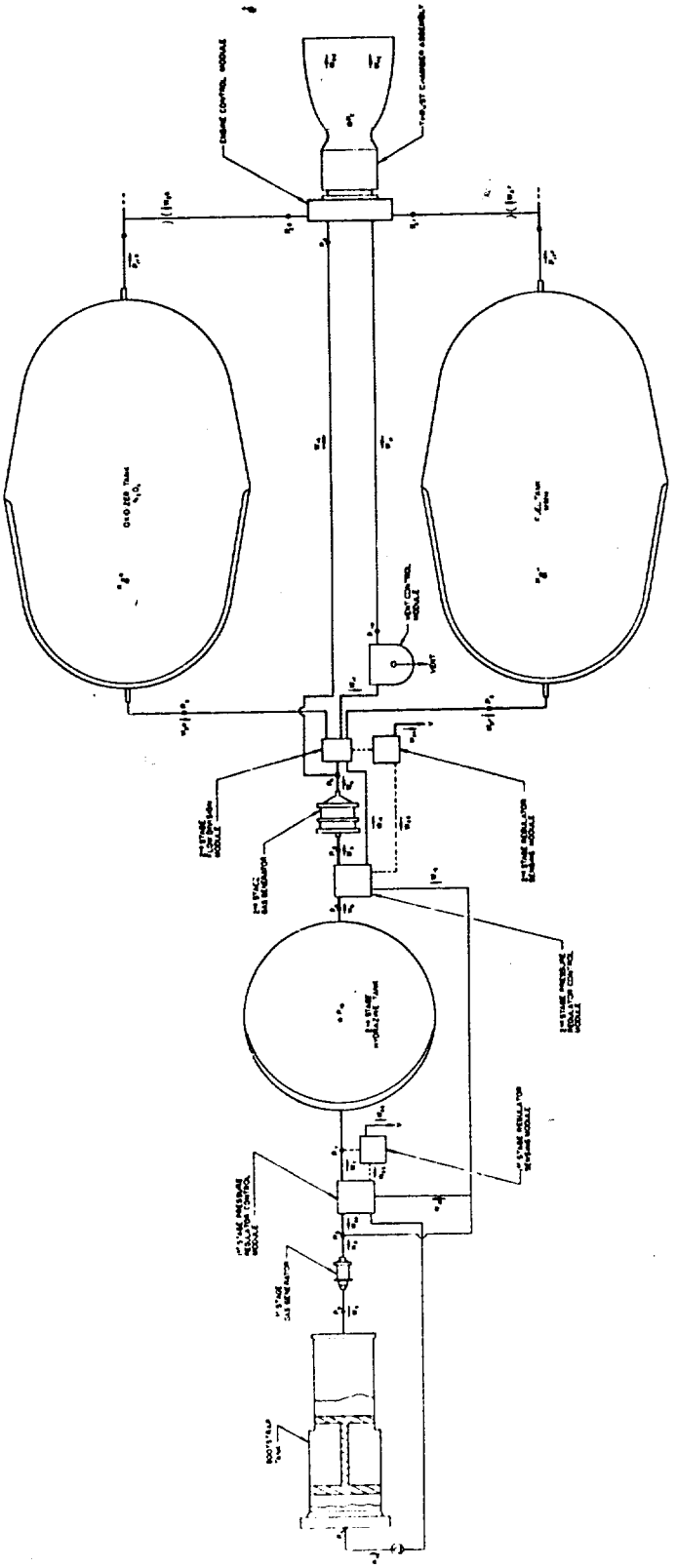

Figure 2. PBPS Controls Schematic

TABLE III

SYMBOL LIST FOR PBPS CONTROL SUBSYSTEM SCHEMATIC

W_{oc} and W_{Fc} = Propellant weight flow to chamber

$W_{2,0}$ and $W_{2,F}$ = Supply-port weight flow, vortex throttle

$W_{3,0}$ and $W_{3,F}$ = Gas weight flow to propellant tanks

$W_3 = W_{3,0} + W_{3,F}$

W_4 = Gas generator II output weight flow

W_5 = Exit port weight flow, vortex throttle, second-stage regulator

W_6 = Supply port weight flow, vortex throttle, second-stage regulator

W_7 = Exit port weight flow, vortex throttle, first-stage regulator

W_8 = Gas generator I output weight flow

W_9 = Hydrazine tank 1 output liquid weight flow

W_{10} = Hydrazine tank 1 input gas weight flow

W_{14} = P_c control output weight flow to vent

W_{15} = Output gas weight flow from second-stage regulator

W_{16} = P_c control supply gas weight flow

W_{17} = Vent-control weight flow

W_{18} = First-stage regulator supply weight flow

W_{19} = Second-stage regulator supply weight flow

$W_{20} = W_8 - W_{18} - W_{19}$

$W_{21} = W_4 + W_{15} - W_{16}$

W_{22} = Sensor-vent weight flow, first-stage regulator

W_{23} = Sensor weight flow, first-stage regulator

W_{24} = Sensor-vent weight flow, second-stage regulator

W_{25} = Sensor weight flow, second-stage regulator

P_c = Engine chamber pressure

$P_{2,0}$ and $P_{2,F}$ = Supply-port pressure, vortex throttle, engine

$P_{3,0}$ and $P_{3,F}$ = Propellant tank pressure, gas side

P_3 = Regulated gas pressure, second stage

P_4 = Gas generator II chamber pressure

P_5 = Exit port pressure, vortex throttle, second-stage regulator (Also hydrazine supply pressure to gas generator II)

P_6 = Supply port pressure, vortex throttle, second-stage regulator (Also hydrazine tank 2 exhaust pressure)

P_7 = Regulated gas pressure, first stage

P_8 = Gas generator I chamber pressure

P_9 = Hydrazine tank 1 pressure, liquid side

P_{10} = Hydrazine tank 1 pressure, gas side

P_{14} = Engine control output pressure to vent control

P_{15} = Hydrazine tank 1 gas pressure upstream of check valve

$P_{16,0}$ and $P_{16,F}$ = Propellant tank pressure

$P_{17,0}$ and $P_{17,F}$ = Tap-off point pressure, downstream of filter and upstream of trim orifice

P_{18} = Hydrazine tank 2 pressure, liquid side

TABLE IV

PRESSURE AND FLOW-RATE SCHEDULE

Pressures, psia			Flow Rates, lb/sec						
Function	Engines On	Engines Off	Function	Engines On	Engines Off	Axial On	Engines Off	ACS On	Engines Off
Pc	150	2.5	W_{oc}			1.23	0.0433	0.154	0.00541
$P_{2,0}$	304	260	W_{fc}			0.77	0.0347	0.0962	0.00434
$P_{2,F}$	304	260	$W_{2,0}$			1.23	0	0.154	0
$P_{3,0}$	304	276	$W_{2,F}$			0.77	0	0.0962	
$P_{3,F}$	304	276	$W_{3,0}$	0.0438	0				
P_3	304	276	$W_{3,F}$	0.0448	0				
P_4	494	435	W_3	0.0886	0				
P_5	606	573	W_4	0.3266	0.4488				
P_6	656	623	W_5	0.3260	0.4488				
P_7	657	632	W_6	0.3060	0.4488				
P_8	707	682	W_7	0.00686	0.01004				
P_9	848	797	W_8	0.0283	0.0315				
P_{10}	677	637	W_9	0.0283	0.0315				
P_{14}	458	149	W_{10}	0.000785	0.000872				
P_{15}	677	637	W_{14}	0.238	0				
$P_{16,0}$	304	270	W_{15}	0	0.0206				
$P_{16,F}$	304	270	W_{16}	0.238	0.392				
$P_{17,0}$	304	267	W_{17}	0	0.0774				
$P_{17,F}$	304	267	W_{18}	0.00308	0.00422				
P_{18}	657	626	W_{19}	0.0206	0.0206				
			W_{20}	0.00457	0.00669				
			W_{22}	0.0001	0.0001				
			W_{23}	0.0001	0.0001				
			W_{24}	0.0001	0.0001				
			W_{25}	0.0001	0.0001				

III, B, Preliminary System Design (cont.)

the potential application of fluidic controls to satisfy design objectives was to be evaluated. The inherent reliability and storeability of fluidic controls make them more desirable than electrical-mechanical controls.

The change in PBPS system size necessitated a re-evaluation of the system as well as subsystem designs early in Phase I. Following this, the subsystem subcontractors were selected and approved. These subcontractors were:

Pressurization Subsystem - Hamilton Standard Division of United Aircraft Company, Windsor Locks, Connecticut

Controls Subsystem - Bowles Engineering, Silver Spring, Maryland

Tankage/Expulsion Subsystem - Arde, Inc., Paramus, New Jersey

After these subcontractors were selected, appropriate liaison was accomplished with them, Air Force project personnel, and Aerojet-General project personnel to jointly identify system requirements and the basic subsystem configurations. A preliminary system pressure and flow rate schedule was formulated. The necessary interface requirements were identified. Figure No. 3 summarizes these preliminary interface specifications and drawings.

The Phase I effort was completed in September 1966 with the receipt of Air Force approval to proceed with Phase II.

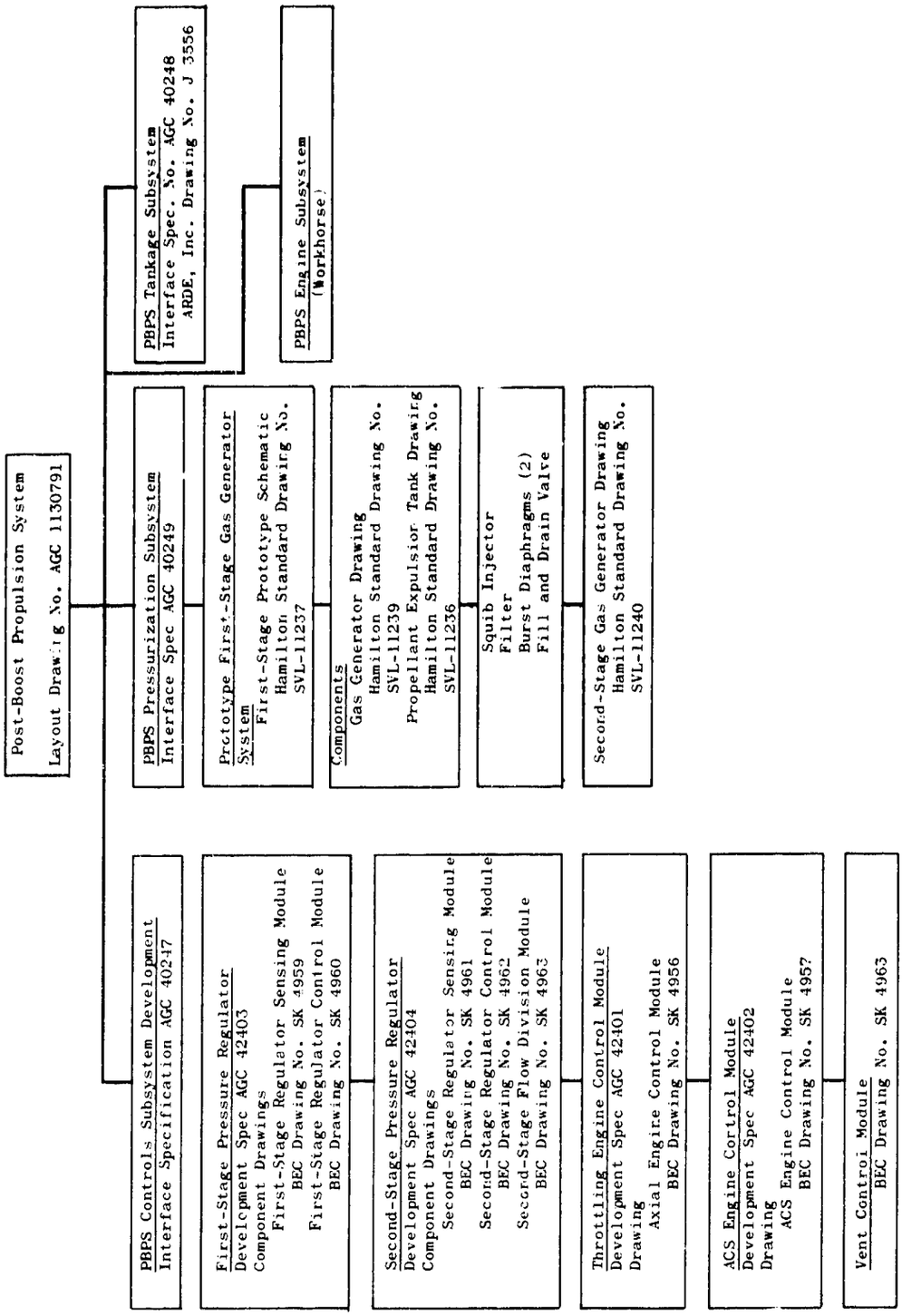

Figure 3. Preliminary Interface Specication and Drawing List

SECTION IV

PHASE II - SUBSYSTEM DEVELOPMENT

A. PRESSURIZATION SUBSYSTEM

1. Requirements

The pressurization subsystem design requirements evolved from an over-all PBPS limit condition system analysis. Each participant (including the subsystem subcontractors) exerted a degree of influence upon these requirements, which significantly affected the type of pressurization subsystem selected. The following are the nominal parametric requirements:

Propellant: Anhydrous hydrazine

Propellant Quantity: 20 lb (first-stage tank)

First-Stage Output Pressure: 700 psia

First-Stage Flow Rate: 0.0315 lb/sec ± 10%

Second-Stage Output Pressure: 435 psia

Second-Stage Flow Rate: 0.30 to 0.45 lb/sec

Output Gas Temperature: 1400°F

Over-all Action Time: 800 sec

Storage Life: 10 years

Storage Temperature: 0°F to +150°F (later modified to +20°F to +125°F)

Operating Temperature: +40°F to +120°F

Preliminary design investigations were accomplished and the following additional criteria were established for selecting the design point:

Bootstrap Area Ratio: 1.4:1 (workhorse tank)

Proof Pressure: 1.5 x normal working pressure

Burst Pressure: 2.5 x normal working pressure

Tank Material: AM 350(1)

Allowable Working Stress: 66,000 psi

Maximum Allowable Length: 28-in.

Vapor Pressure Storage is allowable

(1) AM 355 was selected for the prototype piston-piston tank material rather than AM 350 because of its availability in the form of forgings.

IV, A, Pressurization Subsystem (cont.)

2. Operation

a. Prototype

The prototype first-stage pressurization subsystem, shown schematically on Figure No. 2, has a differential-area, piston-tank assembly for propellant storage and positive expulsion. Feedback gas pressure acts upon a large piston area while pressurizing a smaller propellant area to achieve a self-feeding (bootstrap) system. The flightweight concept differs only slightly from the prototype in that a shear seal is located between the tank and piston for positive sealing during long-term storage. This seal was omitted in the prototype tank to permit its reuse for development testing. The shear seal development program is detailed in the development discussion, Section IV,A,4,d. A teflon insert was placed on the knee of the piston to preclude possible galling during experimental testing.

System operation is initiated by firing a small solid propellant gas generator which pressurizes the ullage at the large area side of the piston. A normally-closed squib valve is fired simultaneously with the gas generator and positively seals off the propellant from the reaction chamber during long-term storage. When these two pyrotechnic devices are activated, hydrazine begins to flow out of the tank. The hydrazine flow is directed through a downstream filter which traps any debris from the squib valve as well as any contaminants in the propellant or in the system. A trim orifice, located upstream of the reaction chamber, is used to calibrate the system to the desired operating conditions. Controlled feedback pressure enters the tank after passing through a one-way burst disk. This disk prevents outflow from the tank during the start transient and ruptures when the pressure in the feedback line is approximately 5 psi higher than it is in the tank. Approximately one-third of the first-stage generator output is used to pressurize the second-stage hydrazine tank; the remainder is available as control fluid for the second-stage pressure regulator. The second-stage unit is used to control the propellant going to the engines (approximately 80% of the output) and for pressurization of the main propellant tanks.

A propellant fill and drain valve is provided for propellant servicing. In the flightweight design concept, a cap is welded over the fill and drain valve for positive sealing during long-term storage.

b. Workhorse

The workhorse system is shown schematically on Figure No. 4. It is very similar to the prototype system discussed above and differs from it only to the extent needed to enable independent and rapid test evaluation of the subsystem.

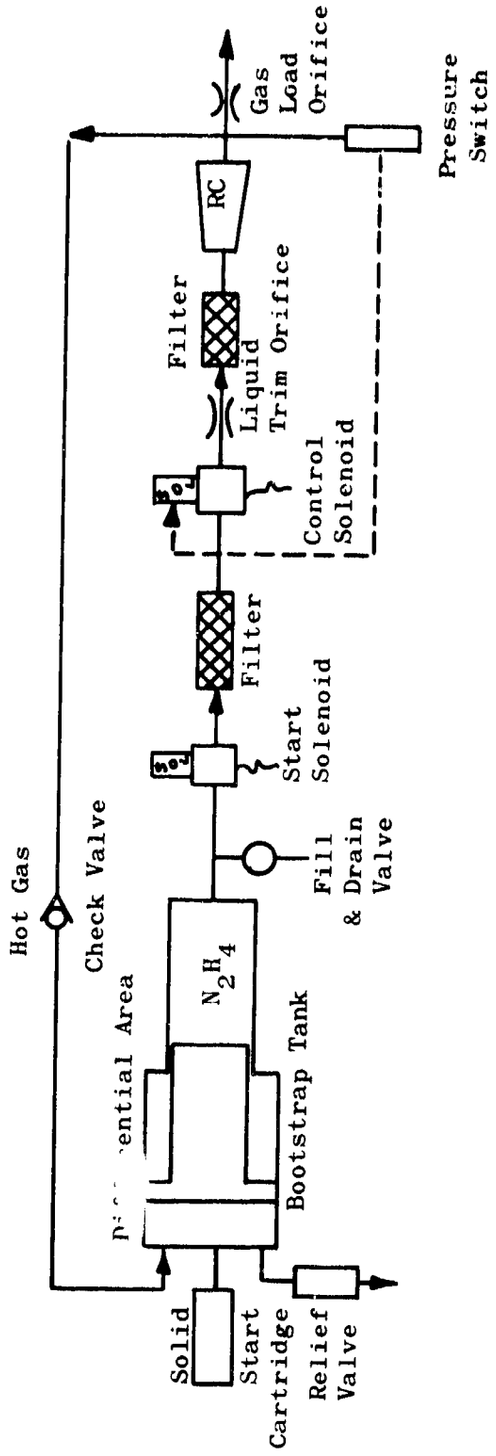

Figure 4. Schematic of First-Stage Workhorse Pressurization Subsystem

IV, A, Pressurization Subsystem (cont.)

The system is activated by a solid propellant gas generator. A normally-closed solenoid valve, located between the propellant-tank outlet and the filter, is used for safety and as a substitute for the squib valve of the prototype system. The filter prevents contaminants from clogging the injector or causing seat leakage across the main solenoid control valve, which is activated by a pair of pressure-sensing switches that monitor output and feedback gas pressures, respectively. A trim orifice is used to calibrate the system to the desired operating conditions. The propellant then passes through the injector and into the reaction chamber. Just downstream of the reaction chamber, the gas flow splits off into three paths.

One part of the flow passes through an orifice to simulate the fluidic controls demand flow. A second portion of the flow goes back to the tank through the feedback line. A hot gas check valve is used in this line to prevent tank outflow while the system is starting. This check valve opens when the pressure in the feedback line is approximately 2 psi higher than in the tank. The third portion of the flow passes to the simulated load. This part of the load consists of an orifice which simulates the pressure drop across the fluidic pressure regulator and a tank which simulates the second-stage pressurization load. A tank outlet loading orifice and a solenoid control valve command the output flow from the tank.

Two pressure switches, one located downstream of the load orifice and the other located in the feedback line, control the flow of propellant to the reaction chamber. The pressure switch downstream of the load orifice senses when the load pressure exceeds a pre-set value and shuts off the solenoid valve, stopping flow to the reaction chamber. The second pressure switch is in the feedback line to prevent a runaway system. Built-in switch hysteresis prevents high-frequency limit cycling. This deadband is an approximate representation of the regulation accuracy of the first-stage pressure-regulating valve.

3. Design Considerations

a. Parametric Study

(1) Preliminary

A preliminary parametric design study of the first-stage gas generator system was conducted for use in the initial system analysis. The data generated were of particular value in evaluating control subsystem concepts which involved numerous variables with potentially wide ranges of values. The following are the significant pressurization subsystem variables and the range over which they were analyzed:

IV, A, Pressurization Subsystem (cont.)

Bootstrap tank differential area gain	1.2 to 4.0
Usable hydrazine	2 to 25 lb
Output pressure	400 to 1600 psia

The effects of these variables upon system weight, volume, reliability, cost, and development risk were analyzed for the six design concepts shown on Figure No. 5. Initial criteria dictated that the design must be self-pressurizing and have positive mechanical closures to ensure zero leakage and long-term storability without any maintenance. Complex mechanisms and fabrication procedures had to be avoided. Volume compensation during temperature cycling was to be achieved by positive displacement rather than vapor pressure storage. It should be noted that some of the initial criteria differed from the final design point requirements.

If the bootstrap gain is fixed at 1.4 and output pressure at 800 psia, the design best suited (conceptually) for hydrazine weights to approximately 7 lb is the piston bellows configuration; above 7 lb the concentric bellows design appeared attractive (see Figure No. 6). The primary limitation of the piston-bellows concept is the high internal pressure in increasing diameters. Primary advantages of both concepts are the apparent simplicity and minimization of critical seals.

(2) Detailed

Following the over-all system optimization, during which the required weight of hydrazine for the first-stage unit was fixed at 20 lb, the parametric study was repeated with detailed emphasis upon a system with 20 lb of hydrazine, 1.4 gain, and 700 psia output pressure. The results of the study are presented on Table V, where a comparison is made between the relative volumes, weights, reliabilities, costs, and development risks of the six systems. Based upon the study parameters, the piston-piston system is best suited for this application. The piston-piston Configuration II system weighs more, involves more development risk, and has lower reliability than the selected system, while the last three bellows systems require high differential pressure bellows. It was determined that bellows were not sufficiently developed for use in this particular application. Each of the study parameters was analyzed and weighting factors were applied to what were considered the most important items. Reliability was judged as the most important factor because failure of the system results in a mission failure. This was weighted as 50% more critical than nominal. Because the application implies large-quantity production, unit cost was weighted as 30% more critical than nominal. Weight, volume, and development risk were not given any additional weighting because they were considered to be roughly equal in importance.

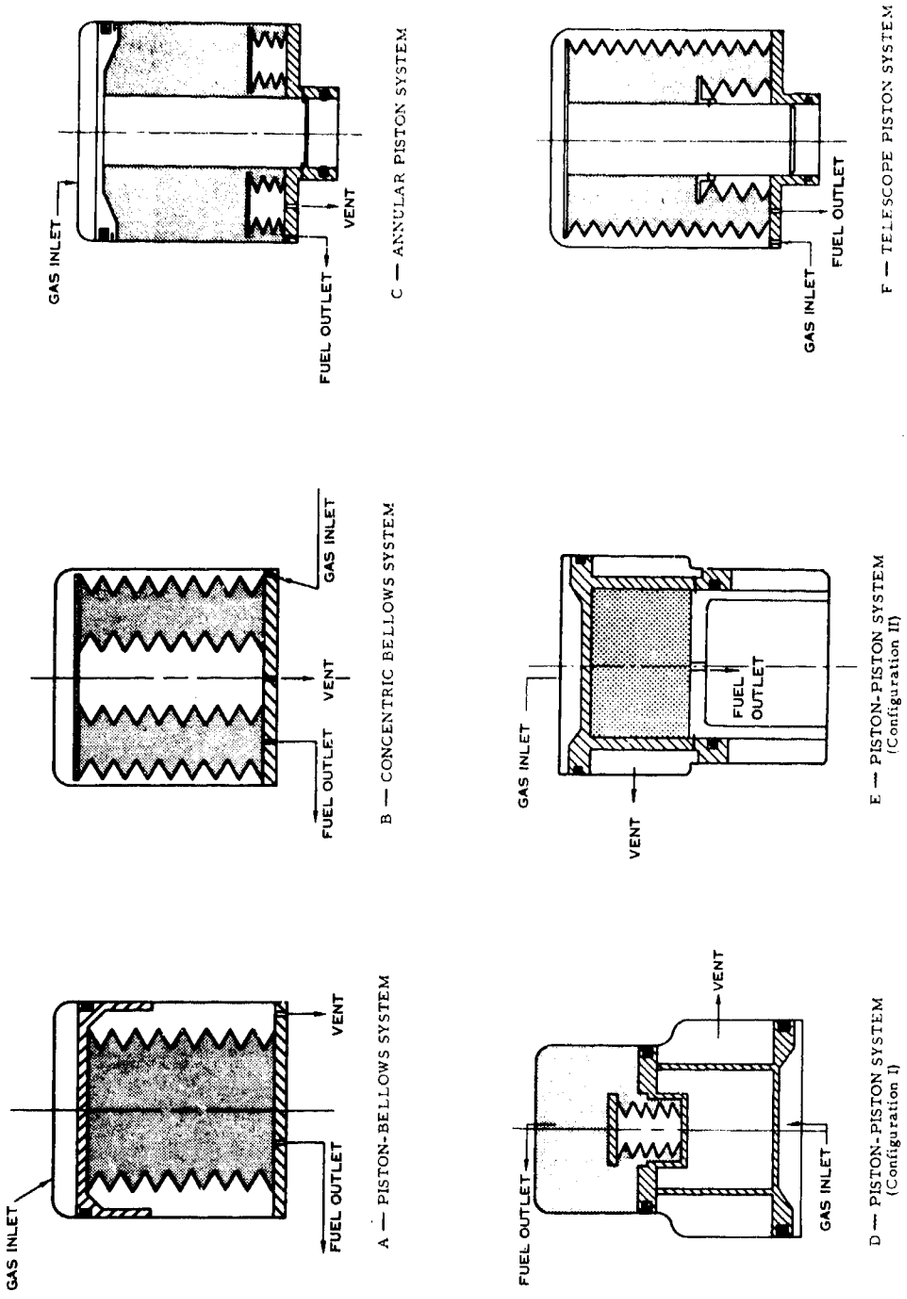

Figure 5. Bootstrap Tank Design Concepts

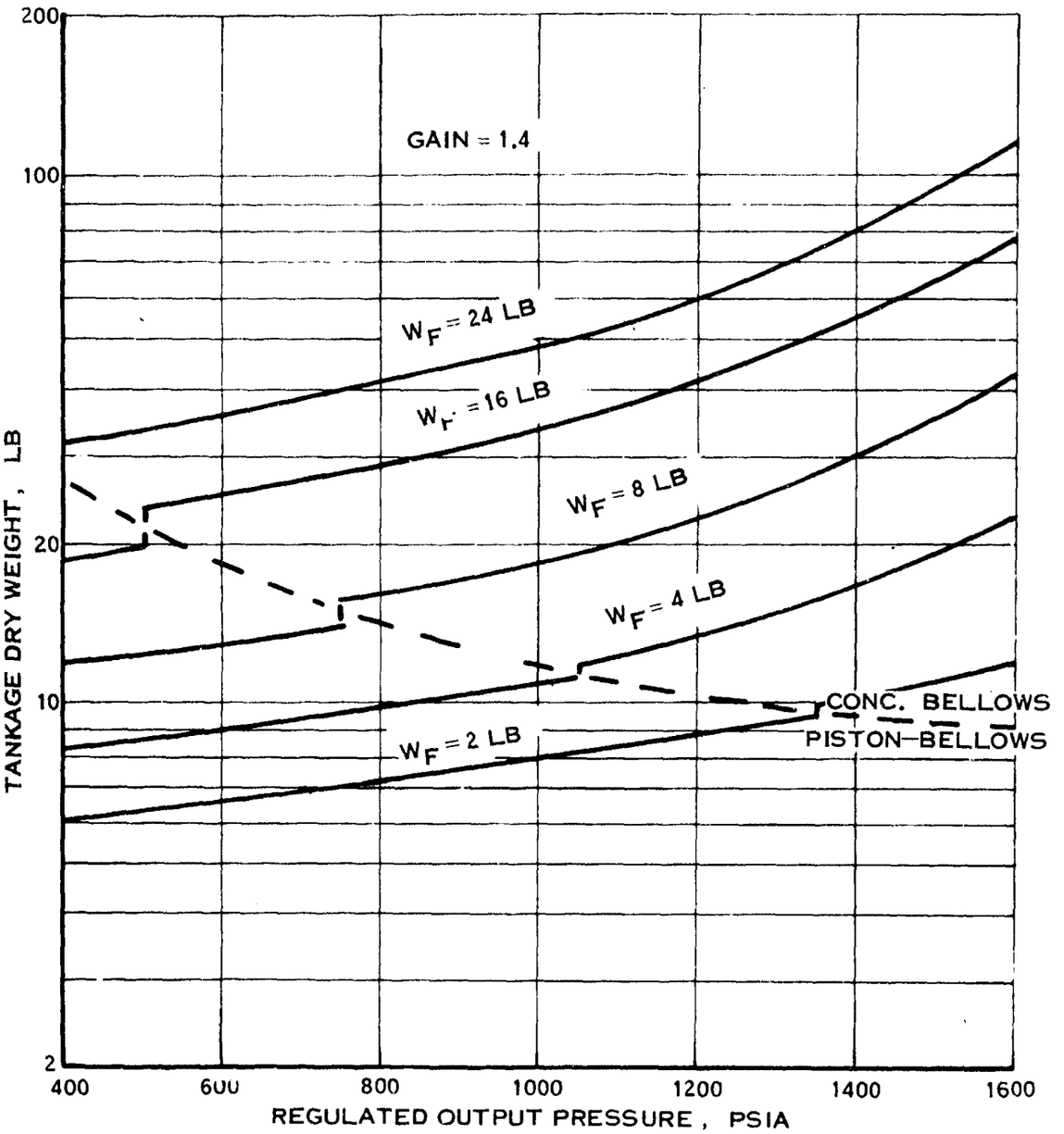

Figure 6. Parametric Tank Weight vs Output Pressure

TABLE V

DESIGN POINT CONDITIONS

SYSTEM	Relative Volume	Relative Weight	Relative Reliability (Weighted X 1.5)	Relative Cost (Weighted X 1.3)	Relative Develop. Risk	$\sum$
Piston-Piston Conf. I	1.50	1.00	1.65	1.43	1.00	6.58
Piston-Piston Conf. II	1.50	1.32	1.50	1.30	1.30	6.92
Annular Piston	1.58	1.23	2.40	1.82	1.60	8.63
Piston Bellows	1.00	1.20	3.15	1.82	1.50	8.67
Concentric Bellows	1.10	1.14	3.00	1.95	1.60	8.79
Telescoping Piston	2.14	1.30	4.50	2.21	1.60	11.75

Bootstrap Area Ratio	1.40
Minimum Expelled Propellant Weight	20 lb
Gas Generator Chamber Pressure	750 psia

IV, A, Pressurization Subsystem (cont.)

Design sketches were made for each system to identify design problems and potential manufacturing difficulties. A tabulation of the advantages and disadvantages of each system is presented on Table VI. Each system was evaluated over a range of diameters. Those diameters resulting in over-all length exceeding 28-in. (envelope limit) were eliminated. Figures No. 7, No. 8, and No. 9 show the weights and volumes of each system as a function of propellant tank diameter (liquid end).

This design point selected imposed the requirement that the first-stage hydrazine tank expel a minimum of 20 lb of propellant. The necessary propellant volume (at +70°F) to satisfy this requirement is approximately 570 $in.^3$. When bellows are considered for the propellant storage and expulsion device, they must withstand an internal pressure differential of approximately 1000 psi and this becomes a limiting design requirement. The volume capacity and pressure differential currently exceeds existing bellows design technology. A survey of various bellows manufacturers indicates that, even with contemplated advances in technology, the operating requirements cannot be satisfied. Fabrication of high-pressure, multi-cycle bellows in the size required for this application is very costly and difficult to control. Even concepts requiring a differential internal pressure capability only (i.e., the concentric-bellows concept) entailed a significant development risk. Only one bellows manufacturer (Gardner Products) indicated potential satisfactory production of a bellows for this application. This bellows would be hydroformed by a proprietary process; however, none had been made for this type of service. As a result, the use of bellows in this application would have represented a substantial development risk.

Current and expected operating pressure limits obtained from bellows manufacturers are summarized below:

Sealol Inc.

Current limit--40 psi
Future limit--800 psi

Metal Bellows

Current limit--250 psi
Future limit--500 psi

Belfab

Current limit--200 psi
Future limit--no comment

Bell-Metrics

Current limit--250 psi
Future limit--no comment

Gardner Products

Current limit--2700 psi

TABLE VI

PRESSURIZATION SUBSYSTEM DESIGN CONCEPTS

Design Concept	Advantages	Disadvantages
Piston-Piston	1. Well within present SOTA technology 2. Not pressure and/or volume limited 3. Lightest weight system 4. High expulsion efficiency 5. Hot gases are substantially remote from propellant 6. Hot gas dynamic seal leakage is vented	1. Requires a shear seal to provide leak-tight storage 2. Requires two dynamic seals 3. Two diameter tank and piston requires special manufacturing care and precision 4. Three point "redundant" guide required to maintain piston wheelbase while avoiding seal damage 5. Either vapor pressure storage or volume compensating bellows required
Inverted Piston	1. Not pressure and/or volume limited 2. High expulsion efficiency 3. Hot gas dynamic seal leakage is vented 4. Piston wheelbase is easily maintained 5. Outer tank can be made self-aligning to reduce manufacturing cost	1. Requires a shear seal 2. Requires two dynamic seals 3. Difficult structural design due to long and tortuous stress paths 4. Hot gases impinge on piston in direct contact with propellant 5. Either vapor pressure storage or volume compensating bellows required 6. Heaviest system
Annular Piston	1. Well within present SOTA technology 2. Not pressure and/or volume limited 3. High expulsion efficiency	1. Requires two shear seals 2. Requires two dynamic seals 3. Piston wheel base is not readily maintained through stroking 4. Dynamic seal damage likely in passing shear seal 5. Hot gases impinge on piston in direct contact with propellant 6. Hot gas dynamic seal leakage enters propellant 7. Either vapor pressure storage or volume compensating bellows required
Piston-Bellows	1. Simple tank design and manufacturing 2. No shear seal required 3. Smallest volume requirement 4. Hot gas dynamic seal leakage is vented 5. Automatic volume compensation	1. Bellows pressure-volume requirements exceeds present SOTA 2. Requires one dynamic seal 3. Short piston wheelbase 4. Hot gases impinge on piston in direct contact with propellant
Concentric Bellows	1. Simple tank design and manufacture 2. No shear seals required 3. No dynamic seals required 4. Low volume requirement 5. Automatic volume compensation	1. Bellows pressure-volume requirement exceeds present SOTA 2. Hot gases impinge on bellows in direct contact with propellant 3. Difficult dual bellows header assembly 4. Low expulsion efficiency
Telescoping Piston	1. Simple tank design and manufacture	1. Bellows pressure-volume requirement exceeds present SOTA 2. Highest volume requirement 3. High weight requirement 4. Requires one shear seal 5. Requires one dynamic seal 6. Dynamic seal damage likely in passing over shear seal 7. Hot gases impinge on bellows in direct contact with propellant 8. Either vapor pressure storage or volume compensating bellows required 9. Requires addition of piston wheelbase

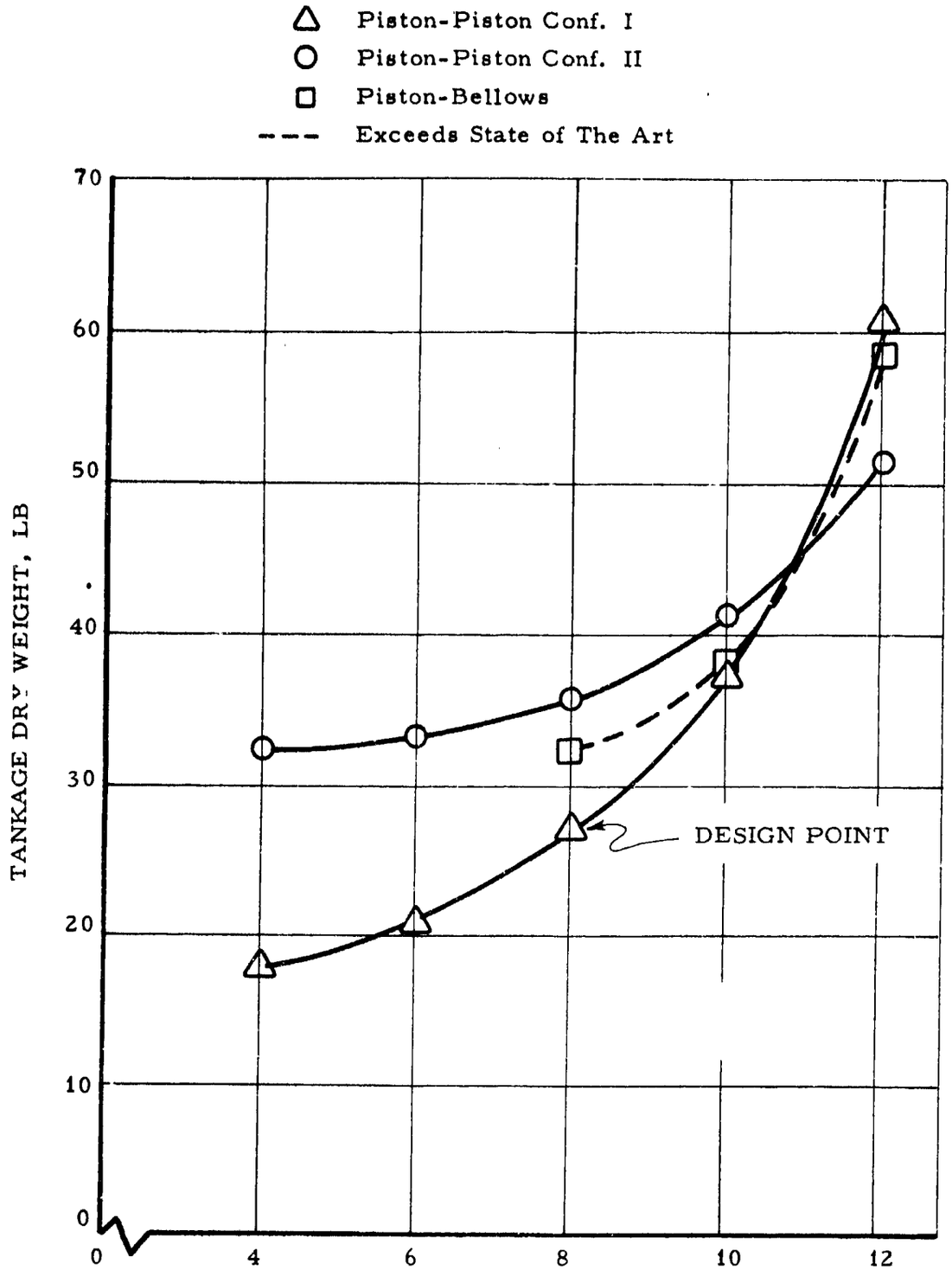

Figure 7. Tankage Dry Weight vs Propellant Tank Diameter

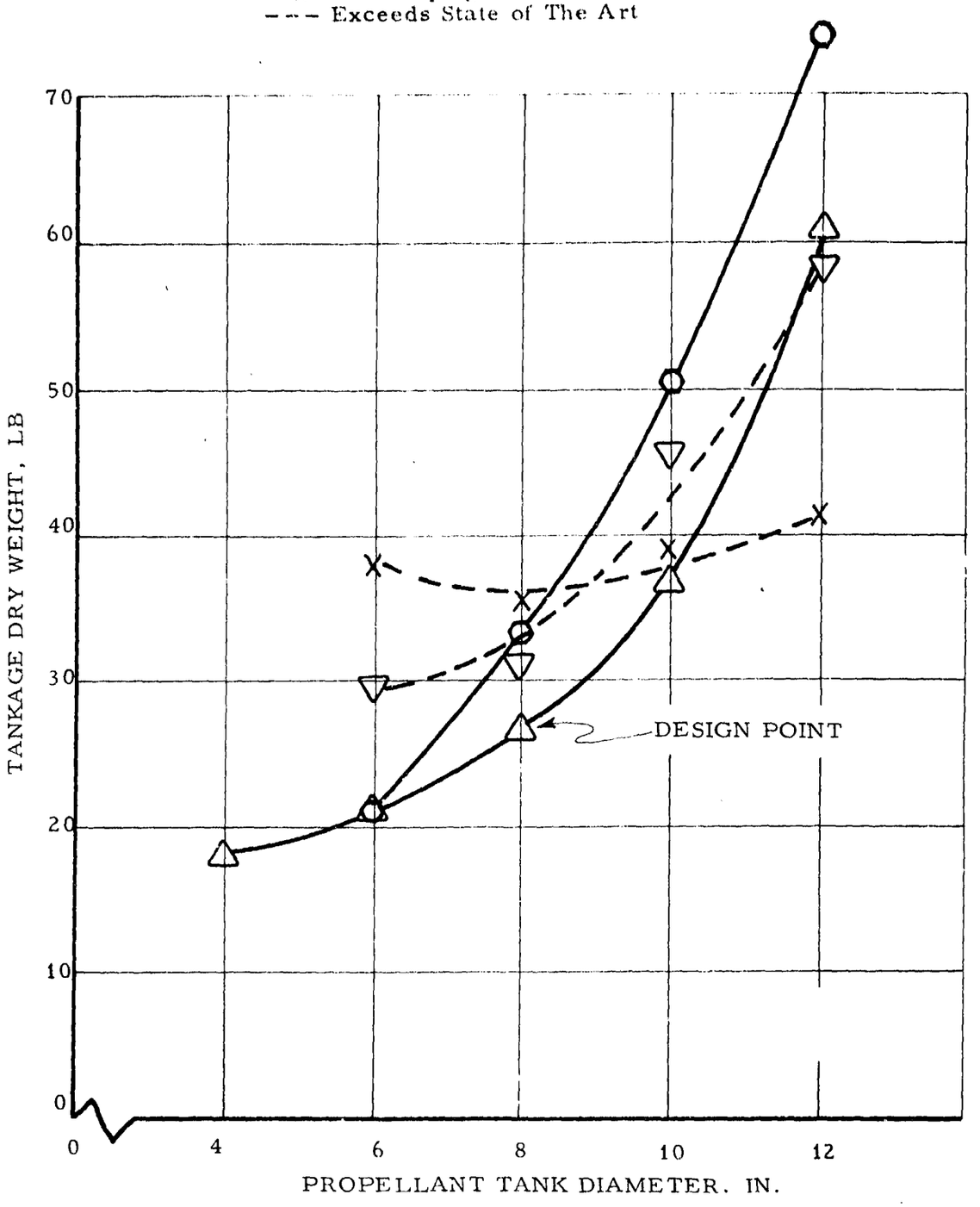

Figure 8. Bootstrap Tank Sizing Study - Tank Weight vs Diameter

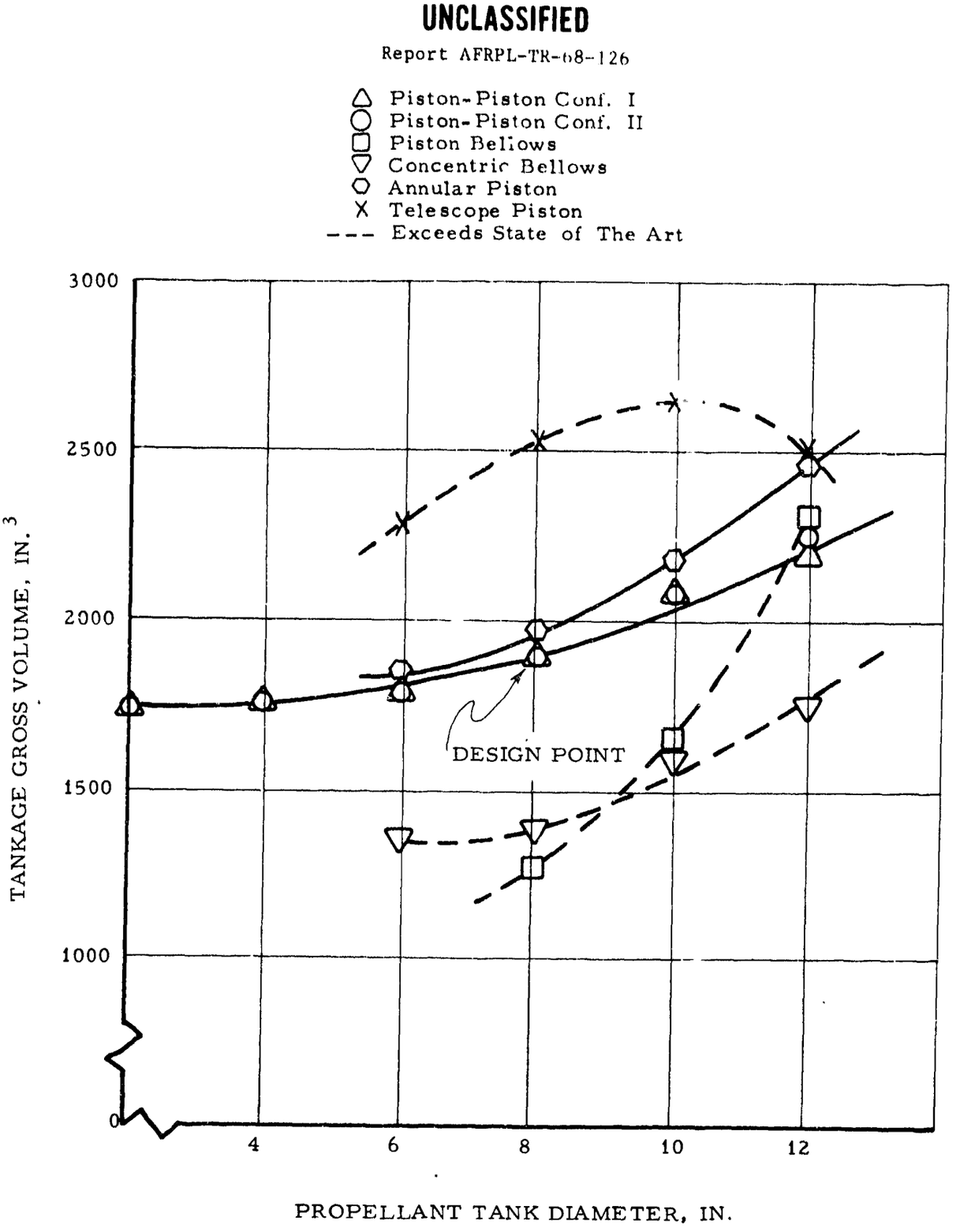

Figure 9. Bootstrap Tank Sizing Study - Tank Gross Volume vs Diameter

IV, A, Pressurization Subsystem (cont.)

b. Gas Generator

(1) Description

The initial design layout of the first-stage hydrazine gas generator is shown on Figure No. 10. The gas generator assembly consists of an injector, reaction chamber, and an exhaust outlet. The injector utilizes capillary tubes in a stand-off configuration to provide proper propellant distribution into the catalyst bed and to minimize heat soak-back. The reaction chamber consists of a chamber wall welded to the injector, the Shell 405 catalyst bed, along with a screen and back-up plate to retain the catalyst. A bolted flange joint is utilized in the workhorse unit to attach the exhaust outlet fitting to the reaction chamber. This facilitates cleaning, catalyst bed inspection, and repacking. A metallic "O-ring" seal is used at this joint to prevent leakage. Integral instrumentation ports are provided to permit evaluation of reactor performance. The materials selected for the gas generator include AISI 347, Inconel 600, and Haynes 25.

The initial design layout of the second-stage gas generator is shown on Figure No. 11. Its basic application is identical to that of the first-stage gas generator; therefore, the basic design of the second-stage gas generator is similar. The only significant differences occur in the over-all size because of the much greater flow, a bolted flange between the chamber and injector for greater developmental flexibility, and materials. A greater strength stainless steel (Greek Ascoloy) was utilized for the injector to minimize weight because the flat plate stress is relatively high as a result of the relatively large size and high chamber pressure. A bolted mounting flange with a teflon seal is provided on the injector as an interface for the vortex throttle valve.

(2) Sizing

The following three basic design criteria were applied in determining the first-stage gas generator size:

- A flow of 0.0315 lb/sec $\pm$ 10% at an outlet pressure of 700 psia and a gas temperature of 1400°F
- 80% ammonia dissociation
- Stable operation with minimum pressure drop through the injector and catalyst bed

Based upon the results from previous research and development programs, it was decided to concentrate upon achieving stability by selecting the proper bed loading and catalyst grain size. With a low bed

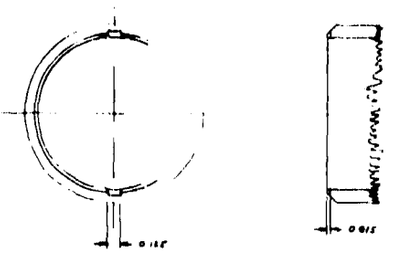

SLOT DETAIL

40-50 IN-LBS TORQUE

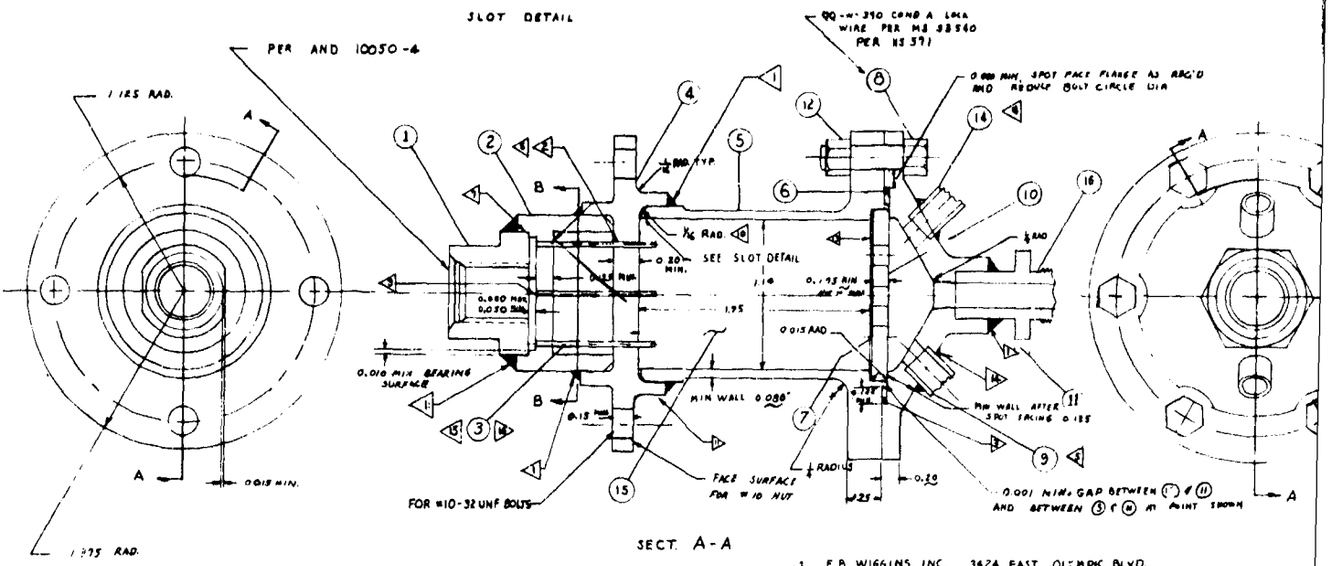

SECT. A-A

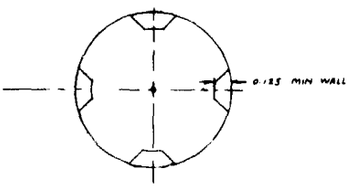

SECT. B-B

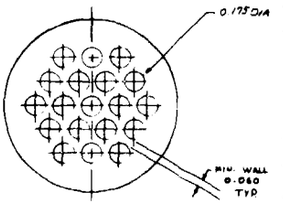

(10) RETAINER, SCREEN

(17) E.B WIGGINS, INC., 3424 EAST OLYMPIC BLVD. LOS ANGELES, CALIFORNIA, 90023

(6) PER MIL-T-8808 AND AMS 5571

(5) I.D TOLERANCE - NO BURRS PERMITTED IN TUBES A

(4) WELD PER MIL-W-8611 PER HS 191 CL II C

(3) CIRCUMFERENTIAL SPOT WELD 7 TO 10 AT 12 EQUALLY SPACED INTERVALS

(2)

(1) LENGTH SUFFICIENT FOR 3 REWELDS

MINIMUM CHAMFER FOR MINIMUM VOID

MOUNT TUBES FLUSH (0 TO 0.010 RECESSED)

(9) SHELL 405 AS PER SHELL REPORT NO. S-13947 CONTAINING 32-34% ACTIVE MATERIAL BY WEIGHT WITH A 20-30 MESH SIZE CATALYST TO BE TUMBLED AND SIEVED PRIOR TO LOADING BFO.

(8) MINIMUM OF 0.050 IN. BEARING SURFACE BETWEEN 1 AND 2

(7) BRAZE FITS PER TFS-30

(16) P_c TAP CONSISTS OF 1.5 IN. LENGTH OF ⅛ TUBING FLARED PER MS 33584 WITH DL-100-4K BY (SEE NOTE 17)

(15) T_c TAP CONSISTS OF 1.5 IN. LENGTH OF ⅛ TUBING FLARED PER MS 33584 WITH DL-100-4K BY (SEE NOTE 17)

(14) INSTALL O-RING PER DESIGN NOTE 37

(13) BRAZE PER HS 1414 TYPE I

(12) WELD PER MIL-W-8611 PER HS 191 CL II A

1

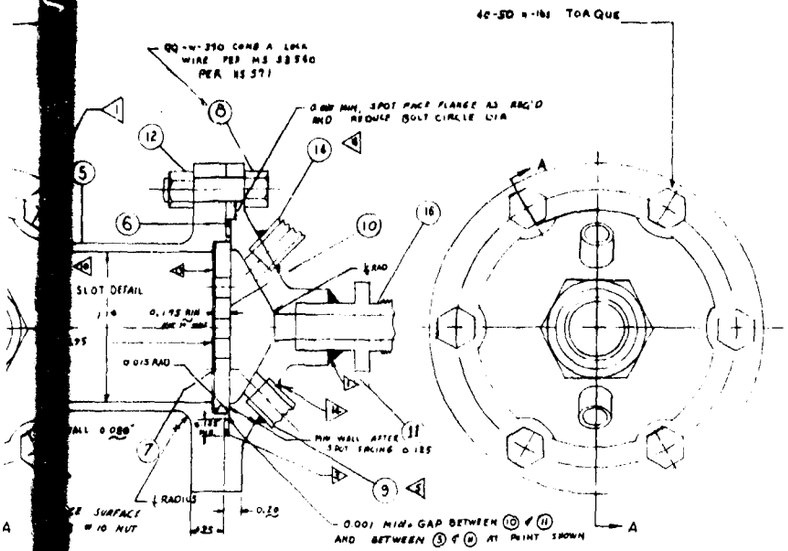

16	1		FITTING, OUTLET	AN 815-4S (TYPE 347) REMOVE THREAD AS SHOWN
15			CATALYST	SEE NOTE 8
14	1		T_c FITTING	0.25 O.D x 0.035 WALL, MIL-T-8808 TYPE I, COMP 347
				DEFINED BY ENGINEERING
12	6	69687-6	NUT	AMS 5525 (A-286)
11	1		OUTLET, EXHAUST	QQ-S-763 CLASS 347 COND A
10	1		RETAINER, SCREEN	AMS 5665

9	1		P_c FITTING	0.250 O.D x 0.035 WALL, MIL-T-8808 TYPE I, COMP 347
8	6	69408A10-8	BOLT	AMS 5616 (32-38 RC)
7	1		SCREEN	HAYNES 25, 50 X 50 MESH, .009 WIRE (AMS 5796)
6	1	69701E38	O-RING	MATL INCONEL, SEE NOTE
5	1		CHAMBER, COMBUSTION	QQ-S-763 CLASS 347 COND A
4	1		FLANGE	QQ-S-763 CLASS 347 COND A
3			INJECTOR TUBE	AMS 5646 TUBING, .931 O.D
2	1		THERMAL STANDOFF	QQ-S-763 CLASS 347 COND A
1	1		INLET VALVE	QQ-S-763 CLASS 347 COND A
DET	NO	PART NO	PART NAME	MATERIAL & REMARKS

17. E B WIGGINS, INC., 3424 EAST OLYMPIC BLVD. LOS ANGELES, CALIFORNIA, 90023
16. PER MIL-T-8808 AND AMS 5571
15. I.D TOLERANCE - NO BURRS PERMITTED IN TUBES AFTER CUTTING
14. WELD PER MIL-W-8611 PER HS 191 CL II C
13. CIRCUMFERENTIAL SPOT WELD 7 TO 10 AT 12 EQUALLY SPACED INTERVALS
12. LENGTH SUFFICIENT FOR 3 REWELDS
11. MINIMUM CHAMFER FOR MINIMUM VOID
10. MOUNT TUBES FLUSH (0 TO 0.010 RECESSED)
9. SHELL 405 AS PER SHELL REPORT NO. S-13947 CONTAINING 32-34% ACTIVE MATERIAL BY WEIGHT WITH A 20-30 MESH SIZE CATALYST TO BE TUMBLED AND SIEVED PRIOR TO LOADING BED.
8. MINIMUM OF 0.050 IN BEARING SURFACE BETWEEN 1 AND 2
7. BRAZE FITS PER TFS-30
6. P_c TAP CONSISTS OF 1.5 IN LENGTH OF ¼ TUBING FLARED PER MS 33584 WITH DL-100-4K BY (SEE NOTE 17)
5. T_c TAP CONSISTS OF 1.5 IN LENGTH OF ⅛ TUBING FLARED PER MS 33584 WITH DL-100-4K BY (SEE NOTE 17)
4. INSTALL O-RING PER DESIGN NOTE 97
3. BRAZE PER HS 1414 TYPE I
2. WELD PER MIL-W-8611 PER H. 191 CL II A

Figure 10. Workhorse First-Stage Gas Generator, SVL 11239

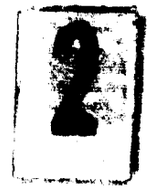

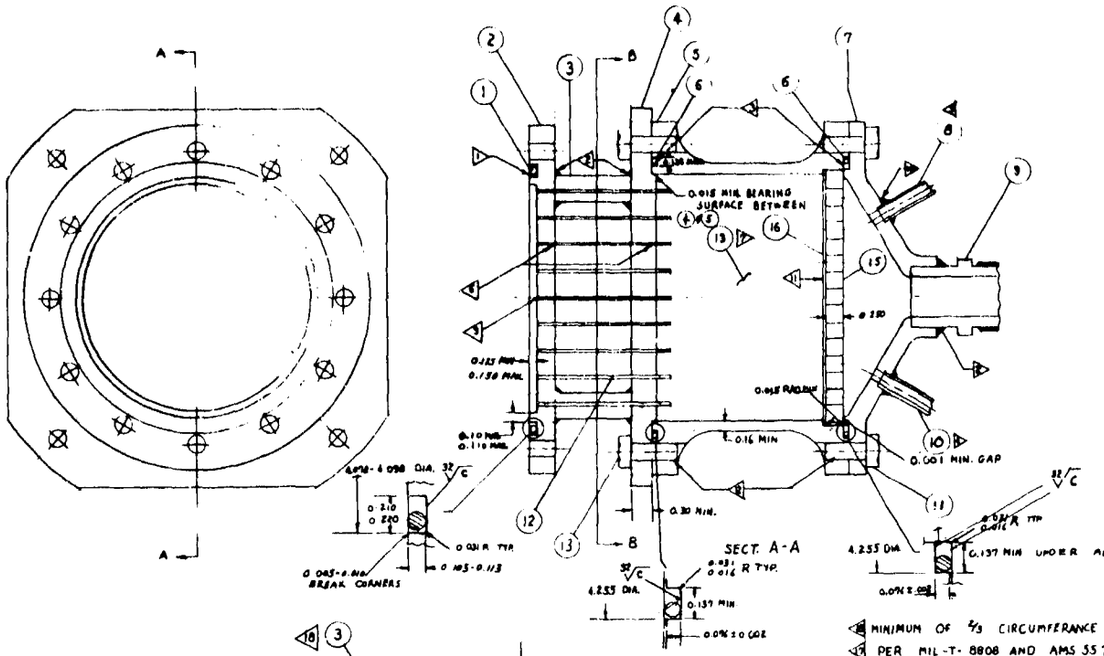

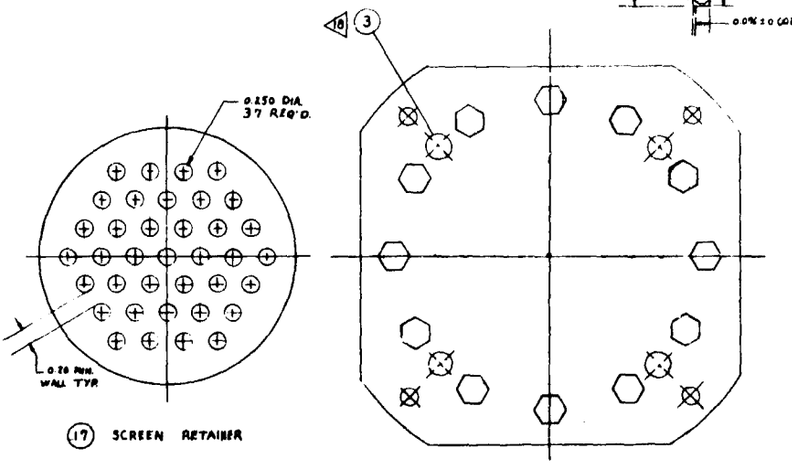

(17) SCREEN RETAINER

- MINIMUM OF 2/3 CIRCUMFERANCE TO BE WELDED
- PER MIL-T-8808 AND AMS 5571
- I.D. TOLERANCE - REMOVE ALL BURRS IN TU
- E.B. WIGGINS, INC., 3424 EAST OLYMPIC BLVD. LOS ANGELES, CALIFORNIA, 90023
- BRAZE FITS PER TPS-30
- TAP PART 3 FOR 3/4 - 28 UNF - 2B THREADS AT 12 EQUALLY SI
- CIRCUMFERENTAL SPOT WELD 13 & 16 AT 12 EQUALLY SPACED PLA
- WELD PER MIL-W-8611 PER HS 191 CL II A
- MOUNT TUBES FLUSH (0.0 TO 0.010)
- BORE REQ'D DIA TO 0.050 DEPTH IN PARTS 2 & 4 TO LOCATE POSITION OF PART 3
- SHELL 606 AS PER REPORT NO. S-13847 CONTAINING 32-36% ACTIVE MATERIAL BY WEIGHT WITH A 20-30 MESH
- BRAZE PER HS 1616 TYPE I
- P, TAP CONSISTS OF 1.5 IN LENGTH OF ½ TUBING FLARED PER HS 33584 WITH A DL100-4K BY (SEE NOTE 15)
- T, TAP CONSISTS OF 1.5 IN. LNGTH OF ½ TUBING FLARED PER HS 33584 WITH A DL100-4K BY (SEE NOTE 15)
- 32 MICROINCH FINISH ON SEALING SURFACES
- WELD PER MIL-W-8611 PER HS 191 CL II A
- 32 MICROINCH FINISH ON SEALING SURFACE

1

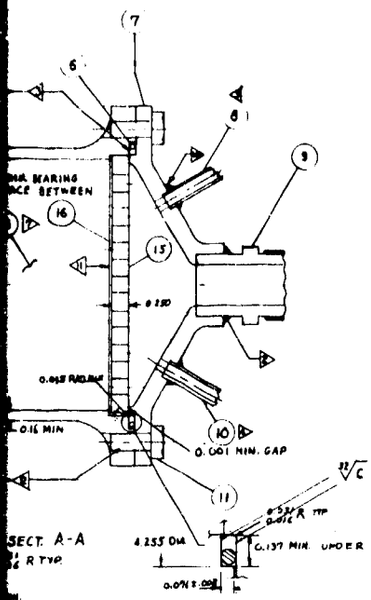

16	1		SCREEN	HAYNES 25, 50 x 50 MESH (AMS 5796)
15	1		RETAINER, SCREEN	AMS 5665
				DEFINED BY ENGINEERING
13			CATALYST	SEE NOTE 7
12			INJECTOR TUBE	0.062 OD
11	24	68408A25-10	BOLT	AMS 5616 (32-38RC)
10	1		T_c FITTING	0.25 O.D x .005 WALL, MIL-T-8808 TYPE I, COMP 347
9	1		UNION (FLARED TUBE)	AN 815-12 S TYPE 347 (REMOVE THREAD AS SHOWN)

8	1		P_c FITTING	0.25 O.D x 0.035 WALL, MIL-T-8808 TYPE I, COMP 347
7	1		OUTLET, EXHAUST	QQ-S-763 CLASS 347 COND A
6	2	69708E79	O-RING	MAT'L INCONEL
5	1		CHAMBER, COMBUSTION	QQ-S-763 CLASS 347 COND A
4	1		FLANGE, MOUNTING	AMS 5616 (32-38 RC)
3	4		THERMAL STANDOFF	QQ-S-763 CLASS 347 COND A
2	1		FLANGE, INLET	AMS 5616 (32-38 RC)
1	1		O-RING	MS 28775-240 (TEFLON)
DET	NO	PART NO	PART NAME	MAT'L & REMARKS

1. MINIMUM OF 2/3 CIRCUMFERANCE TO BE WELDED
2. PER MIL-T-8808 AND AMS 5571
3. I.D. TOLERANCE - REMOVE ALL BURRS IN TUBES
4. E.B. WIGGINS, INC., 3424 EAST OLYMPIC BLVD. LOS ANGELES, CALIFORNIA, 90023
5. BRAZE FITS PER TPS-30
6. TAP PART 3 FOR 1/4-28 UNF-2B THREADS AT 12 EQUALLY SPACED PLACES
7. CIRCUMFERENTIAL SPOT WELD 15/16 AT 12 EQUALLY SPACED PLACES
8. WELD PER MIL-W-8611 PER HS 191 CL II A
9. MOUNT TUBES FLUSH (0.0 TO 0.010)
10. BORE REQ'D DIA TO 0.050 DEPTH IN PARTS 2 & 4 TO LOCATE POSITION OF PART 3
11. SHELL 406 AS PER REPORT NO. 3-13347 CONTAINING 32-36% ACTIVE MATERIAL BY WEIGHT WITH A 20-30 MESH
12. BRAZE PER HS 1614 TYPE I
13. P_c TAP CONSISTS OF 1.5 IN LENGTH OF 1/4 TUBING FLARED PER MS 33580 WITH A DL100-4K BY (SEE NOTE 15)
14. T_c TAP CONSISTS OF 1.5 IN. LENGTH OF 1/8 TUBING FLARED PER MS 33584 WITH A DL100-4K BY (SEE NOTE 15)
15. 32 MICROINCH FINISH ON SEALING SURFACES
16. WELD PER MIL-W-8611 PER HS 191 CL II A
17. 32 MICROINCH FINISH ON SEALING SURFACE

Figure 11. Workhorse Second-Stage Gas Generator, SVL 11240

loading of 0.03 lb/sec/in.^{2}, the catalyst bed pressure drop is reduced and stable operation can be achieved with a minimum of injector pressure drop. The use of a finer mesh catalyst also contributes to reactor stability with only a slight increase in bed pressure drop resulting from the relatively high gas density at a chamber pressure of 700 psia. A bed length of 1.75-in. was selected to achieve the required 80% minimum ammonia dissociation. The resultant injector pressure drop was 190 psid and the bed drop was 10 psid, which gave a total drop of 200 psid.

The sizing criteria for the second-stage generator were similar to those of the first stage except that flow rate was 0.30 lb/sec to 0.45 lb/sec at an outlet pressure of 435 psia and a temperature of 1400°F. A slightly higher bed loading of 0.041 lb/sec-in.^{2} was utilized to minimize the reactor weight. A bed length of 2.5-in. was required to obtain a minimum of 80% ammonia dissociation. The total gas generator pressure drop was approximately 75 psid (a 53-psid injector pressure drop and a 22-psid bed pressure drop).

Testing of the first-stage and second-stage gas generators is discussed in Section IV,A,4,a.

c. Bootstrap Tank

(1) Workhorse Configuration

(a) Design Analysis

The workhorse bootstrap tank configuration was designed to simulate a flightweight bootstrap tank except for allowable deviations because of material availability, instrumentation needs, hardware re-use requirements, and developmental flexibility. Other factors influencing the design of the workhorse tank were component costs and procurement time.

The numerous operating parameters affecting the pressurization subsystem were examined. Of these, the steady-state operating parameters of primary concern included: propellant flow rate to the reactor; reactor output pressure; feedback pressure; component pressure drops, piston friction and leakage losses; and piston area ratio. These parameters were examined and are discussed further in the following paragraphs. Where applicable, analysis data also are given for the prototype tank configuration.

1 Pressure and Flow

The subsystem design was based upon the pressure and flow rate schedule shown on Table VII. A preliminary reactor design study was accomplished to ascertain the catalyst bed pressure drop and

TABLE VII

ESTIMATED SYSTEM HYDRAULIC CHARACTERISTICS

PRESSURE AND FLOW RATE SCHEDULE	Pressure, psia		Flowrate, lb/sec	
	Engines On	Engines Off	Engines On	Engines Off
1st Stage Gas Generator Input	848	797	0.0283	0.0315
1st Stage Gas Generator Output	707	682	0.0283	0.0315
1st Stage Fluidic Pressure Regulator Control Input	707	682	0.00457	0.0067
2nd Stage N_2H_4 Tank Pressure Input	657	626		
2nd Stage Pressure Regulator Control Input			0.0206	0.0206
Feedback Decomposed N_2H_4 to Differential Area Tank	677	637	0.00079	0.00087
2nd Stage Gas Generator Input	606	573	0.326	0.449
2nd Stage Gas Generator Output	494	435	0.326	0.449

ESTIMATED FEED-SYSTEM PRESSURE DROP	Pressure Drop--psid	
	Workhorse	Prototype
Solenoid Valves and Lines	30	--
Squib Valve	--	5
Filter	5	5
Trim Orifice (Nominal)	35*	35
Injector	70**	70
Catalyst Bed	10	10
Piston Friction	20***	20
Estimate Total	170	145
Actual Total	330	270

*Actual (nominal flow) approximately 90 psid, **Actual injector pressure drop after development was 196 psid, ***Actual piston friction 5 psid.

the injector pressure drop needed to provide stable operation. A trim orifice was added for calibration purposes. As shown on Table VII, the actual injector pressure drop achieved after development was almost 2-1/2 times greater than the calculated value. This additional pressure drop was required for stable operation of the gas generator. The pressure drop allowances for the solenoid valve, squib valve, and filter were selected to allow the use of off-the-shelf hardware.

2 Friction and Leakage

The effective propellant pressure loss was determined by means of a friction analysis based upon a preliminary design estimate of the tank operating conditions. This estimate included the effects of seal friction and piston cocking. Seal friction loss was based upon an allowance of 12 pounds-per-circumferential-inch. Friction caused by piston cocking was based upon a 1-degree out-of-squareness for each piston face and a 0.3 coefficient of friction.

The effect of piston seal losses was found to be negligible. Propellant leakage did not affect the piston force balance. However, gas leakage past the seal would require make-up flow with its consequent feedback line pressure drop. Substantial leakage flow would be required to sustain any significant pressure drop in this 1/4-in. line.

The initial analysis indicated an estimated total pressure drop of 170 psi, but in actual practice, the total was approximately 330 psi at nominal flow.

3 Area Ratio

Table VIII shows the range of expected operating conditions along with the area ratio needed to satisfy each condition. The most severe operating condition occurs with the prototype system at minimum chamber pressure and minimum feedback pressure. An area ratio of 1.3, which corresponds to this condition, was selected as the minimum design target. However, in consideration of over-all system pressure prediction accuracies and the selection of standard tank bore sizes, a final area ratio of 1.40 was selected. This provided a design safety factor of 9%.

(b) Design Description

The workhorse tank design (see Figure No. 12) has a stepped-diameter bore and outer shell with flanges at both the gas and the propellant ends. These flanges are sealed with face-type O-ring seals to prevent gas and propellant leakage. The flange construction minimizes the manufacturing problems (i.e., maintaining roundness and concentricity of the tank bores) that would occur if the propellant header were welded to the 6061 T-6 aluminum tank shell.

TABLE VIII

BOOTSTRAP TANK AREA RATIO REQUIREMENTS

	WORKHORSE*	PROTOTYPE
Flow, lb/sec	0.0315 - 0.0315	0.0315 - 0.0283
Pressure (P_c), psia	682 - 707	682 - 707
P (feed system), psid	170 - 170	145 - 117
Required Feed System Pressure, psia	852 - 877	827 - 824
Feedback Pressure, psia	682 - 707	637 - 677
Required Bootstrap Area Ratio	1.25 - 1.24	1.30 - 1.22

*Workhorse system with pressure-switch - solenoid control

Actual area ratio for workhorse tank was 1.4 which provided a feed pressure of 990 psia for a generated feedback pressure of 707 psia which was sufficient to compensate for the additional pressure drops encountered during development.

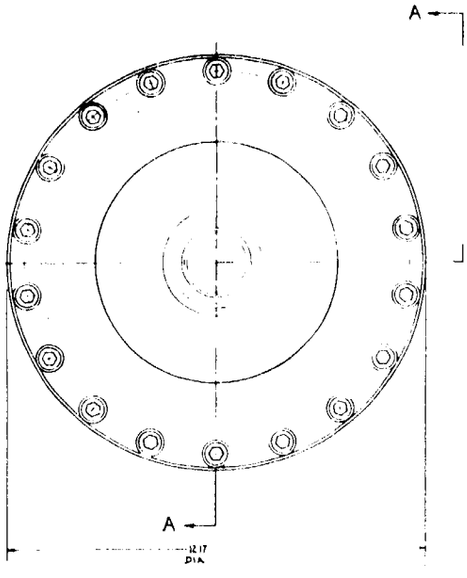

TANK
END VIEW

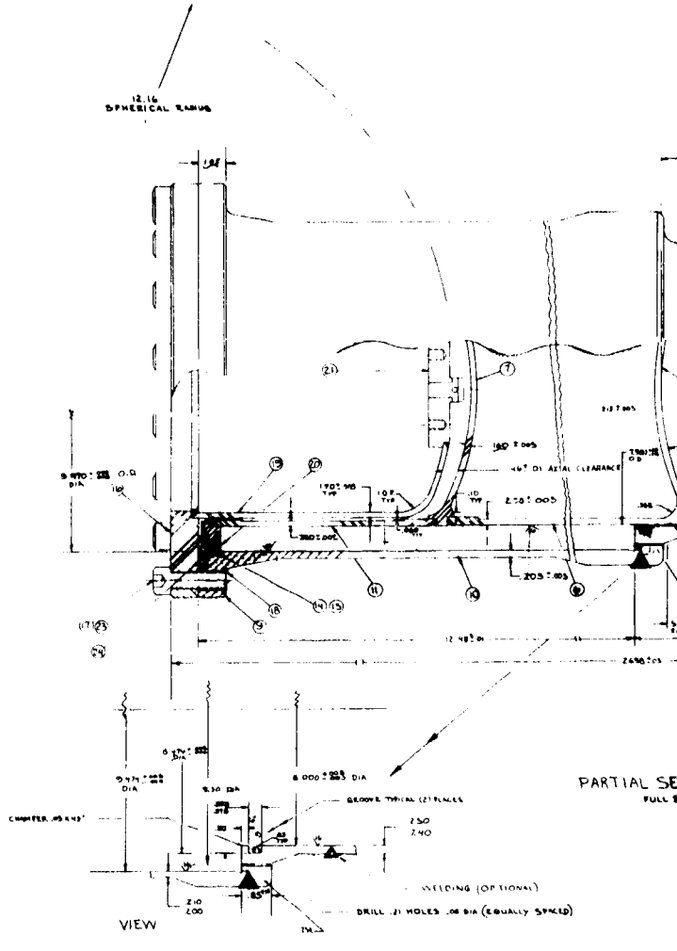

VIEW

1

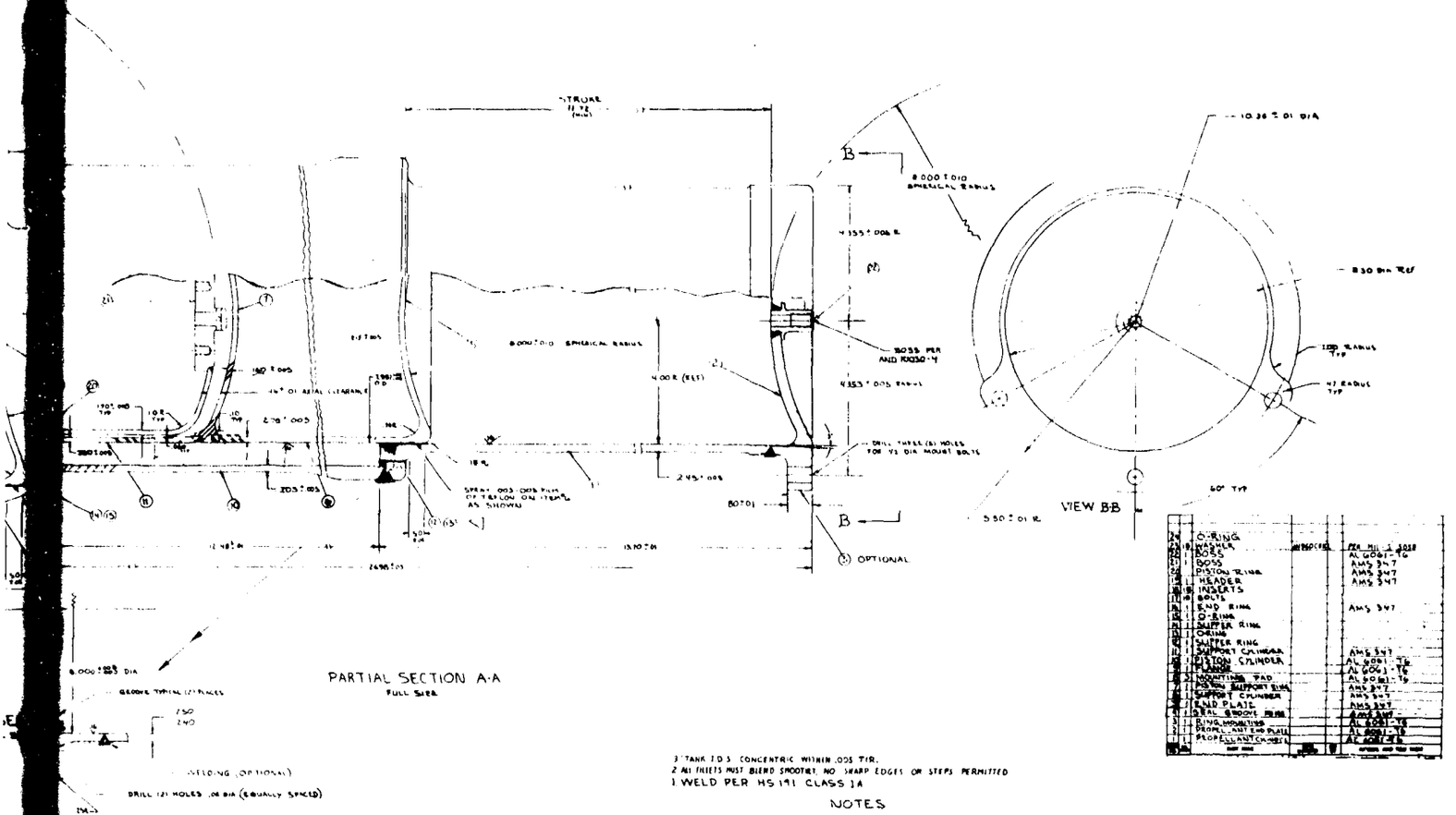

Figure 12. Workhorse Bootstrap Tank Assembly, SVL 11236

IV, A, Pressurization Subsystem (cont.)

The piston assembly was built-up from AISI 347 sheet and plate stock welded together and teflon-coated on the sliding surfaces. One dynamic seal was located on the gas side of the piston and a second seal was located in the tank body to contain the propellant.

Ports for the solid gas generator, feedback line, and necessary instrumentation were located on the gas-side flange, which was fabricated from AISI 347 corrosion-resistant steel.

(c) Tank Sizing

Three considerations influenced the selection of tank diameters (8-in. on the liquid end and 9-1/2-in. on the gas end). First, the estimated over-all length did not exceed the maximum envelope length of 28-in. Secondly, the area ratio of 1.40 (using standard seal sizes) gives an adequate safety margin over the minimum design target of 1.30. Thirdly, minimum tank diameter provides minimum weight and volume, which is significant for the flightweight unit. The purpose of the workhorse system was to approximate the flightweight configuration; therefore, the smallest practical diameter consistent with available seal diameters was selected. The following propellant storage volume requirement was established:

Consideration	Volume, $in.^3$
20 lb of usable propellant at 70°F	550
Weighing tolerance, 1%	6
Residuals	10
Thermal expansion, 70 to 140°F	22
Safety factor to limit maximum pressure at +140°F to shear-seal rupture pressure if sea-level pressure is inadvertently established at the minimum temperature of +20°F	2
Total	590

The gas-end volume was established at a nominal value of 30-$in.^3$ to minimize the free-volume change with temperature. Consequently, at the maximum operating temperature, the free volume to be pressurized was 44.5-$in.^3$, while at the minimum operating temperature the volume after shearing the seal was:

$$V = V \text{ nominal} + V \text{ (+40 to +140°F)} = 30 + 45 = 75 \text{ in.}^3$$

The resultant pressure ratio for initiation of system operation was 1.7:1 over the range of operating conditions.

IV, A, Pressurization Subsystem (cont.)

(d) Tank Material

A survey of materials considered for the workhorse and prototype tank assembly is presented as Table IX. The materials are listed from left to right in the order of their specific strength. AM 350 steel is the preferred tankage material for a practical minimum weight tank. An extensive survey of material suppliers, forging manufacturers, and tank subcontractors indicated that fabricating the tank from AM 350 would adversely affect the program cost and be particularly detrimental to the program schedules. AM 350 is not available in commercial forgings. It is produced in sheet stock which is readily available to 1/8-in. thickness. As a result, it was necessary to select an alternative material. It was found that the most favorable alternative material was aluminum alloy 6061-T6 followed by AISI 347 stainless steel. The 6061-T6 aluminum alloy was selected for the tank external member to reduce weight as well as material and machining costs. A further consideration was to approximate the expected tank wall deflection of the flightweight unit under pressure. This deflection would be proportional to the ratio of the working stress and the modulus of elasticity. For aluminum, this value is 0.0017, which is similar to that of AM 350 (0.0022). If AISI 347, which has a ratio of 0.0007, were used, the deflection would only be one-third that of the flightweight tank and could have been considered inadequate for concept evaluation. The high thermal capacity and conductivity of the tank external member had no appreciable effect upon squib gas generator temperature because of its remoteness and minimum contract area.

AISI 347 was selected for both the piston and inlet gas end flange because of the high temperature gas from the squib and the feedback. Gas would impinge directly upon the piston surface, which if it were aluminum could become fully annealed and require excessively heavy wall sections, thereby adding unnecessary weight.

Both materials exhibited poor galling properties; therefore, it was judged that a dissimilar metal combination would have a better probability of working. To further offset this problem, the nose of the piston was coated with teflon.

(e) Dynamic Seals

A number of dynamic seal configurations were examined for possible use in the piston/tank application. The requirement for a 10-year dry storage period eliminated most seals. Seal suppliers and seal specialists indicated that a spring-loaded teflon lip seal which could be pressure energized during actual operation would be most practical. The spring would lightly load the lips which both reduces the creep rate of the teflon and also adjusts for creep deflection. Further, it would provide initial lip contact during the pressurizing cycle.

TABLE IX

TANK MATERIAL SURVEY

MATERIAL	17-7 PH	TI-GAL-4V	AM-350	INCONEL 716	AM-355	INCONEL X 750	GRK. ASCOLOY	6061-T6	5052-4134	AISI410	AISI347	INCONEL 600
DENSITY lb/in^3	0.276	0.160	0.282	0.297	0.282	0.298	0.286	0.096	0.097	0.28	0.28	0.307
YOUNGS MODULUS PSI	$28x10^6$	16×10^6	$29x10^6$	$29.6x10^6$	$29x10^6$	$31x10^6$	$29x10^6$	$10x10^6$	$10.2x10^6$	$29x10^6$	$29x10^6$	$29.6x10^6$
ULTIMATE, MIN. PSI	240,000	130,000	200,000	180,000	165,000	170,000	153,000	42,000	34,000	90,000	75,000	80,000
ULTIMATE, MAX. PSI	---	---	---	---	184,000	---	170,000	---	41,000	95,000	105,000	100,000
YIELD, MIN. PSI	230,000	120,000	180,000	150,000	140,000	115,000	135,000	35,000	31,000	60,000	20,000	30,000
YIELD, MAX. PSI	---	---	---	---	165,000	---	150,000	---	---	---	---	---
ALLOW. DESIGN WORKING PSI	96,000*	52,000*	80,000*	72.000*	66,000*	68,000*	61,200*	16,800*	13,600*	34,000*	30,000	32,000
STRESS FOR BURST ALLOW. DESIGN WORKING PSI	153,000	80,000	120,000	100,000	93,300	76,600	90,000	23,300	20,700	40,000	20,000	20,000
STRESS FOR PROOF ELONGATION - %	1	10	10	15	10	18	10	10	7	20	40	40
COMPATIBILITY WITH N_2H_4	CLASS 3 160°F	CLASS 1 160°F	CLASS 1 160°F	UNKNOWN	CLASS 1 160	CLASS 1 140	UNKNOWN	CLASS 1 160	CLASS 1 80	CLASS 2 277	CLASS 1 200	CLASS 1 200
MACHINEABILITY	POOR	FAIR	FAIR	FAIR	FAIR	POOR	POOR	GOOD	GOOD	POOR	FAIR	POOR
WELDABILITY	GOOD	GOOD	GOOD	GOOD	GOOD	POOR	NOT REC	GOOD	GOOD	FAIR	EXCEL.	GOOD
WEAR-GALLING	MUST BE NITRIDED	POOR	POOR	POOR	POOR	POOR	GOOD	POOR	POOR	SOME	POOR	POOR
CORROSION RESISTANCE	GOOD	GOOD	GOOD	V GOOD	GOOD	GOOD	GOOD	GOOD	GOOD	GOOD	GOOD	GOOD
SPECIFIC STRENGTH $\frac{PSI}{lb/in^3}$ AT ALLOWABLE DESIGN STRESS	347,000	325,000	284,000	242,000	234,000	228,000	214,000	171,500	140,500	128,500	68,000	65,100
PROBLEM AREAS												
COMPATIBILITY	x			x		x	x		x	x		
WELDABILITY						x	x					
STATE-OF-THE-ART		x										
AVAILABILITY		x	x		x		x					

NOTES 1) ALL STRENGTH VALUES FOR SHEET OR PLATE AT ROOM TEMPERATURE

2) *DENOTES MAXIMUM ALLOWABLE DESIGN WORKING STRESS

IV, A, Pressurization Subsystem (cont.)

The seals selected for the dynamic application in the workhorse tank assembly were the Hamilton Standard-designed chevron seals. The chevron seal was machined from a high-grade, pure virgin teflon (TRE-6C) and spring-loaded with garter springs.

(2) Prototype Configuration

(a) Tank Description

The prototype tank design, which is shown on Figure No. 13, is similar in concept to the workhorse tank design except for its flanges and the material it was made from. The design was guided by the objective of providing the lightest possible tank while retaining the tank reuseability feature. The tank was manufactured from high-strength, corrosion-resistant AMS 5547 (AM 355) steel.

AM 355 steel alloy was developed from AM 350 technology for heavy cross-section applications. With a maximum strength heat treatment, AM 355 had been found to be susceptible to stress corrosion cracking in some application in the NASA Saturn program. However, investigations revealed that, by changing the heat treatment from sub-zero cooling and tempering at 850°F to sub-zero cooling and temperature at 1000°F, the resistance of AM 355 to stress corrosion was provided. The SCT-1000 heat treatment was selected for this application. The tank manufacturer (Pressure Systems Incorporated) consistently demonstrated obtainable yield strengths with AM 355 at 165,000 psi and ultimate strengths at 184,000 psi. These properties were possible only if the heat treatment was carefully controlled.

The only drawback of the AM 355 was that, in an as-welded (without heat treatment after weld) condition, the material transforms from austenite (as-welded) to martensite (after a sub-zero treatment). A significant amount of the austenite transforms as high as 32°F. Apparently, the austenite weld is not stable under normal temperature zone weather conditions, but the use of the SCT-1000 process heat treatment results in the complete stabilization of the material.

Except for the mounting arrangement and the omission of the shear seal approach, the prototype design is very similar to a flightweight configuration. Figure No. 14 is a picture of the assembled unit. The heavy flanges used for the workhorse configuration were eliminated and the use of a higher strength material allowed reduced wall thicknesses. The weight of the prototype tank assembly shown on Figure No. 14 is approximately 65 lb. The dynamic seals used were Aeroquip Omniseals® which fit into standard O-ring grooves. A teflon bearing insert was installed and machine finished at the sliding point (propellant end) of the piston to prevent metal galling during development testing. This extended the experimental life of the piston/cylinder combination.

® Registered Trademark of Aeroquip Corporation-Aircraft Division.

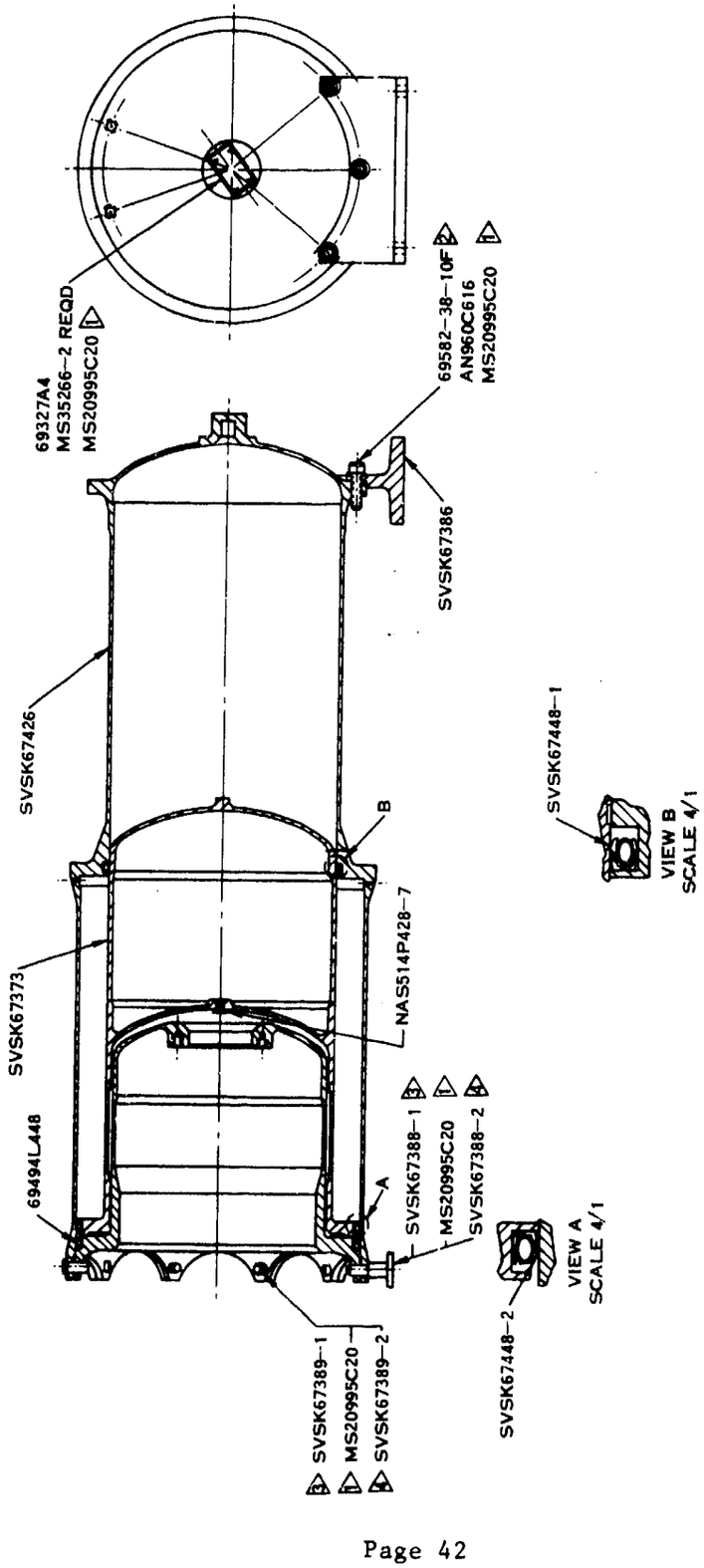

Figure 13. Tank Assembly - Prototype PBPS

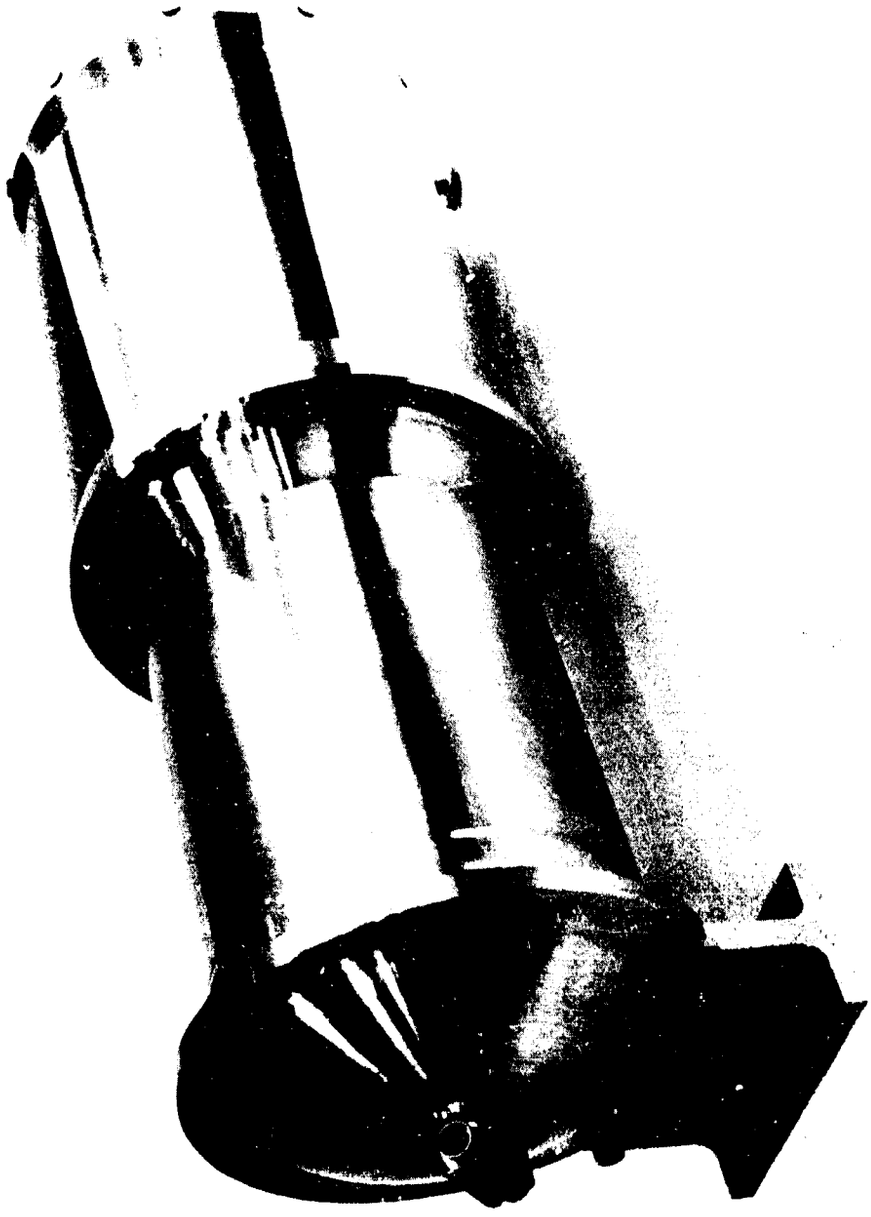

Figure 14. Prototype Pressurization Bootstrap Tank

IV, A, Pressurization Subsystem (cont.)

(b) Tank Size

Originally, the prototype tank was designed for a area ratio of 1.4:1, which was similar to the workhorse configuration. However, to provide additional system operating margin, the area ratio was increased to 1.56:1. It was desirable to maintain the same over-all length of approximately 28-in.; therefore, the piston diameter (propellant end) was kept at 8-in. It was intended to apply standard parts wherever possible, and 10-in. was the next standard O-ring groove size above the equivalent size for an area ratio of 1.4. Therefore, the gas-side of the piston was constructed with a 10-in. diameter which provided a 1.56 area ratio. This large an area ratio meant that the feed pressure could be as high as 1100 psia for a generated feedback pressure of 707 psia.

d. Component Descriptions

The components used for the workhorse development testing are shown on Figure No. 15. The philosophy used in selecting components for this program was predicated upon a tradeoff between minimum procurement time, necessary level of operational flexibility, and cost. Operational flexibility was significant for items such as the solid propellant gas generator and pressure switches because these components required some development for optimum performance. A brief description of each component follows along with a summary of individual operational requirements. The components are listed in the order of system function.

(1) Fill and Drain Valve (Hoke Valve Company)

A manually-operated, 1/4-turn ball valve was selected for the hydrazine fill and drain function. This valve is fabricated from stainless steel (AISI 300 series) and has teflon seals.

(2) Solenoid Valves (Marotta Valve Corporation)

Two solenoid valves were used in the workhorse system. An isolation valve served to isolate the main propellant storage from the remainder of the system and a start valve controlled the propellant flow to the first-stage reaction chamber. These valves were direct-acting, normally-closed solenoid valves (24 to 28 volts, dc) operating on a balanced poppet principle. A spring held the poppet in the closed position. The valves were of the medium response (50 msec to 80 msec from signal to full-open) types. They were intended to serve only as a flexible, economical means of providing minimum control for pressurization system feasibility testing.

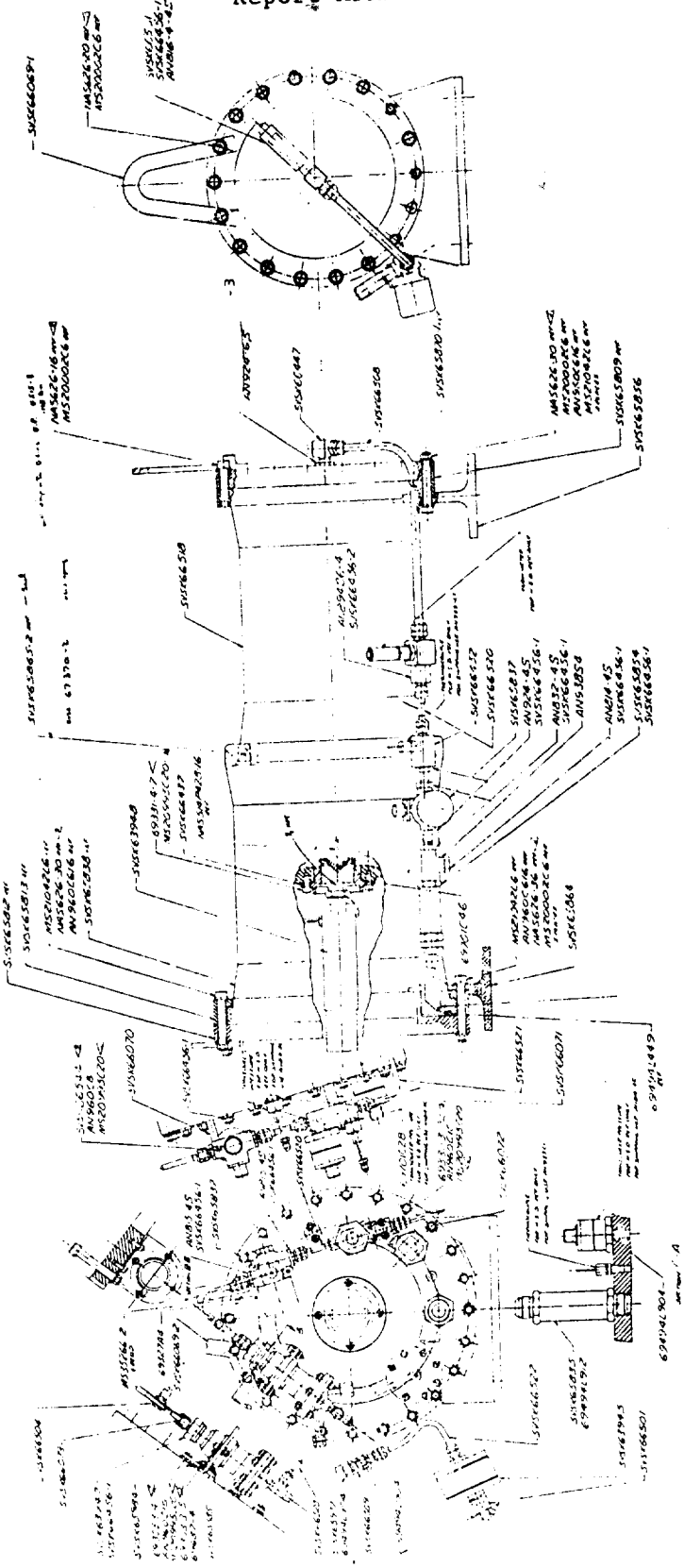

Figure 15. First-Stage Workhorse Gas Generator Assembly

IV, A, Pressurization Subsystem (cont.)

(3) Primary System Filter (Microporous Filter, Division of Circle Seal)

The primary system filter was designed to remove particles generated downstream in the differential area bootstrap tank and propellant feed lines. It will remove 90% of all particles that are 5 microns or larger and 100% of all particles that are 20 microns or larger. The filter element is a pleated, stainless steel wire mesh which provides minimum pressure drop and maximum contaminant capacity.

(4) Injector Inlet Filter (Microporous Filter, Division of Circle Seal)

A small line filter of pleated disk construction was placed into the system to protect the first-stage injector from contaminants which might be generated in the lines and the solenoid valve preceding it. Flow is directed perpendicularly across the filter disk. This filter was not designed for high contaminant capacity, but it has sufficient open area to minimize pressure drop.

(5) Pressure Switches (Gorn Corporation)

The operational mode selected for the workhorse system feasibility testing governed whether one or two pressure switches were used. Without a simulated downstream second-stage hydrazine propellant tank load, only one pressure switch was required. This switch was set to open the control solenoid circuit at 735 psig $\pm$25 psi and close the circuit within 50 psig (lower) of the opening pressure. Using the second-stage hydrazine tank load, the second pressure switch was located downstream of the load orifice near the tank itself and sensed tank pressure. When two switches were used, they were connected electrically in series and controlled the system operation by switching the propellant valve on and off at the proper preset pressures. These switches operated by means of a series of Belleville washers making or breaking contact with a microswitch. The washers are carefully selected in matched sets to control the hysteresis band.

(6) Hot Gas Check Valve (James Pond and Clark, Inc.)

The hot gas check valve was used instead of the one-way burst disk for all initial testing. It proved to be extremely flexible and there was no increase in leakage after repeated use. This stainless steel (AISI 300 series) valve had a high temperature, easily replaceable Inconel 600 spring and a lapped poppet seat.

IV, A, Pressurization Subsystem (cont.)

(7) One-Way Burst Disk (Calmec Mfg. Corporation)

The purpose of the one-way burst disk was to keep the ullage (gas) volume to a minimum when the solid charge gas generator was fired. Without the burst disk, a larger squib charge would have been needed or the time it took the system to reach equilibrium would have increased. These disks were replaceable after each system start, thereby allowing for different burst-away pressures to be set if necessary. The disk was designed to fail in one direction only when a differential pressure was applied across the unit in one direction only. It was designed to withstand a pressure differential in excess of 700 psid in the opposite direction.

The unit was bench tested to determine operational procedures as well as to verify the rupture pressure achieved by the manufacturer. Two disks were used to verify the burst pressure. Burst-away was at 23.8 psid and 24.7 psid, respectively. It was feasible to reduce the burst pressure to as low as 5 psid, which offered a possibility of improving the start transient.

(8) Solid Grain Squib Gas Generator (Holex, Inc.)

The solid grain squib gas generator operated from a source voltage of 28 dc which initiated squib firing and, in turn, ignited the solid grain. The solid charge was sized to pressurize the tank ullage volume (24 $in.^3$) at 70°F to 7 psia within 500 milliseconds. The maximum temperature of the resultant gases was 1800°F. However, expansion occurred through the tank solid gas generator inlet fitting. Therefore, the resultant temperature was limited to prevent local tank or propellant overheating. At the maximum operational temperature (140°F), the ullage volume was 32.8 $in.^3$, which could have been pressurized to 1430 psia approaching the burst pressure of the tank(2). At the minimum operational temperature (40°F), the ullage volume was 75 $in.^3$, which could have been pressurized to 680 psia and was sufficient to start the system. The gas generator, which was easily removed for replacement, was threaded into the tank boss. All components were fully compatible with the system propellant and the solid charge was sealed prior to its use, thereby preventing damage. The gas generator could be refurbished by replacing the charge cartridge.

(9) Relief Valve (James Pond and Clark, Inc.)

A pressure relief valve was provided on the gas pressurant side of the expulsion tank, upstream of the one-way burst disk. It prevented burst failure of the tankage or feed system caused by any unanticipated overpressurization of the system during both the starting transient and

(2) The pressure relief valve limits tank pressure to 900 psig maximum.

steady-state operation. A poppet was used in the valve for flow control and an O-ring for backup sealing, thereby preventing leakage during normal operation. A drain line was used to route the flow to a safe sump area in the workhorse system.

The valve was set to crack at 900 ± 45 psi and reseat at 855 ± 45 psi. These valve settings were selected to prevent system pressure from rising to system proof pressure while providing a margin for transient pressure fluctuations during development testing. All components of the valve were fully compatible with the propellant. Corrosion-resistant steel was used for all metallic parts and teflon for the sealing elements.

(10) Workhorse Bootstrap Tank

This major component was discussed in Section IV,A,3,c.

(11) Prototype Bootstrap Tank

This major component was discussed in Section IV,A,3,c.

(12) Squib Safety Valve (Prototype Subsystem Only)
(Pneu-Hydro Valve Corporation)

To ensure against leakage into the first-stage gas generator during storage, a N/C squib valve was placed immediately downstream of the tank in the prototype only.

The redundant squib valve had a plunger actuated from an electrical 28 vdc command signal, which sheared a metallic diaphragm. The command signal was transmitted to the squib valve simultaneously with that of the squib gas generator.

The squib valve components could be refurbished by replacing the charge cartridge and diaphragm inserts.

All fire current:	1.5 amp min
No fire current:	0.5 amp (1 min)
Bridgewire resistance:	0.90 to 15 ohm

e. Subsystem Packaging Description

The flightweight, first-stage packaging concept utilized the recessed gas end of the propellant storage tank for mounting the squib valve, filter, trim orifice, reaction chamber, and solid gas generator. The fill and drain valve would be mounted in the recessed propellant end of the tank and only the propellant feed line would be external to the tank envelope.

IV, A, Pressurization Subsystem (cont.)

The general procedure that was followed for the workhorse system assembly was to approximate the flightweight configuration without compromising either accessability or maintainability of the components. All components, other than the propellant feed-line instrumentation, were mounted on the gas-side tank flange. The first-stage gas generator was mounted on an adjustable bracket, which provided for alignment adjustment. The gas-side instrumentation, relief valve, and feedback line were installed into integral parts on the gas-side tank flange to provide the least expensive manufacturing and the most direct gas path. The solid gas generator was installed at the center of the flange in the deep recessed section to eliminate unnecessary projection and to provide a central distributing port for the hot gas to eliminate direct impingement of the hot gas on the tank shell.

The propellant feed-line instrumentation was line-mounted on the side of the tank while the fill and drain valve were attached to the propellant end of the tank. The feed system components were connected with replaceable hydraulic tubes. Standard AN flared fittings, except for Wiggins Type-DL nuts and sleeves, were used.

The entire assembly was mounted to a cradle at the tank flanges for ease in handling and testing. Figure No. 15 illustrates the first-stage workhorse subassembly packaging.

4. Development

a. Gas Generator Development

There were three categories of development testing activities associated with the hydrazine gas generators; first-stage gas generator development, second-stage gas generator development, and gas generator vortex valve throttling. The first-stage and second-stage gas generator development testing is discussed in this section, while the gas generator vortex valve throttling is discussed in Section IV,C,1,b.

After initial development, the first-stage gas generator was integrated into the workhorse system for continued testing. This development paced the workhorse system integration, while the second-stage gas generator development was primarily an independent program. The development testing program for each gas generator is presented in the ensuing discussions.

(1) First-Stage Gas Generator

The development program for this generator established the injector pressure drop as well as the injection distribution to provide maximum chamber pressure stability for minimum injector drop. Three

basic injector configurations were evaluated during the 28 tests that were performed. The number of injection elements was the primary variation in injector configurations. Figure No. 16 illustrates these configuration changes.

Table X summarizes the testing performed during this development program. The first (7 element) configuration required an excessive injector drop to achieve chamber pressure stability. Subsequent configurations were designed for increased flow distribution and uniformity as well as lower injector pressure drop. These configurations were development tested without the aid of a downstream receiver volume. Adding volume, such as that contained in the feedback path of the bootstrap tank, would have dampened the pressure perturbations (pressure attenuation) and effectively increased the stability margin (decreasing chamber pressure roughness).

Leakage was observed during development testing, and this led to the redesign of the single flange/seal joint. The vented, unplated, metal O-ring was replaced by a gas-filled, silver-plated, stainless steel O-ring. A drilled and tapped split-ring stiffener was added to provide support for the exhaust outlet flange. High temperature, A-286 bolts were used to secure the split-ring to the reaction chamber. Subsequent testing indicated that these changes minimized flange leakage although some relaxation of the bolts occurred.

The final first-stage gas generator configuration had an injector with 10 distribution elements and provided a pressure drop of 190 psid at rated flow (0.0315 lb/sec). The ΔP inj/P_c was approximately 27% for this configuration based upon flow bench data.

The catalyst bed was filled with 14-18 mesh (standard sieve size) Shell 405 catalyst and the bed pressure drop was approximately 10 psid.

The first-stage generator was acceptance tested by running an 800-sec duty cycle. The maximum chamber pressure roughness recorded during this test was $\pm$5%, which occurred during the middle of the run. Roughness was appreciably less at the end of the run, approximately $\pm$2% to $\pm$3%. This generator was transferred to the workhorse system and recorded combustion chamber pressure roughness was less than 1% during the system tests.

(2) Second-Stage Gas Generator

Similar in concept to the first-stage unit, the second-stage generator also was developed to achieve minimum injector pressure drop for maximized chamber pressure stability. The major difference between the units was their size. Second-stage maximum flow rate was 0.45 lb/sec.

ORIGINAL DESIGN SVL – 11239

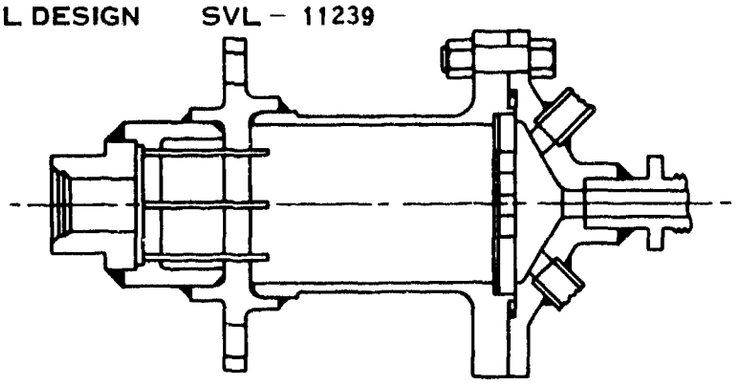

GENERATOR ON TEST

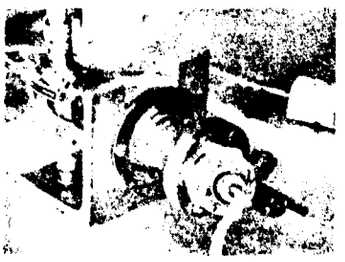

CONFIGURATION CHANGES		ΔP
CONF #1	7 TUBE	70
CONF #2	19 TUBE	200
CONF #3	13 TUBE	170
CONF #4	10 TUBE	190

FINAL ASSEMBLY SVSK 65585

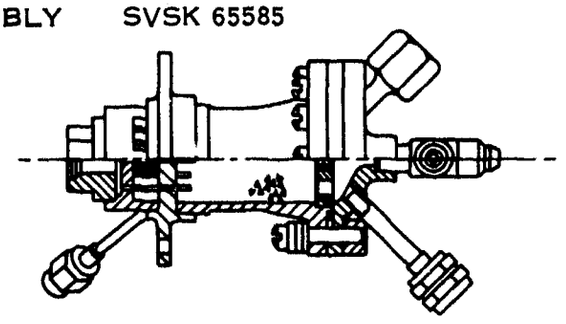

Figure 16. Development of First-Stage Gas Generator

TABLE X

SUMMARY OF FIRST-STAGE GAS GENERATOR DEVELOPMENT

INJECTOR S/N	DESCRIPTION OF INJECTOR	INJECTOR PRESSURE DROP PSID	NO. OF TESTS	TOTAL RUN TIME SEC.	PERFORMANCE	CONCLUSIONS
1	7 capillary tubes, I/D .018. Upstream restriction .031-in. dia.	45 (at rated flow of .0315 lb/sec.	2	20	Catalyst 20-30 mesh Pc= 670 psig, roughness ± 14%. Increased upstream restriction .024-in, Pc= 595 psig, roughness ±24%. Catalyst bed packed, causes high bed pressure drop.	$\Delta P_{inj}/Pc$ is too low (<5%) resulting in a coupling between chamber and the feed system. Catalyst mesh size too small evidenced by packing. Install wire restrictors into capillary tubes increasing ΔP_{inj}.
1	7 capillary tubes, I/D .018, wired. No upstream restriction.	185	1	~10	Catalyst 20-30 mesh. Chamber stability substantially increased, Pc=615 psig, roughness ± 8.7%.	Increased injector pressure drop. Reduced Pc roughness. $\Delta P_{inj}/Pc$ = 30% which is higher than desirable for gas generators.
1	7 capillary tubes I/D .018, wired upstream restriction added I/D= .043-in.	235	1	~10	Catalyst 20-30 mesh. Chamber stability increased. Pc=718 psig, roughness ± 1.5%.	Investigating the influence of added upstream restriction to stabilize Pc. Data indicates an improvement by sacrificing ΔP.
1	7 capillary tubes I/D .018, wired upstream restriction increased to I/D = .031-in.	250	1	~10	Catalyst 20-30 mesh. Chamber roughness increased slightly. Pc= 730 psig, roughness ± 4%.	Catalyst bed packing observed, influencing roughness data and orifice investigation. Upstream orifice appears not the most beneficial location for isolating the feed system from the chamber dynamics.
1	7 capillary tubes I/D .018, wired	185	3	30	Catalyst 14-20 mesh. Pc=560 psig, roughness ± 5.36% $\dot{\omega}$= .026 lb/sec. Load orifice not properly sized. Changed orifice size next two run to size load.	Increasing catalyst mesh size reduced the bed packing tendency and bed drop, orifice load size established by the third iteration. Decided to increase number of injection points on next injector to achieve lower ΔP.

TABLE X (cont.)

INJECTOR S/N	DESCRIPTION OF INJECTOR	INJECTOR PRESSURE DROP PSID	NO. OF TESTS	TOTAL RUN TIME SEC.	PERFORMANCE	CONCLUSIONS
2	19 capillary tubes I/D = .010, no upstream orifice.	90	1	108	Catalyst bed charged with 20-35 mesh around injector and 14-20 for residual. Pc=750 psia. Roughness ±15%. Initially very stable, became increasingly unstable with time. $\dot{W}$ = .028 lb/sec.	Catalyst bed found packed due to chamber roughness. still have a feed/system coupling stability problem. Increasing feed system pressure drop may help.
2	19 capillary tubes I/D = .010, upstream restriction .043-in.	90 plus	2	134	Catalyst bed rebuilt with 14-20 mesh. Pc=750 psig roughness ±20% $\dot{W}$ = .0315 lb/sec. Sinusoidal roughness start 2.3 seconds into the run. Second run, water-cooled injector to determine if instability was thermally initiated. Pc = 720 psig, roughness ±22% $\dot{W}$ = .0315 lb/sec.	Increasing pressure drop ahead of capillary tubes showed little or no benefit. Instability is not thermally initiated through the injector but still appears to be a feed system coupling. Blocking off some of the 19 capillary feed tubes should decouple the two systems.
2	19 capillary tubes 6 tubes blocked I/D = .010, no upstream restriction	~200	2	139	Catalyst 14-20 mesh. At Pc = 530 psig, roughness ±2.83% $\dot{W}$ = .0235 lb/sec (first test). Second test run to accumulate time on generator, Pc = 700 psig, roughness ± 2.8%, $\dot{W}$ = .0315 lb/sec.	This configuration is extremely stable over a wide Pc variation (as low as Pc = 200 psig' However ΔP_{inj} is too high, $\Delta P_{inj}/Pc > 25\%$. Try to decrease by optimizing the number of injection elements.
3	19 capillary tubes 6 tubes blocked	170	2	100	Pc = 780 psig, roughness ± 15%. Pc = 275 psig, roughness ± 10%.	This configuration appears fairly stable, not as stable as the 200 psid injector. Note the difference between the two injectors. The I/D tolerance of injector capillary tubing is sufficient to result in this change, in otherwise identical injectors.
3	19 capillary tubes 6 tubes blocked	170	2	207	Catalyst 14-20 mesh Pc = 740 psig, roughness ±8% Suspected leakage during this run but none detected after a check.	Rerun to accumulate time on the generator. Leakage could start an instability.

TABLE X (cont.)

INJECTOR S/N	DESCRIPTION OF INJECTOR	INJECTOR PRESSURE DROP PSID	NO. OF TESTS	TOTAL RUN TIME SEC.	PERFORMANCE	CONCLUSIONS
3	19 capillary tubes 6 tubes blocked Cleaned entrances & exits of capillary tubes.	156	1	85	Catalyst 14-20 mesh Pc = 580 psig, roughness ± 7%. Flange bolts yielded and leaked, bed packed.	Injector drop decreased after cleaning operation. Suspected flange leakage was our major problem. Bolts retorqued. Rebuild generator and retest.
3	19 capillary tubes 6 tubes blocked	156	1	95	Catalyst bed 14-20 mesh recharged. Stable operation Pc = 720 psig, roughness ± 4.4%. Flange leakage (small) observed.	Flange leakage confirmed as a problem. But the amount is difficult to determine. Run a longer test.
3	19 capillary tubes 6 tubes blocked	156	1	522	Catalyst bed 14-20 mesh Reran same configuration, tighten flange bolts. Pc=710 psig, roughness ± 5.6%. Occasional spike (peak to peak) ± 10%. Maximum injector temperature 280°F, Tc=1490 °F.	With the leakage controlled, the generator ran very stable. These tests established that 13 tubes with 156 psid would run generator stable. Increasing distribution definitely influence generator stability. This test completed development of the injectors. A new flange seal, stiffener and high temperature bolts would be adapted to the final workhorse configuration.
4	13 capillary tubes 2 tubes blocked	169	1	47	Catalyst bed 1 -18 mesh. Pc=630 psig, roughness ±10% ΔP across bed = 20 psid, Tc = 1470°F. Showed signs of feed system instability possibly causing bed packing. Flow rate not recorded.	Generator was disassembled and checked for bed packing. Catalyst did not pack; however. it was removed an repacked. Rerun test.
4	13 capillary tubes 2 tubes blocked	169	1	44	Catalyst bed 14-18 mesh Pc=665 psig, roughness ± 4.5% ΔP across bed = 15 psid, Tc = 1460°F $\dot{W}$ = .0326 lb/sec.	Generator dynamics still appear as though some feed system coupling is present. Rerun test without rebuilding the catalyst bed.
4	13 capillary tubes 2 tubes blocked	169	1	31	Catalyst bed 14-18 mesh Pc = 715 psig, roughness ± 7% ΔP across bed = 5 psid, Tc = 1435°F $\dot{W}$ = .0314 lb/sec.	Rerun of same configuration still indicating feed system coupling. Load orifice sizing changed to establish correct Pc & $\dot{W}$. (Pc=682-707 psia & $\dot{W}$ = .0283-.0315 lb/sec).

TABLE X (cont.)

INJECTOR S/N	DESCRIPTION OF INJECTOR	INJECTOR PRESSURE DROP PSID	NO. OF TESTS	TOTAL RUN TIME SEC.	PERFORMANCE	CONCLUSIONS
4	13 capillary tubes 2 tubes blocked	169	1	80	Catalyst bed 14-18 mesh at 14 sec: Pc = 590 psig roughness ± 12%, $\dot{\omega}$ = .0258 lb/sec, Tc = 1310°F at 78 seconds: Pc=680 psig, roughness ± 16% $\dot{\omega}$ = .0303 lb/sec, Tc = 1455°F ΔP across bed = 10 psid.	Generator run once again for longer period to confirm suspicion of feed system coupling. With time, the chamber pressure roughness increases. This confirms feed system coupling; i.e., insufficient injector pressure drop. Individual pressure transducer readings indicate that the injector pressure drop during a firing at rated flow is approximately 140 psid compared to 169 psid which is a water flow calibration equivalent. This indicates more ΔP is required.
4	13 capillary tubes 3 tubes blocked	196	1	25	Catalyst bed repacked with 14-18 mesh. Stable operation. Pc=690 psig, roughness ±2% $\dot{\omega}$ = .0303 lb/sec. Tc = 1450 °F. ΔP across bed = 10 psid	Generator ran extremely stable with the increased injector pressure drop. Pressure transducer readings indicate approximately 160 psid across injector. Generator ready for acceptance run.
4	13 capillary tubes 3 tubes blocked	196	1	825	Catalyst bed 14-18 mesh. Stable operation through run. Pc = 700 psig, max roughness ± 5%, $\dot{\omega}$ = .031 lb/sec, Tc = 1500°F (max) ΔP across bed = 10 psid.	Development completed, generator acceptable for workhorse system integration.

IV, A, Pressurization Subsystem (cont.)

It was designed with a larger bed loading (G = 0.04 lb/sec-in.^{2}) than the first-stage unit (G = 0.03 lb/sec-in.^{2}). This increased bed loading served to reduce the amount of catalyst required; however, it did increase the bed drop. The resultant catalyst bed configuration used in the second-stage gas generator was a multi-layered combination of 20-30 mesh, 14-18 mesh, and 1/8 x 1/8 pellets of Shell 405, respectively, from the injector to the exit port. This bed configuration best satisfied the development criteria by minimizing bed drop and maximizing stability while at the same time providing the desired ammonia dissociation of 80%. Aside from several catalyst bed configuration changes, the only two other development changes were incorporated into the basic design. These were a higher pressure drop injector and a stiffened exhaust outlet flange (plus silver-plated, gas-filled O-rings and high temperature bolts). The development changes and final configuration are shown on Figure No. 17. The testing performed during this development program is summarized on Table XI.

The chamber pressure stability of the generator with the mixed catalyst bed consistently demonstrated pressure roughness of less than $\pm$1%.

b. Workhorse System

The first-stage workhorse pressurization subsystem was a totally self-contained unit with all the necessary components mounted to the tank. Integral instrumentation ports were provided for measuring critical parameters. A schematic of this first-stage workhorse system was shown schematically as Figure No. 4. Figures No. 18 and No. 19 show the fully instrumented system installed in the test stand. This workhorse system was necessarily heavy. It weighed approximately 125 lb dry (no propellant load) and was provided with lifting eyes on each end of the tank flanges to ease handling problems. Stabilizing feet were provided to allow horizontal anchoring to the test installation. The mounting feet also cradle the tank and allowed for removal as well as reinstallation of the two end flanges without any need for other supports. All of the components and instrumentation ports offered easy access for any necessary maintenance.

The system had a built-in natural (seeks and finds) steady-state operating point. This point was difficult to determine physically because it was extremely dependent upon such things as the orifice (exit) load size and the flow coefficient of the load orifice. Calculations were performed and a set of orifices selected for the initial workhorse system tests. Figure No. 20 is a schematic showing the values of these orifice sizes and flow rates along with the pressure estimates throughout the system. These values were used as "guide posts" for the initial testing. Changes were made to achieve desired system pressure levels. Figure No. 21 is a plot of liquid propellant pressure and gas generator chamber pressure in relationship to total system

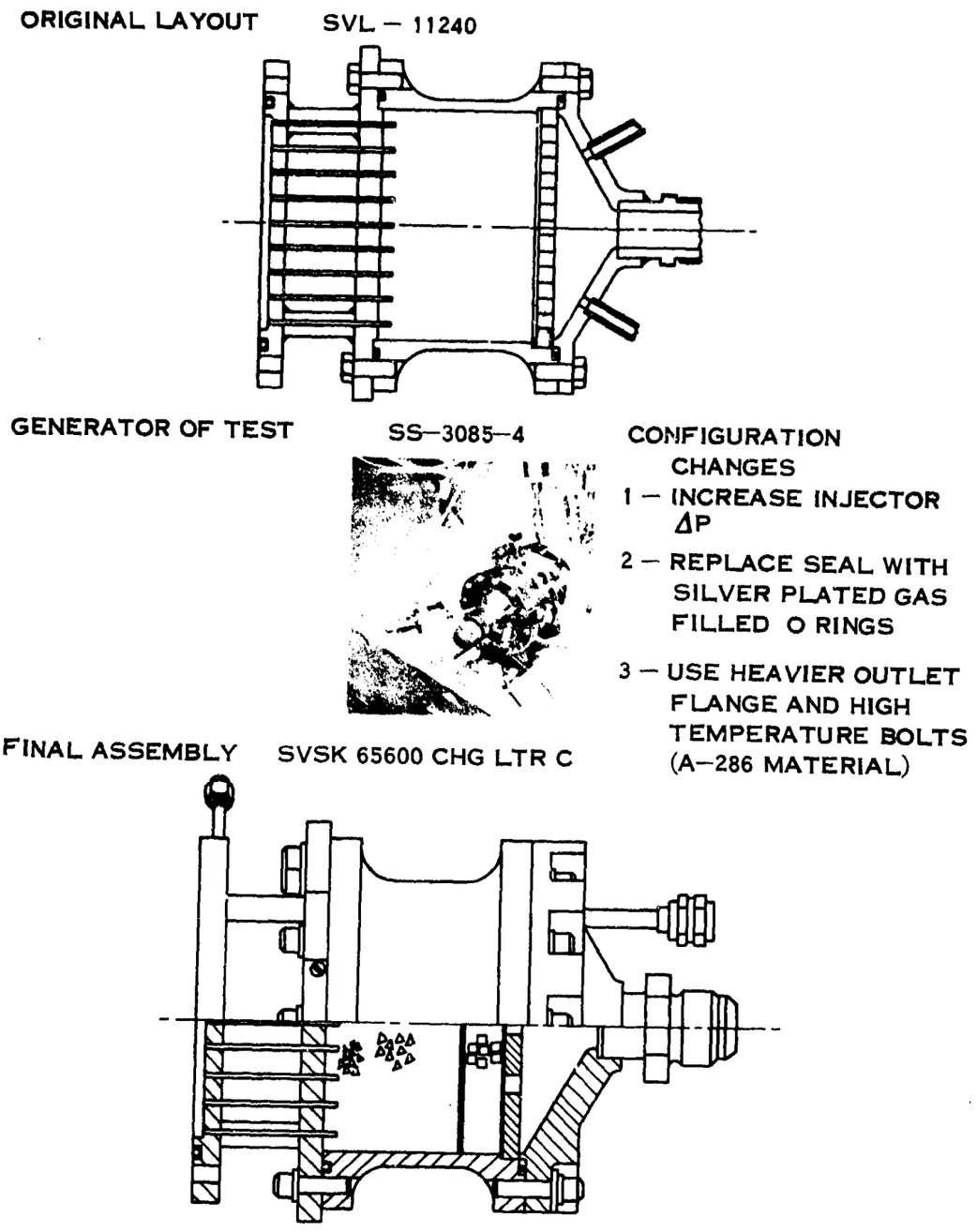

Figure 17. Development of Second-Stage Gas Generator

TABLE XI

SUMMARY OF SECOND-STAGE GAS GENERATOR DEVELOPMENT

INJECTOR S/N	DESCRIPTION OF INJECTOR	INJECTOR PRESSURE DROP PSID AT RATED FLOW	NO. OF TESTS	TOTAL RUN TIME SEC.	PERFORMANCE	CONCLUSIONS
A	61 capillary tubes I/D = .022-in.	53	8	55	Catalyst bed 20-30 mesh runs were initially stable but with each additional start, the generator became progressively unstable. Pc=400 psig, roughness ±1% at start increasing to ±12%.	Test stand pressure drop approximately 200 psid at rated flow ($\dot{\omega}$ =.45 lb/sec) resulted in initial injector pressure drop as high as 600 psid which is approximately 3.4 times rated flow. This caused hard starts which packed the catalyst bed. Changed test procedure, start at low tank pressure, increase to rated conditions. Reduce bed drop by changing catalyst size.
1	61 capillary tubes I/D = .022-in.	53	4	40	Catalyst bed 20-35 mesh, 14-20 mesh, 1/8 x 1/8 pellets. Pc=390 psig, roughness less than 1%. Extremely stable. $\dot{\omega}$ = 0.42 lb/sec. Tc=1300°F. The flow rate and resulting Pc were progressively increased by raising tank (supply) pressure. The 3 gpm flowmeter saturated after the second run.	Generator ran extremely stable during these calibration runs. Chamber exhaust temperature consistently reached 80% NH_3 dissociation point. layered catalyst bed stabilizes chamber pressure. Exit orifice load size requires a change to match Pc and $\dot{\omega}$.
1	61 capillary tubes I/D = .022-in.	53	6	39	Catalyst bed 20-35 mesh, 14-20 mesh, & 1/8-in. x 1/8-in. pellets. Generator performed extremely stable. Pc=450 psig, roughness $<$ 1% $\dot{\omega}$ = .45 lb/sec. Tc=1360°F P_{inj} = 525 psig. Exit orifice (final) .406-in. dia.	Exit orifice reduction matched Pc & $\dot{\omega}$. Generator ready for vortex throttle testing. Development of this generator essentially completed.
1	61 capillary tubes I/D = .022-in.	53	1	10	Catalyst bed (same as previous run). Unit run with vortex throttle valve - all liquid flow. (steady-state) Pc=370 psig, roughness ±3% P_{inj} = 480 psig, P_{inlet} = 510 psig, $\dot{\omega}$ = .371 lb/sec, Tc=1260°F	Data indicated that Pc roughness with the vortex valve installed was larger. The generator was hard started which logically accounts for the increased instability; i.e., bed packing.
1	61 capillary tubes I/D = .022-in.	53	4	107	Catalyst bed (three layers as previously outlined). Attempted throttling by continually increasing supply pressure, but did not achieve any.	GN_2 orifice apparently choked and must be increased to raise GN_2 flow rate.
1	61 capillary tubes I/D = .022-in.	53	2	30	Catalyst bed (same as previous run). First successful run to demonstrate throttling with the vortex valve.	Injector pressure drop increases with throttling (adding GN_2) resulting in more stable operation.
	61 capillary tubes I/D = .022-in.	53	1	42	Catalyst bed (same as previous run) Achieve a 60% and 95% throttling capability. P_{inj} psig / Pc psig / $\dot{\omega}$ lb/sec 480 / 325 / .35 325 / 210 / .182 350 / 125 / .028	The diffusion of hydrazine and nitrogen through the 61 tube injector appears to have no adverse effect on chamber pressure roughness. Generator stability increased with throttling. Bed packing observed upon disassembl

TABLE XI (cont.)

INJECTOR S/N	DESCRIPTION OF INJECTOR	INJECTOR PRESSURE DROP PSID AT RATED FLOW	NO. OF TESTS	TOTAL RUN TIME SEC.	PERFORMANCE	CONCLUSIONS
2	61 capillary tubes I/D = .019-in.				Based upon the results of vortex throttle testing, an increased injector pressure drop was decided upon for the next injector.	This particular injector was scrapped out during fabrication.
3	61 capillary tubes I/D = .019-in.	140			Pressure drop with water flow at $\dot{\omega}$ = .45 lb/sec was too high, indicating large entrance & exit losses.	Injector tube entrances and exits were deburred and cleaned, reducing the pressure drop at rated flow to 115 psid.
3	61 capillary tubes I/D = .019-in.	115	1	70	Catalyst bed 20-35 mesh, 14-20 mesh and 1/8-in. x 1/8-in. pellets. Generator went unstable after 60 sec of operation. Flange leakage (at ambient temperatures) increased considerably. Flange bolts at high temperature and yielded and lost their torque. Pc=425 psig, roughness ±6% $\dot{\omega}$ = .456 lb/sec, Tc = 1440°F. Pressure oscillations ~9.1 cps.	Generator operated stable until flange bolts yielded and leakage occurred. Leakage caused a sudden loss in chamber pressure and an accompanying increase in flow rate - result, unstable operation. Replacing the bolts with high temperature material should reduce flange leakage. A-286 material selected. Catalyst bed did not pack.
	61 capillary tubes I/D = .019-in.	115	1	60	Catalyst bed rebuilt to same configuration as above. Generator ran extremely stable throughout test. Flange leakage less at end of run. Pc=425 psig, roughness $<$ ±1% $\dot{\omega}$ = .475 lb/sec, Tc=1400°F P_{inj} = 510 psig, P_{bed} = 500 psig.	Leakage solved by high temperature bolts; generator stable. Silver-plated gas-filled O-rings and a stiffened exhaust flange will also be incorporated to ensure leakage prevention, particularly for longer runs.
	61 capillary tubes I/D = .019-in.	115	1	45	Catalyst bed configuration: 20-30 mesh, 14-18 mesh 1/8-in. x 1/8-in. pellets. Exit orifice decreased slightly from .406-in. to .390-in. dia. Pc = 450 psig roughness $<$ ±1% $\dot{\omega}$ = .41 lb/sec, Tc=1450°F, P_{inj} = 550 psig, P_{bed} = 470 psig, bed drop = 20 psid.	Pre-acceptance test run. Generator extremely stable. No apparent flange leakage. The change in exit orifice sizing helped to match the loading requirements. Pc = 435-494 psia $\dot{\omega}$ = .326-.448 lb/sec Run acceptance test - fuel tank capacity limited to approximately 40 pounds of N_2H_4.
3	61 capillary tubes I/D = .019-in.	115	1	90	Catalyst bed same as above. Results after 40 seconds: P_{inj} = 625 psig $\dot{\omega}$ = .425 lb/sec, P_{bed} = 510 psig, Tc = 1450°F Pc = 490 psig, roughness $<$ ±1% ΔP_{bed} drop = 20 psid Results after 90 sec: P_{inj} = 640 psig $\dot{\omega}$ = .427 lb/sec, P_{bed} = 525 psig, Tc = 1470°F Pc = 500 psig, roughness $<$ ±1%, ΔP_{bed} drop = 25 psid	Generator appeared extremely stable throughout run. Unit met its acceptance criteria. No leakage observed. This completes the testing and development on this workhorse unit.

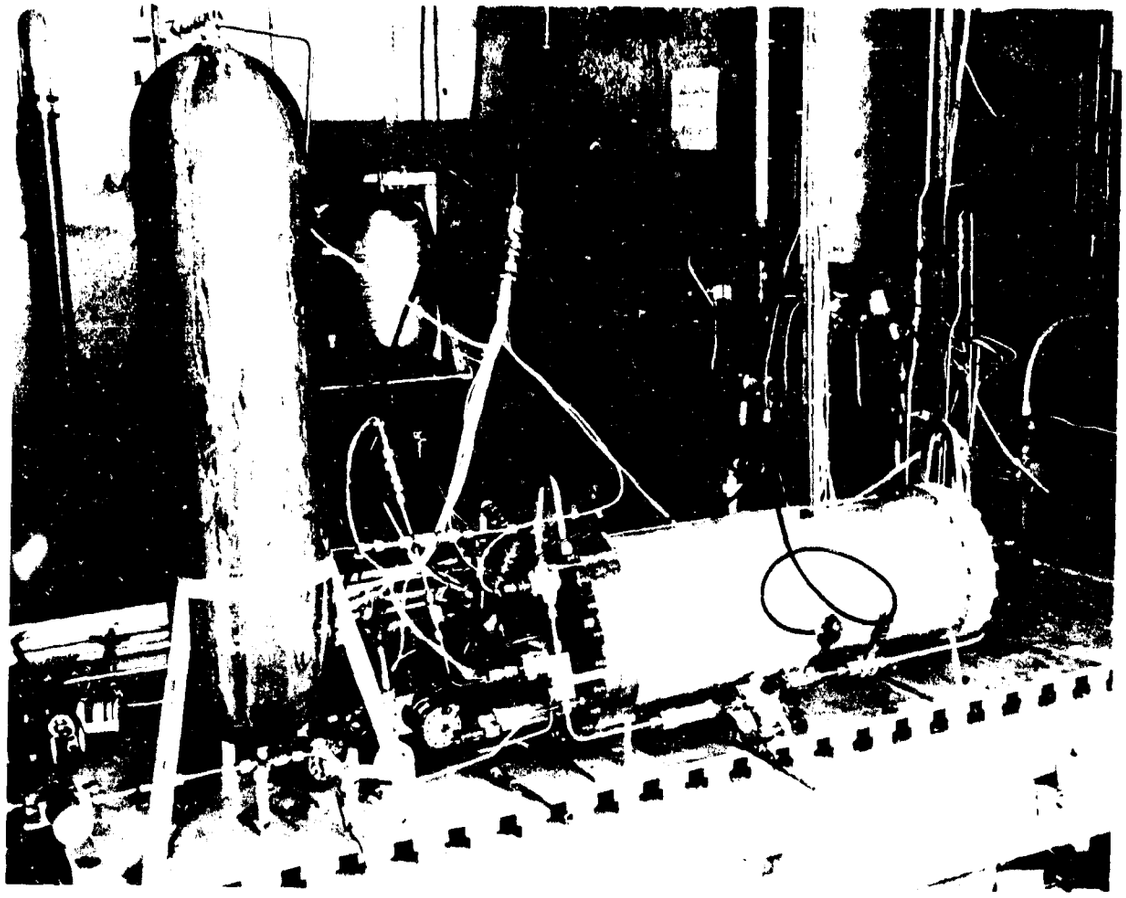

Figure 18. Hamilton Standard Test Set-Up for First-Stage Gas Generator Workhorse System

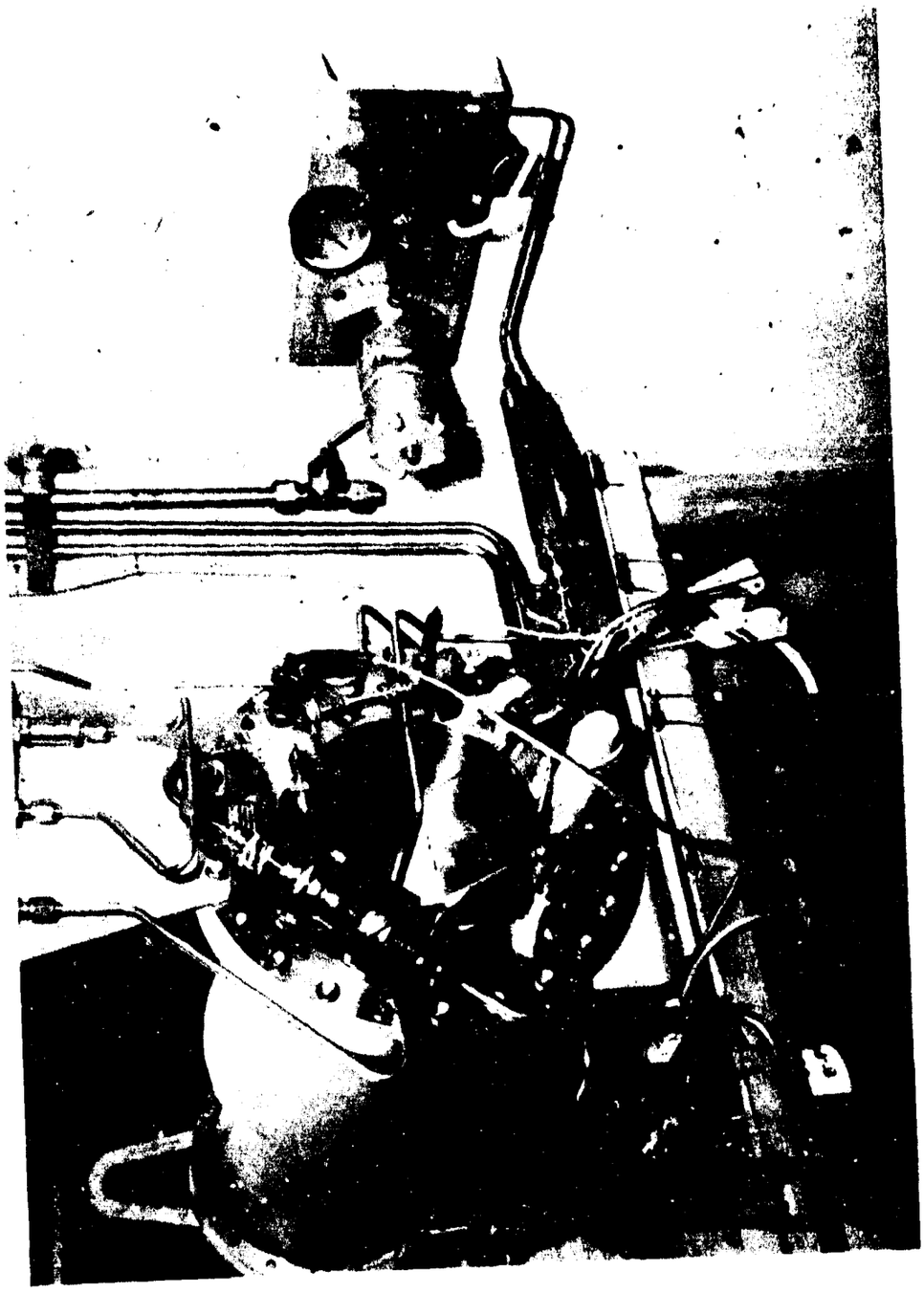

Figure 19. Integrated Subsystems Testing - Test Stand

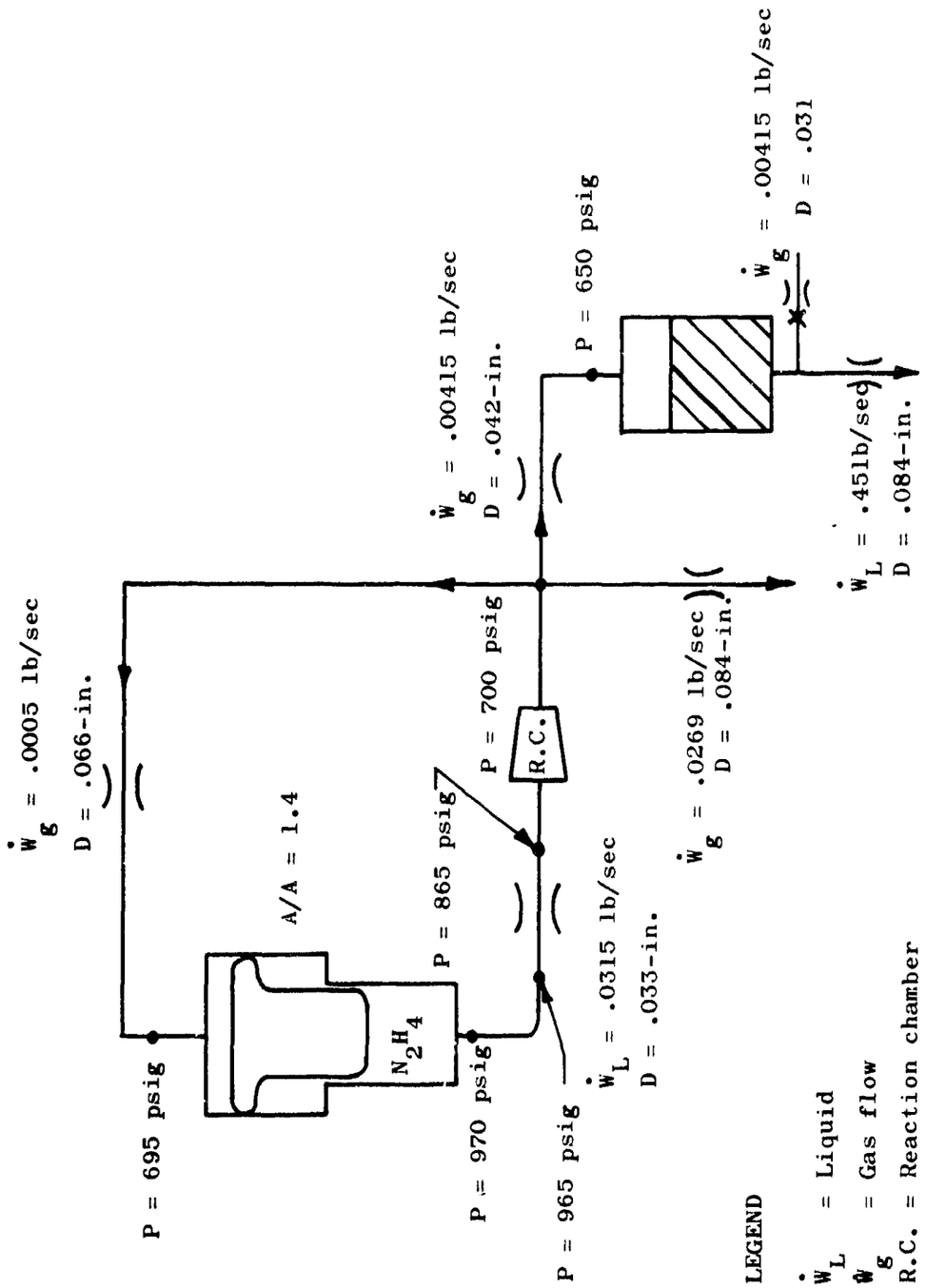

Figure 20. Workhorse System Orifice Sizing

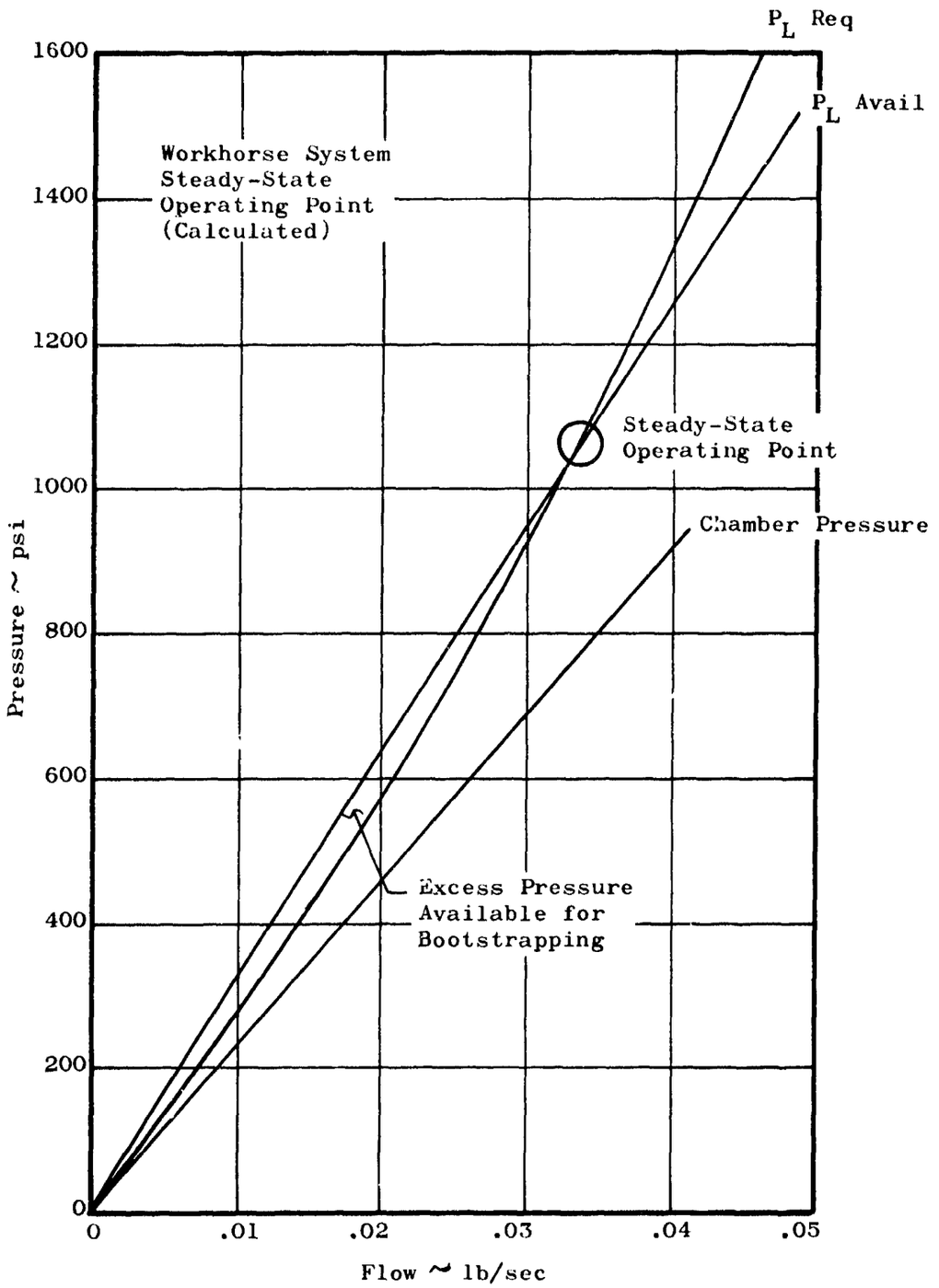

Figure 21. Calculated Equilibrium Performance for Workhorse System

IV, A, Pressurization Subsystem (cont.)

flow rate. This curve demonstrates that the unit would seek a natural steady-state operating point. In effect, this is a built-in limiter. The liquid flow curve is plotted to show available output pressure as a function of the hydraulic characteristics of the line components. The gas flow curve was obtained by relating the output pressure to the difference between the liquid flow rate and the feedback gas flow rate. The steady-state operating point occurs where the required liquid pressure is exactly the same as the available liquid pressure. If there is excess pressure (P_L available greater than P_L required), it will ensure that the system will bootstrap itself up to the desired operating point. For the case studied, the curve shows a steady-state chamber operating pressure of 770 psia at a flow rate of 0.0338 lb/sec. Pressure switches and a solenoid shut-off valve constituted the simple "bang-bang" control system used in this evaluation to guarantee positive limit control in the event of a malfunction during the testing sequences.

(1) Instrumentation

The workhorse system was fully-instrumented to evaluate all necessary performance levels, system pressure, and stability levels during the starting transients and steady-state operations.

(2) Testing

The first-stage gas generator and bootstrap tank, along with the selected components, were successfully integrated to form a first-stage workhorse system. Testing demonstrated that the system will successfully bootstrap and sustain stable gas generation for a full mission period.

The first testing performed prior to system build-up was the determination of workhorse tank expulsion efficiency. This test set-up is shown on Figure No. 22. Running the expulsion efficiency test provided the opportunity to check out the dynamic seals. The results from the initial testing were most favorable. There was no detectable leakage even with only 10 psid applied across each seal. The tank had a usable propellant capacity in excess of 20 lb and an expulsion efficiency of approximately 98%.

Twenty-three first-stage workhorse system tests were conducted during the program. The first eight of these tests were accomplished at the Hamilton Standard facility. The remaining 15 tests were conducted at the Aerojet-General facility.

(a) Hamilton Standard Testing

The workhorse system was assembled with the first-stage workhorse gas generator. It was tested to determine system transient and steady-state operating characteristics. The initial start

Figure 22. Expulsion Efficiency Testing

IV, A, Pressurization Subsystem (cont.)

signal for the first few tests was supplied by a GN_2 source rather than a solid gas generation. The output load was sized to provide a simulation of the fluidic demand and tank pressurization. (Figure No. 18 shows this test set-up.) In subsequent tests, the tank pressurization simulation was eliminated and replaced by a single fluidic orifice load simulation. The reduced test results are summarized on Table XII.

The workhorse system was designed to deliver a gas flow rate of 0.0315 lb/sec at 700 psia. Only a small portion of this flow is feedback for bootstrap operation. Approximately two-thirds of the flow was designed to feed the fluidic elements and the remainder was used for second-stage hydrazine tank pressurization.

The initial test runs were confined to short (under 2 min) durations for the purpose of determining load orifice sizes. Depending upon the initial propellant loading in the tank, the transient start-up times to reach maximum system pressure (700 psia) varied. With a full load of propellant, the system took approximately 70 sec to reach 700 psia. The transient start-up also is influenced by the initial start pressurization provided by the squib gas generator. The test previously cited achieved a start pressurization of 140 psig provided by the squib gas generator. However, this could be raised to a higher value depending upon the size of the solid grain. With this low start pressurization (140 psig), the system began to bootstrap within 2 sec. Once the orifice sizes were selected, the system was fired for acceptance and allowed to run for approximately 5 min before shutdown. Reaction chamber pressure roughness was less than $\pm 1\%$ over the entire test period. The control system was an essentially open-loop run with orifice flow limiting used to attain the proper chamber pressure and flow rate. During the acceptance test, the chamber pressure reached 750 psig at a flow rate of 0.030 lb/sec.

The solid grain squib gas generator (supplied by Holex) was assembled and test fired into a simulated ullage to obtain some sizing data for the full workhorse system simulation. This grain is relatively slow burning; 6-in. in approximately 23 sec. Hamilton Standard used an approximately 1/2-in. grain to achieve the 140 psig start pressurization. The simulation rig used for grain sizing consisted of a long length of small diameter tubing which generated both the equivalent surface area and gas-side ullage volume of the workhorse tank assembly.

(b) Aerojet-General Testing

Fifteen tests were conducted at Aerojet-General with the first-stage pressurization system. Nine of these tests were accomplished to check out the first-stage pressurization system incorporating the workhorse bootstrap tank at the operating levels identified on Figure No. 20.

TABLE XII

SUMMARY OF FIRST-STAGE WORKHORSE SYSTEM DEVELOPMENT

TEST SERIES NUMBER	DESCRIPTION OF LOAD	TOTAL RUN TIME SEC.	APPROX. FUEL LOAD % CAPACITY	INITIAL PRESSURIZATION PSIG	TIME TO BOOT STRAP SEC.	PERFORMANCE	CONCLUSIONS
1	Gas orifice to simulate fluidic load. 8 gal H_2O tank to simulate 2nd stage load.	10.59	18	~250	~3.5	At 4 seconds: Gas side press. = 260 psig. Liquid side press. = 362 psig Liquid above drop orifice 280 psig. Chamber press = 260 psig; 2nd stage load press. = 0 psig. Gas side temp. = 60°F. Chamber temp. = 1150°F At 10 seconds: P_{GS} = 280 psig, T_{SG} = 60°F, P_{LS} = 382 psig, P_{LDO} = 310 psig, Pc = 290 psig, Tc = 1310°F, P_{2ND} = 20 psig, $\dot{W}$ = N/R	Initial test demonstrated bootstrap feasibility - fuel load was approximately 18% of total capacity leaving a large gas ullage volume to be filled with feedback flow. The two loads, Fluidic orifice = .042-in. 2nd stage orif. = .082-in. take most of the gas flow produced, leaving little for ullage pressurization. System was very stable, less than 1% Pc roughness. Increase initial pressurization.
2	Same as Test 1	10.69	10	~360	~3.0	At 4 seconds: P_{GS} = 350 psig T_{GS} = 50°F, P_{LS} = 475 psig, P_{LDO} = 380 psig, Pc = 350 psig, Tc = 1310°F, P_{2ND} = 15 psig At 10 seconds: P_{GS} = 370 psig T_{GS} = 50°F P_{LS} = 505 psig P_{LDO} = 400 psig Pc = 380 psig Tc = 1390°F P_{2ND} = 25 psig $\dot{W}$ = N/R	Increasing the initial pressurization did improve the bootstrapping time. Flow rate was not recorded, prevented checking load sizing. System was extremely stable. Rerun test with new flowmeter, add more propellant and run longer duration.
3	Same as Test 1	25.4	~25	~350	3.0	At 4 seconds: P_{GS} = 400 psig T_{GS} = 70°F P_{LS} = 535 psig P_{LDO} = 405 psig Pc = 370 psig Tc = 1280°F P_{2ND} = 65 psig $\dot{W}$ = .021 lb/sec At 20 seconds: P_{GS} = 495 psig T_{GS} = 110°F P_{LS} = 665 psig P_{LDO} = 505 psig Pc = 460 psig Tc = 1400°F $\dot{W}$ = .025 lb/sec	System response is gradually improving with each test. Major difference is the reduced gas side ullage. Reload with more fuel and run a longer test.

TABLE XII (cont.)

TEST SERIES NUMBER	DESCRIPTION OF LOAD	TOTAL RUN TIME SEC.	APPROX. FUEL LOAD % CAPACITY	INITIAL PRESSURIZATION PSIG	TIME TO BOOT STRAP SEC	PERFORMANCE	CONCLUSIONS
4	Same as Test Series No. 1	100	~40	320	4.0	At 10 seconds: P_{GS} = 360 psig T_{GS} = 55°F P_{LS} = 490 psig P_{LDO} = 465 psig Pc = 360 psig Tc = 1050°F P_{2ND} = 105 psig [illegible] = N/R At 70 seconds: P_{GS} = 710 psig T_{GS} = 66°F P_{LS} = 975 psig P_{LDO} = 950 psig Pc = 700 psig Tc = 1486°F P_{2ND} = 440 psig At 80 seconds, the pressure switch started to shut down the system. At 100 seconds: P_{GS} = 750 psig T_{GS} = 70°F P_{LS} = 1035 psig P_{LDO} = 1010 psig Pc = 740 psig Tc = 1495°F P_{2ND} = 455 psig [illegible] = N/R	System successfully bootstrapped and came up to system pressure (682-707 psia). Pressure switch set to shut down at 740 psia and back on at 680 psig. The pressure switch is located close to the fluidic load orifice. The pressure decays vary rapidly because there is no appreciable volume. Switching becomes oscillatory at 3 cps if allowed to continue but controls the system pressure. Without flow rate, there was no check of load orifice sizing. 2nd stage simulated load probably not sized correctly.
5	Same as Test Series No. 1	34	~40	350	3.0	Firing was terminated because of leakage at one of hot gas fitting. 1st stage gas generator S/N 4 injector used for this test.	Post-firing investigation showed loose "B" nut connections. These were retightened while still hot.
6	Single gas orifice load ~ .086-in. dia.	85	~50	350	2.5	Pc reached 640 psig at shutdown. [illegible] = .030 lb/sec	Several firings were conducted to determine the proper load orifice in order to reach system pressure, without actuating the pressure switch (740 psig). Started with a .094-in. orifice and worked down to .086-in. dia.

TABLE XII (cont.)

TEST SERIES NUMBER	DESCRIPTION OF LOAD	TOTAL RUN TIME SEC.	APPROX. FUEL LOAD % CAPACITY	INITIAL PRESSURI-ZATION PSIG	TIME TO BOOT STRAP SEC.	PERFORMANCE	CONCLUSIONS
7	Same as Test Series No. 6	300	~60	350	~2.0	Pc reached 700 psig in approximately 90 sec. Slowly increased to Pc = 740 psig and was shut down when the power switch started controlling. ṁ = .030 lb/sec. Steady-state.	This test was conducted to allow the system to achieve steady-state operation. Load orifice sizing based upon this test is satisfactory to demonstrate system capability. Acceptance testing shall be conducted using this load configuration.
8	Same as Test Series No. 6. First-stage gas generator S/N 4 injector used.	~300	100	-	~1.0	Squib gas generator fired to initially pressurize the system. Pressurization reached max. of 140 psig in 2.5 sec. Bootstrap operation occurred 1.0 sec later. At 10 seconds: P_{GS} = 250 psig T_{GS} = 64°F P_{LS} = 360 psig P_{LDO} = 345 psig Pc = 260 psig Tc = 525°F At 100 seconds: P_{GS} = 710 psig T_{GS} = 75°F P_{LS} = 1020 psig P_{LDO} = 998 psig Pc = 730 psig Tc = 1285°F At 200 seconds: P_{GS} = 720 psig T_{GS} = 84°F P_{LS} = 1050 psig P_{LDO} = 1028 psig Pc = 740 psig Tc = 1340°F At 220 seconds, the system's control (pressure switch) started actuating. The control system was by-passed so that the system could proceed on a steady-state basis. System shut-down at 300 sec.	With a minimum gas side ullage of approximately 35-in.^{3}, the system reached rated pressure in 50 sec. This was achieved with an initial gas side pressurization of 140 psig. Transient start performance could be further improved by increasing the initial pressurization. Chamber pressure was extremely stable. The addition of a pressurized volume (gas side of tank) helps to dampen out the pressure oscillations created in the generator. This run constituted acceptance of the workhorse system. It met the functional requirement established by this program. Continued development testing will be conducted at Aerojet in preparation for system integration.

IV, A, Pressurization Subsystem (cont.)

The remaining six tests incorporated the prototype bootstrap tank and operated at a pressure level reduced to 400 psi output pressure. These tests were conducted to provide a hot gas source for subsequent system integration tests (see Section IV,E for discussion).

Three of the nine workhorse system checkout tests included the expulsion of water from the tank which simulated the second-stage hydrazine supply. The remaining tests were made with a single sonic orifice load simulation. The objectives of these tests were to check out the test set-up and instrumentation, develop test procedures, and determine the characteristics of the system. The primary quantitative objectives were to determine flow/pressure balance criteria for use as a "norm" during subsequent fluidic component testing. In addition, test data were obtained to assist in analytical predictions of the bootstrap loop performance. These tests are summarized on Table XIII, while a representative sample of testing is detailed below.

1 Test Description

A schematic of the basic first-stage system test set-up and instrumentation is shown as Figure No. 23. The physical location of the components is shown on Figures No. 19 and No. 24. Each test was initiated by external nitrogen pressurization of the bootstrap tank. The nitrogen supply pressure was pre-set to 700 psia. To begin a test, the nitrogen supply valve was opened just long enough to pressurize the ullage behind the piston to approximately 500 psia. An orifice in the nitrogen supply line was sized to provide a 3-sec to 4-sec duration pressure rise to 500 psia, which prevented hard starting of the gas generator. Two pressure switches were utilized in the system for output control. These switches controlled the position of the "run" solenoid valve (ROV-4). Pressure switch No. 2 limited the expulsion tank pressure to approximately 650 psia. Pressure switch No. 1 limited the feedback pressure to the bootstrap tank to approximately 750 psia.

2 Tests SP-16A-101 and -102

The first test was an attempt to duplicate the final test conducted at Hamilton Standard. A single sonic orifice (0.086-in. diameter) load simulation was used. The bootstrap tank was pressurized to 520 psia in 3.85 sec. All pressures rose simultaneously. Bootstrap operation occurred approximately 1 sec after the nitrogen supply valve was closed. The generator output pressure rose to 90% of its maximum value within 13 sec at an average rate of 12.3 psi/sec. The pressure exceeded the feedback line pressure switch setting (750 psia) at 38 sec. The test was terminated at 43 sec.

TABLE XIII

FIRST-STAGE PRESSURIZATION SUBSYSTEM TEST SUMMARY

TEST NUMBER	DATE	DURATION SEC.	OVERBOARD LOAD ORIFICE DIA.-IN.	EQUIL. PRESS. PO_2-psia	TIME TO BOOTSTRAP SEC	START PRESSURE PSIA	TIME TO 90% PO_2 SEC	AVG. RATE OF RISE PSIA/SEC	OUTPUT TEMP. TO_2-°F	FLOW RATE MAX LB/SEC	BOOTSTRAP TANK ULLG. IN³	REMARKS
SP 16A-101	4-17-67	43	.086	>750	1.0	515	13	12.3	1450	N/A	35	System as delivered - 0.034 dia liquid trim orifice
102	4-18-67	50	.086	>750	1.0	540	15	9.4	1450	.0317	70	
103	4-18-67	110	.089	630	3.5	485	18	5.7	1450	.028	35	
104	4-19-67	112	-	>750	3.0	525	13	19.6	1100	0→.033	35	.089-in. dia orifice - Direct to tank-tank pressure = 640 ± 15 psia
105	4-21-67	27	.089	>750	1.0	505	10.6	16.0	1380	.036	35	No trim orifice
106	4-26-67	43	.067	<300	---	500	---	---	---	---	35	Tank vent open - 0.098 orifice to tank
107	4-26-67	103	.067	660	2.4	505	32	4.7	1420	0→.029	35	0.098-in. dia orifice to tank-tank pressure = 640 ± 10 psia
108	4-27-67	62	.096	600	5.5	520	12	4.6	1420	.031	35	No trim orifice
109	4-27-67	67	.086(P)	650	3.2	515	15	4.7	1420	.029	80	Load orifice has rounded inlet

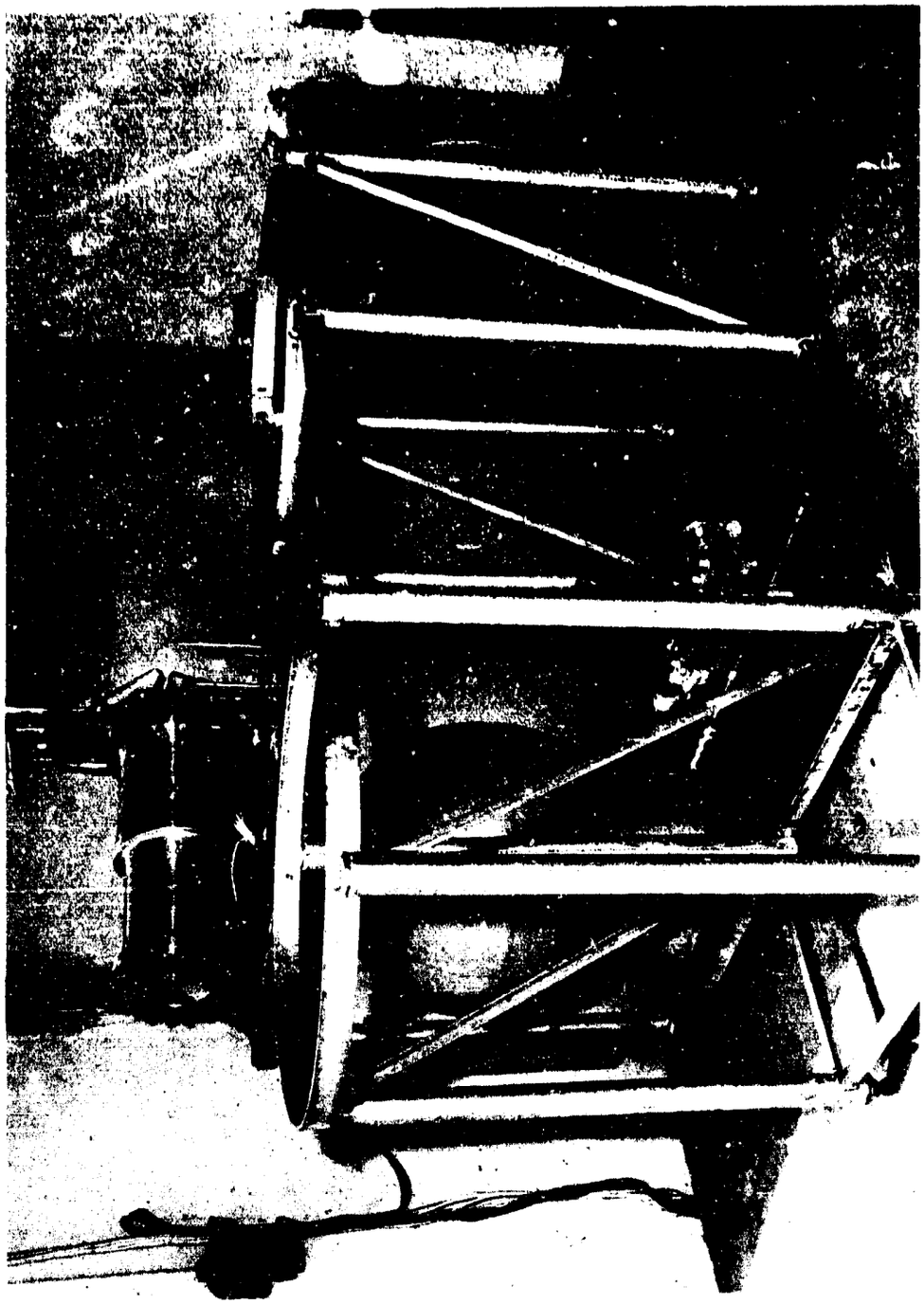

Figure 23. First-Stage Pressurization Subsystem-Test Schematic

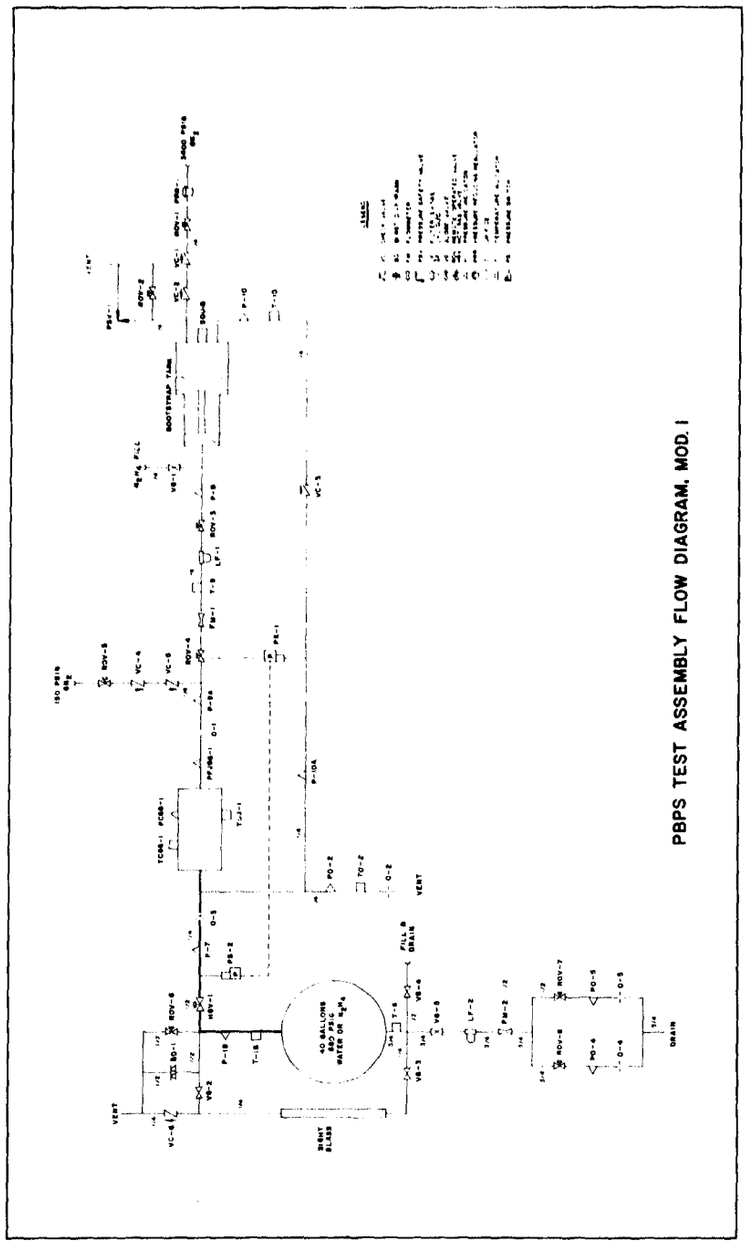

Figure 24. Integrated Subsystems Testing Test Stand

IV, A, Pressurization Subsystem (cont.)

The second test was identical to the first one except that the bootstrap tank ullage was approximately twice that of the first test. Output pressure reached 90% of its maximum value within 15 sec of the bootstrapping point at an average rate of 9.4 psi/sec. The test was terminated at 50 sec.

3 Tests SP-16A-104, -106, and -107

For Test -104, the output of the gas generator was plumbed through an 0.089-in. diameter orifice directly to a 40-gal tank filled with water. Dual-load orifices provided water flow rates of 0.3 lb/sec and 0.5 lb/sec to simulate flow demand to the second-stage gas generator. A pressure switch was mounted on the tank to limit tank pressure to approximately 650 psia. A second pressure switch was used to limit the feedback pressure to the bootstrap tank to approximately 750 psia. With a 0.089-in. orifice exhausting to atmosphere, the equilibrium output pressure of the bootstrap system was 630 psia (Test -103). With the back-pressure supplied by the water tank, the output pressure exceeded the 750 psi pressure switch setting, closing the fuel valve. The initial closing of the valve occurred when the water tank pressure reached 615 psia. Subsequent valve closing signals came from both switches as required to maintain their limiting pressures. Tank pressure was maintained at 640 $\pm$ 15 psia for the entire run duration. Gas generator operation and the water outflow was terminated at 115 sec to observe the tank pressure decay caused by heat loss from the gas. Significant data obtained during the test are shown on Figure No. 25.

Tests -106 and -107 were planned as water expulsions with a constant overboard gas bleed upstream of the tank inlet orifice. The 0.089-in. inlet orifice was replaced with a 0.098-in. diameter orifice and a 0.067-in. diameter orifice was used for overboard bleed to simulate the fluidic control gas requirements. Test -106 was aborted because the water tank vent valve was inadvertently opened during the start sequence.

Test -107 was a 103-sec run, during which the water tank pressure was held to 640 $\pm$ 10 psi. Control was achieved by the tank pressure switch throughout the test.

4 Test Results

No major difficulties were experienced in the operation of the first-stage gas generator system. There were no obvious signs of either hydrazine or hot gas leakage. The system was run both with and without the liquid trim orifice and with various load orifices to obtain pressure drop characteristics of each component as a function of hydrazine flow rate.

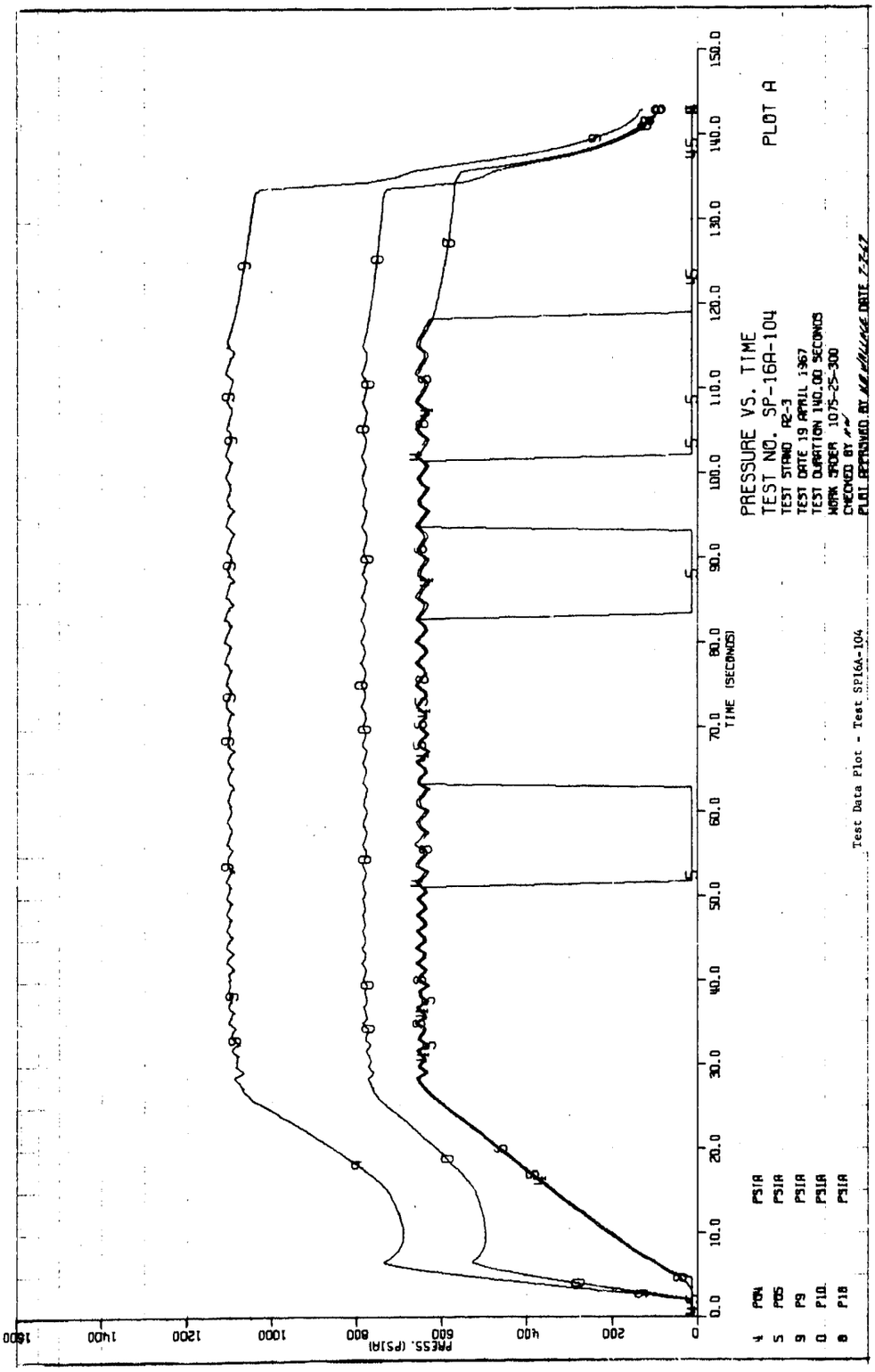

Figure 25. Test Data Plot - Test SPI 6A-104

IV, A, Pressurization Subsystem (cont.)

System operation was extremely stable during every test. No significant effort was expended to investigate transient response because the test set-up did not adequately simulate operation with the fluidic pressure regulator. No attempt was made to alter the "as-delivered" performance of the system.

The need for accurate determination of component pressure drops is illustrated by Figure No. 26, which is a plot of output pressure versus liquid flow rate. The characteristics of the liquid circuit and the gas circuit are plotted separately. These two lines cross at the equilibrium pressure and flow rate. The liquid flow curve is plotted showing available output pressure as a function of the hydraulic characteristics of the line components. The gas flow curve was obtained by relating the output pressure to the difference between the liquid flow rate and the feedback gas flow. The gap between the two liquid flow plots represents the trim capability of the existing system. The two gas flow curves represent a single load orifice with a 0.9 and a 1.0 discharge coefficient. They indicate the sensitivity of equilibrium pressure to the load characteristics.

c. Prototype Tank Testing

The prototype tank (see Figure No. 14) was fabricated from AMS 5743 (AM 355) material, heat-treated to SCT-1000. It was tested for structural integrity, weld porosity, dynamic seal leakage, and expulsion efficiency.

The piston assembly was fabricated with several welded sections. Then, it was submerged in water and pressurized with GN_2 to 700 psia and held at pressure for 2 min to observe any leakage. The cylinder assembly had only one welded section (propellant flange end), but the tank had to be completely assembled for this test. Once the propellant cavity was pressurized with 700 psia GN_2 and no leakage was observed, the proof pressure tests were undertaken.

Proof pressure tests were successfully conducted on both ends of the assembly using filtered distilled water at the design proof pressures for nominal operating levels. The gas-side of the tank was pressurized to 1120 psig and the propellant side of the tank pressurized to 1590 psig.

Expulsion efficiency tests were conducted to determine the maximum tank capacity and the useful propellant expelled by the piston device. The average expulsion efficiency was 99.2%. A check also was made to determine if the dynamic seals leaked. No leakage occurred. The following expulsion test results gave an average expulsion efficiency of 99.2%.

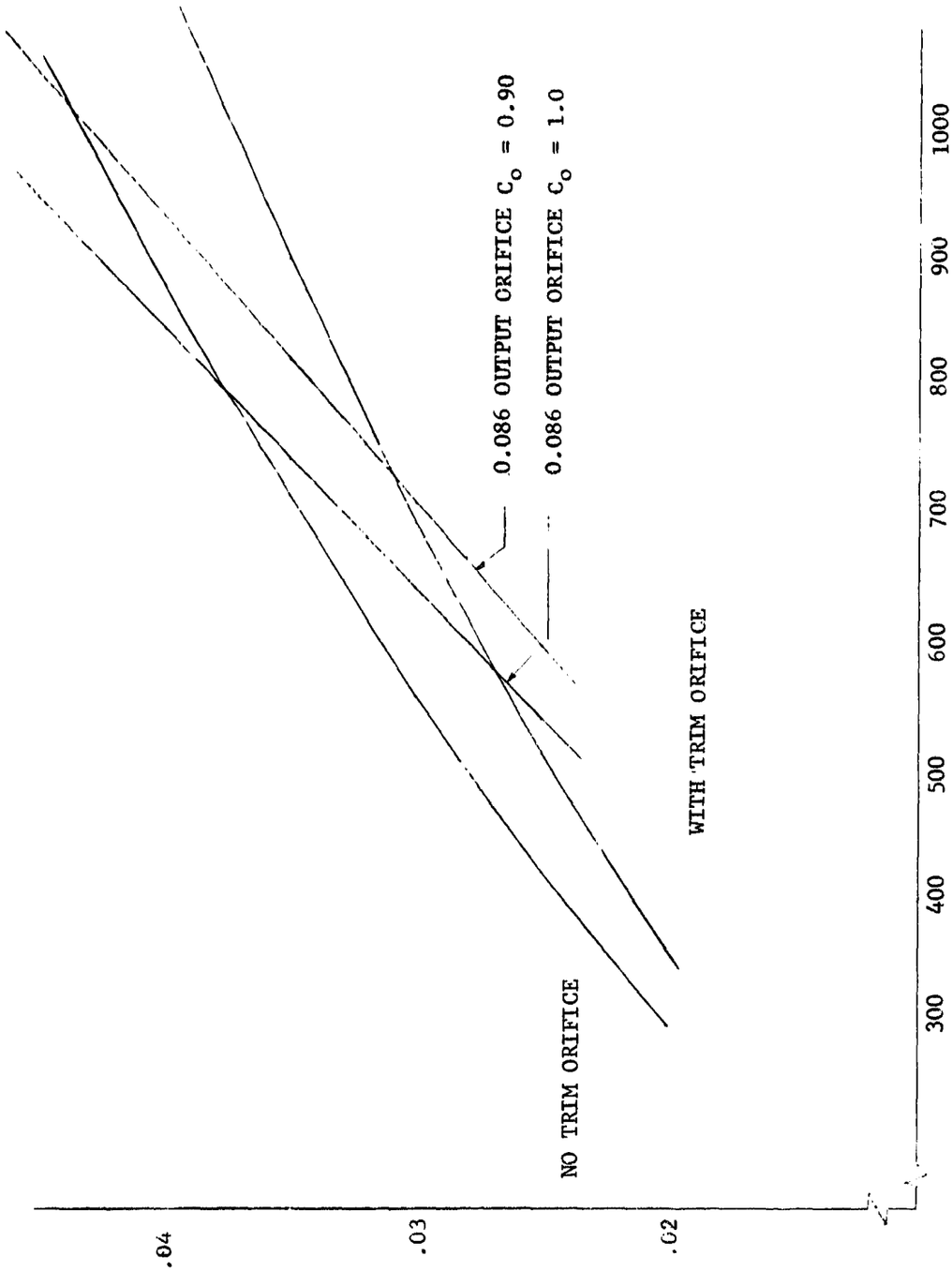

Figure 26. Bootstrap System Flow Characteristics

IV, A, Pressurization Subsystem (cont.)

Run	Maximum Propellant Load, lb	Residual Volume - CC
1	21.16	73
2	21.17	81
3	21.18	75

d. Shear Seal Weld Program

A basic requirement for the flight-type pressurization system was that the stored propellants must not make contact with any non-metallic seal used in the system during the 10-year storage life. Many of the bootstrap tank concepts studied used no non-metallic seals (i.e., bellows and collapsing diaphragm configuration). However, when piston-type devices are used, seals are required. Preventing the exposure of these seals to the propellants presents a problem. With the selection of the piston-type positive expulsion bootstrap tank came the related problem of protecting seals from propellant exposure. The approach selected to provide separation of propellant from seals was to weld an actual joint between the piston and the cylinder, thereby isolating the propellant from the seals. This weld joint would be sheared at the time the system was activated.

The shear seal was required to meet the following criteria:

- Maintain the propellant separate from the seals
- Shear when the proper force is applied
- Withstand many thousands of pressure cycles (vapor pressure storage of propellants required without compensators)
- When sheared, no interference in any way (i.e., tearing the seals or galling the sliding surfaces)
- The shear seal should preferably be the same material as the tank material for compatibility

It should be noted that the shear seal concept was being developed for the flight type pressurization subsystem and not for use in either the workhorse or prototype units being developed for this program. The tankage fabricated for this program had to be reusable as well as minimum cost. For these reasons, the shear seal was evaluated in test devices which only simulated the actual tankage.

Although the design of the workhorse and prototype piston and tank did not contain the shear seal, the internal configuration of these components did provide for incorporation of the shear seal at a later date if desired.

IV, A, Pressurization Subsystem (cont.)

The original shear seal design is illustrated on Figure No. 27. It consists of a narrow electron-beam weld (EBW) between the cylinder and the nose of the piston. The weld penetrates the cylinder wall while only slightly penetrating the surface of the piston.

Hamilton Standard performed all of the shear seal development program work in conjunction with their basic contract for the pressurization subsystem development.

(1) Subscale EBW Shear Seal Effort

Subscale investigations were performed early in the program to determine the feasibility of shearing an electron-beam weld. Seven test samples, approximately 3-in. in diameter, were welded using weld widths varying from 0.008-in. to 0.026-in. These specimens were checked for cracks using the Zyglo method and tested for leaks at 50 psi ΔP with air and a Halide leak tester. Weld penetration and weld width were examined by metallurgical means and the shear load required to cause the weld to fail was determined using a simple test fixture. These preliminary tests demonstrated the feasibility of the electron-beam shear weld concept to break the seal at moderately low pressures while the piston moved freely to expel propellant. Based upon these successful results, the full scale shear weld program began.

(2) Full-Scale EBW Shear Seal Effort

(a) Design and Fabrication

A development program was performed to determine if the EBW shear seal concept could be successfully applied to the differential area bootstrap tank which was designed, fabricated, and successfully tested during the course of this program. The same approach was followed for the full scale program as was used during the subscale program, namely:

- Weld penetration and width correlations
- Weld leakage
- Weld shear strength test

As previously noted, full-scale testing using actual tankage hardware for shear seal evaluation testing would have been too expensive. A reasonable facsimile had to be designed that would be at least full-scale in dimensions and manufactured from the identical materials used for the full-scale tank (AM 355). The method selected was to machine two concentric rings having the same dimensions as the prototype dimensions in the location of the intended shear weld. The diameter where the two concentric rings met had a 0.060-in. wide land and was accurately machined (8.002/8.000-in. diameter). A slight force was required to assemble the two pieces. Then, the

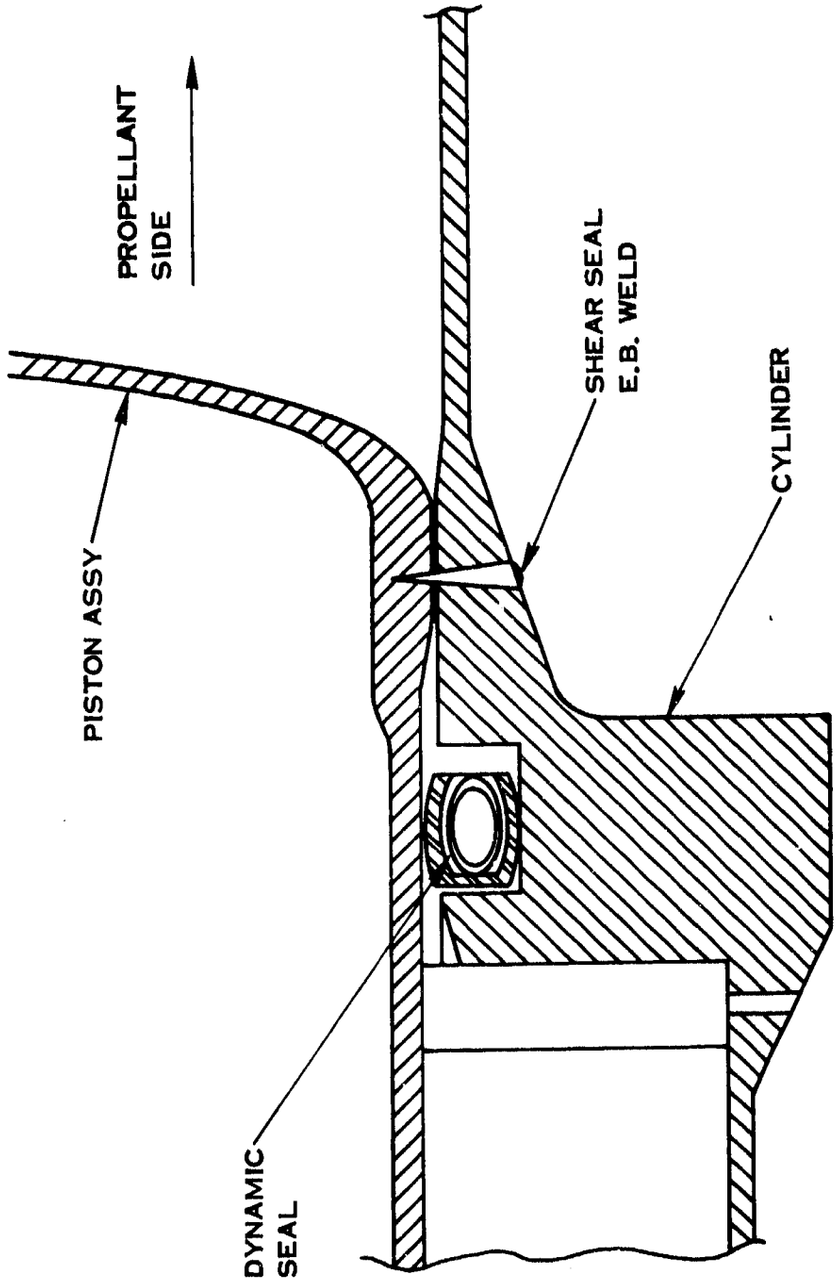

Figure 27. Electron-Beam Welder Shear Seal

assembly was tack-welded together at four locations to ensure there would be no movement prior to electron-beam welding. After the assembly was EB welded, the four tack welds were removed and the inside as well as outside diameters cleaned. The weld bead formed on the periphery of the outside diameter surface was machined off prior to testing.

A special test fixture was designed and fabricated for testing both leakage and shear strength. The ring-set assembly was bonded (epoxy resin) into the fixture as shown schematically on Figure No. 28. Once the test specimen had been bonded in place, the end plates were assembled and bolted together with steel through-bolts.

Ten concentric ring sets were machined from a ring forging of AMS 5547 (AMS 355) material. Eight of these sets were tested with the following results.

(b) Testing

The main objectives of the EBW testing program were to uncover and correct problem areas while demonstrating that the shear seal weld concept is feasible for a flightweight PBPS tank assembly. A summary of all full-scale EBW ring set results is presented on Table XIV.

The first full-size EBW shear seal specimen was welded to determine proper machine setting for various weld penetration depths as well as widths. These initial tests established the feasibility of making the weld required for the prototype tank size and configuration. A photomicrograph of two of these welds is shown as Figure No. 29.

The EBW machine schedules that were established for this first test piece essentially involved only one variable, that of current setting. It produced weld widths from 0.013-in. to 0.028-in. at the shear surface. The welds are wider and penetrated deeper with the higher current settings. Defects noted from the photomicrographs included some porosity at the shear joint interface, shrinkage voids parallel to the shear plane, root porosity, and cracking in the weld plane. None of these defects were considered detrimental to the function of the system and no special attempt was made to eliminate them in this program. There was no evidence of weld cracking or shrinkage in the plane of the shear joint. Such defects would have been considered very serious. No difficulty was experienced in centering the weld on the shear load.

Based upon the experience obtained from Sample No. 1, Assemblies No. 2 and No. 3 were welded using the preferred machine setting. These assemblies, which were welded over these entire

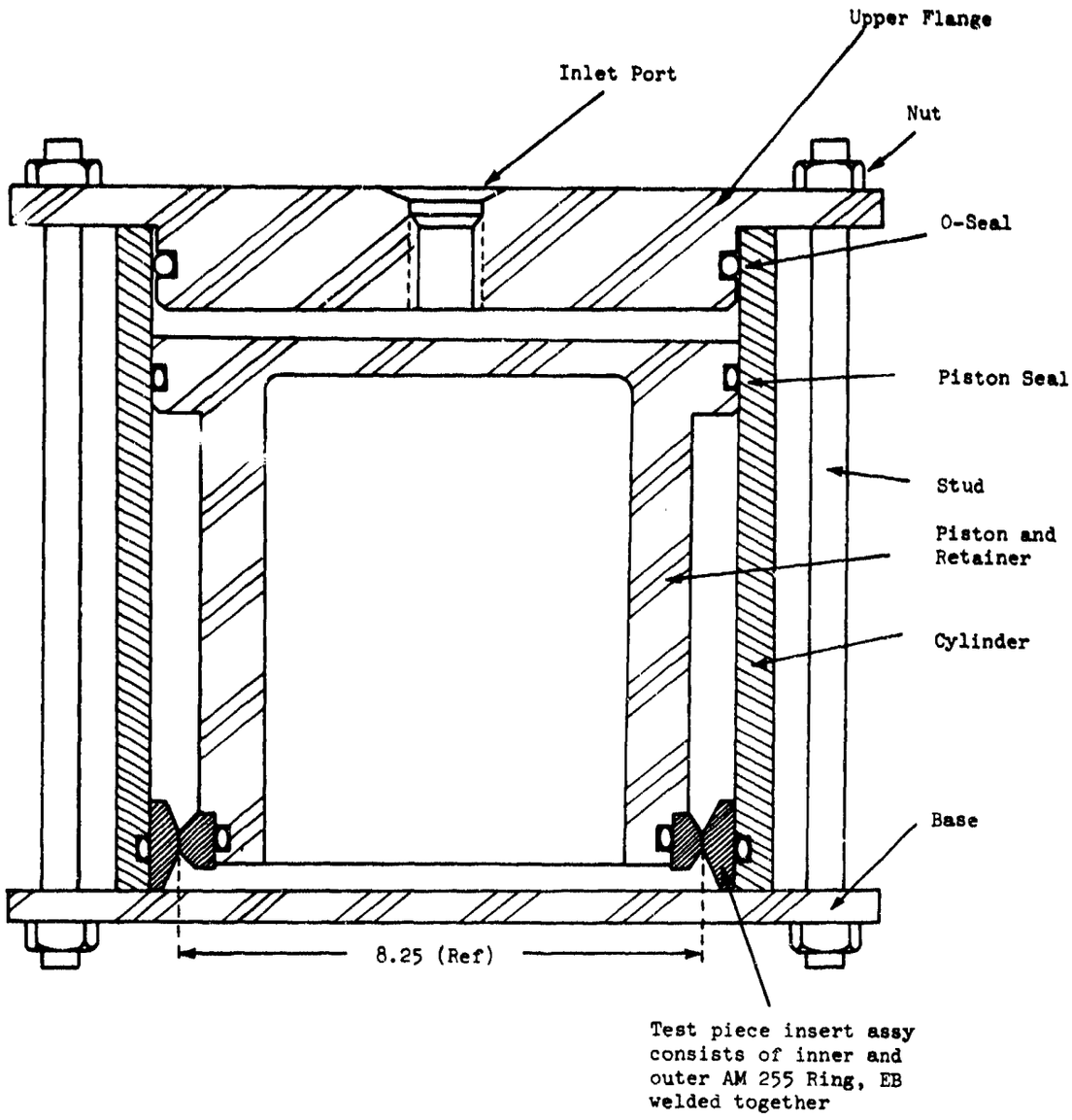

Figure 28. Shear Seal Test Fixture

TABLE XIV

STATUS AND RESULTS OF ELECTRON-BEAM WELDED RING SETS

NO.	RING-SET CONFIG-URATIONS	WELD SCHEDULES			APPROX WELD WIDTH IN.	LEAKAGE TEST	SHEAR PRESSURE 8-IN.DIA TANK PSIG	PRESSURE REFLECTED BACK TO 1.56 AREA RATIO PISTON	COMMENTS
		VOLTAGE KV	CURRENT MA	SPEED RPM					
1		150	16-26	60	0.015-0.029	Destructive samples	NA	NA	Weld schedules were initially established on this ring-set 6 different setting 30-degree segments.
2		150	24	60	0.032-0.035	Parts gapped at weld joint	NA	NA	Beam sharp focused 1/8-in. below surface. Rings were not leak tight - parts bridged when outside ring expanded during welding.
3		150	24	60	0.032-0.035	Parts gapped at weld joint	NA	NA	Same as No. 2. Both ring-sets were destruct tested.
4		150	30	120	0.016-0.020	Destructive sample	NA	NA	Machine settings changed. Beam focused 1/8-in. below surface. Parts were separated and leaked.
5		150	30	120	0.016-0.020	Parts gapped at weld joint	NA	NA	Same as No. 4.
6		160	30	120	0.016-0.020	No leakage	1100	700	Voltage increased but despite decrease in weld width, the ring failed much higher than expected.
7		150	10	83	0.012-0.014	No leakage	1050	670	Modified the outside ring to reduce cross section and changed weld schedules. Width still didn't go small enough but no part separation occurred.
8		150	7.5	120	0.008-0.010	No leakage	750	480	Established new machine setting - worked well. Weld was leak-proof and sheared at a reasonable pressure.
9									
10									

7X

Sample #1

7X

Sample #2

Figure 29. Electron-Beam Depth and Width Determinations

IV, A, Pressurization Subsystem (cont.)

circumferences, experienced separation during the welding process. The separation problem caused small pin holes to form in the shear seal weld and leakage resulted.

Samples No. 2 and No. 3 were used for metallurgical studies. Metallurgical stability of as-welded AMS 5547 (AM 355), particularly over a 10-year storage life, had not been evaluated. It became a concern during the evaluation of the shear seal pieces; therefore, these ring sets were sectioned to provide five as-welded samples. These samples were subjected to the thermal cycles shown on Table XV. The sections then were mounted in Bakelite, HCL-Picral etched, and Zwick 0.2 kg microhardnesses taken in the weld and base material as shown on the table.

TABLE XV

AMS 5547 (AM 355) METALLURGICAL STABILITY

	Condition Thermal Cycle	Weld Hardness--RC	Base Metal Hardness--RC
1.	As welded	15.5/32	39/41.5
2.	32°F/8 hr + 150°F/8 hr 2 cycles	25.5/36.5	36.5
3.	20°F/8 hr + 150°F/8 hr 2 cycles	39/42	36.5
4.	0°F/8 hr + 150°F/8 hr 2 cycles	36.5/43	39/43
5.	-100°F/24 hr	47/49	

The conclusion drawn from these tests was that the weld hardness increases with decreasing exposure temperature as the weld transforms from austenite (as-welded) to martensite (after a sub-zero treatment). It is interesting to note that a significant amount of austenite transforms as high as 32°F. Apparently, the austenite weld is not stable under normal temperature zone weather conditions and the strength of as-welded joints in AM 355 cannot be closely predicted with any degree of accuracy. Based upon the successfully sheared weld widths (Samples No. 6, No. 7, and No. 8, subsequently discussed), the calculated shear strength of the material is somewhere between 86,000 psi and 110,000 psi. The larger value seems to be more consistent with the test results. Attempts were made to stabilize the austenite, but it was determined to be doubtful that true stability, except in the hardened condition, could ever be achieved.

IV, A, Pressurization Subsystem (cont.)

To avoid this separation, which was thought to result from excessive heat input, a new machine setting was tried. This setting was a faster part rotation speed, producing a narrower weld. Specimens No. 4 and No. 5 were used for these experiments. In reviewing the results from these tests, it appeared that the power was too low because the welds were not good. The power setting was raised for Specimen No. 6 and this assembly was welded. Although a good weld was obtained on No. 6, the shear force required to cause weld failure was too high (1100 psig).

At this time, it was decided to reduce the mass of the outer ring, thereby reducing the thickness of material through which the weld beam had to pass. Ring Set No. 7 was modified (i.e., grooved to provide equal amounts of heat to both inner and outer rings and lower penetration requirements) so that less power could be used with a resultant narrower bead width.

Ring Set No. 7 was tested and failure occurred at 1050 psig. This pressure was too high. It was thought that a tight fit between rings could have caused ring binding and, consequently, high pressure for weld failure. Three sets of rings were mechanically assembled and pushed apart (no welding involved). It required 8 psig to separate the assembled ring sets. Thus, the excessive strength of Ring Sets No. 6 and No. 7 must be attributed to weld widths.

Ring Set No. 8 was welded with a smaller width and as a result failed at an acceptable level (750 psig). Also, it was leak tight.

Ring Sets No. 9 and No. 10 were never tested.

Because of the importance of weld widths, a separate evaluation was conducted to determine the significance of various machine parameters on width determination. This evaluation is briefly discussed in the following section.

(c) Weld Bead Studies

Several studies were conducted to minimize bead with the shear joint. This work involved the variation of the following machine parameters:

- Pulsating beam rather than continuous beam
- Distance of EBW gun from specimen
- Weld speed and current setting
- Beam focus

IV, A, Pressurization Subsystem (cont.)

It was found that in all tests using the pulsating beam, the weld width was greater than for comparable depth welds produced conventionally by the continuous beam method. This result was not completely understood. It was believed that the effective beam width might be a function of peak current intensity rather than the PMS value. Pulsation techniques were not pursued further.

Weld beads were run at distances from 6-in. to 16-in. from the EBW gun at speeds of 60 ipm, 90 ipm, and 120 ipm. It was observed that the weld bead width was consistently lower with the test piece closer to the gun.

Tests were conducted to determine weld bead width as a function of weld speed. The results from the speed tests were badly scattered, but the general trend indicated that lower weld currents and higher speeds would be desirable for narrower welds.

Each time a weld set-up is established, the machine operator sets the controls (i.e., voltage, speed, and current). However, it was standard procedure to focus the beam to the finest beam diameter for each set-up by observing it through a microscope on the machine. Usually, the test piece (copper or tungsten target) undergoes some melting while the beam is being focused resulting in some brinneling, which simply means less accuracy in setting up focal lengths.

Many test welds were made to determine if a simple set of weld parameters (voltage, current, speed, and focus coil mount), once determined, could be used in production without readjusting the focus each time the gun, filament or tooling were changed. When gun, filament, or tooling changes were made at the setting used, reproducibility was not obtained. Welds that were not refocused became as much as 50% wider. The same setting gave reproducible results from piece to piece when the gun, filament, or tooling remained unchanged.

Thus, it was determined that all welding parameters can be predetermined and set in the EBW schedule except focus, which controls beam power density and, thus, depth and width penetrations. Within current technology, the focusing parameter remains operator-dependent.

A large variation in pressure was required to fail the weld because of small variations in weld width. Therefore, an attempt was made to revise the existing design to make the failure more dependent upon properties of a material and less dependent upon the width of the weld. This alternative design is described in the following discussion.

IV, A, Pressurization Subsystem (cont.)

(d) Alternative Shear Seal Design Concept

To control the shear seal fracture pressure, it was necessary to control the shear area and/or the shear strength of the material. The shear area is a product of the weld length and width. The length is fixed; therefore, the weld width controls the area. The shear pressure is proportional to the product of the shear area and the material shear strength. As a result, both area and shear strength must be low to achieve a low weld shear pressure. It was determined that weld width was difficult to control and therefore, in the alternative seal design, weld width was controlled by machining the width into the part and then welding it in place. This would result in acceptable weld width tolerances. A material change also was included in the alternative design. By substituting a lower shear strength material in the vicinity of the weld, lower weld shear pressures could be achieved. This alternative design, which is shown on Figure No. 30, has an insert of AISI 347 stainless steel pressed into the piston and cylinder. Then, it is machine-finished to the configuration shown. The 347 stainless steel is compatible with both the tank material (AMS 5547/AM 355) and hydrazine. It has a shear strength in the range of 40 ksi to 44 ksi, which is approximately half that of the AM 355 value. Considering an acceptable shearing pressure to be 380 psi to 550 psi, the maximum shear weld width would be 0.040-in. and the minimum 0.030-in. for a propellant end tank diameter of 8.0-in. and a gas end tank diameter of 10.0-in.

Using 0.030-in. to 0.040-in. for the width of the sealing wall, the tolerance can be easily maintained on the machined interface. The plot of shear pressure and shear seal width shown on Figure No. 31 illustrates the predicted requirements.

This alternative design concept offered several advantages. It is positioned in a low-stressed area of both the piston and cylinder; therefore, it did not require any increase in tank length. Further, the welded bead width could have greater welding tolerance (i.e., control of electron-beam would be less sensitive) and the electron-beam could be accurately positioned axially with respect to the sealing wall on the inside (the length of the AISI 347 bond compensates for the axial tolerances affecting the position of the piston because it can be referenced machined after the insert is press-fit into place). Finally, the sheared edge residue could be cleared away by the piston passing over a sharp edge downstream.

There are a number of alternatives possible regarding the details of this shear seal concept. These include material for the insert ring, the method of installing the ring, and possibly, the ring shape. Alternative material criteria would include compatibility with hydrazine, no corrosive problems, low shear strength, and easy welding to itself as well as to AMS 355.

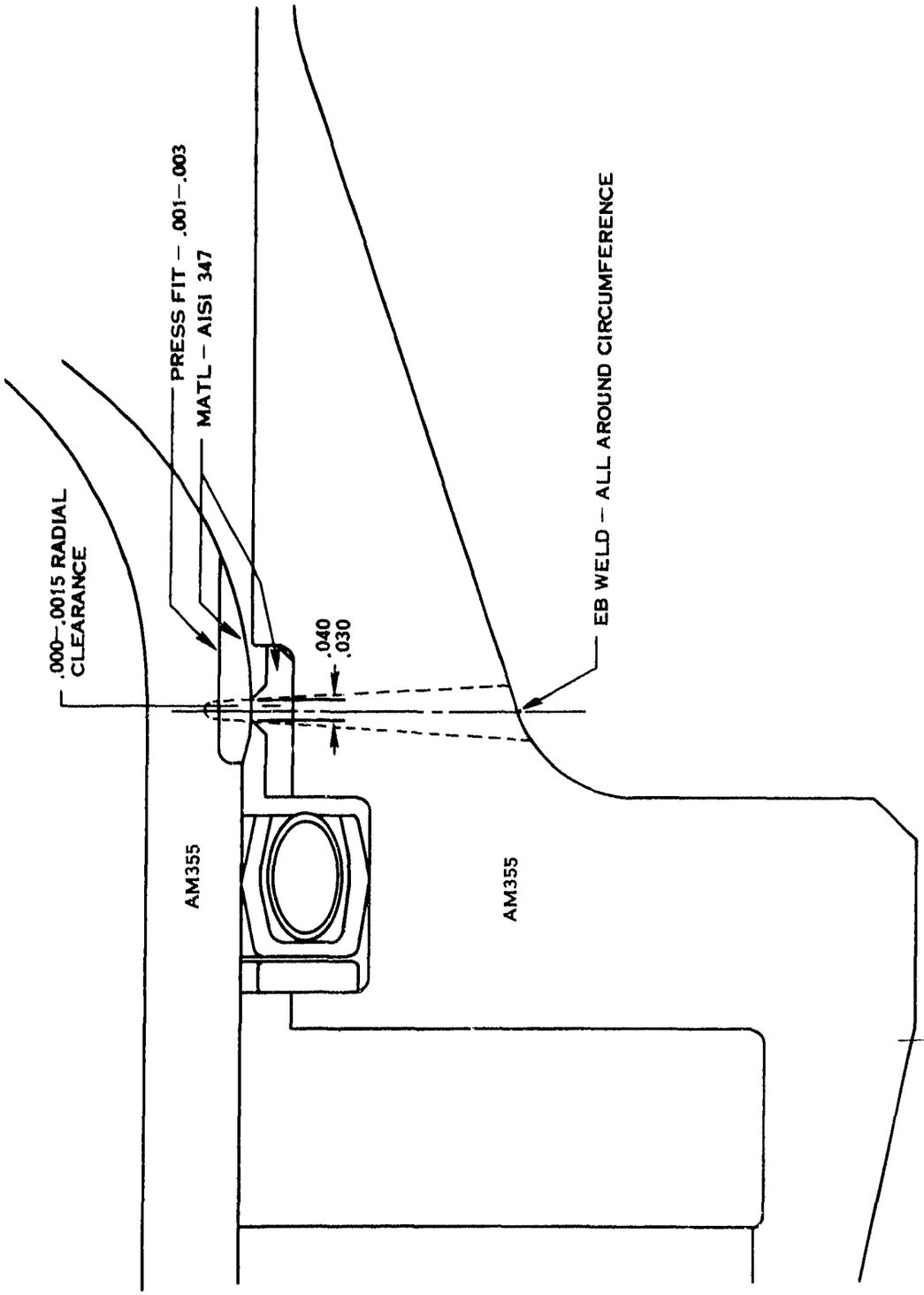

Figure 30. Shear Seal Concept Drawing

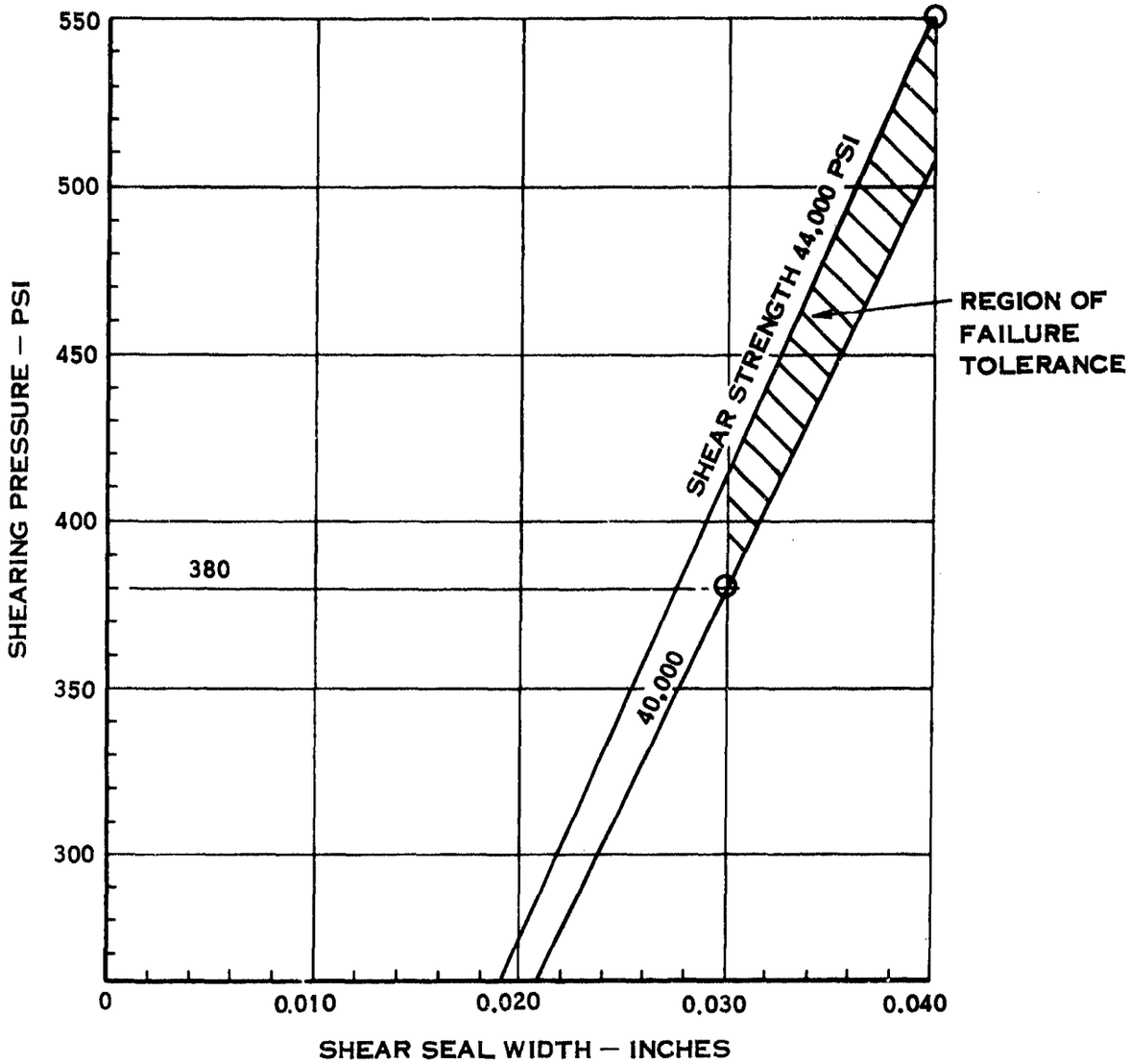

Figure 31. Failure Tolerance

IV, A, Pressurization Subsystem (cont.)

Based upon the experience gained in the EBW shear seal program, it is strongly suggested that, when additional work is performed in this area, consideration be given to the alternative design approach.

5. Problem Areas

No technological problems were encountered during the development of the pressurization subsystem components.

Problems of gas leakage at the gas generator flanges were solved by thickening the flanges and using high-temperature bolts. These problems would not exist in the all-welded prototype units.

Some problems were encountered in predicting injector pressure drops because of small variations in the internal diameter of the capillary tubes.

Hard starting of the generators when they were tested as components severely affected catalyst bed life as a result of the high instantaneous flow rates encountered when the supply pressure was present at its nominal value. The actual system operation provides a gradually increasing supply pressure during the start transient; therefore, the majority of tests conducted did not experience hard starts.

IV, Phase II - Subsystem Development (cont.)

B. PROPELLANT TANK/EXPULSION SUBSYSTEM

1. Design Considerations

The following major design requirements were established for the advanced PBPS tankage/expulsion subsystem:

a. High volumetric and expulsion efficiency at low, constant, differential expulsion pressures.

b. Ability to contain the required propellant volumes in the available packaging envelope, which is usually restricted because of space limitations.

c. Facility to withstand repeated temperature cycling, vibration, shock, and handling loads without degradation of diaphragm integrity.

d. High reliability for liquid containment and for operation after long-term exposure to the propellants.

e. Design and materials to result in all-welded, hermetically sealed, propellant-compatible units at minimum cost.

By the very nature of the subsystem requirements, many of the otherwise variable design features of the tankage expulsion subsystem were initially fixed. To meet the space envelope requirements identified for the main propellant tanks, tank configurations required length-to-diameter ratios greater than one for packaging into the wafer configuration PSV. Corrosion-resistant steel was identified as the best material for all tankage/expulsion subsystem components to satisfy the long-term propellant compatibility requirements. The subsystem had to be completely welded and hermetically-sealed to meet reliability, compatibility, and extended storage life criteria. Positive expulsion, reliability, and long storage life necessitated the use of a metallic diaphragm. High expulsion efficiency at low constant, differential pressure required that a flexible diaphragm be fabricated and that maximum propellant utilization be achieved.

The proprietary ARDEFORM stainless steel tank incorporating the ring-stabilized, stainless steel expulsion bladder developed by Arde, Inc., who was subcontracted to develop and fabricate the tank subsystem shown on Figure No. 32, was selected on the advanced PBPS propellant tank and positive expulsion concept.

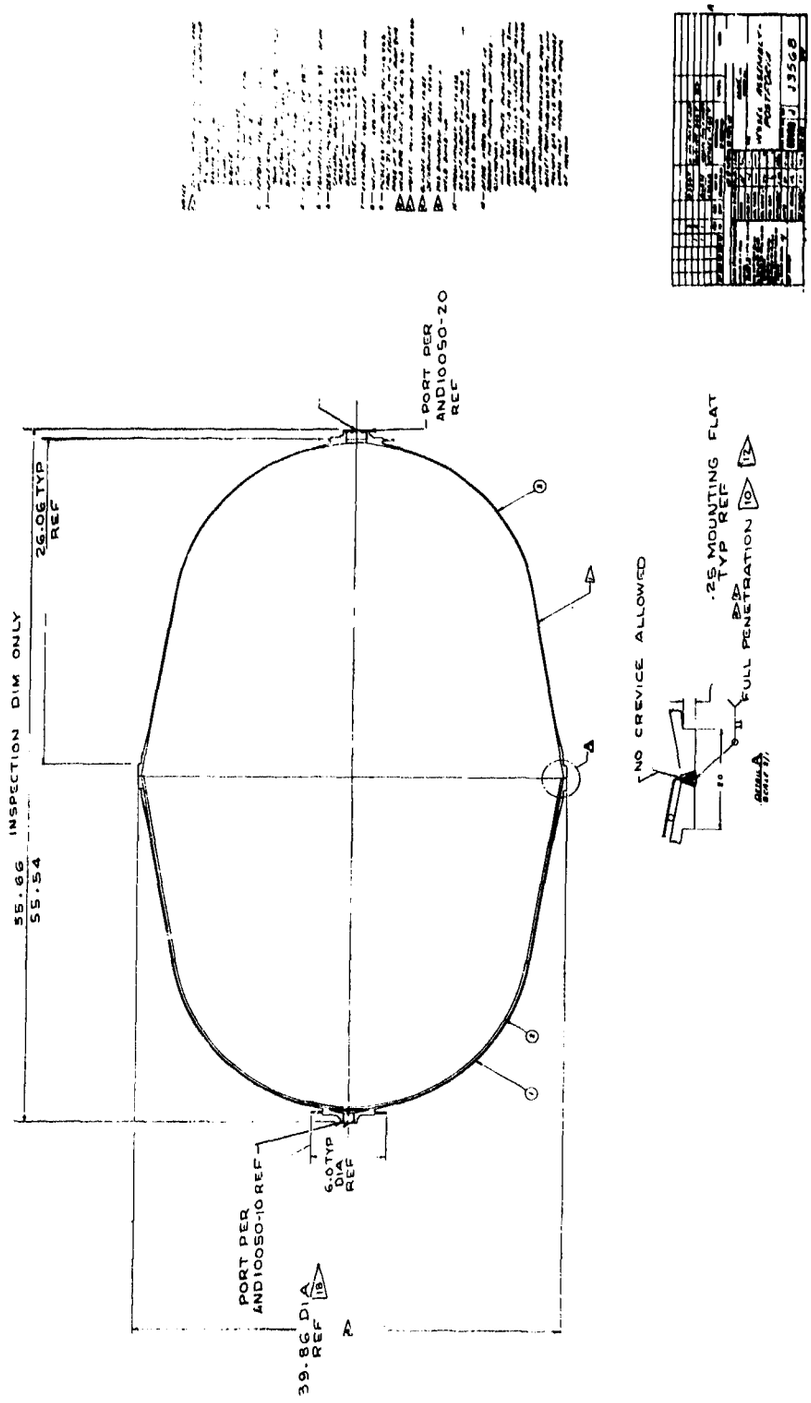

Figure 32. Vessel Assembly Post Form

IV, B, Propellant Tank/Expulsion Subsystem (cont.)

a. Design Criteria

(1) Diaphragm

In the PBPS application, the propellant volume changes as much as 10% over the specified temperature range (20°F to 150°F)(3). If the diaphragm were free to follow the liquid, this motion would degrade the diaphragm reliability potential. Therefore, to prevent diaphragm movement, the pressurization space behind the diaphragm is evacuated to a hard vacuum before propellant loading. The liquid side of the diaphragm also is evacuated and the tank filled with degassed propellant to the required propellant weight. The fill tube was crimped and welded closed. The ullage bubble, which is on the liquid side of the diaphragm, consists of propellant vapor only. When the PBPS is armed, the tanks are pressurized and the vapor bubble condenses, thereby resulting in a hard liquid system. Thus, through the incorporation of this unique evacuated ullage design, the diaphragm is held against the inside of the tank-half at all times by the propellant vapor pressure. This positive pressure differential prevents motion even under the most severe shock and vibration environments, ensuring diaphragm reliability. The techniques for maintaining a vacuum in all-welded steel containers have been in use by industry for more than 40 years and high reliability has been consistently achieved.

Diaphragm structural design considerations involved the selection of shell thickness and contour, reinforcing-wire size and spacing, as well as the method of wire-to-shell attachment. The shell was made as thin as possible to reduce bending strain and to lower the diaphragm actuation pressure during reversal. The size and spacing of the shell reinforcement (stiffeners)were selected to control the diaphragm deformation mode and preclude buckling. A satisfactory design is one which exhibits lower actuation pressures for the complete diaphragm reversal cycle. To obtain the proper design, trade-offs had to be made between conflicting requirements. For low shell strain and actuation pressure, the shell had to be thin and the wires spaced far apart. For increased buckling resistance, the shell thickness and wire diameter had to be increased and the wire spacing reduced. Arde, Inc., successfully developed and verified their design theory on hemispherical or near hemispherical diaphragm shapes. It was necessary to extrapolate this theory, developed on hemispheres, to the new conospheroid-shape diaphragm. However, it was anticipated that the range of permissible trade-offs possible for the more flexible conospheroid shape would be much less than for the stiffer hemispherical shape. Because of the numerous unknowns involved in the design and fabrication of a conospherical diaphragm, it was decided to investigate these questionable parameters in a subscale diaphragm development program before proceeding with design and fabrication of full-size conospherical diaphragms. The subscale diaphragm program is detailed in Section IV,B,2,a.

(3) During the program, this temperature limit was reduced to 125°F.

IV, B, Propellant Tank/Expulsion Subsystem (cont.)

Success in the subscale program established the following diaphragm criteria:

(a) Nominal cone angle - 10-degrees

(b) Nominal diaphragm wall thickness - 0.020-in.

(c) For the first units fabricated, wire size was to be 0.125-in. diameter and wire spacing was to be at 0.80-in. increments except for the first wire which was to be located closer to the flange

(d) A flat diaphragm flange rim

The conospheroid contour had already been established. Modifications to these initial criteria occurred during the course of the development program and this is discussed in Section IV,B,2,c.

(2) Propellant Tank

Within the framework of the design guidelines previously cited, a limited parametric study was performed to assist in selecting the tank design. This study was based upon the use of high-strength stainless steel (work-hardened) as the tankage material. The range of parameters examined included:

Design yield strength for ARDEFORM stainless steel (cryogenically-stretched stainless steel) = 240,000 psi for cone and 200,000 psi for sphere.

Young's modulus for ARDEFORM stainless steel = 30×10^6 psi.

Proof-pressure (internal) = 1.25 x working pressure = 250 psi, 438 psi, and 1000 psi.

Collapse pressure (external) = 1.33 x 15 = 20 psi.

Tank volume = 1500 to 50,000 $in.^3$.

Shapes-Length/Diameter Ratio, L/D = 1.6, 2.0, 0.5, and 1.0 (sphere).

The results of this investigation indicated that:

(a) Buckling controls the structural design at low proof-pressures (i.e., when vapor press of propellant is less than atmospheric pressure because of low temperature)

IV, B, Propellant Tank/Expulsion Subsystem (cont.)

(b) Yielding controls the design at high proof-pressure (high internal pressure, low exterior pressure)

(c) The spherical shape is most efficient from a standpoint when buckling governs

(d) The transition from design control by buckling and control by yielding is approximately 700 psi tank working pressure

As can be seen from the shape ratios indicated above, the primary designs considered for the tankage system were spherical, cylindrical, and conospherical concepts. The spherical and conospherical concepts studies considered the use of ring-stabilized reversing diaphragms while the cylindrical tanks considered the use of a bonded rolling diaphragm.

The conospheroid stainless-steel tank with the ring-stabilized reversing diaphragm was selected principally because its shape provided for optimum packaging of the PBPS wafer-configuration bus.

The critical-pressure design condition for the tank was an external pressure of 1.33 (S.F.) x 15 = 20 psi. This occurred because the vapor pressure of the fuel during storage could be less than 1 psia. A minimum wall thickness of 0.054-in. was required to resist this buckling load. If proof-pressure was defined as 1.25 times the working pressure (1.25 x 430 = 438 psi), the hoop membrane stress in the cone at its maximum radius of approximately 16.7-in. and a thickness of 0.054-in. was

$$\frac{438 \times 16.7}{0.054} = 136{,}000 \text{ psi.}$$

Defining internal burst-pressure as 1.33 x 350 = 465 psi, this produced a membrane stress of 144,000 psi. These stresses were well below the 240,000-psi yield-strength which is obtained by cryogenically-stretching the Type-301 stainless-steel tank.

If the dynamic loads resulting from vibration, shock, and handling do not exceed the implosion loading, the over-pressure condition dictates the tank design. The dynamic loading had to be analyzed for each type of mount as well as mounting arrangement used. Preliminary analysis indicated the dynamic loads were below the yield stress of the material; therefore, the wall thickness, based upon over-pressure criteria, governed the tank design.

Additional design criteria for the tanks included the following:

The tanks were sized to contain internal volumes of 31,213-in.^{3} (not including diaphragm)

The tanks were designed to operate satisfactorily over a temperature range of 20°F to 150°F (this upper limit was later reduced to 125°F)

The ullage allowance was established at 1.5% and a volumetric efficiency of 97.5% was the target along with an allowance of 2.0% for residual propellants at maximum temperature

Minimum weight tankage had to be designed (estimated weight of inch tank assembly was 148 lb, including diaphragm)

b. Materials Selection for Tank and Diaphragm

The selection of materials suitable for use in the PBPS tankage/expulsion subsystem was extremely limited. Corrosion-resistant materials had to be used because of the long-term propellant compatibility requirements. High-strength material was required to meet the stresses developed in the large pressurized conospheroid tanks. Materials that were capable of being severely deformed during the fabrication processes had to be used.

The material selected for the tanks was Type-301 stainless-steel, which was cryogenically-stretched by the ARDEFORM cryogenic-stretching process to achieve extremely high-yield-strength. Yield-strength for the hemispherical section of the tank was 200,000 psi while that for the cone was 240,000 psi.

The material selected for diaphragm fabrication was standard Type-321 stainless-steel sheet-stock. Initially, it was 0.062-in. thick, but it was precision ground to the desired thickness (0.020-in. to 0.035-in.).

c. Fabrication Methods Investigation - Tank and Diaphragm

Tank and diaphragm fabrication methods were evaluated upon the bases of technical feasibility, cost, and schedule. A limited study was conducted early in the program. It showed that:

(1) The number of fabrication options available for tank or diaphragm fabrication decreased as the tank volume increased.

(2) The maximum tank volume compatible with the standard 48-in. wide steel-sheet was 23,000-in.^{3}.

IV, B, Propellant Tank/Expulsion Subsystem (cont.)

(3) The largest one-piece diaphragm or tank-shell that could then be hydroformed (based upon blank size) corresponded to a tank volume of approximately 7000-in.^{3}.

(4) The maximum depth of draw (20-in.) for commercial hydroforming and deep drawing also limited the size of one-piece diaphragms or tank-shells that could be made utilizing the hydroforming or deep drawing fabrication techniques.

The following information shows the maximum tank volume that could be achieved as a function of length-to-diameter ratio (based upon standard sheet-size):

L/D Ratio	Maximum Tank Volume, in.^{3}
2.0	8,000
1.6	12,500
1.0	30,000
0.5	over 50,000

All reasonable methods for diaphragm and tank fabrication were reviewed. For diaphragm fabrication, methods for obtaining the properly prepared raw material (stainless-steel sheet-stock) to manufacture the diaphragm shell as well as to attach the reinforcing rings to the shell were evaluated. The methods selected for full-scale diaphragm fabrication were:

Obtain thick (0.062-in.) stainless-steel sheet and grind it down to the desired thickness

"Inturgescent form" the diaphragm (a proprietary-process of the Bendix Corporation, wherein a combination of drawing and hydraulic-forming is used

Initially attach the stainless-steel wires to the diaphragm by tack-welding, then secure them permanently in place by furnace brazing in a hydrogen atmosphere.

A summary of the various methods investigated is presented as Table XVI.

For tank fabrication, consideration involved selection of the best method for preform manufacture, the condition of the girth-ring (hardened or annealed), the type and method of fabrication for gaining and securing the diaphragm to the tank, and the method for obtaining a high-strength girth-weld. The selected method involved fabrication of a two-piece preform,

TABLE XVI

TANKAGE FABRICATION EVALUATION

	ITEM	FABRICATION METHODS CONSIDERED	FABRICATION METHOD CHOSEN
BLADDER	Diaphragm Shell	Hydroform, deep draw, inturgescent forming, spin or forge and machine, spin and deep draw, explosive forming.	Subscale Diaphragm: Hydroform Full-Scale Diaphragm: Inturgescent Forming
	Diaphragm Sheet Material	Existing sheet stock, sandwich pack roll, grind down thicker sheet to smaller thickness.	Subscale: Existing Sheet Full-Scale: Grind down 72-in. wide x .062-in. thick sheet
	Assembly of Reinforcing rings to diaphragm shell prior to brazing	Tack Welding Fixturing	Tack Welding
TANK	Furnace Brazing	Vacuum GH_2 atmosphere	GH_2 atmosphere - lack of presently available sufficiently large vacuum furnaces
	Tank Preform	One piece conospheroid; deep draw or hydroform hemisphere plus roll and weld cone	Deep draw hemisphere plus roll and weld cone
	Girth Ring	Hardened Annealed	Annealed
	Girth Weld Joint (Diaphragm Tank)	Partial penetration Full penetration	Full penetration - avoids long term storage crevice corrosion problem
	Weld	Cryogenic restretch Room temperature restretch	Room temperature restretch

an annealed girth-ring, a full-penetration weld (selected upon the basis of results obtained from a weld development program), and a room temperature restretch to obtain full weld strength.

2. Tank/Expulsion Subsystem Fabrication and Development

a. Subscale Diaphragm Program

The conospherical shape of the fuel and oxidizer propellant tanks required the use of conospherically-shaped positive-expulsion diaphragms to achieve high volumetric efficiency in the tankage design.

Conospheroid reversing diaphragms had not been fabricated prior to this program; however, hemispherically-shaped and near-hemispherically-shaped reversing diaphragms had been successfully fabricated. At least one vendor (Arde, Inc.) had successfully developed and verified their design theory on hemispherical or near hemispherical diaphragm shapes. The available theory as well as the practical fabrication experience had to be extrapolated to the new conospherical shape. In view of the many unknowns involved in the design and fabrication of a conospherical diaphragm (i.e., shell thickness, cone angle, reinforcing wire-size, and wire spacing), it was decided to investigate these questionable parameters in a subscale diaphragm development program before proceeding with the design and fabrication of full-size conospherical diaphragms.

Arde, Inc. performed the subscale diaphragm work and utilized the information gained during this effort toward later fabrication of full-scale conospherical diaphragms. They fabricated nominal 12-in. diameter units with a length-to-diameter ratio (L/D) of 1.6. These units were manufa tured in both 10 degree and 12 degree taper-cone angles. Diaphragms were to be made from 0.010-in. wall stainless-steel. The 10 degree cone angle was preferred for its high packaging efficiency, but it limited the number of options for wire size and spacing variations. The subscale diaphragms were similar in all respects to the subsequent full-size units.

Initially, eight, 10 degree taper subscale diaphragm shells were received by Arde from the Hydroform Company of America, Chicago, Illinois. These units were fabricated by using an aluminum sandwich-method and this resulted in the aluminum diffusing into the surface of the steel shell. The diaphragms were subjected to a bright anneal and upon close inspection, all eight units displayed longitudinal wrinkles in the cone-section of the flange as well as at the cone-spherical sector juncture. These wrinkles were 0.01-in. to 0.02-in. deep by 0.100-in. to 0.125-in. wide. The parts were determined to be structurally inadequate for testing.

Arde personnel assisted the Hydroform Company of America in resolving the fabrication problems. Two acceptable 10 degree taper subscale

IV, B, Propellant Tank/Expulsion Subsystem (cont.)

shells were completed. These shells were hydroformed using steel back-up sheets. The wrinkles were eliminated by limiting the initial draw operation to 50%. Eight additional 10-degree taper shells were fabricated within drawing and specification requirements.

The hydroform tooling was then modified to fabricate 12-degree taper subscale conospheroid diaphragm shells. Ten, 12-degree taper subscale shells were completed successfully and accepted by Arde.

Fabrication of the first 10-degree taper subscale diaphragm was initiated by Arde and furnace-brazing of the reinforcing rings was completed. Subscale reversal tests were initiated with the successful reversal of diaphragm S/N E3560-1S. A major milepost was achieved in the field of positive-expulsion devices as a result of this successful test. The unit was the first conospheroid diaphragm with an L/D ratio of 1.6 to be tested. All prior units had been spherical with an L/D ratio of 1.0.

Three, 10-degree taper and two, 12-degree taper subscale expulsion diaphragms were tested at Arde. All units were constructed from 0.010-in. thick hydroformed stainless-steel-sheet and reinforced with 0.094-in. diameter wire rings brazed to the shell surface. As a normal result of hydroforming, the shell thickness varied from 0.010-in. at the flange to 0.008-in. at the apex. The design parameters and the test summary for these units is presented on Table XVII.

The wire-spacing selected permitted a maximum amount of information to be obtained from the tests. The 0.6-in. spacing resulted in zero interference; the 0.5-in. spacing yielded physical interference between the rings; and the 0.9-in. spacing was the maximum unsupported cone length where buckling could occur.

All five units were subjected to similar, successful initial reversal tests. All five reversed following the rim-rolling mode of controlled-collapse. The unit walked between the rings, but was completely controlled and rolled, one ring at a time. The amount of walking was proportional to the wire-spacing. The actuation pressure varied from approximately 3 psi to 9 psi, with "apex popping" at approximately 10 psi at the end of the first reversal. A trace of the diaphragm differential pressure during a typical expulsion test is shown on Figure No. 33. Sequential photographs taken during a representative conospheroid diaphragm test are presented on Figure No. 34.

Although the expulsion system in the PBPS application is actually a "one-shot" requirement, a push-back reversal was performed with all five units. They all behaved alike; following the apex-roll mode of collapse

TABLE XVII

SUMMARY OF SUBSCALE DIAPHRAGM TEST SUMMARY

SUBSCALE BLADDER SN	REINFORCING WIRE SIZE, IN.	NUMBER OF WIRES	WIRE SPACING, IN.	NUMBER OF COMPLETE H_2O TEST REVERSAL ACHIEVED	FAILURE EVENT	FAILURE MODE	ACTUATION PRESSURE RANGE	REMARKS
E3560-1S (10°)	0.094 X-Section Diameter	17	0.60	1	Pin-hole leak in cone region about two-thirds the way through second reversal.	Wire interference during apex rolling mode of second reversal caused wire and shell buckling, leading to three corner folds and pin hole.	3 to 8 psi for reversal No. 1 and 5 to 10 psi for reversal No. 2.	First reversal very successful. Rim roll deformation was smooth and well controlled. Shallow angle, apex rolling made, and close wire span led to wire interference in the second reversal.
E3560-2S (10°)	0.094 X-Section Diameter	20	0.50	1	Same as E3560-1S	Same as E3560-1S	Same as E3560-1S	Same as E3560-1S. First mode even better controlled due to smaller wire spacing than on E3560-1S unit.
E3560-3S	0.094	12	First wire at 0.6 and remainder at 0.9.	1	Same as E3560-1S	Shell buckling in second reversal due to large unsupported cone length produced three corner folds and pin hole.	Three to ten psi for reversal No. 1 and 5 to 8 psi for reversal No. 2.	First reversal successful Ring roll mode well controlled. More "walking" of shell between wires during rim rolling was noted due to larger wire spacing. Larger wire spacing, however, did eliminate the severe wire interference during second reversal noted in tests of E3560-1S and E3560-2S units. This test checked out ARDE's actuation pressure range prediction and verified the use of a larger wire spacing to achieve a successful first reversal. Better control of first reversal deflection mode is achieved with closer wire spacing.

TABLE XVII (cont.)

SUBSCALE BLADDER SN	REINFORCING WIRE SIZE, IN.	NO. OF WIRES	WIRE SPACING, IN.	NUMBER OF COMPLETE H_2O TEST REVERSAL ACHIEVED	FAILURE EVENT	FAILURE MODE	ACTUATION PRESSURE RANGE	REMARKS
E3560-4S (12°)	0.094 X-Section Diameter	13	First wire at 0.6 and remainder at 0.8.	1	Pinhole leak in core region about two-thirds the way through second reversal.	Shell buckling produced wire intertwining & severe shell folds causing pin hole.	3 to 10 psi for reversal No. 1 and 5 to 10 psi for reversal No. 2.	First reversal successful. Controlled rim roll type. Cocking during second reversal could not be adequately controlled due to larger wire spacing. However, larger angle and larger wire spacing did result in elimination of severe wire interference observed in tests of E3560-1S & E3560-2S units.
E3560-5S (12°)	0.094 X-Section Diameter	17	0.6 Same as unit S/N E3560-1S					Scheduled for use in the subscale tank-weld model to be tested in February 1967.

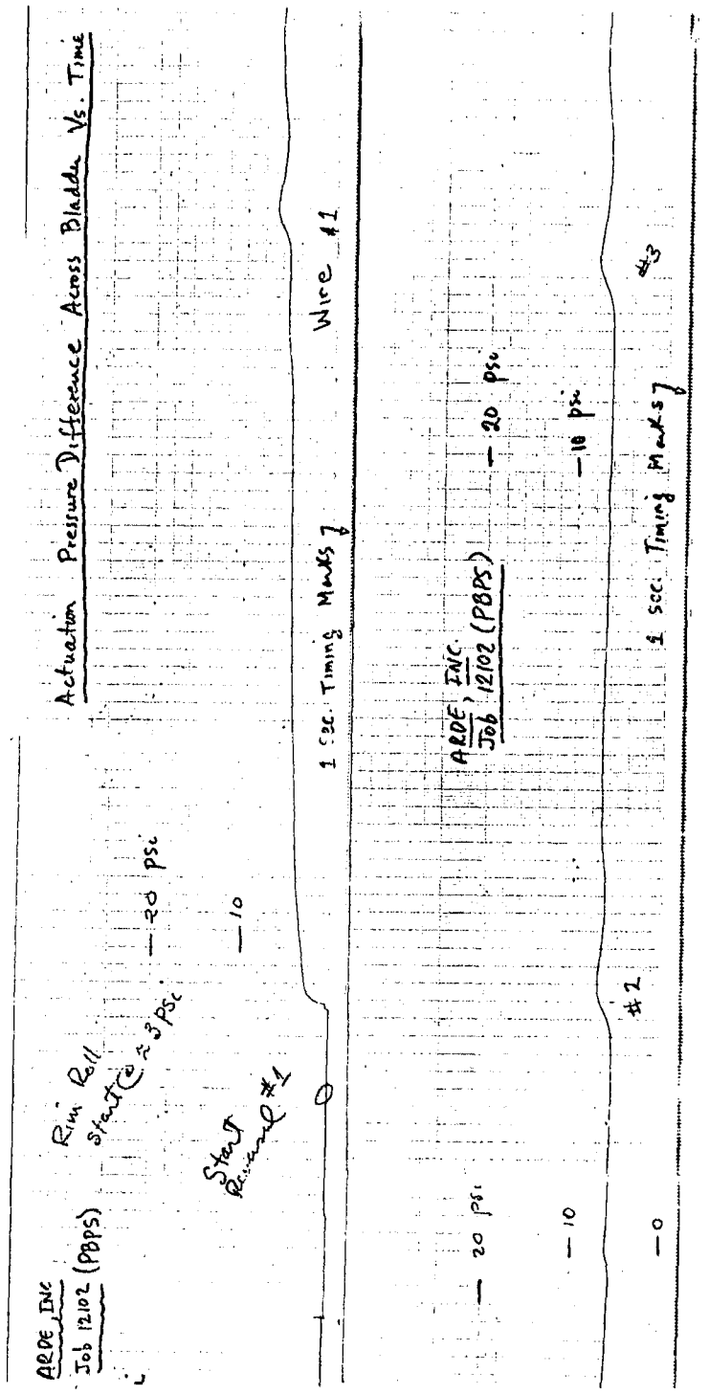

Figure 33. Typical Diaphragm Pressure Differential vs Time

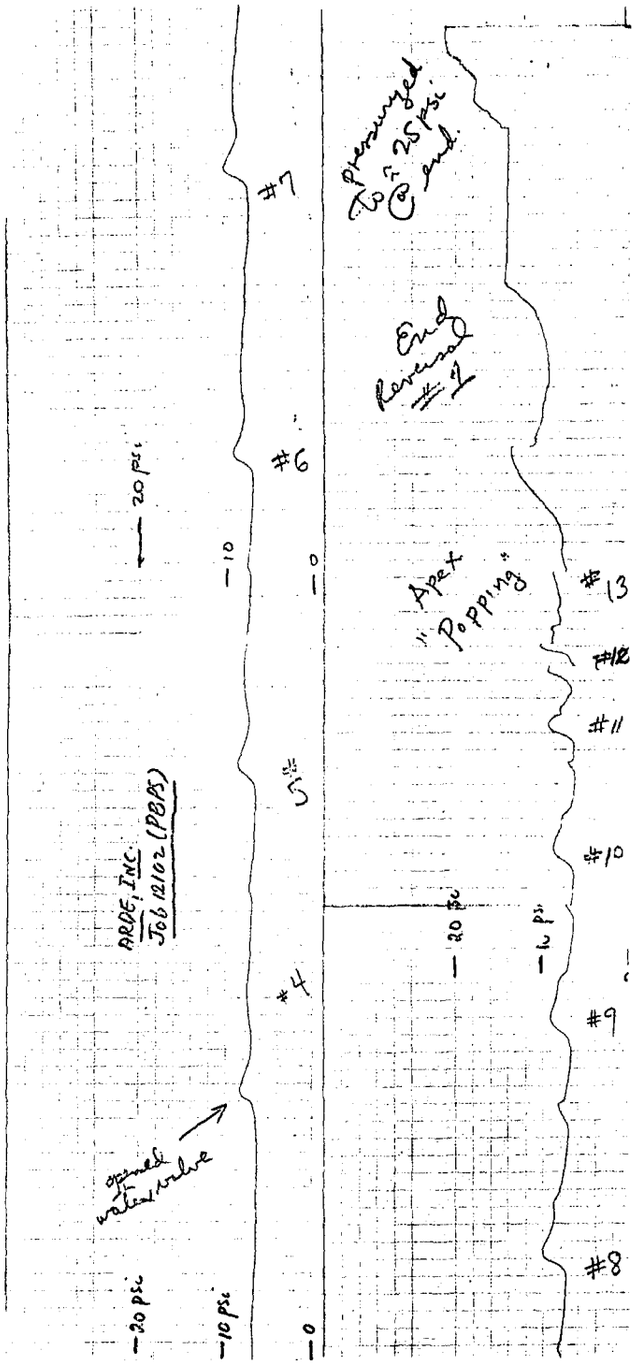

Figure 33. Typical Diaphragm Pressure Differential vs Time

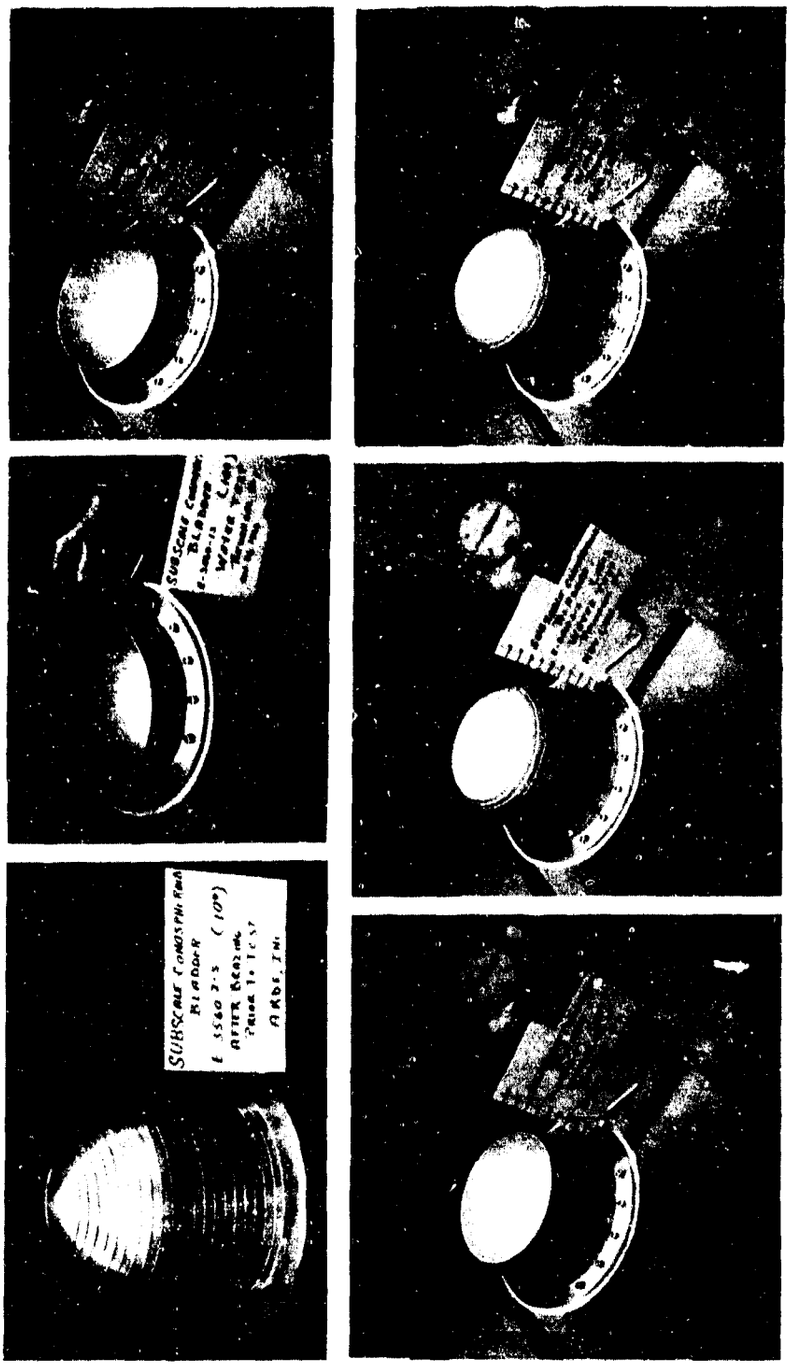

Figure 34. Tankage/Expulsion Subsystem

during the second reversal. The results with S/N 3560-1S and S/N 3560-2S were identical. Both units followed a controlled mode of apex-rolling through the spherical dome sector and through the transition into the cone. However, because of the very close wire-spacing and the walking of the unit, one wire bound underneath the next wire preventing it from passing on through. Consequently, from this point on, the reversal was uncontrolled. More than one wire passed through one side of the diaphragm before the other. The shell buckled and three-corner folded between the wires. The reversal cycle was completed, but pinholes occurred at several of the three-corner folds.

Unit S/N 3560-3S followed the pattern of S/N 3560-1S and S/N 3560-2S in apex-rolling during the second reversal. However, as a result of the large wire-spacing, no serious wire interference was observed. In this case, wire spacing was at the limit condition and the shell buckled between the rings in the cone section, approximately midway through the expulsion cycle. At that point, the collapse became uncontrolled with the same results; additional buckling, three-corner folds, and pinholes when the cycle was continued to completion. The actuation pressure varied from approximately 5 psi to 10 psi during the second reversal.

The results of the second reversal with units S/N 3560-4S and S/N E3560-5S (the only 12-degree taper-units tested) were essentially identical to those obtained with S/N 3560-3S. Shell-buckling between the rings produced the same results. However, the larger angle and wire-spacing did eliminate the severe wire interference obtained with units S/N 3560-1S and S/N 3560-2S.

The following conclusions and observations are based upon the design, analysis, fabrication, testing, and development experience gained during this subscale diaphragm program:

(1) A reliable, single reversal conospheroid diaphragm of a small cone angle (10-degree to 12-degree) was successfully demonstrated five times.

(2) The Arde "hemisphere" theory for predicting bladder actuation pressures, shell-thickness, and contour, as well as wire size and spacing was verified as being a reasonable design guide for the conospheroid shape.

(3) Cycle life can be increased by:

  (a) Increasing the cone angle in excess of 12-degree (13-degree to 15-degree is the anticipated range required). However, this would reduce the "packaging efficiency" of the subsystem.

IV, B, Propellant Tank/Expulsion Subsystem (cont.)

(b) Mechanically forcing rim-rolling, at least for the first few wires during the second and other even-numbered reversals.

b. Weld Development Program

Early in this program, it was recognized that one of the critical items in the tankage design was the girth joint between the tank-halves and the positive-expulsion diaphragm. It was planned that initial tank fabrication would be with flanged joints to facilitate development work but the prototype tanks would be of all-welded construction. Figure No. 35 shows both the flanged-joint construction and the integral weld-joint construction.

A weld development program was conducted to determine the most promising weld joint configuration, proper welding procedure, and the design data necessary to make the diaphragm-to-tank and girth joint details optimum. It was anticipated that the following problems would be encountered in connection with the tank and diaphragm welding:

- Weld-splatter and weld drip-through causing undercutting, burn-through, or other damage to the diaphragm.
- During long-term storage, weld-associated crevices could cause corrosion. Local cells of different propellant concentration produce corrosion. To eliminate this problem, partial-penetration welds would have to be avoided.
- The weld must be inspected. Inspection techniques available include visual, X-ray, dye-check, and leak-check. Each joint design considered would be evaluated with respect to its inspection capability.
- Increased diaphragm stiffness and welds were to be avoided in the area maximum-strain at the equator.

Lay-outs of several candidate joint concepts were studied before the weld development program was started. Four of these concepts are shown on Figure No. 36 along with a summary of the principal advantages and disadvantages of each joint concept. Analysis of the various concepts resulted in the selection of the joint design designated as No. 3 on Figure No. 36. This joint was considered most promising because crevice-corrosion, splatter, and drip-through problems had been eliminated. Also, a single weld could complete the joint and no increase in stiffness was introduced in the area of maximum flexure. However, visual inspection was limited to only one side of the weld.

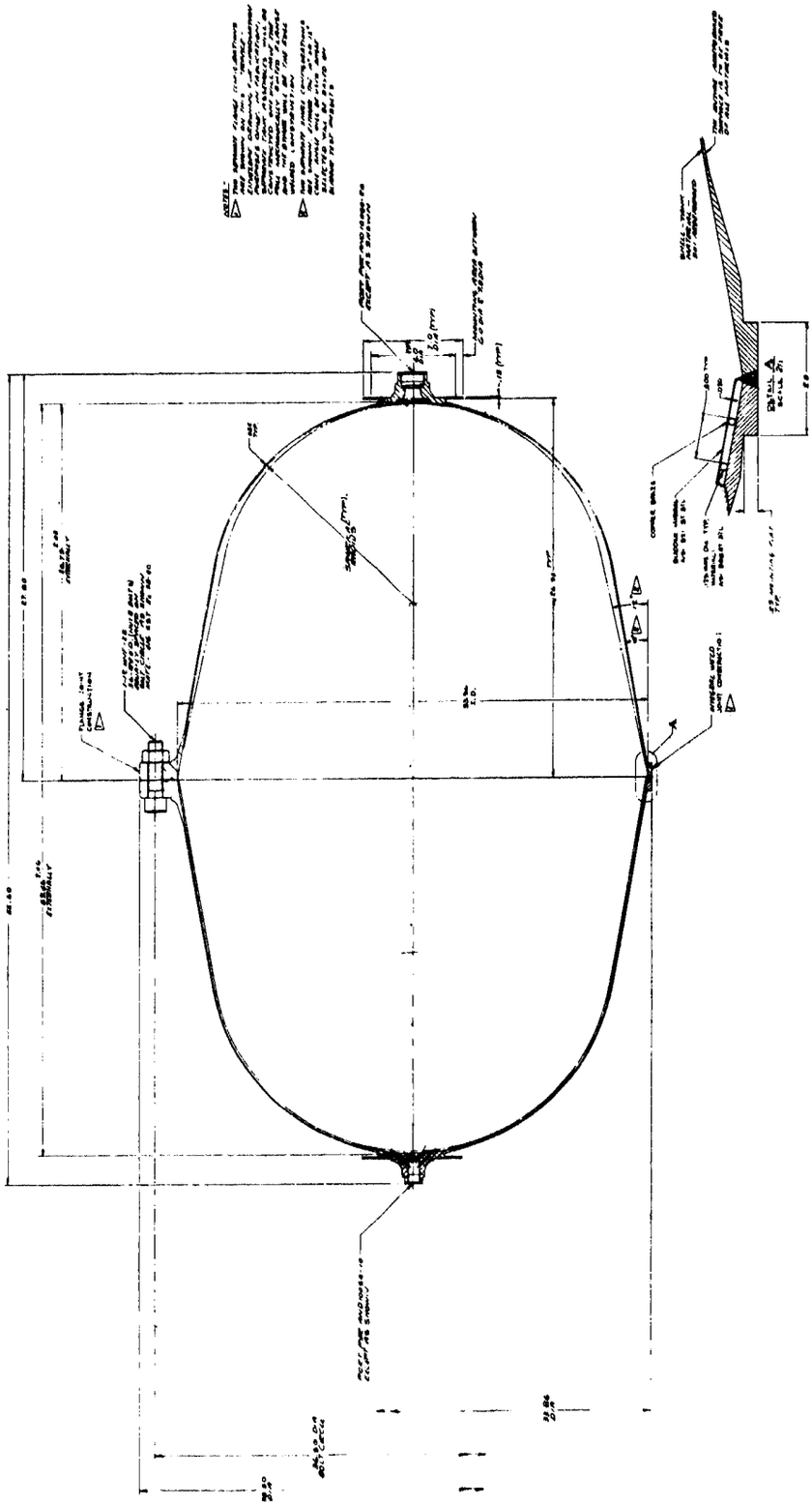

Figure 35. Tankage/Expulsion Subsystem Interface Drawing

Figure 36. Typical Tankage Diaphragm Girth Joints

Joint # 3

ADVANTAGES

1. Single Weld
2. No crevice corrosion due to similarity to brazed joint i.e. fillet.
3. Simple
4. Demonstrated fillet control by gas back-up. No drip-through or splatter problems.

DISADVANTAGES

1. Visually inspectable from one side only, unless bladder is reversed.

Joint # 4

ADVANTAGES

1. Fluid will not contact final structural weld.
2. Bladder weld easily inspected visually.
3. Partial penetration structural weld avoids weld splatter.

DISADVANTAGES

1. Does not lend itself to machine welding of bladder to shell without considerable development.
2. Wires must be attached to inside of bladder; development required.
3. Joint is heavy and bulky.
4. Bladder must be reversed prior to use.

Figure 36. Typical Tankage Diaphragm Girth Joints

IV, B, Propellant Tank/Expulsion Subsystem (cont.)

The weld development program was initiated. Effort was concentrated upon developing proper joint design and welding procedures for the No. 3 type joint design.

Stainless-steel cylinders were fabricated to simulate the tankage while flat-stainless-discs were used to simulate the diaphragms. The diameters of these parts were equivalent to full-size tankage and diaphragms. In addition, subscale cylinders were fabricated.

The primary objectives of the weld development program were twofold. First, a full-penetration weld had to be obtained. Secondly, the size of the fillet between the diaphragm and the tank had to be accurately controlled. To accomplish these objectives, experimental welds were made to ascertain the proper setting of critical weld parameters, including gas back up pressure, voltage, amperage, weld-speed, weld-wire size, and weld-wire feed-rate.

Initial trials showed that:

- The simulated large-diameter cylinders formed by rolling and welding were not fabricated to tolerances representative of the actual tankage
- The thin metal discs simulating the diaphragm warped excessively during welding
- Some type of joint-chamfering on the outside diameter, inside diameter, or both, would be required to achieve weld-design objectives

Additional tests were performed using subscale cylinders that were accurately machined to simulate joint dimensions and actual subscale diaphragms produced as part of the subscale diaphragm program.

A modified "J-groove" joint preparation with an internal cut-back was machined on a subscale cylinder. This configuration was successfully welded to the diaphragm. The "J-groove" design reduced the amount of weld material required for deposit on the first pass and limited the miniscus formed on the inside diameter; however, considerable remelt of the first-pass weld material was required to fill the remainder of the groove.

A "V-type" groove joint preparation then was machined and successfully welded. Proper melt-through was achieved and accurate groove-filling between diaphragm and tank-halves was accomplished. The "V-groove" weld was tentatively selected as the prototype weld method.

As soon as full-scale hardware became available, a full-sized weld specimen was prepared, using the "V-groove" joint. This specimen

had a full-size CRES 321 forged-ring as the tank section and an actual full-size CRES 321 diaphragm, P/N D104305-S/N 70.

A single-pass-weld was used followed by a cosmetic-weld-pass. The single-weld-pass was made completely around the ring and no weld-wire was used. The cosmetic-weld-pass was made only about two-thirds of the way around the ring using type 308L weld-wire. After welding, the part was helium leak-checked and no leaks were noted. The part was dye-checked and no dye-check indications were found.

Two micro-specimens were cut from the ring. One was cut across the section having both the single-weld-pass and the cosmetic-weld-pass. It also exposed the weld-joint. The other micro-specimen was cut across the single-weld-pass section of the ring to expose the weld-joint.

In addition, two samples, each approximately 2-in. long, were cut from the weld section of the ring. One sample was taken from the single-pass weld area while the other was taken from the double-pass weld area.

The 2-in. long single-pass weld area sample showed excessive weld penetration into the bladder material and undercutting at the bladder. Except for this, the welded joint was considered to be of very good quality.

The weld-joint on the full-scale verification tank assembly was evaluated when the inlet and outlet tank-halves as well as the bladder were welded at the girth-joint. The results of this welding are discussed in Section IV,B,2,e.

All objectives of the weld development program were satisfied. The "V-groove" weld design was selected as the prototype weld method. Figure No. 37 shows the final weld design. Vendor specifications were prepared for both the proper welding procedure (Arde Spec AES 501) and inspection (Arde Spec AES 550) of the weld.

c. Full-Scale Diaphragm Development

(1) Fabrication

Based upon the results of the subscale diaphragm development program, a 10-degree cone taper angle was selected for the full-scale diaphragm. The Bendix Corporation of Santa Ana, California, was the diaphragm-forming vendor. This vendor used a forming process involving a two-step operation. The first-step produced a "preform," which conformed to the general geometry of the final diaphragm but was much smaller in size. In the

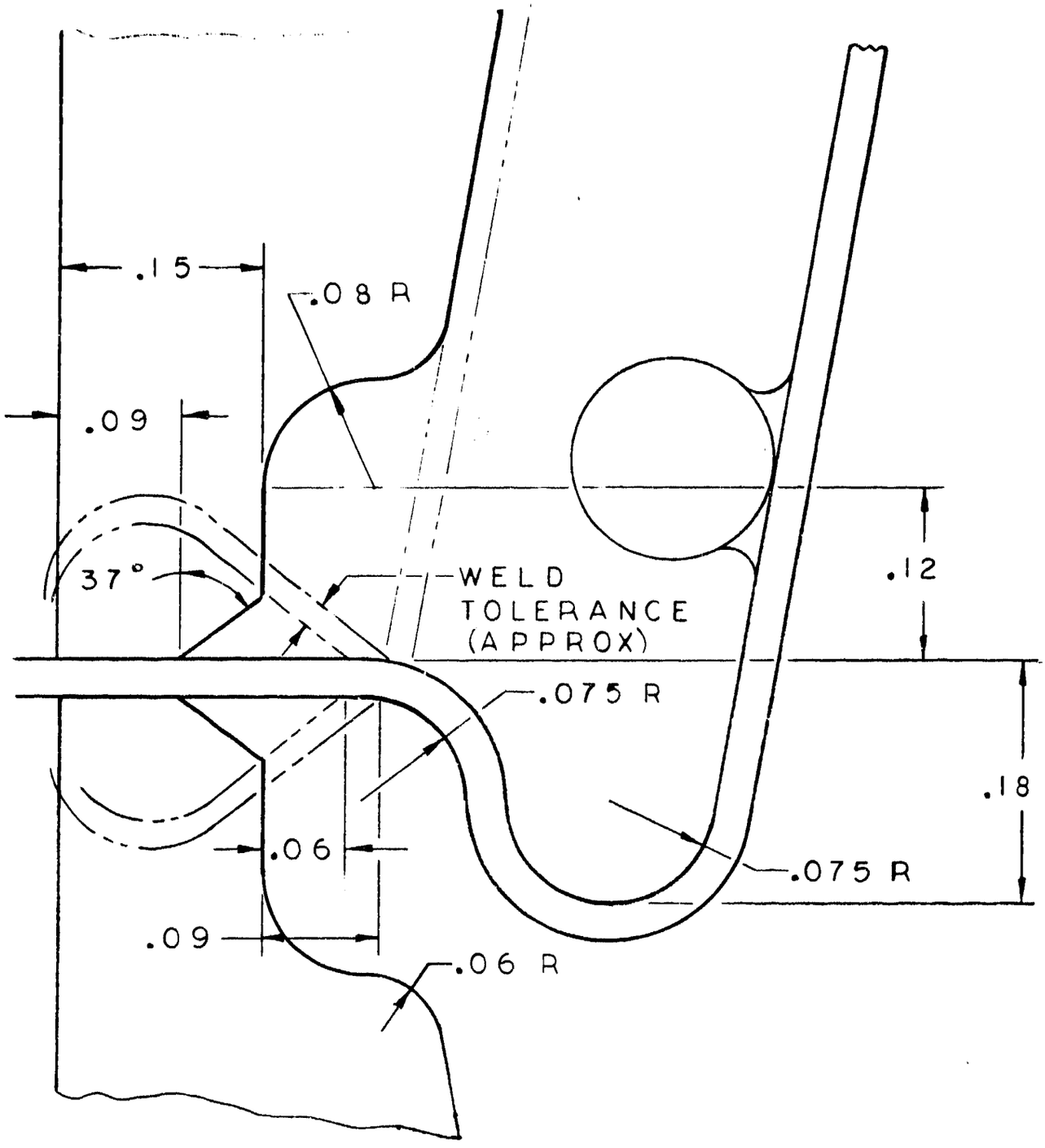

Figure 37. Final Weld Design

second step, the preform was placed into a properly tooled and fixtured female-die; then, it was hydraulically-stretched to its final size and shape.

The vendor encountered considerable difficulties in attempting to produce the 20-mil thick conospheroid shell shown on Figure No. 38.

The primary problem involved the fabrication of the preform. The Bendix "preform" was fabricated using a pack-draw process through a single-draw ring (see Figure No. 39), but the necessary blank size was very large in relationship to the draw-ring diameter because of the required depth of the draw. The flange resistance, friction, draw-ring, and other process forces combined to prevent the metal from flowing through the draw-ring. This resulted in an excessive metal "thin-out" in the "preform" dome, which caused the part to become too thin or to rupture during the stretching operation. The "preform" had to undergo considerable stretching during the final sizing and shaping operation. This problem was not experienced when the more common pure-hemispherical-shape was fabricated.

In analyzing the problem, it was recognized that in a hemisphere, the ratio of the depth of the draw to the ring diameter was L/D = 0.5 and the ratio of the draw-ring diameter to the blank diameter was favorable. As a result, the problems of flange resistance and excessive dome "thin-out" were not encountered. The conospheroid diaphragm shell had a draw-depth-to-part-diameter ratio of 0.8. The conospheroid shape dictated that the draw-ring diameter had to be smaller than the final part diameter to prevent premature lock-up in the stretch-cavity; therefore, the ratio of draw-ring diameter to blank diameter was very poor. To overcome this latter problem, preform fabrication attempts continued at Bendix with the use of staged draw-rings, which served to draw more metal (surface-area) through the draw-rings. A stainless-steel sheet was placed between two sheets of body-metal and this laminated assembly was processed through the staging dies. Bendix made more than 20 attempts to produce a suitable experimental preform.

At the time the preform fabrication problem was first identified, a back-up vendor was engaged. This back-up vendor, B. H. Hubbert and Son of Baltimore, Maryland, used the more conventional mechanical punch-and-draw-ring deep-drawing process. Intensive development of the deep-draw process was conducted to produce the required preforms. A significant problem that quickly became identified with the deep-draw process was the excessive thinning of the preform wall in the transition section between the hemispherical-dome and cylindrical skirt.

The back-up vendor produced six experimental preforms from 25-mil stock. Although these preforms were of marginal wall thickness,

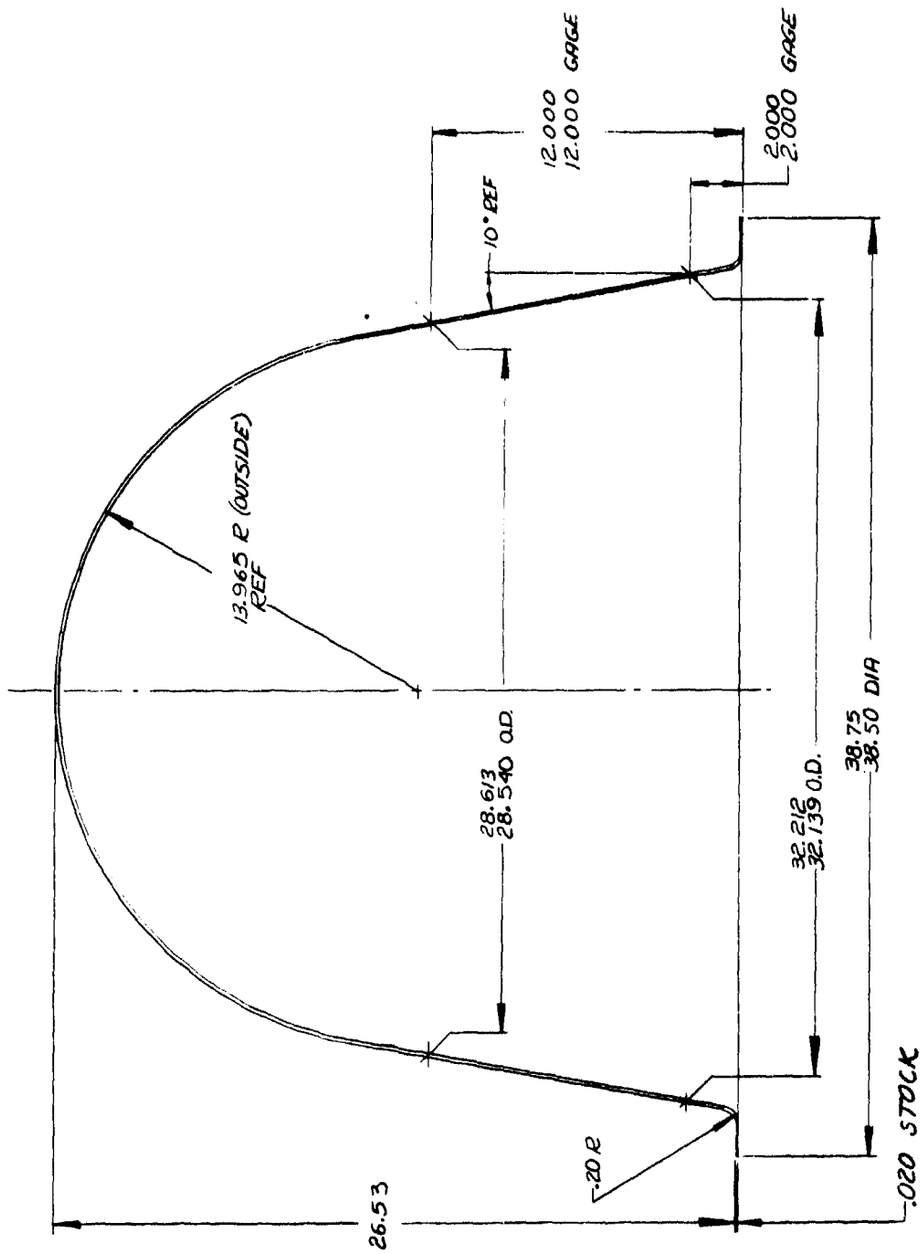

Figure 38. Conospheroid Expulsion Diaphragm Shell

321 SS - First Draw
Free Form Thru Draw Ring

Approx.: - Diameter 28 In.

Height 17.4 In.

Dome Thin Out 35%

321 SS - Second Draw
Unfolding into Cavity

Approx.: Diameter 32 In.

Height 18.6 In.

Note: Free Form Background Comparison

321 Stainless Steel

Left - S/N 1 Second Draw
Right- S/N 2 First Draw

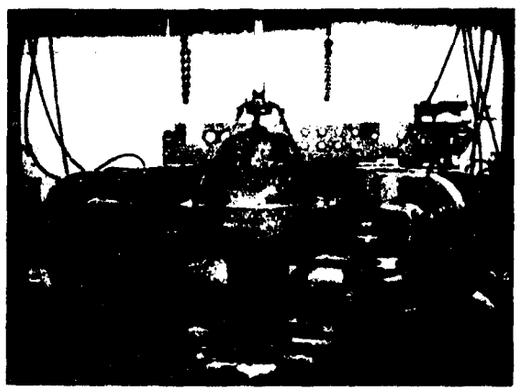

Final Stage Tooling
Cavity Installed

Figure 39. PBPS Propellant Tank Bladder Shell Development

they were shipped to Bendix for stretching to permit further evaluation of the stretching process. Excessive thinning (8-mils to 10-mils) prevented the diaphragm from stretching to full-depth. Three of the preforms ruptured and the remaining three achieved a height range of 22-3/4-in. to 24-in.

Another attempt was made by the back-up vendor to produce preforms wherein 32-mil material was substituted for the 25-mil material previously used. Two experimental 32-mil "preforms" were fabricated, but they exhibited the same characteristic thinning within minimum thickness readings of 13-mils to 15-mils. However, both of these units were delivered to Bendix, where they were successfully stretched to final size and shape. Figure No. 40 shows the first of these units. Measurements indicated a diaphragm shell thickness of approximately 21-mils near the flange, 11-mils at the knuckle, and a dome thickness of 19-mils. The two units were shipped to Arde, Inc. for processing into full-expulsion diaphragm assemblies.

At this time, it was decided to proceed with fabrication of the full diaphragm assembly despite the non-uniform wall thickness. It was judged that the fabrication development of a perfect, uniform wall diaphragm could become unduly costly and time-consuming. Therefore, no further diaphragm shell fabrication development was attempted to provide the more optimum shell uniformity. It was judged that the non-uniform shell could be controlled by proper spacing and sizing of the reinforcing wire rings to produce a satisfactory expulsion diaphragm demonstration. The preform vendor fabricated 25 additional preforms for expulsion diaphragm assemblies.

The following three areas of fabrication work also were under way during the course of initial preform development.

(a) A method was developed for calibrating and checking the Vidigage used to measure the part thickness. A mechanical micrometer was designed and fabricated. It was used to check the part thickness near the shell flange and to establish a base for calibration of the Vidigage.

(b) Stretch procedures were evolved, based upon actual component stretches. Experimental diaphragms were grid-marked for strain evaluation and analyzed at each step of the processing.

(c) Cleaning and annealing procedures were evolved.

The initial full-scale expulsion diaphragms received by Arde, Inc., did not conform to blueprint specifications either in height or thickness. These units were 0.060-in. to 0.070-in. too high and varied in wall-thickness from 0.011-in. to 0.027-in. as previously noted. Corrections were subsequently machined into the Bendix stretch cavity to provide the proper diaphragm height.

Figure 40. Full-Scale Expulsion Diaphragm Shell

IV, B, Propellant Tank/Expulsion Subsystem (cont.)

Braze experiments were performed with a subscale and a full scale diaphragm.

Six of the 25 production preforms were received and stretched at Bendix, after which they were delivered to Arde.

Arde Inc., completed the first full-scale diaphragm assembly by fabricating reinforcing wires, which were installed on the diaphragm. This first diaphragm assembly was identified as S/N 60 (see Figure No. 41). The diaphragm was unsuccessfully tested soon afterward.

As a result of the testing performed with S/N 60, fabrication changes were required for the next diaphragms to be completed. These diaphragms, identified as S/N 61 and S/N 71, incorporated: diaphragm shells that were electro-polished in the critical flange/cone region to 0.016 $\pm$ 0.001-in. shell thickness; a reverse fold gutter in the diaphragm flange (see Figure No. 42); Wire No. 1 was moved as close to the flange "gutter" as possible; and the ring wire diameter was increased from 0.125-in. to 0.188-in. in the region from the flange through the cone-hemisphere joint area. Wire No. 1 and dome wires were 0.156-in. diameter.

Initial electro-polishing attempts were conducted on diaphragm S/N 70, but difficulties were experienced. The rate of material removal was monitored by the electro-polish vendor by means of a control sample. The sample part thickness was checked periodically to determine how long the actual part should be processed. However, the Vidagage inspection of S/N 70 diaphragm indicated that the thickness reduction was considerably more than the sample with the result that the shell was reduced more than had been desired. At approximately 5-in. up from the flange, the thickness was 0.011-in. as contrasted to the blueprint requirement of a 0.017-in. minimum. The cause of this high rate of reduction was attributable to the particular tooling and shell geometry. It was not a problem as long as a running checks of the thickness reduction were made at several intervals during processing.

Based upon the S/N 70 experience, successful electro-polishing of S/N 61 and S/N 71 was completed. This success was achieved in part by a minute Vidagage inspection of the shell and establishing a detailed map of the thickness. The unit was then selectively masked and electro-polished. Intermediate Vidagage inspection was performed during the process to assure proper wall thickness reduction.

The diaphragm reinforcing wires were installed prior to brazing S/N 61 and S/N 71. Tacking the wires to the diaphragm was much more difficult using the larger diameter wire because it was considerably stiffer than that previously used. When the rings were fitted to the diaphragm,

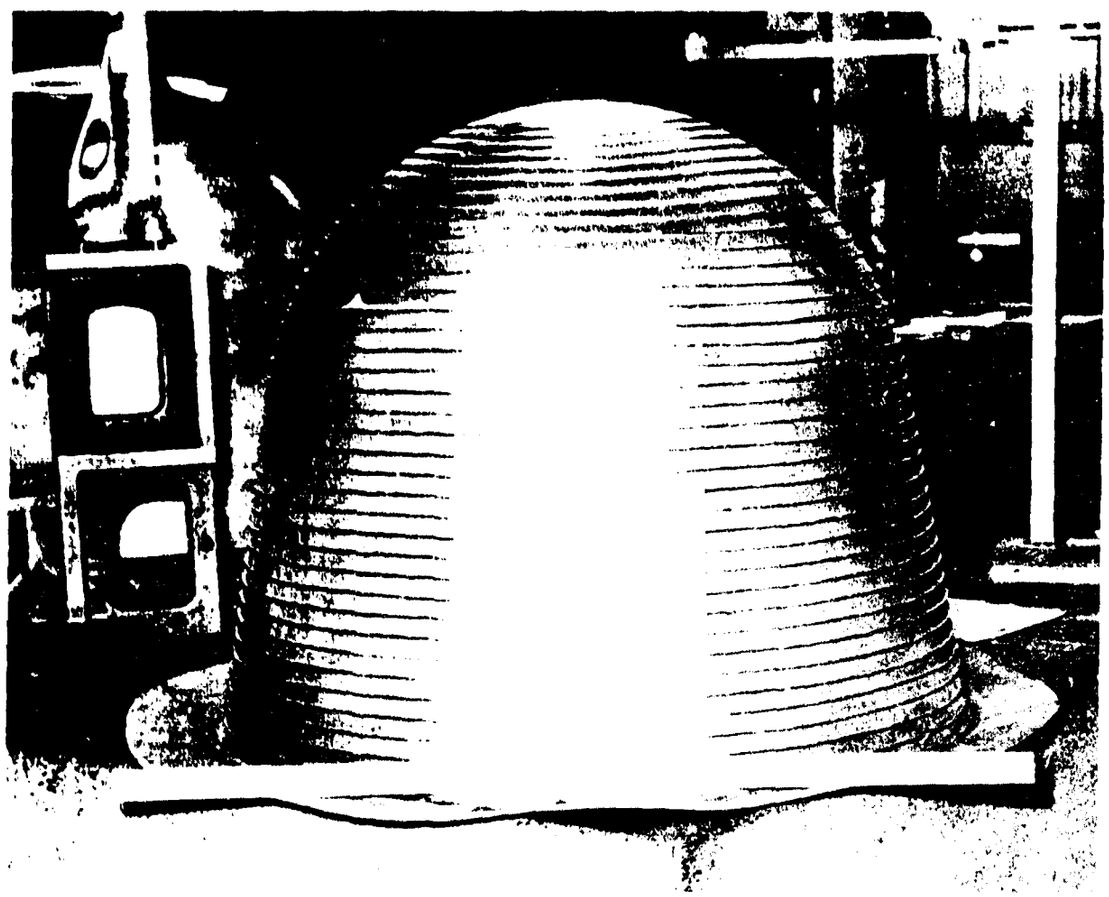

Figure 41. Full-Scale Expulsion Diaphragm

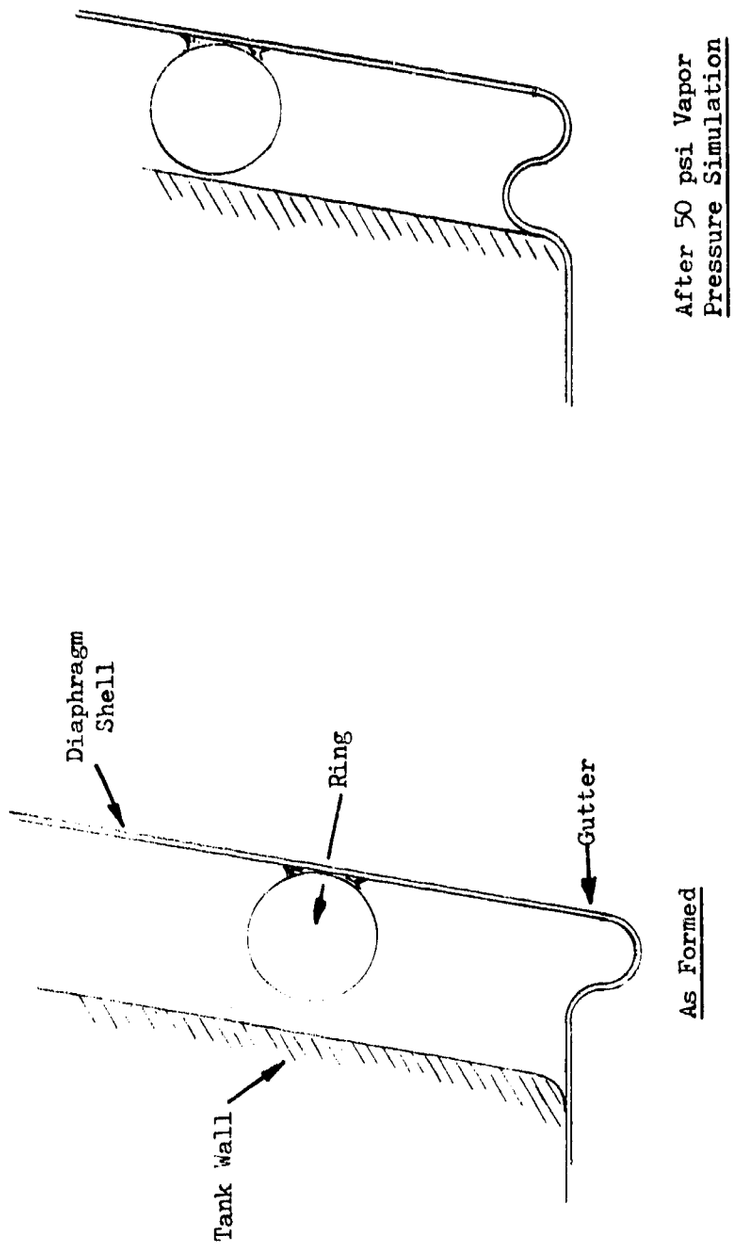

Figure 42. Diaphragm Flange "Gutter" Section

IV, B, Propellant Tank/Expulsion Subsystem (cont.)

these stiffer wires did not readily conform to the contour and required excessive fit-up. This affected the tacking because improper fit-up necessitated a high tacking voltage, which sometimes resulted in a shell burn-through requiring subsequent repair.

An effort was directed toward improving this processing. Some of the items investigated included partial annealing of the wire rings to reduce the ring stiffness and tacking the wire to the diaphragm shell prior to the ends being welded together into a ring. The wire ends would then be helium-arc welded into place. Both of these methods followed by brazing were used to install the wires. The fabrication of two diaphragm assemblies, S/N 61 and S/N 71, was completed. These units were essentially of the same configuration. They were used for demonstration testing.

Based upon the successful diaphragm reversal test of S/N 61 diaphragm, Bendix undertook the forming of the remaining 19 diaphragm shells fabricated by B. H. Hubbard and Son. During the forming of the first six of these shells, five suffered distortions. These distortions ranged from slight depressions (i.e., a pattern of gentle folds in two of the shells) to a random pattern of relatively sharp folds in three of the final formed group. All of the distortions were located in the knuckle area of the shells.

A close examination of the second group of six units, which had been processed through the second forming and anneal cycle, revealed slight depressions in four of the units. Two of the units were then subjected to the third forming cycle. One of the two units was processed in two pressure stages to observe the effect of bulge pressure upon the distortion. Most of the distortion was removed after the high pressure sizing cycle. The next unit was then subjected to the normal, single, high-pressure forming cycle used for the six shells. Examination revealed no evidence of distortion in the original area. However, the same random pattern of sharp folds found in three of the initial six units was observed. The new distortion occurred at approximately the same height but was rotated approximately 75-degrees from the original minor distortion.

The cause of this distortion was undetermined although many possible causes were investigated. These included: distortion caused by relaxation of the forming strains induced in the part at the second forming cycle during the subsequent anneal; handling damage; improper venting of the cavity; eccentricity of the part and cavity on "clamp-up"; racking or elongation of the shell in heat treat causing the cavity to hang up on the part and distort it in compression; and localized "thin-out" causing a blister which is subsequently compressed.

The corrective action implemented by Bendix was to limit the stretched height to less than final size during the second stretch

operation of the part when the cavity is sized. In addition, "spring-back" was taken out during the third cycle only.

The dome section of one diaphragm, S/N 58, was successfully electro-polished to provide a diaphragm assembly that would follow the apex roll mode of collapse. The apex surface within an 8.5-in. diameter circle was reduced to a 0.012-in. to 0.014-in. thickness. This special diaphragm was subsequently tested.

After diaphragm S/N 71 was successfully tested in the rim roll mode, all of the remaining diaphragm fabrication was committed to electro-polishing for the rim roll mode type of collapse.

The effort to improve the tack welding of the wires to the diaphragm had continued with another bladder sample (S/N 67) being fabricated using a two-electrode system and annealed wires. The wires on the cone were pre-welded before tacking and the wires on the hemisphere region were welded closed subsequent to tacking. Wire fit-up was more difficult on the hemispherical portion of the shell; however, only limited imperfections resulted from the tacking. This new method represented a marked improvement over that used for the previous diaphragms fabricated.

Diaphragm S/N 73 was fabricated and was tested in conjunction with the tank verification unit.

All of the remaining bladder shells were successfully fabricated at Bendix. The reduction of shell deformation during the second pass (1/2-in. less part height) eliminated the shell rippling problems. Some part distortion ("stress relief" rippling during the last anneal prior to the final sizing pass) was noted in the cone-to-hemisphere transition region. However, the parts were small enough with respect to the cavity that these "dents" were removed by the final sizing pass. Fabrication of these shells was then completed at Arde.

(2) Testing

Five full scale conospheroid reversing diaphragms were tested during this program. Four of these five diaphragms were subjected to reverse pressure seating tests and full diaphragm reversal tests. One assembly underwent a full diaphragm reversal test only.

Four of the five diaphragms were tested in a test rig or a flanged tank-half while one was tested in actual flight-weight tankage. The four tests using the test rig/flanged tank-half are reported in this section while the verification test evaluating the diaphragm in the flight weight tankage is subsequently discussed. Table XVIII is a summary of all diaphragm testing.

TABLE XVIII

FULL-SCALE DIAPHRAGM TEST SUMMARY

TEST DATE	DIAPH. SN	REINFORCING WIRE SIZE	NO. OF WIRES	WIRE SPACING	DIAPHRAGM DESCRIPTION PRIOR TO TESTING	DESIGN MODE OF COLLAPSE	TESTING CONDUCTED	SUMMARIZED RESULTS
Early May '67	60	0.125 Dia	37	First wire at 0.6-in. from flange. Remainder at 0.8 in. intervals	Shell thickness variation approx. 0.027-in. near flange. Approx. 0.011-in. cone to hemisphere transition area. Approx. 0.019-in. dome. Diaphragm had straight flange joint.	Rim Roll Mode	1.Reverse pressure seating test (1 @ psi) 2.Diaphragm reversal test	Distortion of diaphragm between wires. Height of diaphragm increased 0.22-in. Flange radius decreased from 0.25 to 0.156. Diaphragm axis shift due to eccentric alignment in test rig. Began rim roll at actuation pressure 3-4 psi, then began apex roll mode. Reversal was uncontrolled. Wire buckling occurred, wires jammed, reversal continued to completion but leaks and tears occurred.
2 Aug '67	61	Wire 1 and 22 through 35, 0.156-in dia. Wires 2 through 21-0.188-in. dia.	35	First wire 0.15-in. above flange. Wires 2-13, 1.20-in spacing. Wire 14, 1.10-in. spacing. Wire 15, 0.90-in. spacing. Wires 16-35, 0.70.	Diaphragm had reverse fold "gutter" at flange joint. Shell electropolished to 0.018/0.002-in. critical flange/cone region. Weld & braze repair performed on shell	Rim Roll Mode	1.Diaphragm reversal test	Successful diaphragm reversal. Rim roll collapse began at 3-4 psi actuation pressure. Max. actuation pressure was 7 psi. The collapse was uniform and controlled. Three pin hole leaks occurred all occurred in areas of prior repair.
13 Sep '67	71	Same as SN 61	Same as SN 61	Same as SN 61	Same as SN 61	Rim Roll Mode	1.Reverse pressure seating test (50 psi) 2.Diaphragm reversal test	Successful test distortion of diaphragm between wires similar to SN 60 but not as severe. Flanged "gutter" changed shape from single hump to double hump. Distance from diaphragm flange to apex extended by 0.012 to 0.018-in. Distance from "gutter" to apex shorted by approx. 0.118-in. There was no unusual damage to the diaphragm shell caused by the seating test. Successful diaphragm reversal. Rim roll collapse began at 4-5 psi actuation press diaphragm successfully rolled over wire 1 when shell collapsed between wires 19 & 20. Collapse probably resulted from interference with close fitting tank. With interference relieved, unit again began rim roll. Rim roll and apex roll modes continued until complete reversal was achieved. No jamming or interference of wires

TABLE XVIII (cont)

TEST DATE	DIAPH. SN	REINFORCING WIRE SIZE	NO.OF WIRES	WIRE SPACING	DIAPHRAGM DESCRIPTION PRIOR TO TESTING	DESIGN MODE OF COLLAPSE	TESTING CONDUCTED	SUMMARIZED RESULTS
	71 (cont)							was noted. One weld or braze repair area developed a slight leak.
Mid Oct '67	58	Same as S/N 61	Same as S/N 61	Same as S/N 61	Dome section electro-polished over 8.5-in.dia circle to achieve thickness of 0.012 to 0.014-in.	Apex Roll Mode	1.Reverse pressure seating test (50 psi)	Successful test usual distortion of diaphragm between wires. Diaphragm height increased approx. .03-in. No other significant changes noted.
					Diaphragm had straight flange joint, no "gutter"		2.Diaphragm reversal test	Apex roll mode initiated at 2-4 psi. Wire interference occurred at cone/hemisphere transition section. Actuation pressure increased to 10-12 psi. Wire buckling occurred. Rim began rolling & alternate rim & apex rolling modes until complete reversal was achieved. Maximum actuation pressure was 20 psi. Uncontrolled collapse and considered unsuccessful test.
Mid Nov '67	73 Tested in conjunction with verification tank assy.	Same as S/N 61	Same as S/N 61	Same as S/N 61	Diaphragm sustained one inch dia. hole during electro-polishing but was successfully repaired.	Rim Roll Mode	1.Reverse pressure seating test (50 psi) (Tested in conjunction with verification tank assembly)	Successful test. Gaseous helium leak check showed no indication of leakage after 50 psi ΔP across diaphragm. Visual inspection not performed. (Diaphragm enclosed in welded tank).
							2.Diaphragm reversal test (Tested in conjunction with verification tank assembly).	Successful test. Diaphragm reversal smooth & readily controlled. Actuation pressure [illegible] psi. Water was discharged from tank during this test. Slight diaphragm leakage was indicated after test during helium leak check. Suspected repaired area of diaphragm leak. Visual inspection not performed (diaphragm enclosed in welded tank).

IV, B, Propellant Tank/Expulsion Subsystem (cont.)

The reverse pressure seating test involved pressurizing the interior of the diaphragm at 100 psi (later changed to 50 psi) to seat the diaphragm, with a "glove-like" fit against the interior of the tank. This test simulated the oxidizer vapor pressure loading, to which the diaphragm would be subjected during propellant storage. The vapor pressure of the nitrogen tetroxide varied between approximately 2 psia to 90 psia over the storage temperature range. (This pressure range was subsequently modified to between 2 psia and 50 psia because the storage temperature upper limit was changed.)

The diaphragm reversal test simply involves the pressurization of the exterior surface of the diaphragm causing it to collapse. In the actual application, propellant would be expelled from the tank.

(a) Test of S/N 60 Full-Scale Diaphragm

S/N 60 diaphragm (see Figure No. 43) was the first full-scale assembly to be fabricated and tested. Both the reverse pressure seating and the diaphragm reversal tests were performed. This full-scale diaphragm had been designed to follow the rim roll mode of collapse. There were 37, 1/8-in. diameter wires brazed to the shell exterior. The first wire, No. 1, was spaced 0.6-in. from the flange and the remaining 36 wires were spaced at 0.8-in. intervals.

Pre-test, theoretical calculations indicated that the unit would rim roll to the first wire only and would then follow an apex mode of controlled collapse because of the excessive cone thickness at the girth area.

1 Diaphragm Reverse Pressure Seating Test

The diaphragm assembly was placed into a water test-rig, which simulated a tank half. It was comprised of three parts: a conical tank, a cover plate, and a wooden plug insert. The plug insert was contoured to match the hemispherical portion of the diaphragm assembly, thereby simulating the tank bottom. Also, the plug supported the diaphragm assembly from the apex through the 28th wire, which left an unsupported diaphragm span of approximately 5-in. In addition, a 1/8-in. "out-of-round" condition existed between the conical wall and the diaphragm flange clamping ring.

The diaphragm seating test was performed by placing the diaphragm into the rig, filling the diaphragm with water, installing the cover plate, raising the water pressure to 100 psig, and holding this pressure for several minutes.

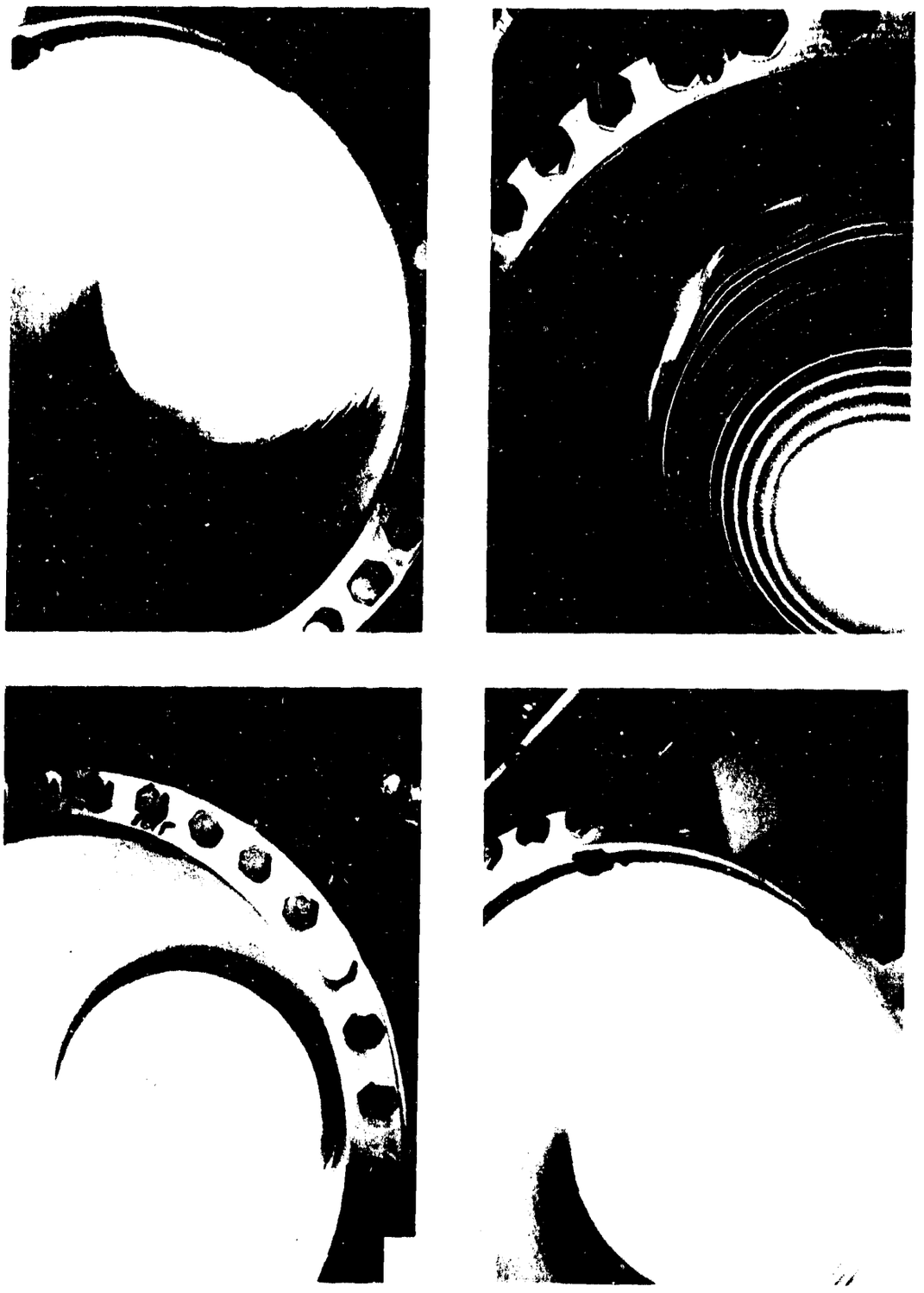

Figure 43. Initial Diaphragm S/N 60 Reversal Test

IV, B, Propellant Tank/Expulsion Subsystem (cont.)

Post-test examination revealed the following:

- A permanent, caternary type of diaphragm shell deformation existed between the wires. This deformation was barely discernible near the flange, but it increased in severity as it progressed towards the apex.

- The diaphragm assembly gained 0.222-in. in height (from 26.603-in.).

- The flange radius decreased from 0.200-in. to 0.156 in.

- The 28th wire, where the plug support ended, was indented into the diaphragm shell approximately 1/16-in. and covering approximately one-half of the ring circumference. This deformation resulted from the conical tank being out-of-round, the axial movement of the diaphragm, and the incomplete support of the diaphragm dome. As the diaphragm was pressurized, the diaphragm shell was forced to comply with the eccentricity of the tank, thereby translating the diaphragm axis. This translation, plus the axial movement of the diaphragm as it rolled the flange, as well as the inability of the plug to shift transversely, forced a localized buckling of the shell about the last wire (the 28th) seated on the plug.

2 Diaphragm Reversal Test

The diaphragm was reinstalled into the water test-rig and subjected to an open-air diaphragm reversal test. Water, controlled through a needle valve, was the actuation medium.

The shell thickness variation of diaphragm S/N 60 was approximately 27-mils near the flange, 11-mils at the knuckle from the conical to the hemispherical section, and tapered to a dome thickness of approximately 19-mils. The wires were numbered 1 through 37 beginning at the flange.

At a diaphragm actuation pressure of 3 psi to 4 psi, the unit began to roll between the 28th and 27th wires at precisely the same area which had sustained the localized shell buckling during the 100 psi seating test. Then, the unit rolled the 29th and 30th wire ring on one side before it completed the 28th wire on the opposite side (see Figure No. 43). At this point, the unit began straightening out, completing the roll of the 29th and 30th wires on the opposite side. When the unit rolled over the 31st wire, it was perfectly symmetrical with the rolled or reversed surface forming the spherical zone between the 27th and 31st wires. From the 31st through the 36th wire, the reversal was completely controlled, rolling only one wire at a time (see Figure No. 43). Here, the unit began to follow the

apex mode of collapse after having rolled over the 27th wire on one side. However, the reversal was uncontrolled and continued to roll over the 26th and 25th wires on the same side, thereby cocking the rolled segment of the diaphragm. As a result of this cocking action, cross-wire buckling was observed through the formation of meridional pleats or nodes (see Figure No. 43). As the cocking became more severe, the nodes became more pronounced and assumed the shape of a ten-pointed star. The reversal was continued in the cocked configuration with the nodes undercutting the shell, interfering with the next wire, and causing horizontal hoop folds between the wires (see Figure No. 43). The cocking action continued until the diaphragm jammed on one side. At this point, a pin-hole leak was observed at one of the nodes between the 16th and 17th wires. The reversal was continued to completion and several folds tore and leaked.

3 Analysis of Test Results

Analysis of S/N 60 diaphragm testing results showed shell thickness to be the major consideration regarding shell buckling resistance and minimum actuation pressure. The wire diameter control led the actuation pressure peaks; therefore, a trade-off was necessary between diaphragm flexibility and buckling resistance.

Based upon the results of this first test, it was decided to redesign the diaphragm to obtain a diaphragm configuration that would follow the rim roll mode of controlled collapse. In addition, the following plan for fabricating and testing the next diaphragm was evolved:

- Electro-polish the diaphragm shell to a thickness of 0.016 $\pm$ 0.001-in. in the critical flange/cone region.
- Incorporate a reverse fold "gutter" in the diaphragm flange to aid in initiating a rim roll mode of actuation.
- Place Ring No. 1 as close to the "gutter" as possible.
- Increase the ring wire diameter from 0.125-in. to 0.188-in. in the region from the flange through the knuckle transition of the cone to the spherical dome to provide improved actuation control.
- Provide 0.156-in. diameter wires in the spherical dome.
- Eliminate the 100 psi vapor pressure simulation test with this unit to permit a more accurate evaluation of the variables involved.

IV, B, Propellant Tank/Expulsion Subsystem (cont.)

(b) Test of S/N 61 Full-Scale Diaphragm

The fabrication of diaphragms S/N 61 and S/N 71, which were almost identical configurations, was essentially completed at the same time. Both units incorporated a reverse fold "gutter" to aid in initiating a rim roll mode of controlled collapse. They were electro-polished to a nominal 0.018 $\pm$ 0.002-in. in the critical flange/cone region where the shell tapered from 0.027-in. to 0.014-in. The electro-polished area was blended into the tapered cone and the nominal wire spacing was as follows:

Wire No. 1: 0.156-in. diameter spaced 0.15-in. above flange.

Wires No. 2 through No. 13: 0.188-in. diameter at 1.20-in. spacing.

Wire No. 14: 0.188-in. diameter at 1.10-in. spacing.

Wire No. 15: 0.188-in. diameter at 0.90-in. spacing.

Wires No. 16 through No. 21: 0.188-in. diameter at 0.70-in. spacing.

Wires No. 22 through No. 35: 0.156-in. diameter at 0.70-in. spacing.

1 Diaphragm Reversal Test

A successful diaphragm reversal test with the S/N 61 unit was accomplished. Sequential photographs of the diaphragm reversal are shown on Figure No. 44. The reversal was controlled, rolling one wire at a time. Photograph 1 of Figure No. 44 shows the unit prior to test while Photograph 2 shows it at the initiation of the rim roll mode of collapse. Photographs 3 through 8 show the progressive stages of reversal with the numbered wire positions being visible. Photograph 9 is a picture of the inside of the diaphragm showing the control rings after a complete reversal. The metal scale running across the diameter as a unit of reference was 36-in.

The rim roll mode of collapse was initiated at an actuation pressure of 3 psi to 4 psi. This actuation pressure rose to 5 psi for the 33rd wire, 5.25 psi for the 34th wire, and 7 psi for the 35th wire.

Three pin-hole leaks occurred during the reversal test. All of these leaks were in areas of heavy braze and weld repair. The heavy braze fillets sheared the diaphragm as they rolled through the sharp bend radius of the reversing shell.

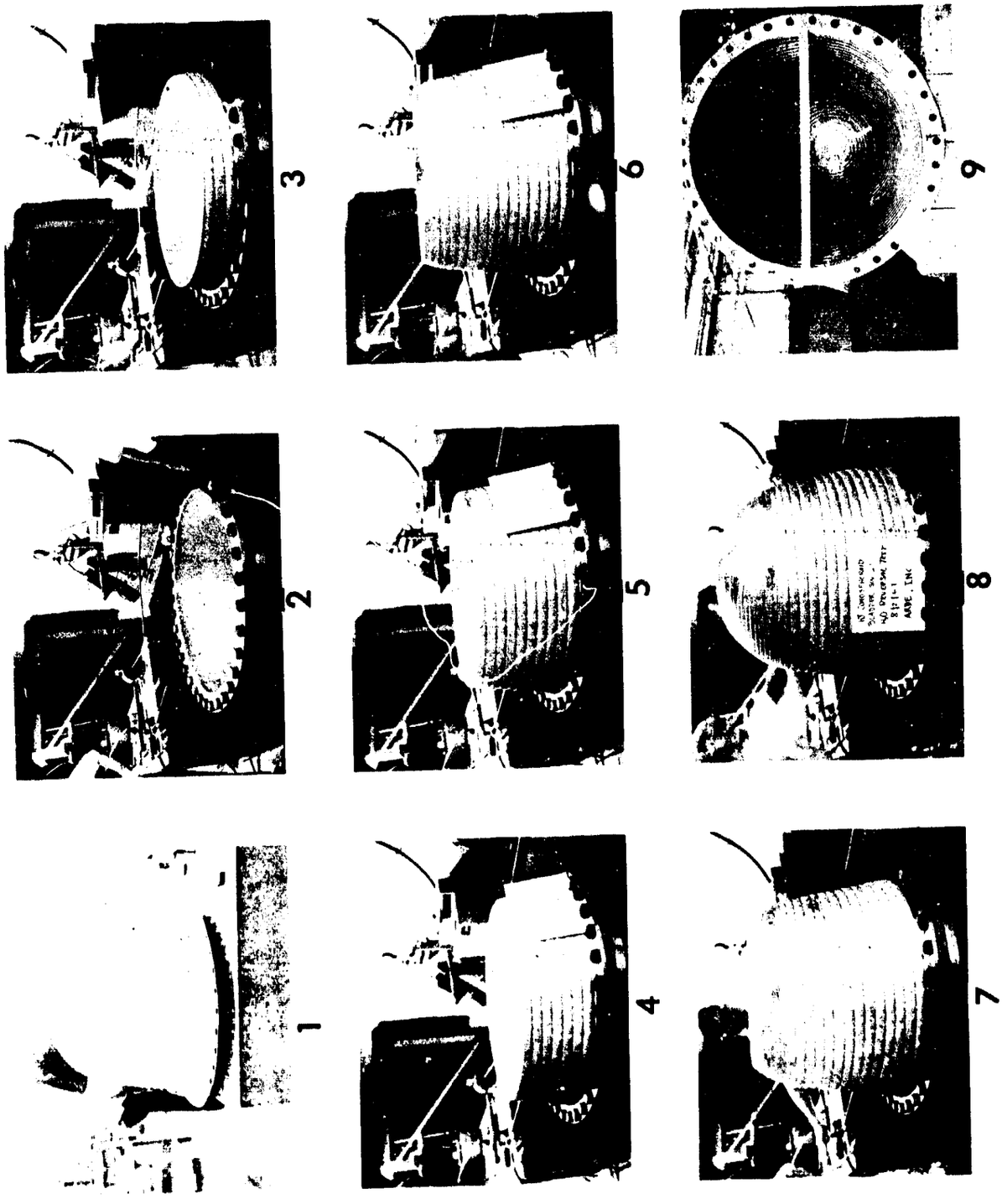

Figure 44. Diaphragm Reversal Test - S/N 61

IV, B, Propellant Tank/Expulsion Subsystem (cont.)

(c) Test of S/N 71 Full-Scale Diaphragm

The requirement for pressure seating the diaphragm was re-examined. It was re-established that a "glove-fit" of the expulsion diaphragm and tank was mandatory to ensure success in withstanding the vapor pressure loads and shipping handling criteria. This minimum clearance between diaphragm and tank reduced axial motion to that compatible with the capability provided by the "gutter" in the diaphragm while providing structural support for the various loads. The final diaphragm size would be achieved by stretching each one into a typical tank containing a suitable liner to compensate for the control wire thicknesses. Match-fitting bladders to each tank instead of using a liner would be another way to ensure this fit.

1 Diaphragm Reverse Pressure Seating Test

Diaphragm S/N 71 was subjected to a 50 psi vapor-pressure-simulation seating test. In this test, the oxidizer vapor pressure loading to which the diaphragm would be subjected during propellant storage was simulated and corresponded to a propellant temperature of approximately 125°F. The diaphragm was assembled into a flanged tank-half which was lined with hard rubber to provide a "glove-fit" between the diaphragm and tank. This fit simulated the tolerances that would be obtained between the "stretched" diaphragms and welded tanks. Then, the cover plate was installed, the diaphragm filled with water, the water pressure was raised to 50 psig, and held for several minutes.

Post-test examination revealed the following:

- Permanent catenary type diaphragm shell deformation existed between the wires. The deformation was barely discernible near the flange but increased in severity towards the apex. This deformation was very similar but not as severe as that obtained with diaphragm S/N 60 which was subjected to a 100 psig seating test (based upon a maximum potential N_2O_4 storage temperature at 150°F). Subsequently, the maximum storage temperature was identified as 125°F.

- The flange section was changed from a single hump to a full, single cycle, sine sweep as shown on Figure No. 42. The second half of the sine cycle was created when the diaphragm flange was formed around the tank flange inner radius.

- The distance from the diaphragm flange to the apex length extended by 0.012-in. to 0.040-in.

IV, B, Propellant Tank/Expulsion Subsystem (cont.)

- The distance from the "gutter" to the apex shortened by approximately 0.143-in.
- There was no unusual damage to the diaphragm shell caused by the seating test.

2 Diaphragm Reversal Test

The diaphragm was reinstalled into the tank half and subjected to an open-air reversal test. The actuation medium was water controlled through a needle valve. Figure No. 45 contains a set of sequential photographs of the successfully controlled diaphragm reversal.

The unit began to rim roll at the flange "gutter" at a diaphragm actuation pressure of 4 psi to 5 psi as shown on Photograph 1 of Figure No. 45. The unit successfully rolled over wire No. 1 at 6 psi and continued to roll toward wire No. 2 when the shell collapsed between wires No. 19 and 20 (shown on Photograph 2) at the same radial locations where maximum "rim-walking" was obtained. This collapse occurred in the area of minimum shell thickness.

As the unit "walks," the shell is forced to cock for a distance equal to the wire spacing. This cocking causes the dome section to swing or translate. Therefore, it is hypothesized that as the diaphragm translated, the dome section was forced to bear on the close-fitting tank in a localized area. This local pressure caused eccentric loading of the diaphragm shell and its collapse in the same area.

The unit rolled the 20th and 21st wires at an actuation pressure of approximately 3.5 psi to 4.0 psi. The, the unit rolled the 22nd wire on one side before completing the 21st wire on the opposite side. Again, it rolled over the 23rd wire on one side before completing the 22nd wire on the opposite side. Following this, the unit straightened out and completed rolling wire No. 23 (as shown on Photograph 3) at an actuation pressure of 3.5 psi to 4.0 psi. Then, under complete control, the unit rolled the 24th through the 30th wires, one at a time (Photograph 4) at actuation pressures varying from 2 psi to 4 psi. After completing the 30th wire, the unit started to rim roll again in the flange area and rolled wire No. 2 at an actuation pressure of 6.5 psi. The unit then apex rolled wire No. 19 at 7 psi, rim rolled wire No. 4, and apex rolled wire No. 17 in that order (Photograph 5) at an actuation pressure of approximately 9 psi to 9.5 psi. Next, the unit rolled through wire No. 31 in the dome at a pressure of 9.5 psi to 10 psi. The reversal continued predominately in the roll mode of actuation by rolling wires No. 5 through No. 11 (Photograph 6) at an actuation pressure of 10 psi to 11 psi. The unit then apex-rolled wire No. 16 at 11 psi followed by rim

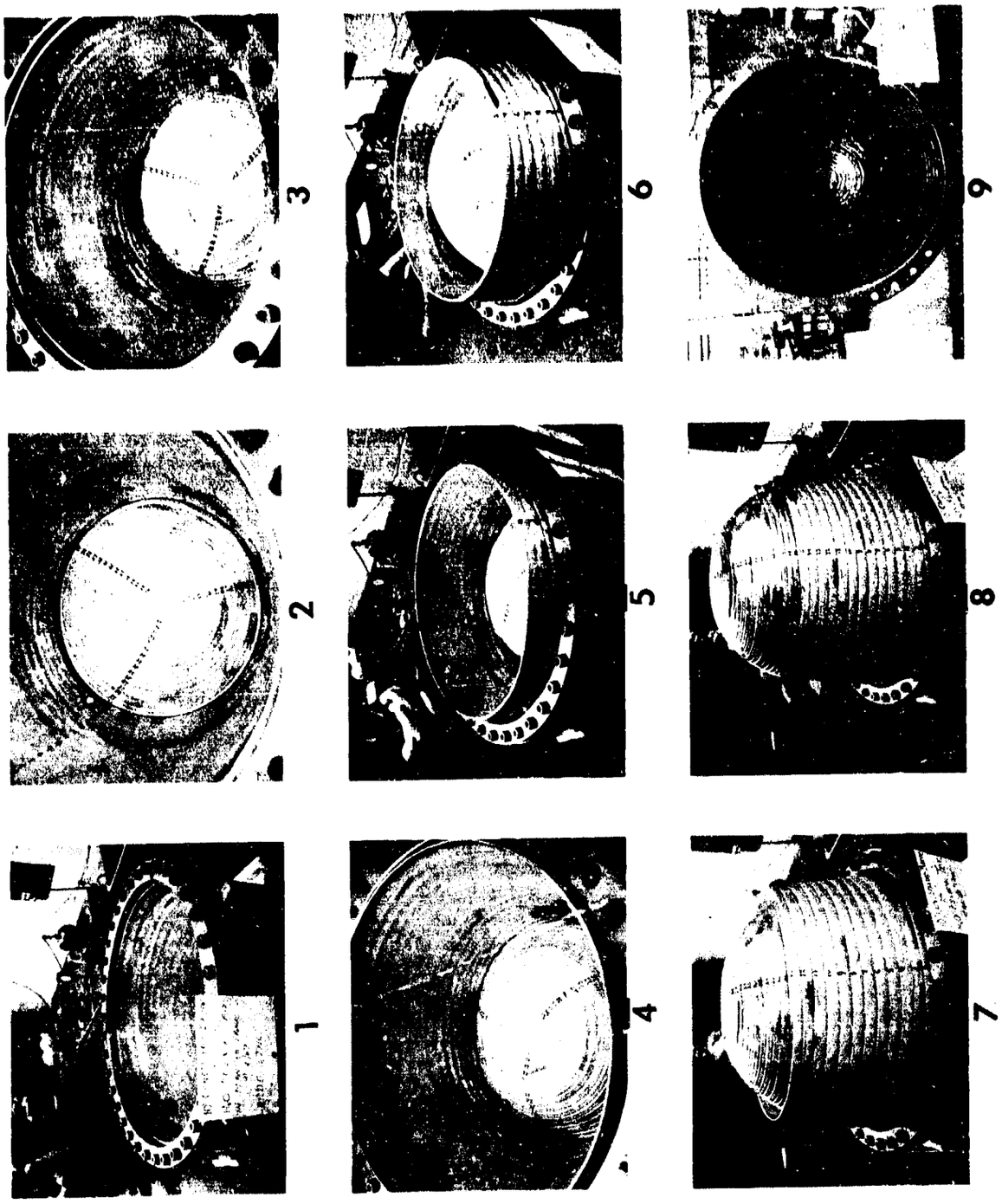

Figure 45. Diaphragm Reversal Test - S/N 71

rolling wires No. 12 through No. 15 (Photograph 7) at 10 psi to 11 psi. The unit satisfactorily rolled through the intersection of both the apex and rim rolling modes of actuation between the 15th and 16th wires. No jamming or wire interference was noted. The reversal was completed by rolling wires No. 32 through No. 35 in the dome with a peak pressure of 12 psi required to "oil-can" the apex. Photograph 8 shows the unit at the conclusion of the reversal cycle while Photograph 9 pictures the inside of the diaphragm showing the control rings after the complete reversal.

(d) Test of S/N 58 Full-Scale Diaphragm

During the course of the development program, it was determined that an apex mode of controlled diaphragm collapse would be a more desirable mode for diaphragm units subjected to transverse acceleration loads. Appropriate parametric studies (i.e., wire size, spacing, shell thickness, and actuation pressures) were completed. Results indicated that the upper dome of the shell would require electro-polishing to obtain the desired mode of collapse. This electro-polishing was completed and the apex mode diaphragm was subjected to a diaphragm reverse pressure seating test and a diaphragm reversal test.

1 Diaphragm Reverse Pressure Seating Test

The apex roll mode bladder (S/N 58) was tested using the lined, flanged tank-half to simulate the "glove-fit" desired between the tank and bladder. The test consisted of a 50 psi internal set pressure test. A 0.18-in. thick spacer ring was reworked to a 33.34-in. inside diameter and was used in the internal set pressure test to compensate for the absence of a diaphragm gutter (0.18-in. deep) at the equator region.

The "apex roll" diaphragm (S/N 58) was successfully tested at the 50 psi set pressure test. The diaphragm height increased approximately 1/32-in. because of the internal pressurization and the occurrence of some puffing between the wires. No other significant bladder geometric changes were noted.

2 Diaphragm Reversal Test

In the reversal test, the small apex region thinned out by electro-polishing, first reversed at approximately 2 psi. This was followed by an apex roll of the top wire at 4 psi. The apex roll behavior continued until wire interference was noted at the cone hemisphere transition region and on the cone. The actuation pressures increased to approximately 10 psi to 12 psi and there was buckling across wires and in the sheet between the wires. Then, the rim started to roll to relieve the wire

IV, B, Propellant Tank/Expulsion Subsystem (cont.)

interference effects. Alternate apex and rim roll behavior continued with actuation pressures increasing to approximately 20 psi as a result of the wire interference until the bladder was completely reversed. The sequenced photographs of S/N 58 diaphragm reversal are shown on Figure No. 46.

The significant aspects of the S/N 58 diaphragm reversal test are as follows:

- Despite wire interference and the buckling of some wires and sheet, the bladder was completely reversed. This demonstrated the "ruggedness" of the wire-reinforced bladder and its ability to function completely under extreme conditions.
- "Squeezing" the bladder together by the actuation pressure during the apex roll deformation, which enhances wire interference possibilities particularly on the shallow angle cone region, was again demonstrated.
- The bladder rim rolled to relive the wire interference effect.
- This test was not a satisfactory demonstration even though complete reversal was achieved since the reversal was not controlled by the wire rings.

d. Tank Shell Development

(1) Fabrication and Testing

The original tank fabrication plan was to fabricate a complete welded preform assembly, cryostretch the assembly, separate the tank into halves for diaphragm installation, and to reweld the assembly.

Several problems associated with this method of fabrication became evident during the detailed fabrication planning stages. There was difficulty in maintaining preform position in the stretch die, uneven stretching of each half of the tank within the die, and the loss of both halves if one-half failed. As a result, the original fabrication plan was modified.

The improved fabrication technique provided for each tank half to be made separately and stretched individually in the same die. This afforded better physical control of the preform in the die and resulted in more uniform pieces, reduced scrap loss, and lower die cost. This process is shown on Figure No. 47. The cryogenic stretch die was fabricated by the Standard Tool Co. of Los Angeles, California.

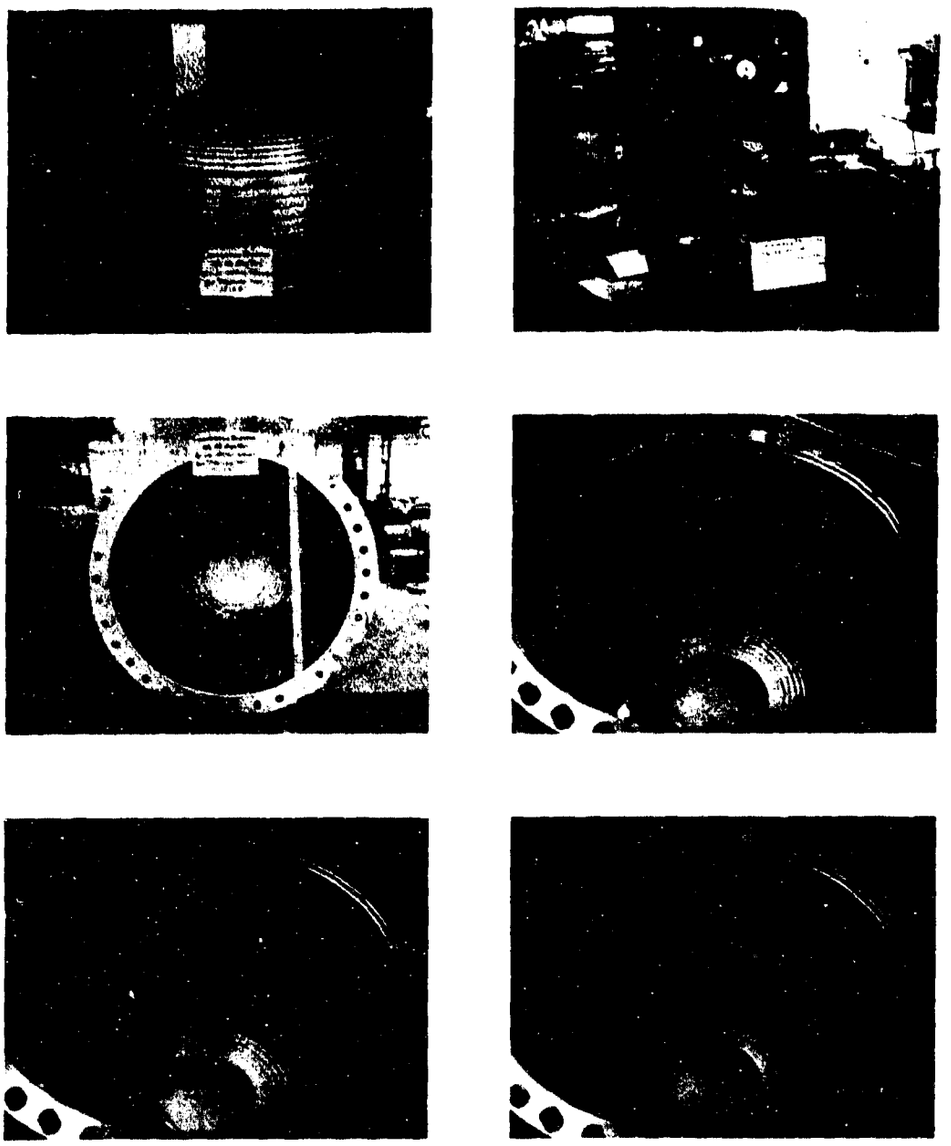

Figure 46. Conospheroid Apex Roll Bladder - S/N 58

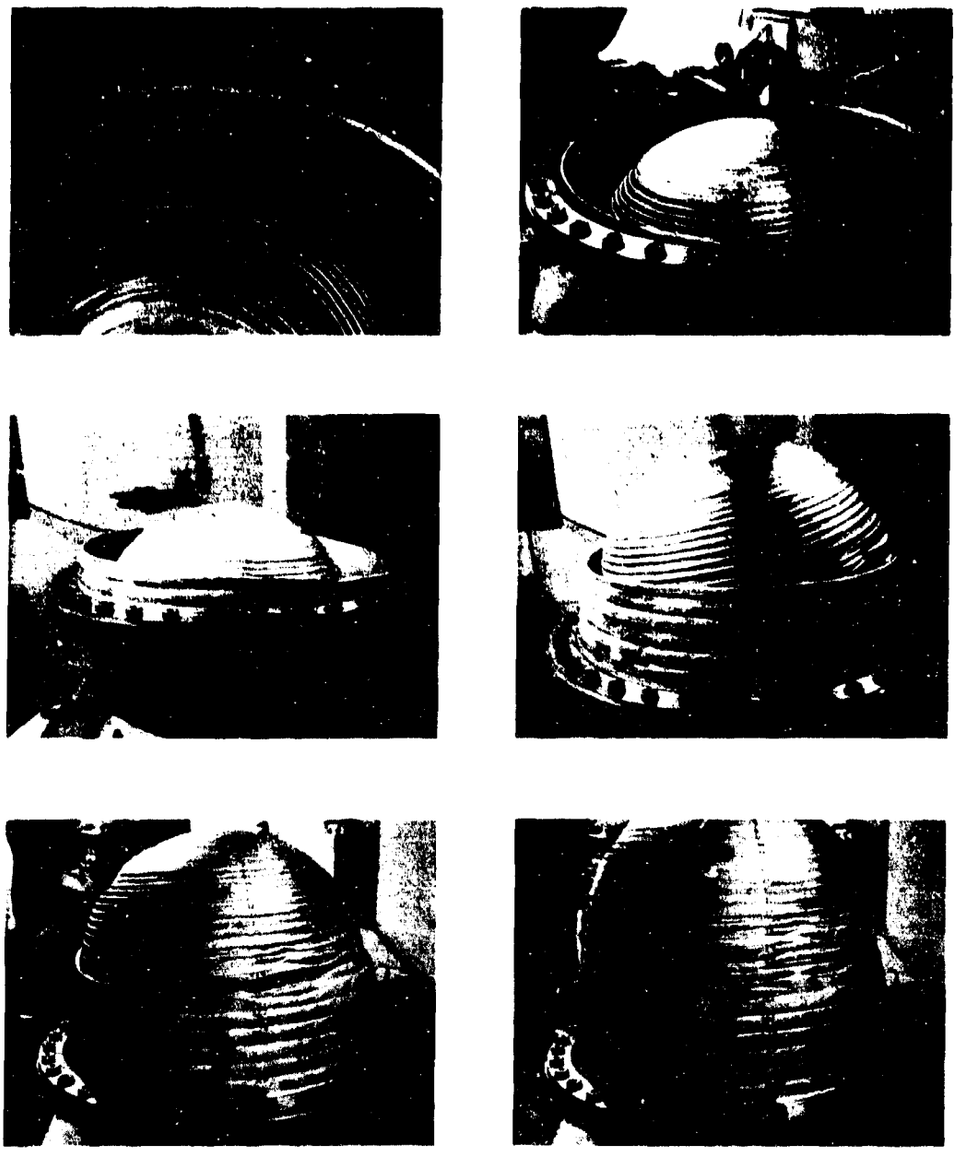

Figure 46. Conospheroid Apex Roll Bladder - S/N 58

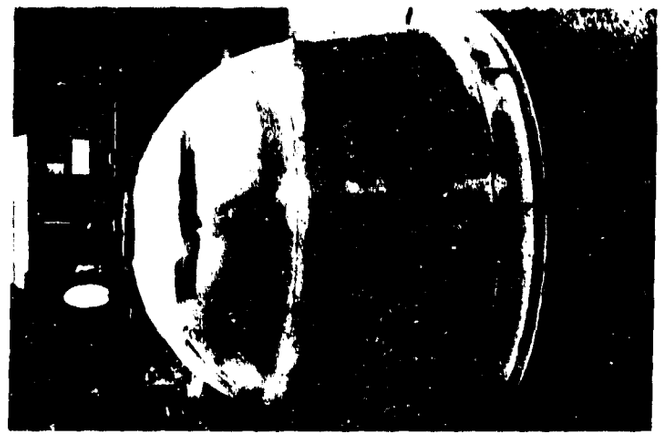

COMPLETED TANK-HALF

TANK-HALF IN STRETCH DIE

TANK-HALF PREFORM
PRIOR TO STRETCH

Figure 47. Advanced PBPS - Tankage Expulsion Subsystem

IV, B, Propellant Tank/Expulsion Subsystem (cont.)

Some problems were encountered in deep drawing the tank heads, but were corrected by a tooling modification.

The first two tank-half preforms were completed in April 1967. Each preform was fabricated from three separate pieces welded together (i.e., a hemispherical head, conical sides, and a flanged section on the girth ring). The first tank half was cryostretched at 1200 psi. Post-stretch examination revealed that it was approximately 1/2-in. short. Analysis showed that the shell stiffness provided by the end boss was greater than anticipated and thereby prevented the dome from fully seating into the die. New alloy bolts were provided for higher pressure capability.

Cryostretching of the second tank-half was then attempted. All of the 36 bolts holding the die closure plate failed at 1170 psi and the die parted, permitting the liquid nitrogen to escape. Examination revealed that the stretch die and the tank preform were undamaged. The bolts failed at approximately the same pressure as the maximum used during the first preform stretch; therefore the second preform also was approximately 1/2-in. short. Metallurgical examination of the bolts revealed that the heat treatment was not in accordance with specifications.

New, properly heat-treated bolt material was obtained and bolt fabrication was completed. These new bolts had a load capability of sustaining up to 2000 psi in the die.

The first flanged tank-half was successfully stretched during July 1967 at 1800 psi. This tank, which was 1/4-in. shorter than the original blueprint limits, was compatible with the "guttered" diaphragms which had a reduced height. However, the tank girth ring did not achieve the expected geometry during the cryogenic stretch operation. It was believed that the girth area was not properly formed because the flange ring locked into the die before the ring could fully expand. The tank was pressurized with water to further unfold the girth ring. A spacer was placed into the die to relieve any ring restraint and the water forming was done at 325 psig. The tank inside diameter and structure was found to be satisfactory.

The first flanged tank-half was completely fabricated and the tank-half was lined with rubber. It was utilized for the S/N 71 diaphragm test series and the S/N 58 apex roll mode diaphragm test. (Flanged tanks were subjected to low pressures during diaphragm seating and diaphragm reversing tests.)

The second flanged tank-half was successfully cryostretched at 1800 psi and hydrostretched at 440 psi. However, during the cryostretching of the third tank-half, the stretch die cover plate reinforcing

welds failed at 1700 psi. The stretch die was reworked and the stretching of the third unit was completed. This third tank-half was successfully hydrostretched at 750 psi.

Four tank-halves were fabricated. These flanged tank units were used only to support the full-scale diaphragm test program. Figure No. 48 is a photograph of a flanged tank-half.

In the latter part of this program, inlet and outlet verification tank preform halves were hydrostretched to 750 psi. The seal plate weld on the outlet half-leaked at low pressure. It was rewelded and then the tank half hydrostretched. Internal tank measurements were taken on the inlet tank half and it was found that the tank was too short to contain the verification tank diaphragm. The verification tank diaphragm, S/N 73, was slightly warped in the hemisphere region to permit installation into the short verification tank.

(2) Acrylic Tank

Only one side of the diaphragm could be viewed during the test in each full-scale diaphragm reversal test performed using the open air test rig. This did not provide an understanding of the tank-shell-to-diaphragm proximity, thereby making evaluation of the collapse mode from the wire ring side difficult.

An acrylic tank was fabricated by the American Polytherm Co. of North Sacramento, California. This would permit the diaphragms to be viewed from the pressurized side during tests.

Considerable difficulty was encountered in the fabrication of the tank. At least seven attempts were made to fabricate the tank shell before an acceptable unit was produced (see Figure No. 49). However, when the acrylic tank was finally completed, insufficient time was available in this program to use the assembly.

e. Tankage/Expulsion Subsystem Development

During the final month of this program, a full-scale welded tank and expulsion diaphragm assembly was satisfactorily demonstrated. The verification tank was assembled, welded at the girth joint, inspected, and tested. The welded tank assembly was inspected using dye penetrant, a gaseous helium leak check, and X-ray. Then, the tank was subjected to a 50 psi diaphragm internal set pressure equivalent to propellant vapor pressure during storage; also, a 440 psig proof pressure, a diaphragm reversal with water expulsion, and a tank burst test. All tests were successful. There was an

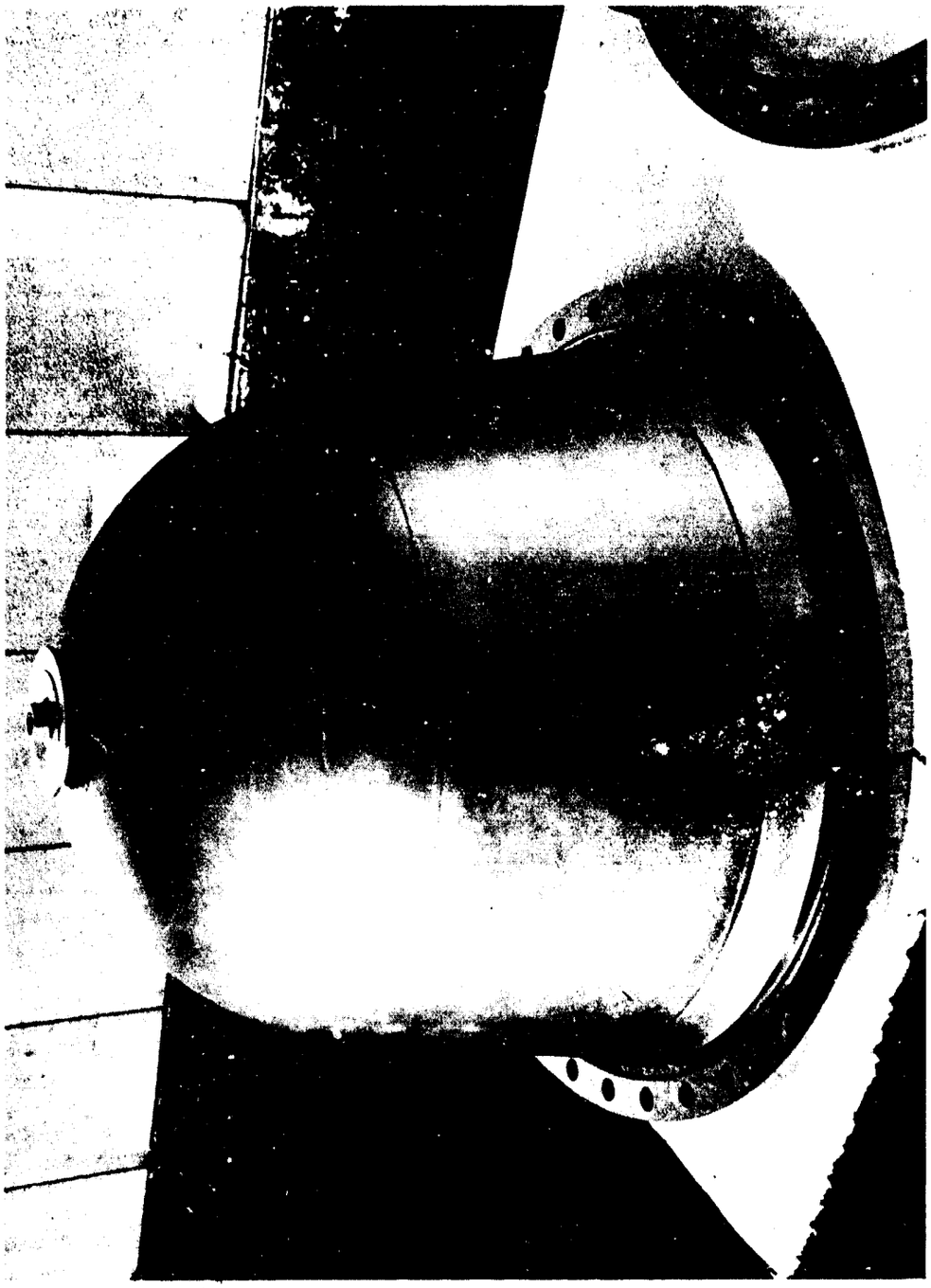

Figure 48. Flanged Tank-Half

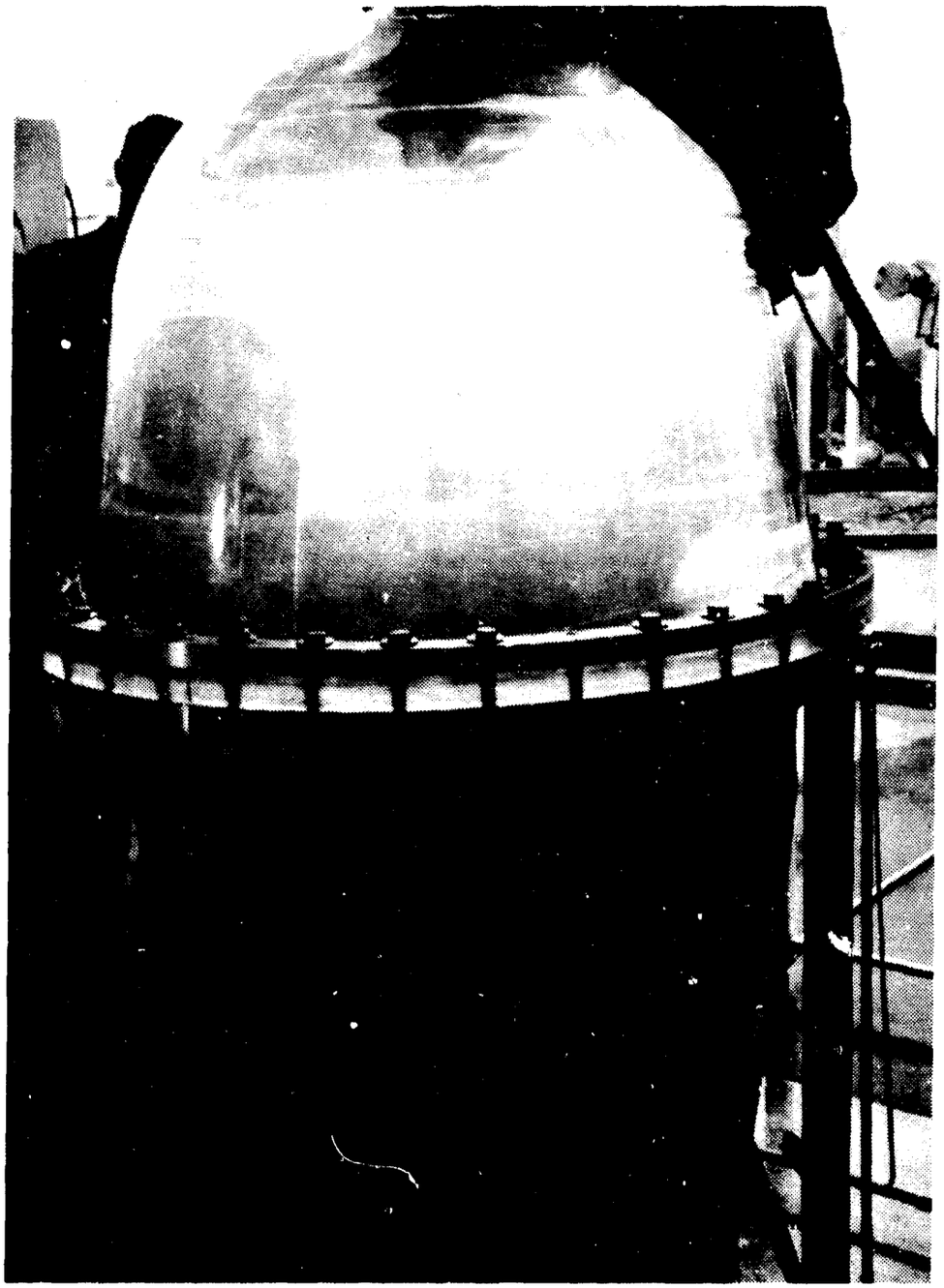

Figure 49. Acrylic Tank Reversal Test Set-Up

IV, B, Propellant Tank/Expulsion Subsystem (cont.)

indication of a small amount of expulsion diaphragm leakage with gaseous helium after complete diaphragm reversal. The tank burst at 1320 psig, which corresponded to the demonstration of a nominal hoop burst strength in excess of 250,000 psi. Sequential photographs of the verification tank assembly fabrication and test are shown on Figure No. 50.

The verification tank assembly (PN J3568 S/N 1) consisted of the S/N 73 diaphragm as well as inlet and outlet welded tank-halves (PN D3574, S/N 1 and PN D3567, S/N 1), welded together. The details of the verification tank inspection and the testing are outlined below.

(1) Tank-to-bladder-girth joint dye check: No surface crack indications.

(2) GHe leak check (ΔP across diaphragm of 50 psi simulates set pressure, ΔP across tank was 15 psi): No leakage indication.

(3) X-rays of girth joint: No significant porosity. Full penetration achieved but the "V" of the weld preparation was not completely filled in some spots.

(4) Tank assembly was proof tested at 440 psig with no significant yielding observed.

(5) Diaphragm reversal followed by GHe leak check: Diaphragm reversal smooth and readily controlled, ΔP range 3 psi to 8 psi, expulsion time one hour corresponding to approximately 18 ft^3 hr average water outflow rate. Slight diaphragm leakage was indicated by the GHe leak check after reversal. It was not possible to determine where the diaphragm leaked. This diaphragm assembly had a repaired area of a hole "burned" in during electro-polishing and this could have been the source of the slight leak.

(6) Tank burst test (1320 psig burst pressure): The failure was in the vicinity of the girth-ring-to-cone-girth weld. In the cone failure region, the radius r2 was equal to 16.5-in. and wall thickness was 0.06-in. It the structure acted as a cone, the membrane hoop stress was

$$\frac{P\ 2}{t} = \frac{1320 \times 16.5}{0.06} = 363.000 \text{ psi.}$$

This indicated the cone yielded in hoop direction because the expected yield strength of the material was approximately 230,000 psi and a finite radius of curvature was formed in the longitudinal direction. Assuming the structure acted locally as an intermediate between a cone and a sphere, the membrance shell theory would give 5 hoop = 0.75 x 363,000 = 272,000 psi as the hoop burst strength of tank. It was significant that the bladder-to-tank-girth weld joint did not limit the burst pressure and that a high strength tank was demonstrated.

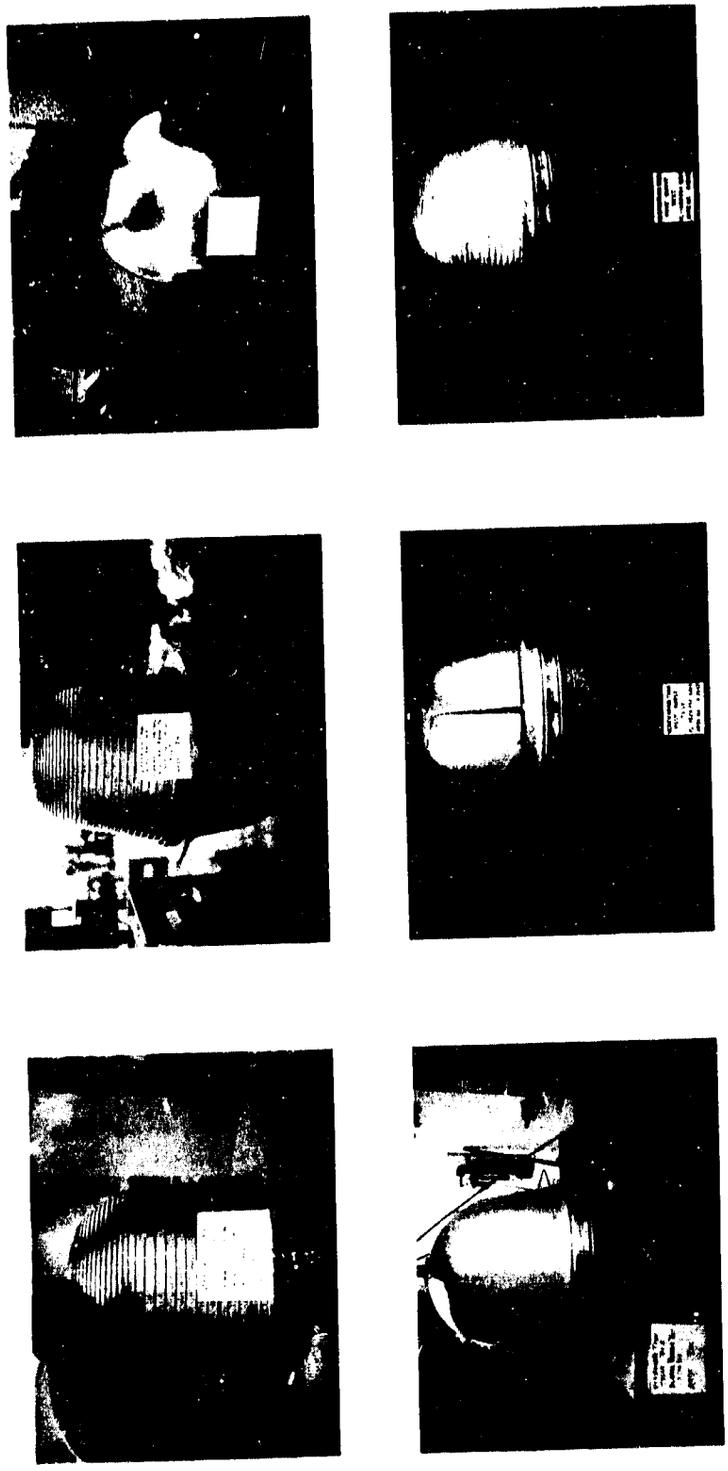

Figure 50. Verification Tank Assembly Fabrication and Test

IV, Phase II - Subsystem Development (cont.)

C. FLUIDIC CONTROL COMPONENTS

(C) The controls subsystem being developed was based upon the application of fluidic controls technology to perform the controls function of the PBV propulsion system. This fluidic controls subsystem development was performed by the Bowles Engineering Company of Silver Spring, Maryland. The controls subsystem performs two primary functions. First, it provides control of the pressurization subsystem. Secondly, it serves to control the propellant flow to the engines in response to demands from the PBPS guidance system. Hot gas from the pressurization system is the fluid used to perform the control functions concerning the propellant flow to the engines. This hot gas also is used for control of the two stages of the pressurization subsystem. Figure No. 51 is the controls subsystem schematic for PBPS application. Basically, this subsystem is comprised of six major fluidic components:

First-stage pressure regulator
Second-stage pressure regulator
Axial engine control module
ACS engine control module
Flow division module
Vent control module

The fluidic components contained within each of the control modules are shown on Sheet 2 of Figure No. 51.

(C) In operation, a pyrotechnic squib, fired on the upstream side of the first-stage bootstrap tank, provides the force necessary to shear a circumferential propellant isolation weld on the fluid side of the differential area piston. Hydrazine (N_2H_4) is then fed under pressure to the first-stage gas generator where it is decomposed in a Shell 405 catalyst bed. The resulting reaction provides 1400°F gas to the second-stage hydrazine tank as well as to the gas-side of the differential piston bootstrap tank. A metal burst diaphram isolates the system during storage. The gas flow to the bootstrap tank is controlled by the first-stage pressure regulator which senses the second-stage hydrazine tank ullage pressure and provides an error signal calling for additional flow until the second-stage hydrazine tank reaches the desired pressure level. The output of the second-stage tank passes through the second-stage pressure regulator which controls a liquid vortex throttle metering hydrazine to the second-stage gas generator. The resulting decomposed hydrazine gas pressurizes the main oxidizer and fuel tanks while providing gas flow to the ACS and Axial engine(s) vortex throttles.

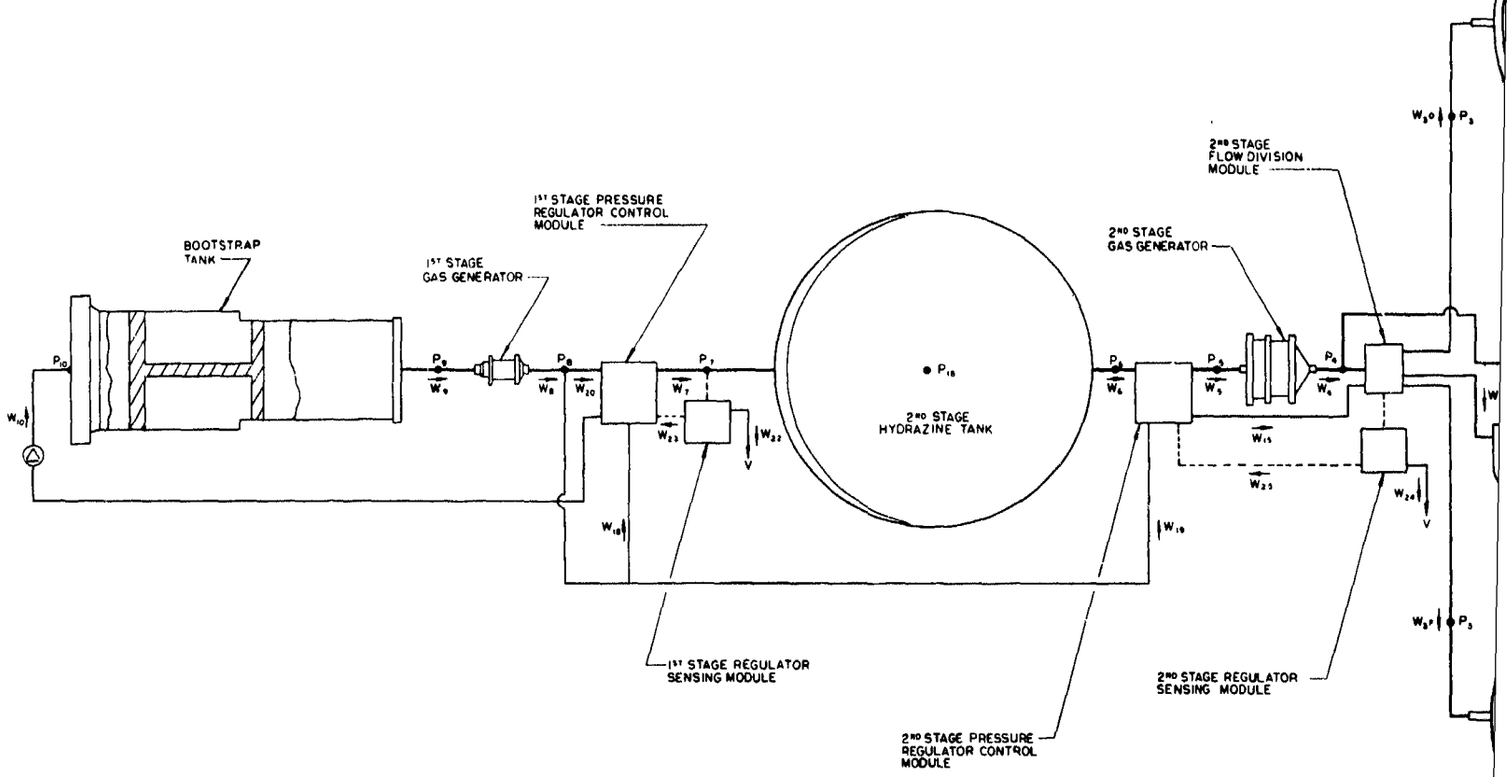
BOOTSTRAP TANK
1ST STAGE GAS GENERATOR
1ST STAGE PRESSURE REGULATOR CONTROL MODULE
2ND STAGE HYDRAZINE TANK
2ND STAGE GAS GENERATOR
2ND STAGE FLOW DIVISION MODULE
1ST STAGE REGULATOR SENSING MODULE
2ND STAGE PRESSURE REGULATOR CONTROL MODULE
2ND STAGE REGULATOR SENSING MODULE

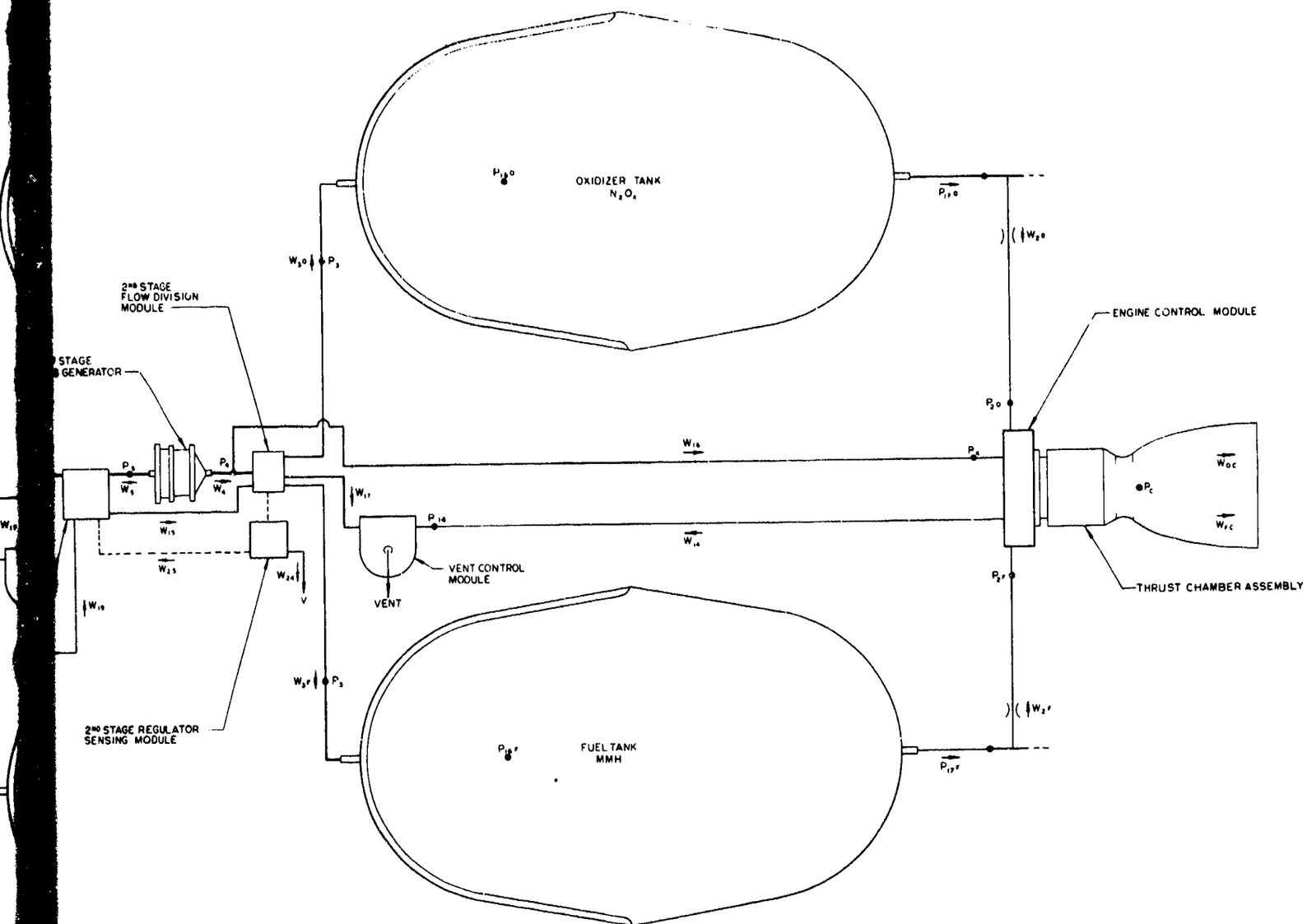

Figure 51. PBPS Controls Schematic (Sheet 1 of 2)

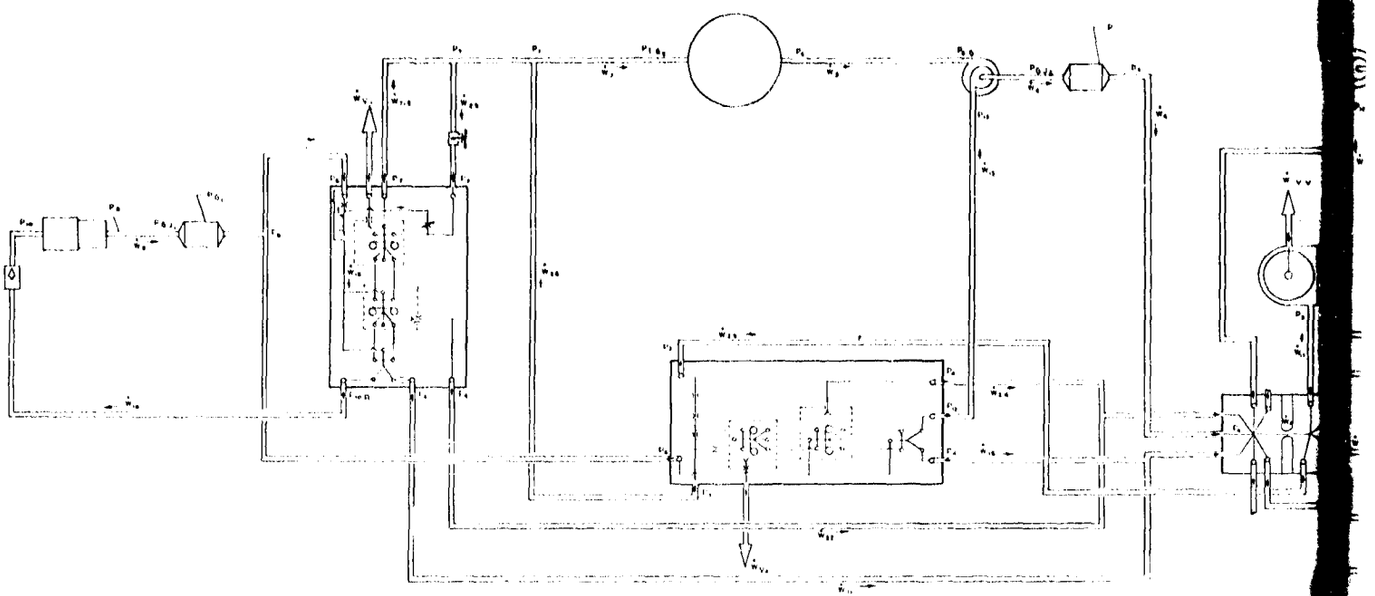

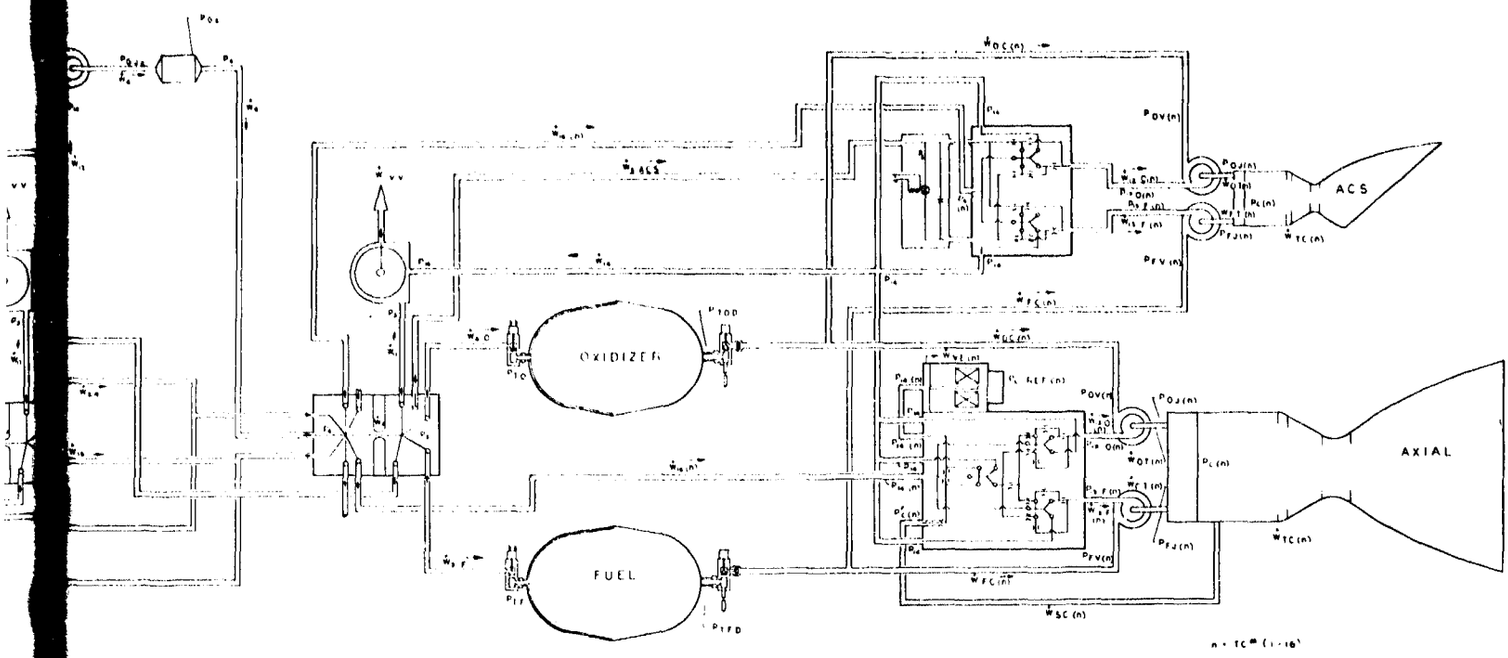

Figure 51. PBPS Controls Schematic (Sheet 2 of 2)

IV, C, Fluidic Control Components (cont.)

1. Pressurization Controls

The pressurization controls include the first-stage and second-stage pressure regulators, a flow division module, and a vent control module.

a. First-stage Pressure Regulator

(1) Function and Basic Operation

The function of the first-stage pressure regulator is to monitor the Stage I gas generator downstream pressure, supply pressurant as required to the Stage II propellant tank, and control the pressurant supply rate to the Stage I gas generator bootstrap propellant feed tank. This must be done relative to the propellant needs of the second-stage generator which supplies pressurant to the main propellant vessels. In turn, these vessels supply both the axial thrustors and the attitude control engines. Supply gas to the first-stage regulator is the monopropellant decomposition product of hydrazine (N_2H_4) propellant from the Stage I gas generator.

Pressure regulation is accomplished through the use of two fluidic devices. The first of these is the diverter valve or fluid amplifier, which operates on the principle of fluid interaction (i.e., if a small jet of fluid is properly directed normal to the flow path of a larger stream, it can divert the larger stream to a new flow path). This is shown in Figures No. 52 and No. 53 which represent vented and non-vented diverter amplifiers, respectively. These devices require flow at all times and therefore, e sometimes referred to as "open center" devices. The advantage of the non-ve ed diverter over the conventional vented types is that it conserves availal e fluid and as a consequence, it is more efficient because fewer stages are required to achieve a desired pressure or flow gain.

However, the non-vented diverter is more load sensitive than the vented type and any pressure changes or fluctuations downstream of the receivers or output legs is reflected in unit performance. The nomenclature used to describe the fluid amplifier or diverter valve is introduced at the supply port or power nozzle of the unit. Then, it is diverted through any one of the receivers or output ports by applying small amounts of gas through either of the control ports. In the case of the first-stage pressure regulator, gas is directed to either the gas-side of the bootstrap tank or away from it as required. Modulation or thrust control also can be achieved by varying the amount of control gas introduced so that the supply gas is only partially diverted, which provides intermediate stages of flow diversion.

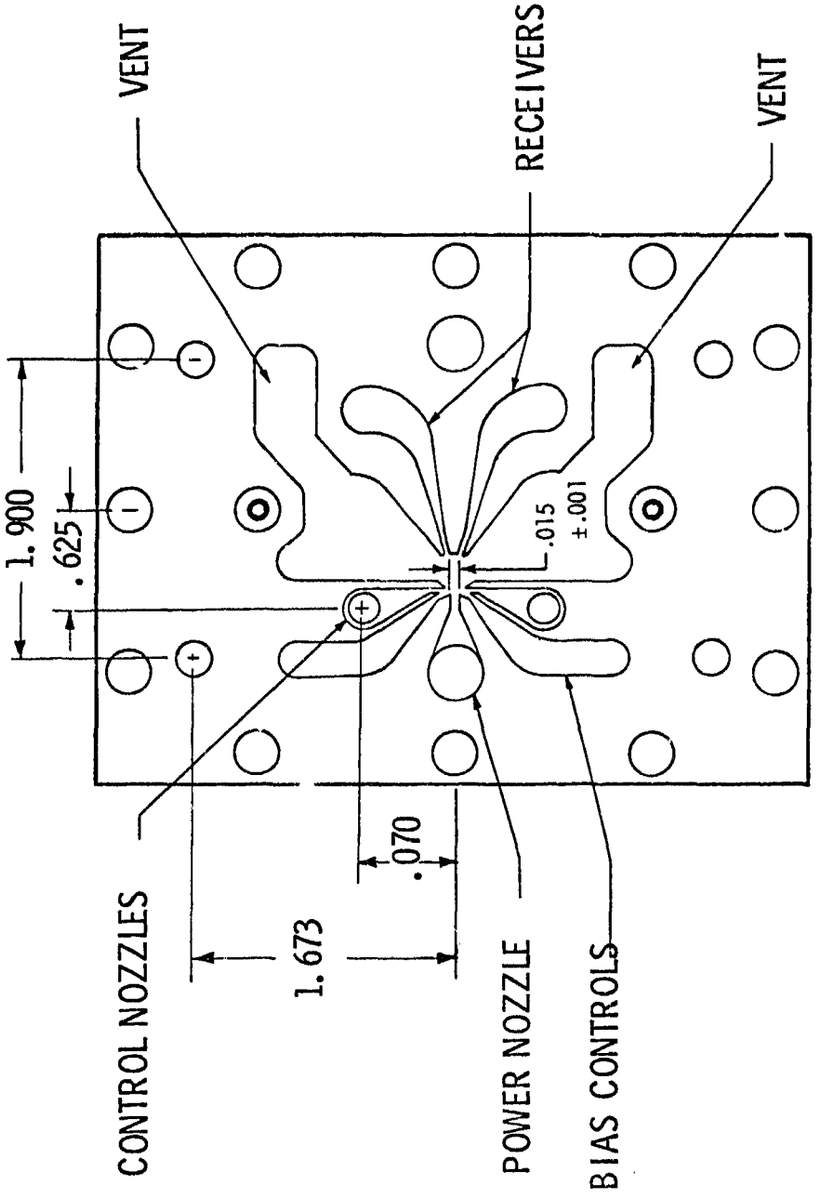

Figure 52. Vented Fluidic Amplifier

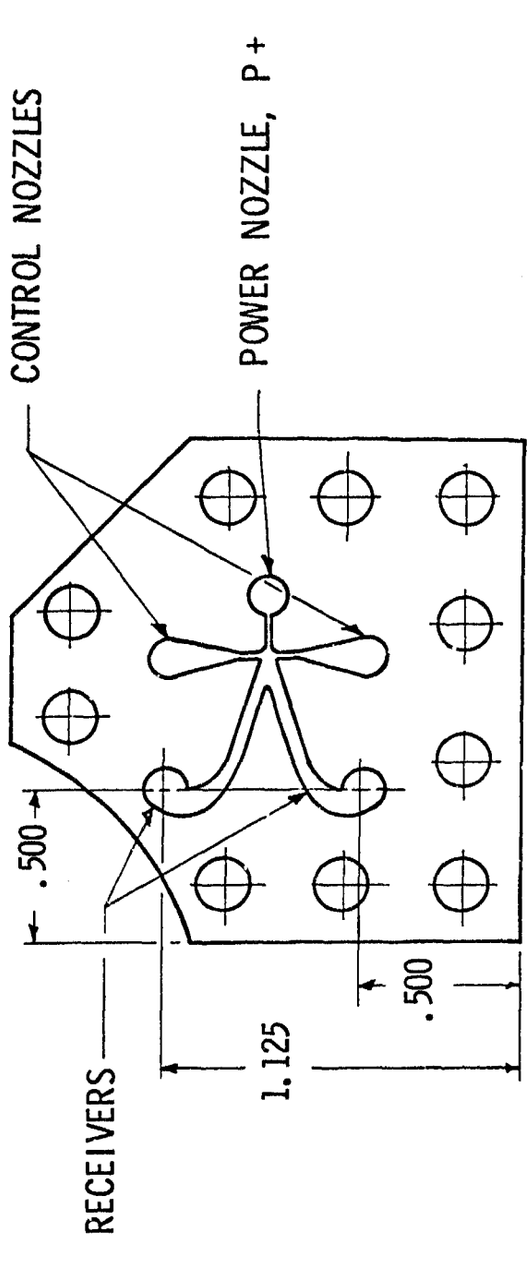

Figure 53. Non-Vented Fluidic Amplifier

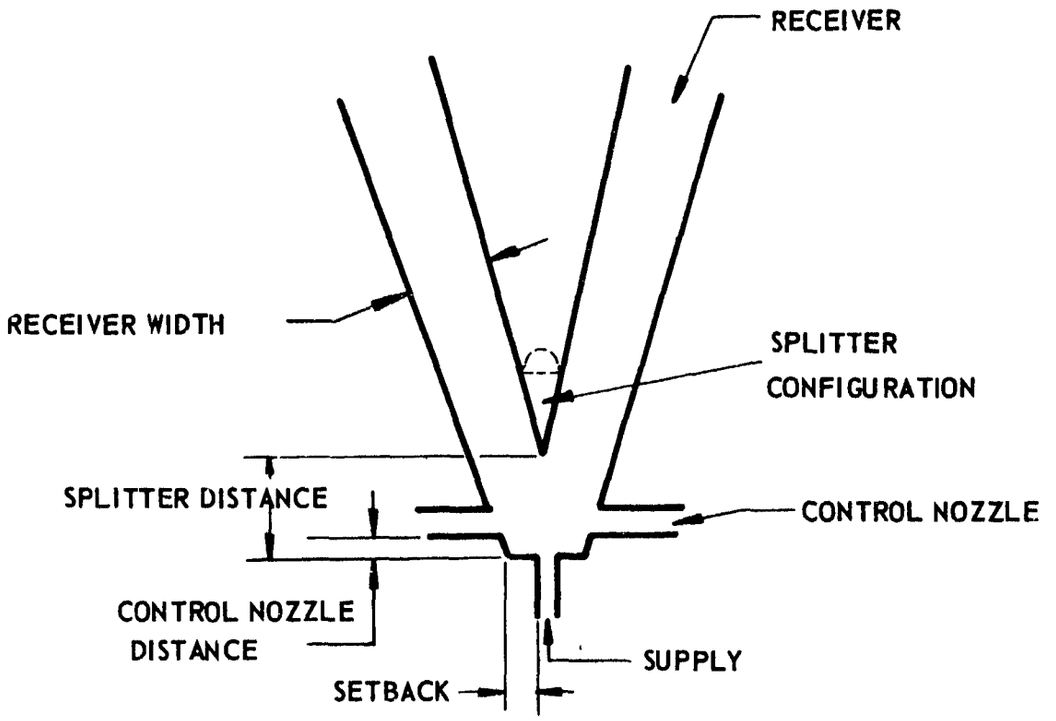

Figure 54. Diverter Valve Nomenclature

IV, C, Fluidic Control Components (cont.)

In addition to providing flow diversion, several diverter amplifiers are staged in series to perform another two functions. In one of these functions, the relatively low error signal or pressure differential (2 psi) out of the pressure sensing module is amplified to approximately 30 psi. The second function is to elevate the output pressure level of the pressure sensing module (Stage I amplifier) from 480 psia to approximately 645 psia as required at the gas-side of the bootstrap tank. Therefore, by using several stages of amplifiers/diverters in series, where each successive stage provides the control flow for the succeeding stage, amplification of a pressure differential error signal and an increase in pressure level can be achieved to provide working pressures at the gas-side of the bootstrap tank.

The second fluidic device required for pressure regulation is a sensing control unit. The PBPS first-stage pressure regulator utilizes a laminar capillary tube/orifice bridge circuit (see Figure No. 55) to produce the initial error signal required to operate the diverters. Supply gas at the pressure side of the second-stage hydrazine tank ullage (sensed pressure) is admitted to both sides of the bridge. The pressure drop through the laminar flow capillary leg is linear with the flow rate while the pressure drop through the orifice leg of the bridge varies exponentially with the flow. Consequently, system equilibrium is satisfied only at that flow rate which produces equal pressure drops in the two bridge legs. Then, the two legs of the bridge are fed directly into opposite control ports of a diverter. When pressure in the Stage II propellant tank is below the set point of the regulator, more flow passes through the orifice side of the bridge diverting supply pressure to increase the Stage I bootstrap tank pressure. Conversely, higher than desired Stage II tank pressure results in more flow through the capillary bridge leg diverting supply pressure away from the Stage I tank. The desired tank pressure setting is adjusted by means of a parallel, adjustable orifice in the orificed leg of the bridge.

A thermal transient is encountered in reaching steady-state because the steady-state operation of the unit is at a temperature approaching the working temperature of 1400°F. An increase in regulated pressure is encountered with increasing temperature because of different flow characteristics with temperature in the orifice and capillary bridge legs. This results in a calculated 1 psi increase for every two-degrees of temperature rise. To compensate for this set pressure thermal drift, a thermal compensating device is used as shown on Figure No. 56. A shaped pintle made from a material with a high thermal coefficient of expansion expands and contracts within an orifice assembly. This assembly is made from a different material to provide the necessary temperature compensation and automatically adjust the regulator set pressure as a function of temperature.

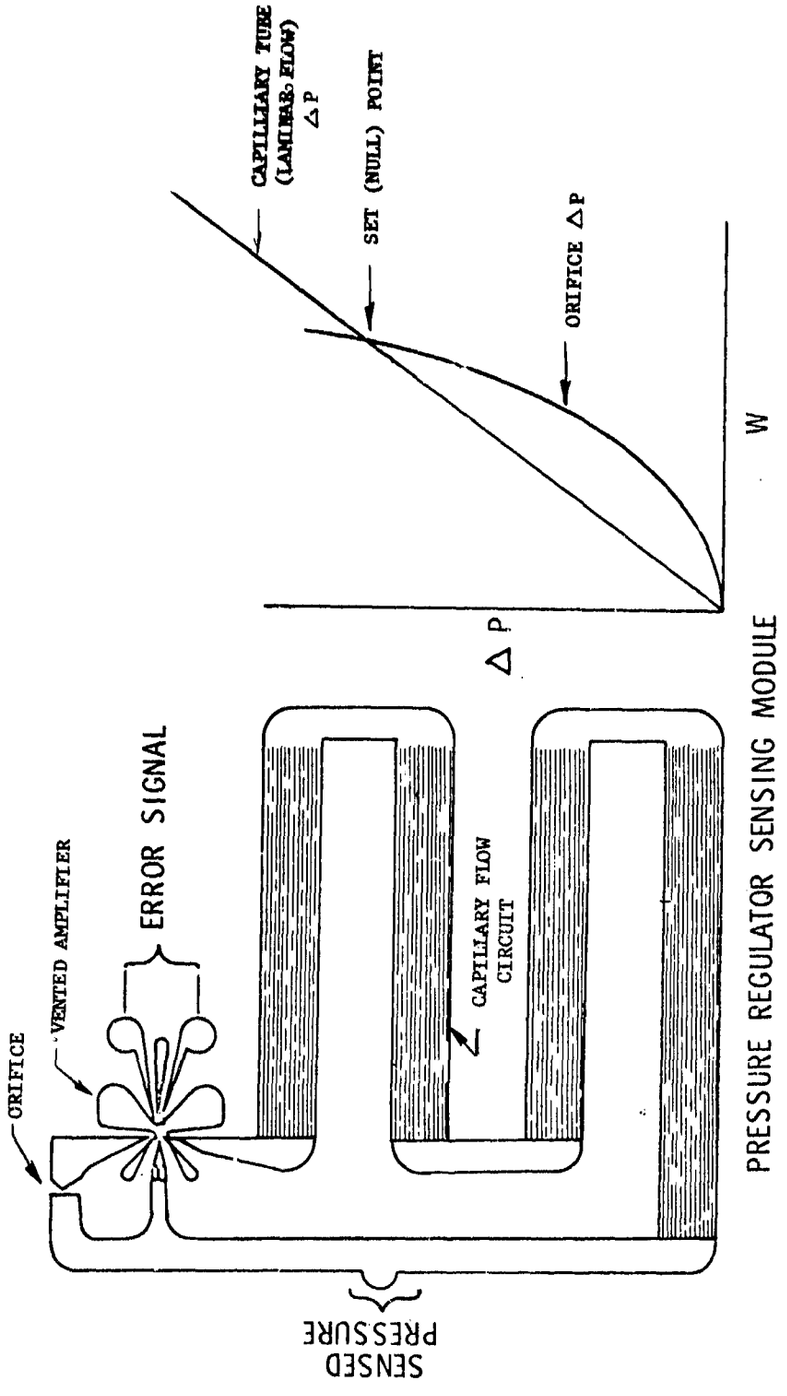

Figure 55. PBPS First-Stage Pressure Regulator

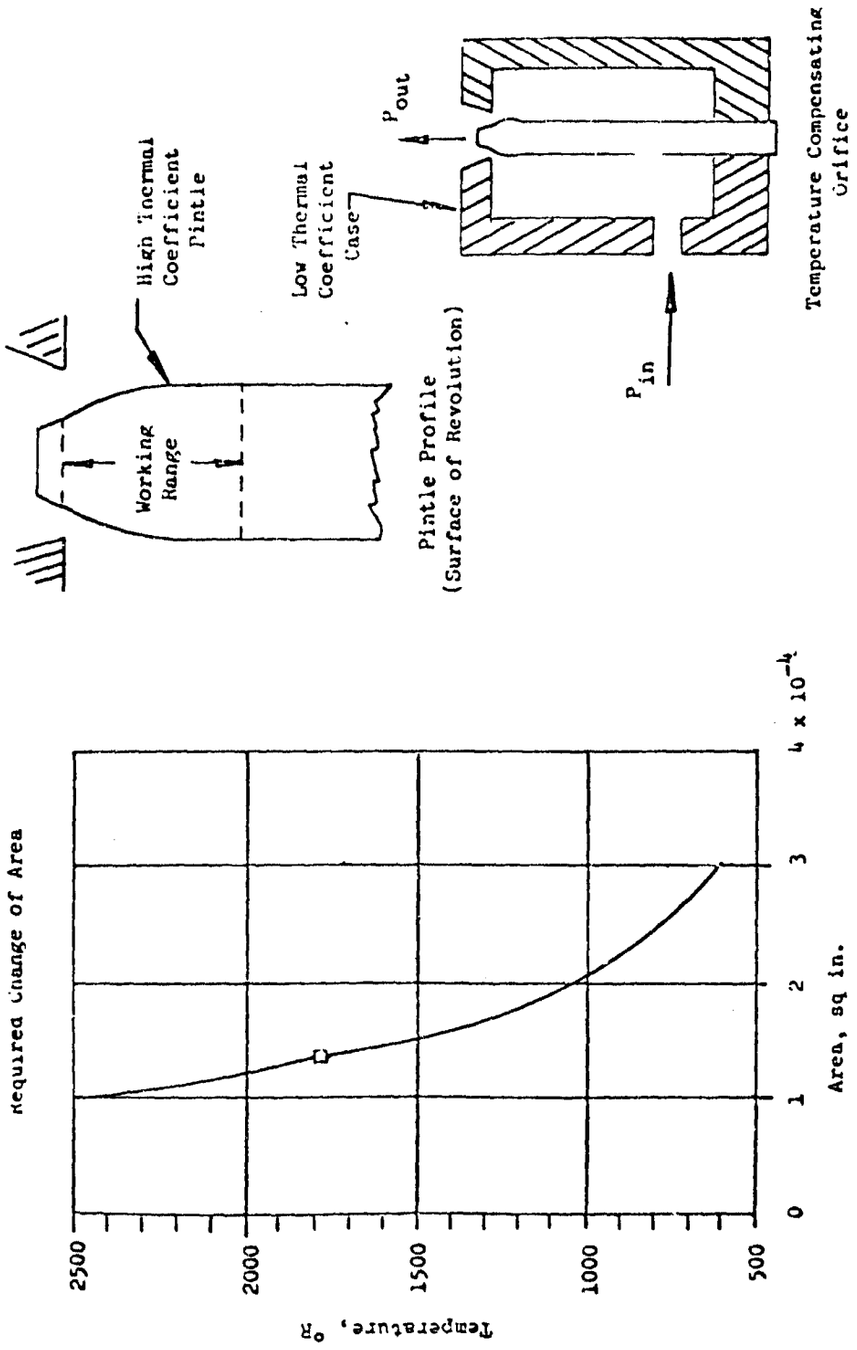

Figure 56. Characteristics of a Thermal Compensating Orifice

IV, C, Fluidic Control Components (cont.)

The initial concept of a pressure sensing unit considered for the PBPS first-stage regulator application is shown on Figure No. 57. This unit utilized a pressure controlled oscillator (PCO), which would receive an input signal from the pressure source that is to be regulated. The PCO incorporated a tuned circuit which would produce an analog signal proportional to the pressure level sensed. A frequency discriminator circuit would produce an error signal and a power amplifier would supply a signal for gas regulation. Difficulty was encountered in obtaining satisfactory performance of the PCO and the discriminator circuit at the high ambient pressures required in this application, although the devices had been used in a one atmosphere ambient pressure application.

(2) Component Description and Specifications

A model representation of the PBPS first-stage pressure regulator is shown on Figure No. 58. This is an experimental unit and its basic construction consists of several bonded fluid amplifier elements, a bonded laminar-capillary flow assembly, orifice plates, as well as supply and vent manifold elements. These modules are stacked in proper orientation, with alternating flat gaskets for sealing. The complete assembly is held together with bolts to facilitate removal and inspection of the individual elements as required. Some typical steel diverter amplifiers in both the unbonded and bonded condition are shown in Figure No. 59. An exploded view representing the 12 platelet laminar-capillary flow assembly is shown on Figure No. 60.

The flightweight version of the regulator assembly would be considerably reduced in size and weight by eliminating the bolts and excess peripheral metal. In addition, the entire unit would be bonded together to eliminate all potential leak paths.

The component receives decomposed hydrazine (N_2H_4) gas from the Stage I gas generator at an inlet pressure of 695 psia and an inlet flow rate of 0.025 lb/sec to 0.035 lb/sec. The gas temperature is approximately 1400°F while the regulated pressure to the Stage II pressurization tank is 645 $\pm$ 30 psia at a gas flow rate of 0.007 lb/sec to 0.010 lb/sec. The regulator outlet pressure to the Stage I bootstrap tank is 660 $\pm$ 30 psia at a gas flow rate of 0.00075 lb/sec to 0.0009 lb/sec.

(3) Amplifier Development

Considerable analysis and testing of diverter amplifier elements were performed at the Bowles Engineering Corporation. A basic diverter amplifier configuration was developed for application to the pressure regulators and engine controls. The basic configuration was scaled

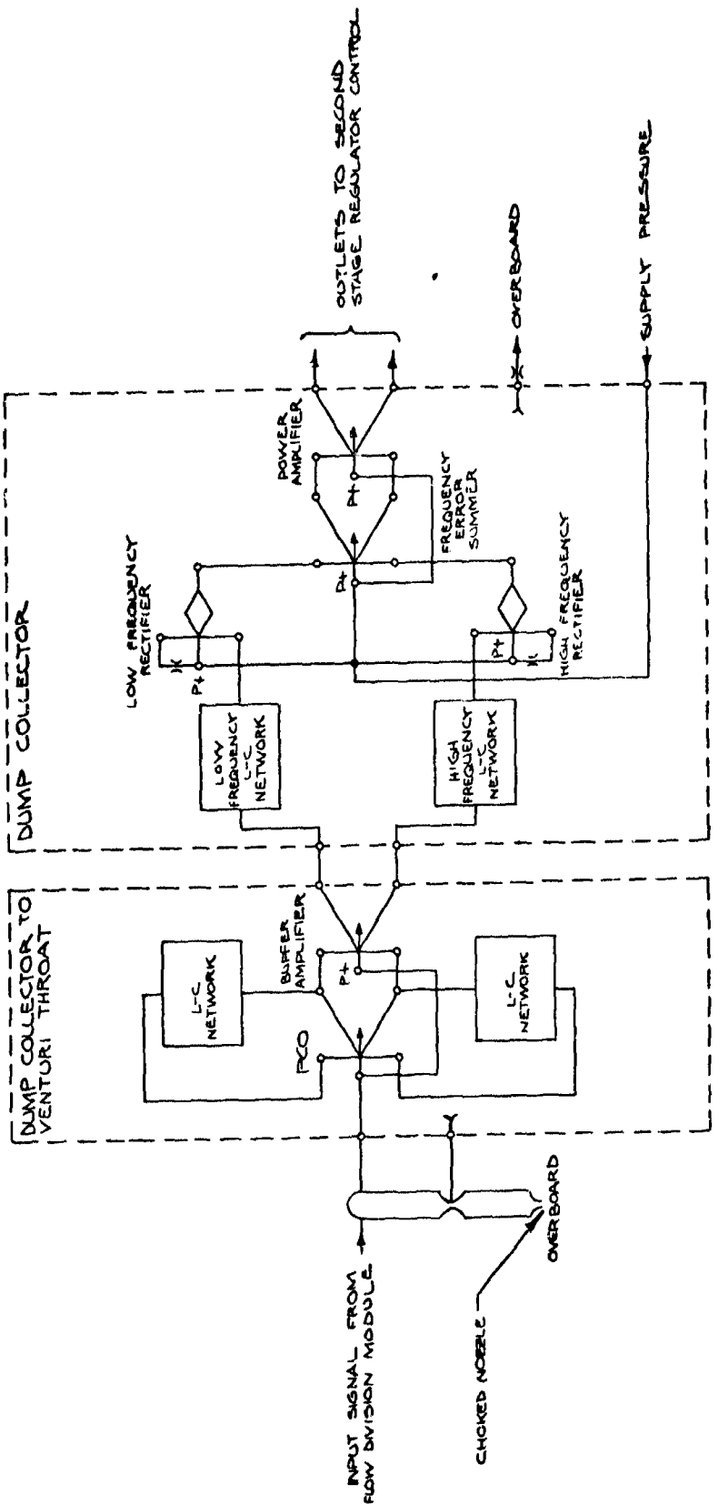

Figure 57. First-Stage Regulator Sensing Module Schematic

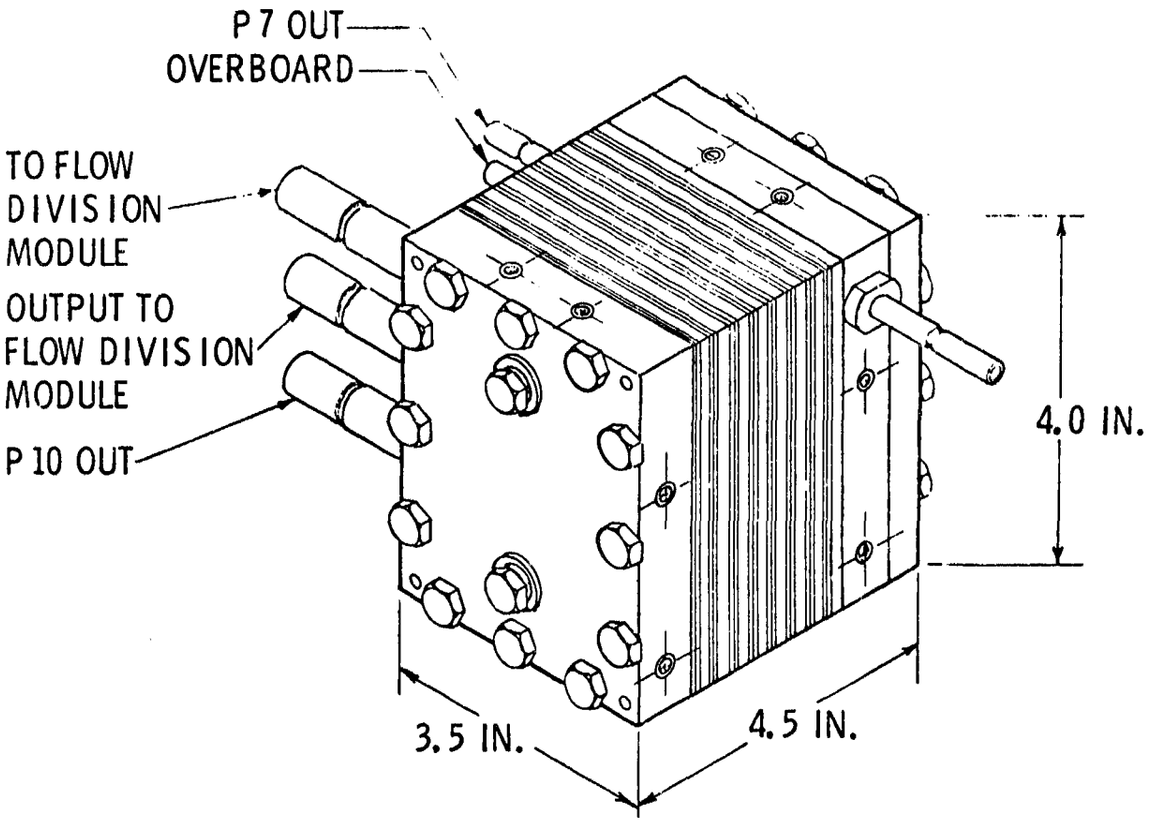

Figure 58. Experimental First Stage Pressure Regulator

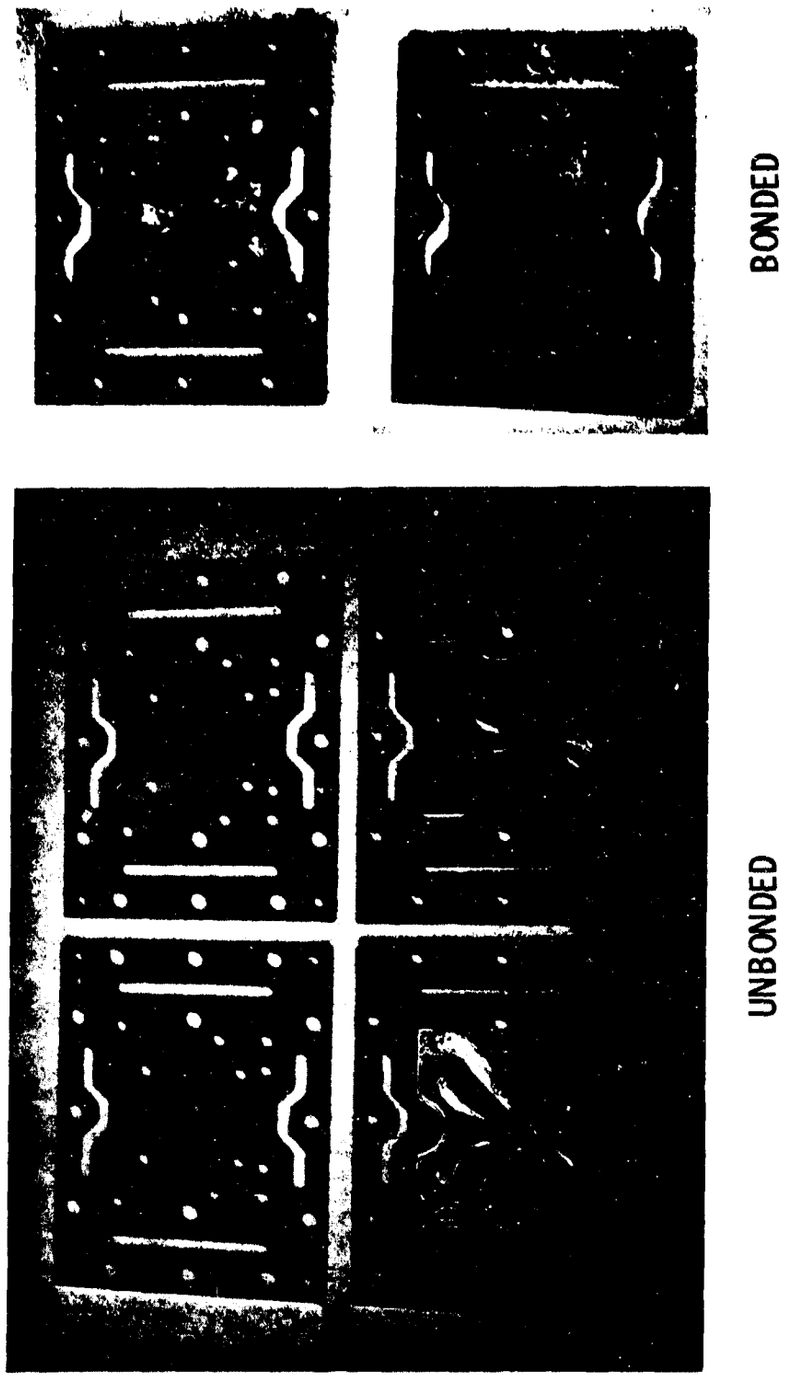

Figure 59. First-Stage Pressure Regulator Amplifier

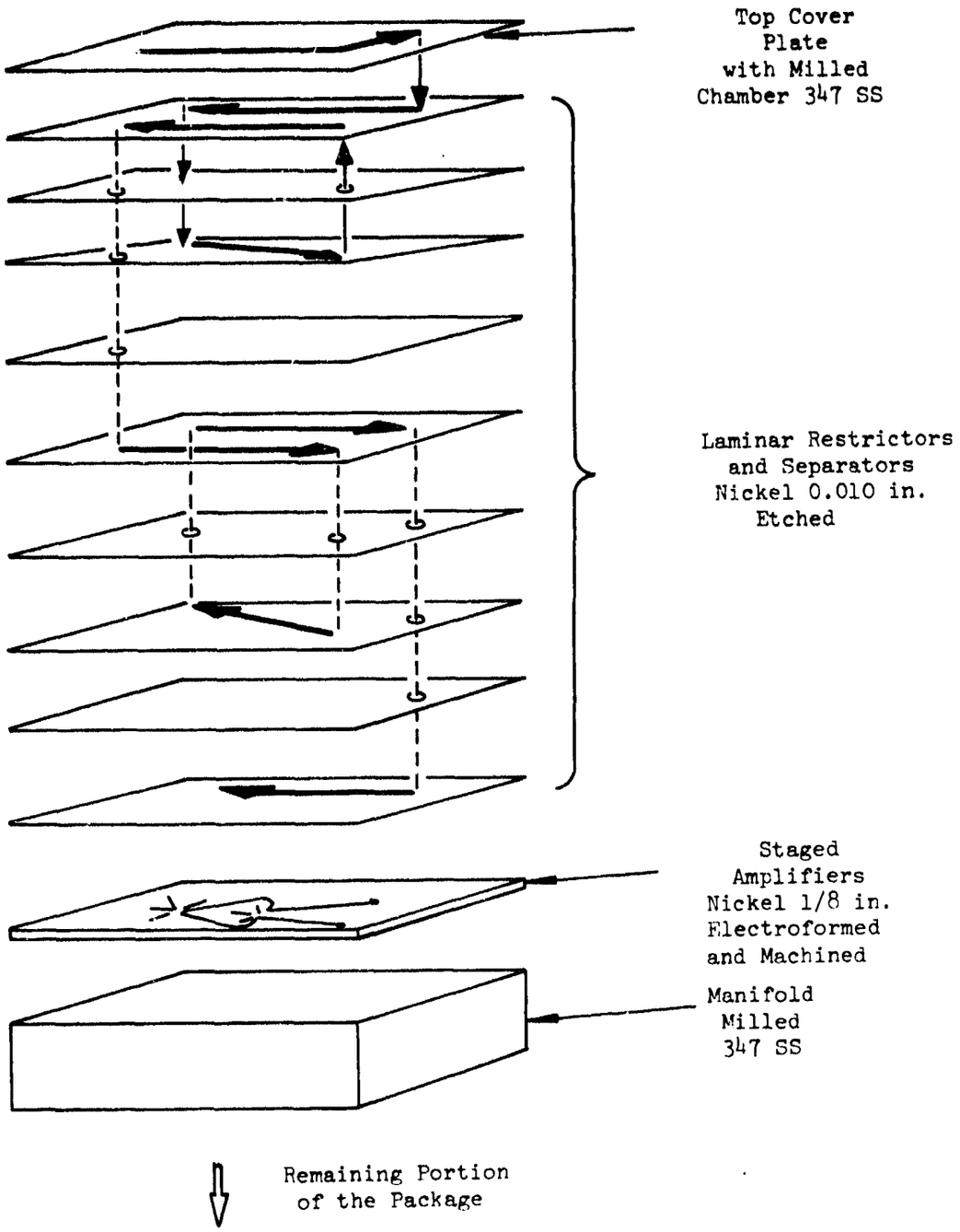

Figure 60. Pressure Sensor Assembly (Exploded View)

IV, C, Fluidic Control Components (cont.)

to meet various pressure and flow requirements encountered in all applications. Preliminary calculations established initial design parameters upon the basis of jet attachment point location. Requirements included analog performance, high pressure recovery, and flow gain.

Nine prototype configurations were constructed and tested with small variations in geometry from the theoretical optimum configuration. The geometric parameters considered were: splitter distance, setback, control nozzle distance, receiver width, and splitter configuration. The laboratory test units were manufactured in a photosensitive plastic material. Air was used as the working fluid.

A set of initial tests was conducted to establish the relative merits of the nine units. This eliminated several units from further consideration. A schematic of the test set-up and the test procedure is presented as Figure No. 61. Output pressure and output flow for both sonic and subsonic operation were measured for each unit to show relative pressure recovery. This was a good indication of diverter amplifier efficiency. The best performance was obtained using a splitter distance that was five times the power nozzle width. This was achieved by module No. 5 which produced the results shown on Figure No. 62. The splitter configuration was slightly blunt in comparison with the other modules and the receiver width was the smaller of two values used in this test series.

Analog performance and flow gain was investigated next using differential pressure across the control ports and monitoring the flow. Figure No. 63 is a schematic of the test set-up and shows the test procedure. All of the amplifiers had a flow gain of approximately 3:1. Flow gain is defined as the ratio of the change in output flow between the two outputs to the change in input flow between the two control ports. Relative pressure level data for several modules appears on Figure No. 64. It is noted that module No. 5, which had the best pressure recovery during the previous testing, maintained the highest output pressure levels in this test. This is an important consideration for staging diverter amplifiers. Upon the basis of these two series of tests, the configuration of module No. 5 was selected for use as the basic diverter configuration. During this evaluation period, water table tests were performed which confirmed the selection of module No. 5.

A set of more detailed tests was performed using the configuration of module No. 5 to obtain information for use in designing the cascades of these elements. The test set-up for these tests are shown on Figure No. 65. Data were taken for fixed supply pressures at various fixed, equal loads. The loads were adjusted by the load valves and monitored with pressure gages and flow meters. The data points were pressure or flow differences between the left and right outputs as well as the left and right control ports. The parameter was the control pressure level. Typical test results appear on Figures No. 66, No. 67, and No. 68.

Test Configuration

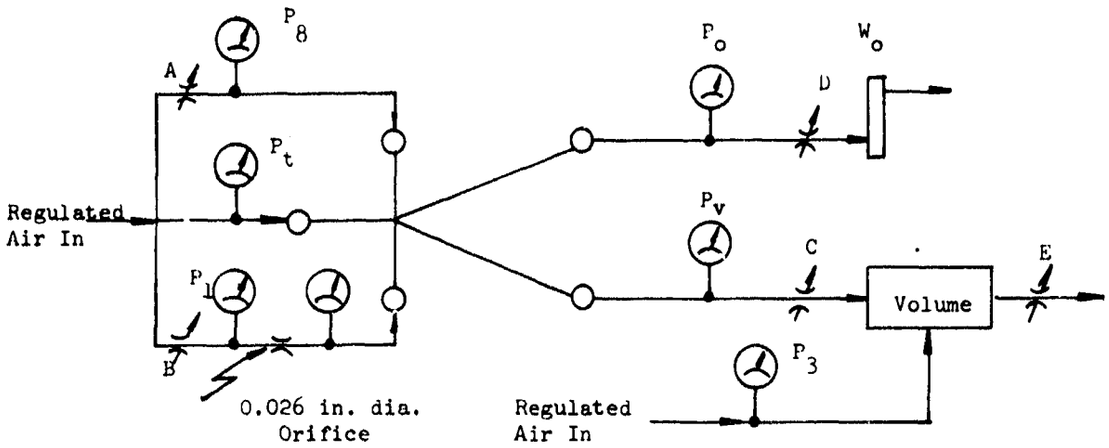

Procedure:

1. Close Valves A and B.
2. Open Valves C and D.
3. Set supply pressure (P_t).
4. Set $P_v = P_3$.
5. Open Valve B until P_2 stops increasing.
6. Record all gages.
7. Close Valve D until P_o begins to increase. Continue closing D, recording P_o and W_o.
8. Open Valve D.
9. Close Valve B to obtain P_2 equal to one-half the value of P_2 used in Step 4.
10. Repeat Steps 5 and 6.
11. Repeat Steps 4 through 10 with new value of $P_v = P_3$.

Figure 61. Test Set-Up and Procedure (Diverter Amplifier)

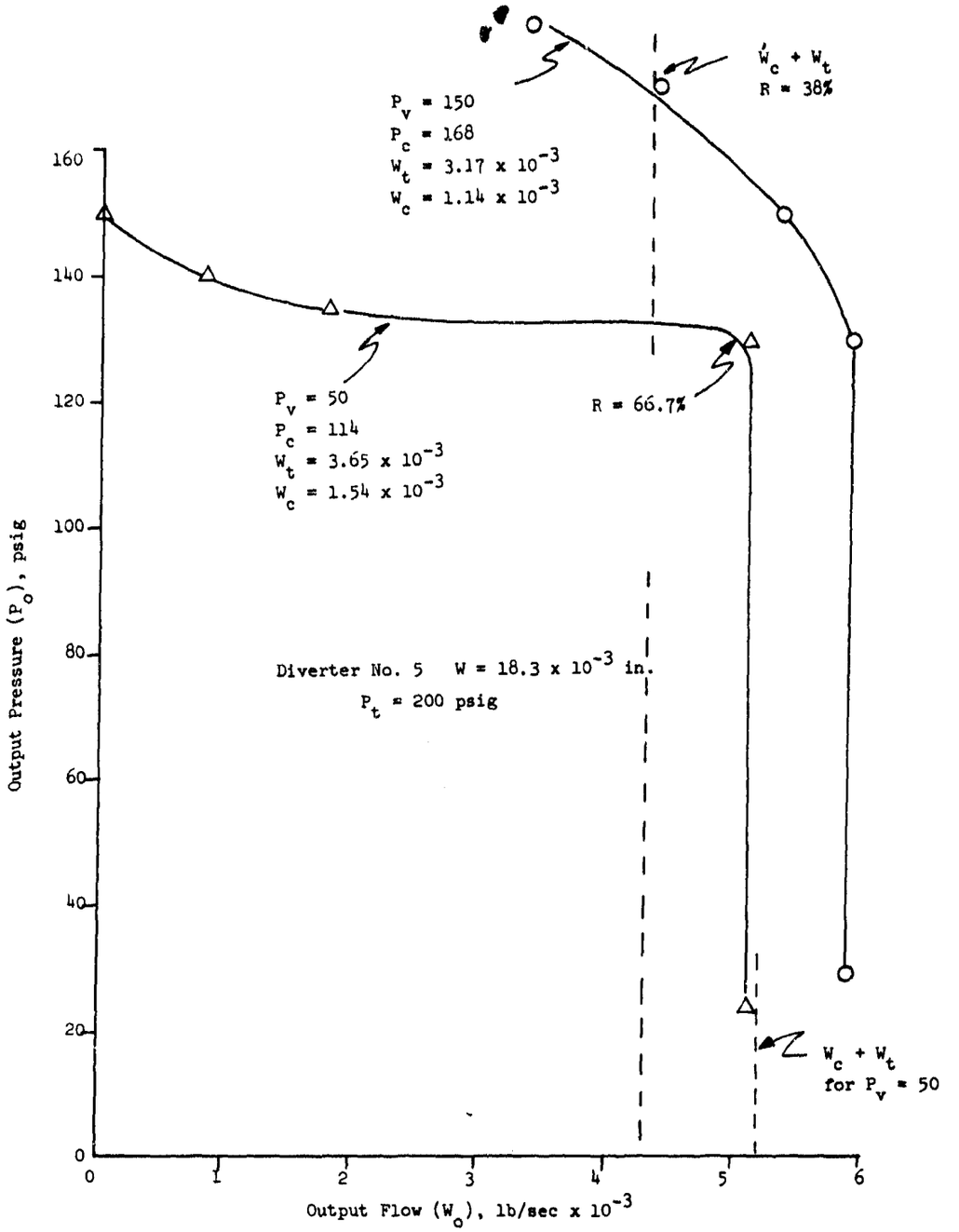

Figure 62. Test Results (Diverter Amplifier Module No. 5)

Test Configuration

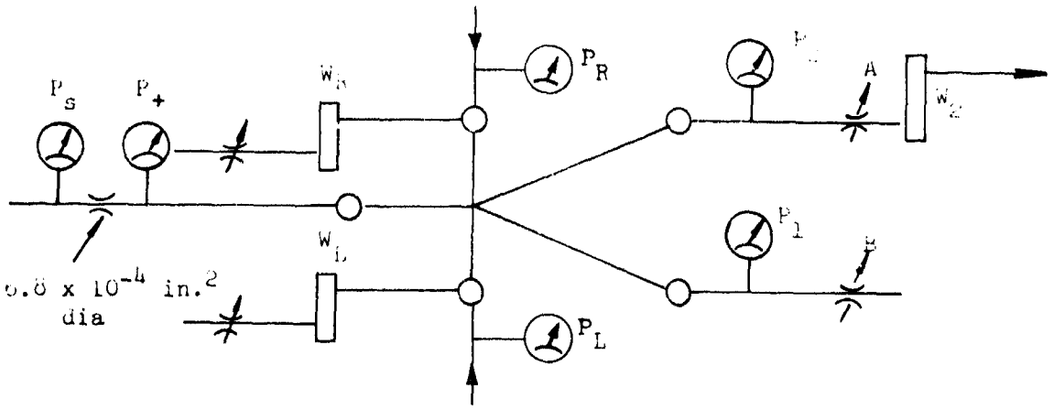

Procedure:

1. Set P_L, P_R and P_+
2. Set Valve A = Valve B (areas)
3. Record all data
4. Repeat Steps 1 through 3 for New Values of P_L, P_R, and P_+.

Figure 63. Test Set-Up and Procedure for Gain Determination

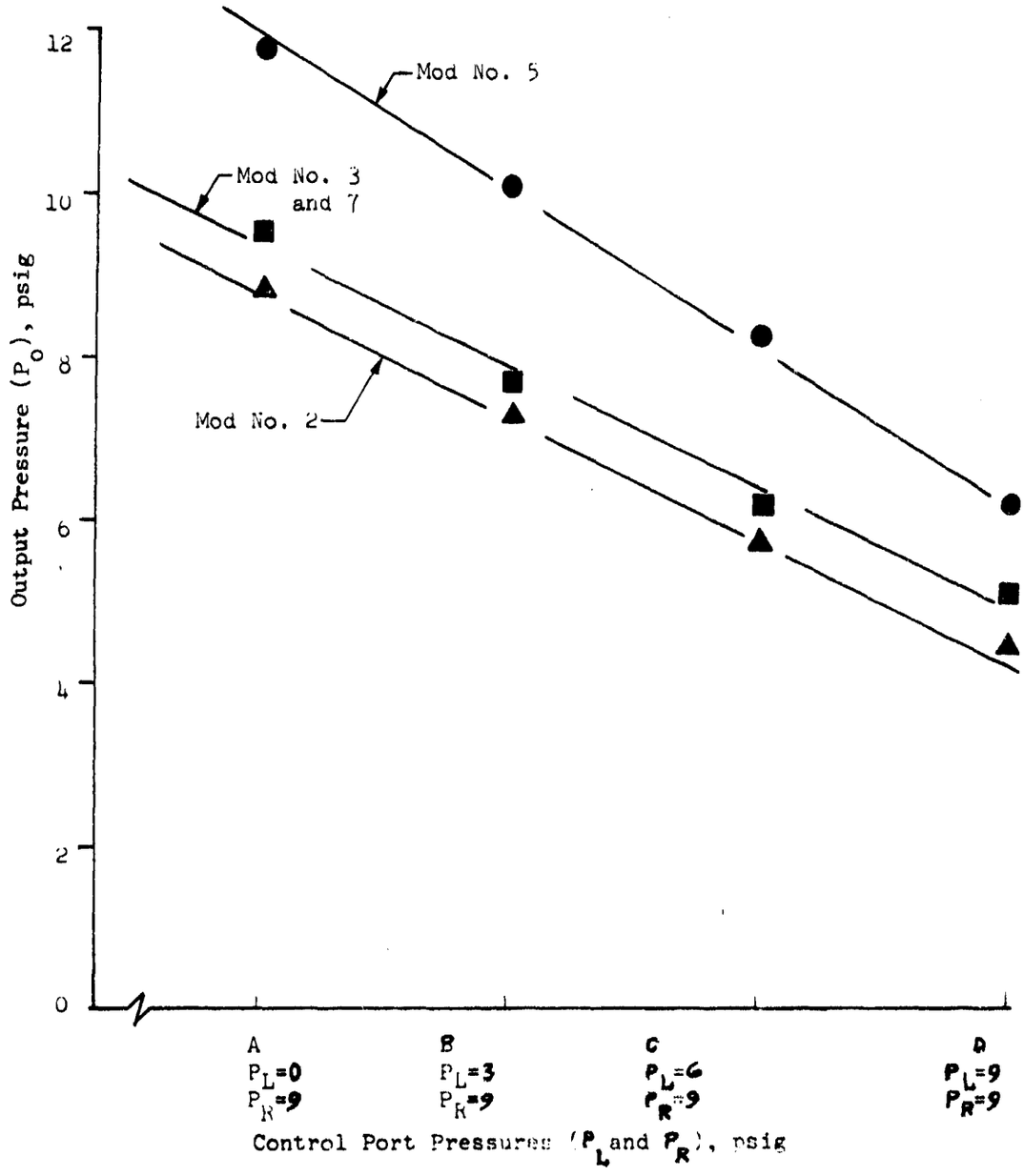

Figure 64. Test Results (Diverter Amplifier Flow Gain Tests)

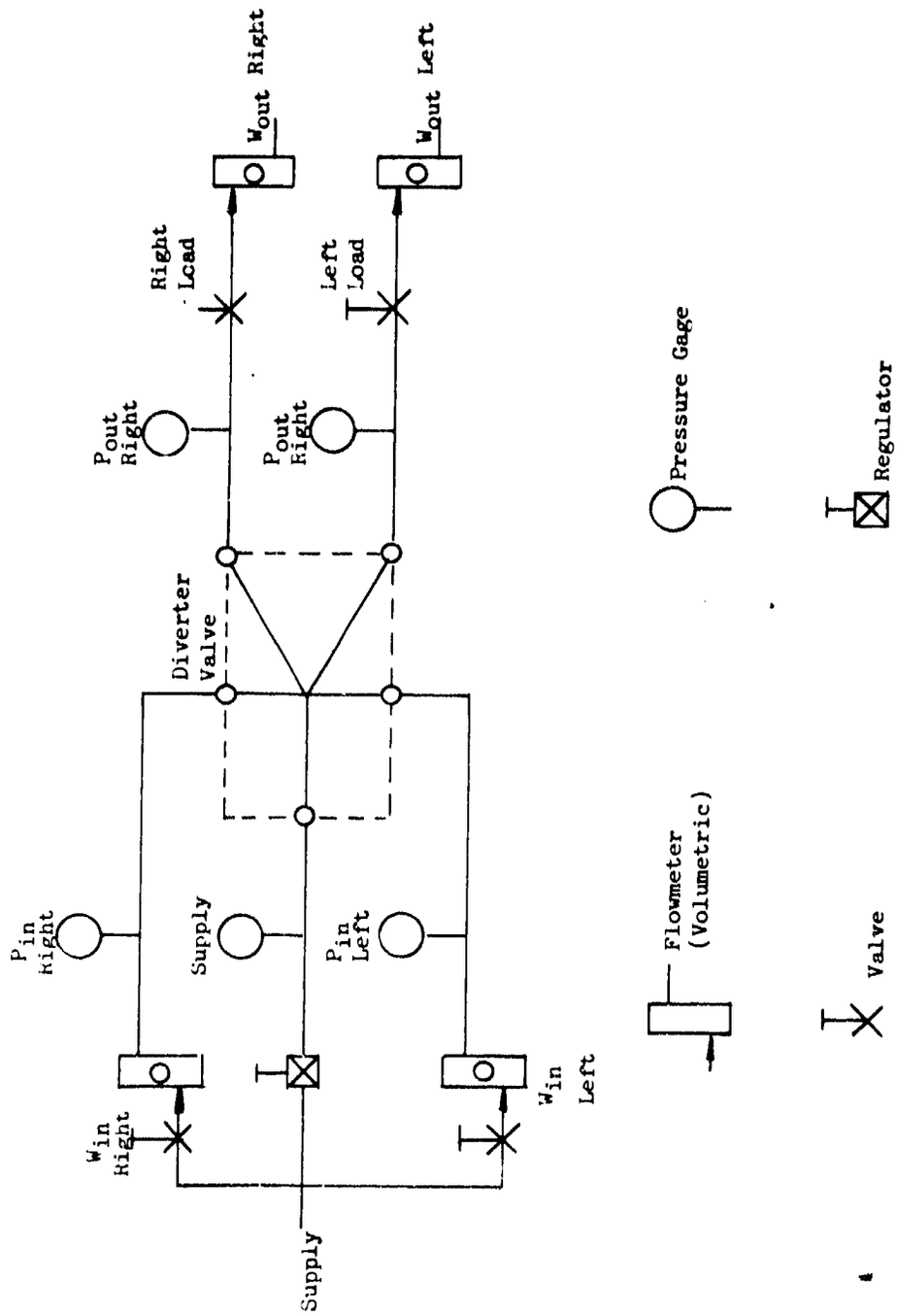

Figure 65. Pressure and Flow Measurements

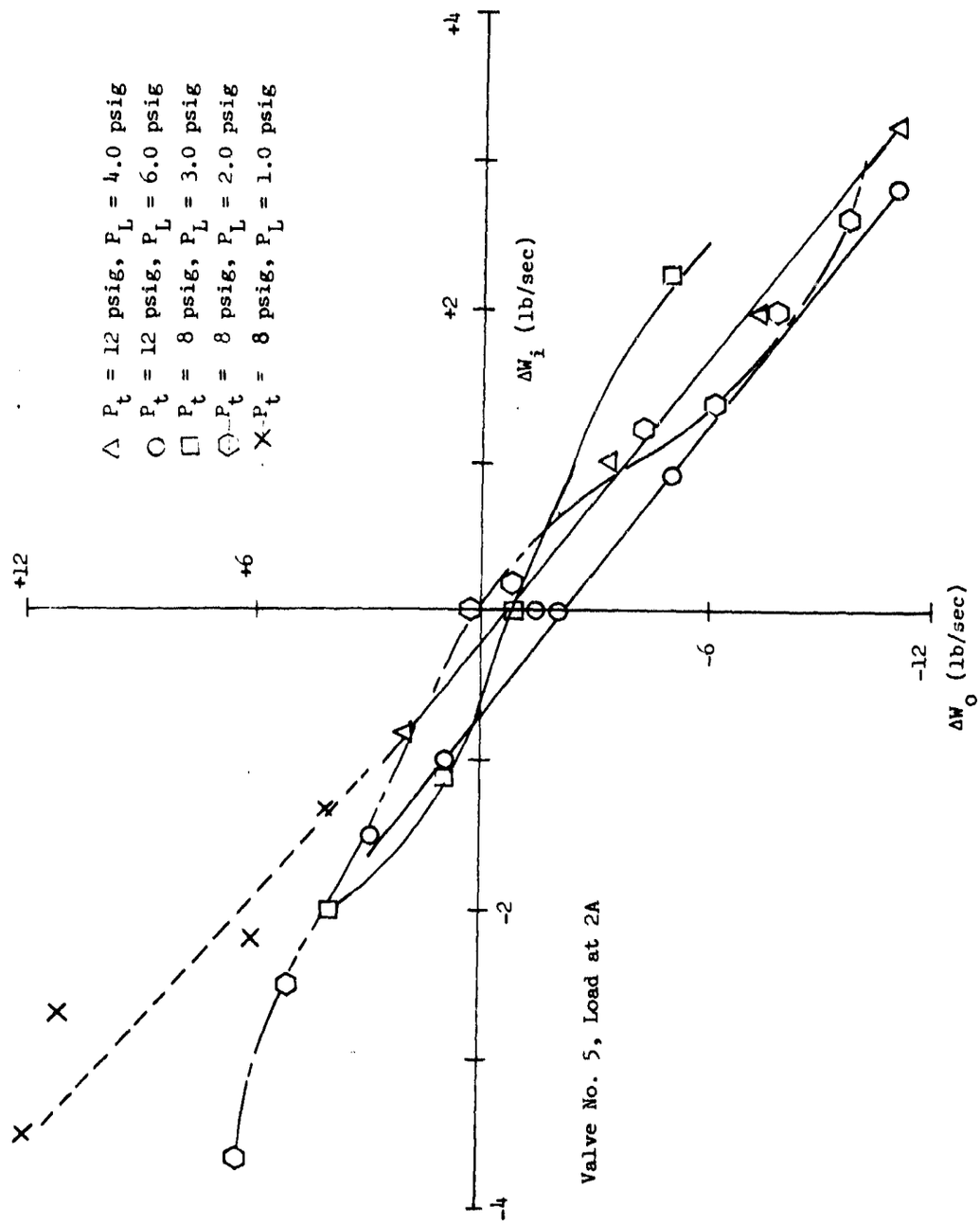

Figure 66. Differential Output Flow vs Differential Input Flow

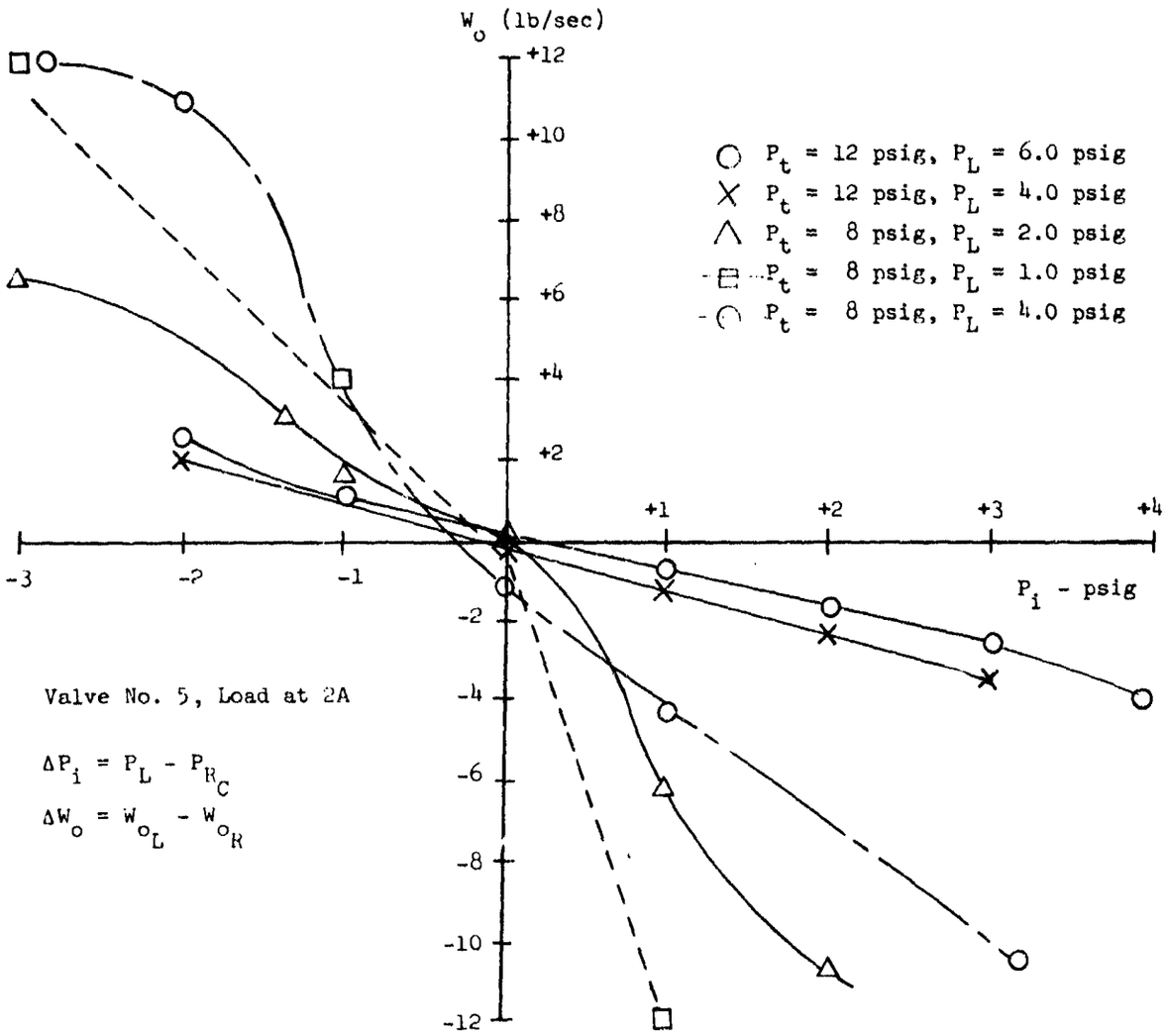

Figure 67. Differential Input Pressure vs Differential Output Flow

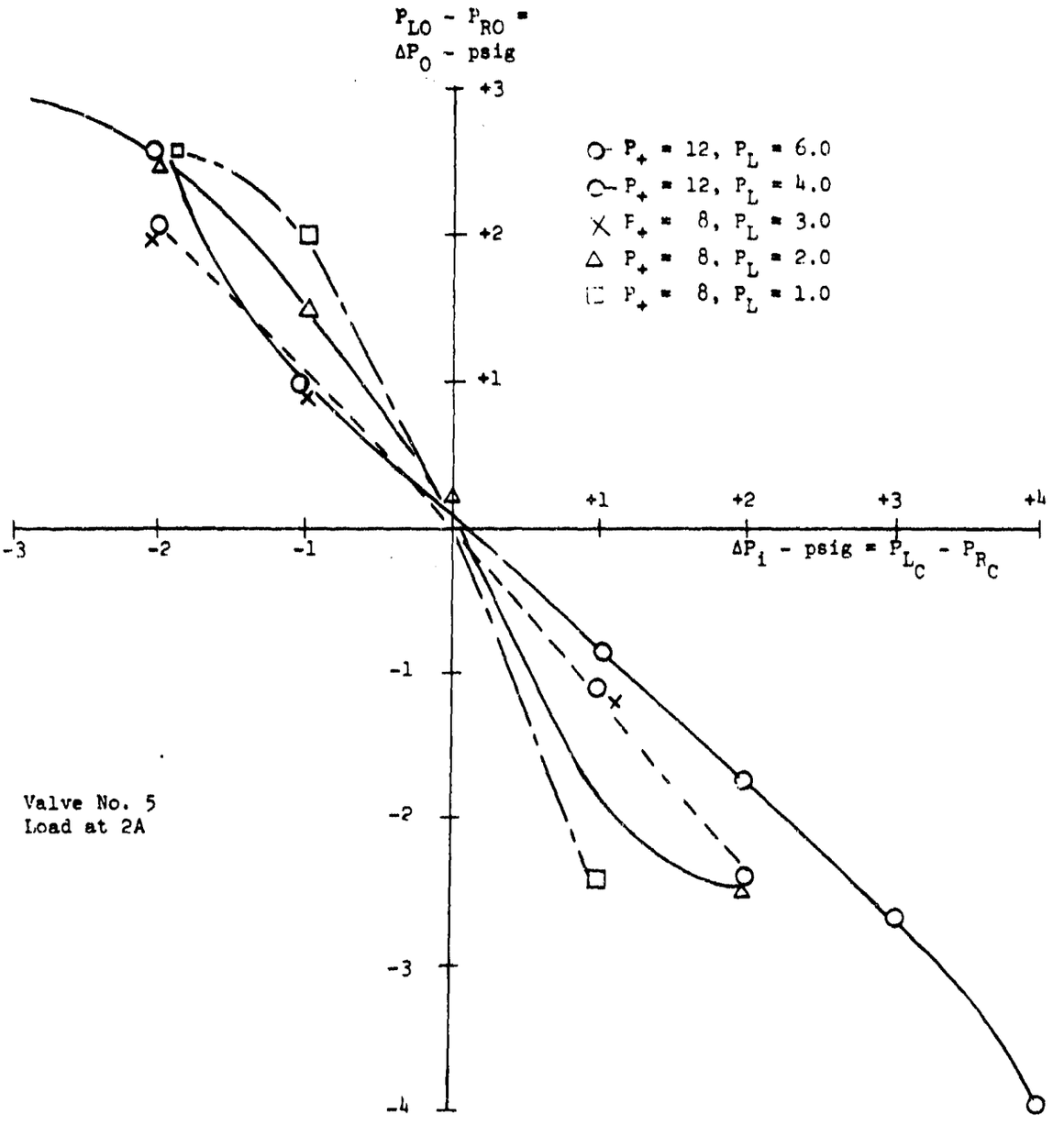

Figure 68. Differential Input Pressure vs Differential Output Pressure

IV, C, Fluidic Control Components (cont.)

It was found that under certain conditions of supply pressure, load, and control pressure level, that either pressure gain or flow gain is obtained. In some cases, both pressure gain and flow gain occur.

A variable geometry non-vented diverter with adjustable control and receiver widths was fabricated and tested. Input and output characteristic curves at various control and receiver widths were recorded at low pressures. Successful operation of the diverter amplifiers was achieved individually. For proper staging of any two diverters to attain greater power and pressure amplification, however, the output characteristics of the first diverter must match the input characteristics of the second diverter. The tests with the variable geometry diverter did not result in a configuration which would properly match the input and output characteristics.

Further studies were implemented to investigate cascading of non-vented diverters for PBPS components application. However, all attempts to achieve satisfactory test results in this area, for the extreme temperature and pressure requirements realized, were unsuccessful. For this reason the pressure regulator designs were changed to incorporate vented diverters which could be successfully staged. This change increased the amount of gas required for control purposes.

(4) Component Testing and Evaluation

An exploded view of the experimental first-stage regulator assembly for PBPS application is provided as Figure No. 69. Only five vented and one non-vented diverter amplifiers were utilized in this experimental model. The three additional vented diverters in the original design were eliminated. This change resulted in a decrease in vented flow and a revision of all stage pressure levels and flow rates. The pressure and flow schematic diagrams for the regulator assembly, pertaining to operation with air at ambient temperatures and N_2H_4 decomposition products gas at 1760°R, are included as Figures No. 70 and No. 71, respectively. The amplifiers were successfully staged with the output diverter element. The gain curve for the five amplifiers driving the diverter, as determined by Bowles Engineering, is shown on Figure No. 72.

Rework of the first-stage regulator assembly was required before the initiation of hot gas functional testing at AGC because the subcontractor had experienced excessive leakage at 50 psig from between the regulator plates. Attempts to correct this problem had been unsuccessful. Inspection of the regulator plates and bonded amplifier modules revealed an out-of-flat condition existed on all units. The plates were machine-ground and lapped, new gaskets of Durabala material were fabricated, and high strength bolts were used to improve regulator sealing capability between the plates up to pressures of 750 psig. The bonded amplifier and laminar-flow capillary units were reworked by edge sealing because there had been some leakage from these joints. Regulator external leakage was greatly reduced as a result of these modifications but there was no way to determine the extent of internal leakage and cross-flow between channels nor what affect it would have upon performance.

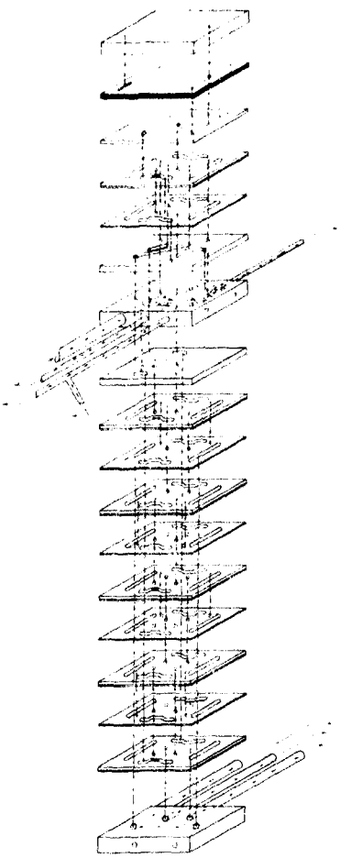

Figure 69. First-Stage Pressure Regulator Sensing and Control Module Assembly

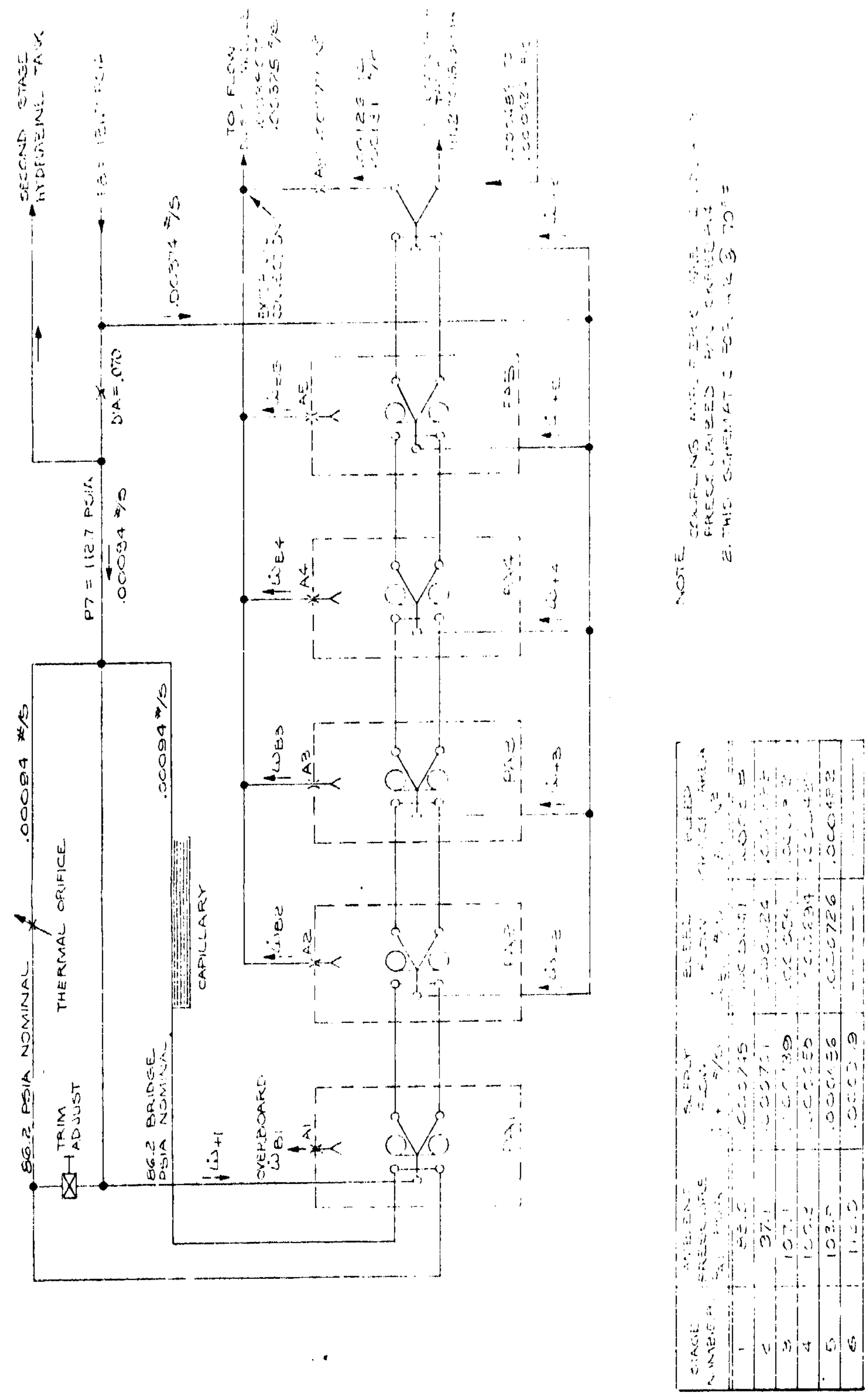

Figure 70. Schematic Diagram - Pressure Regulator No. 1

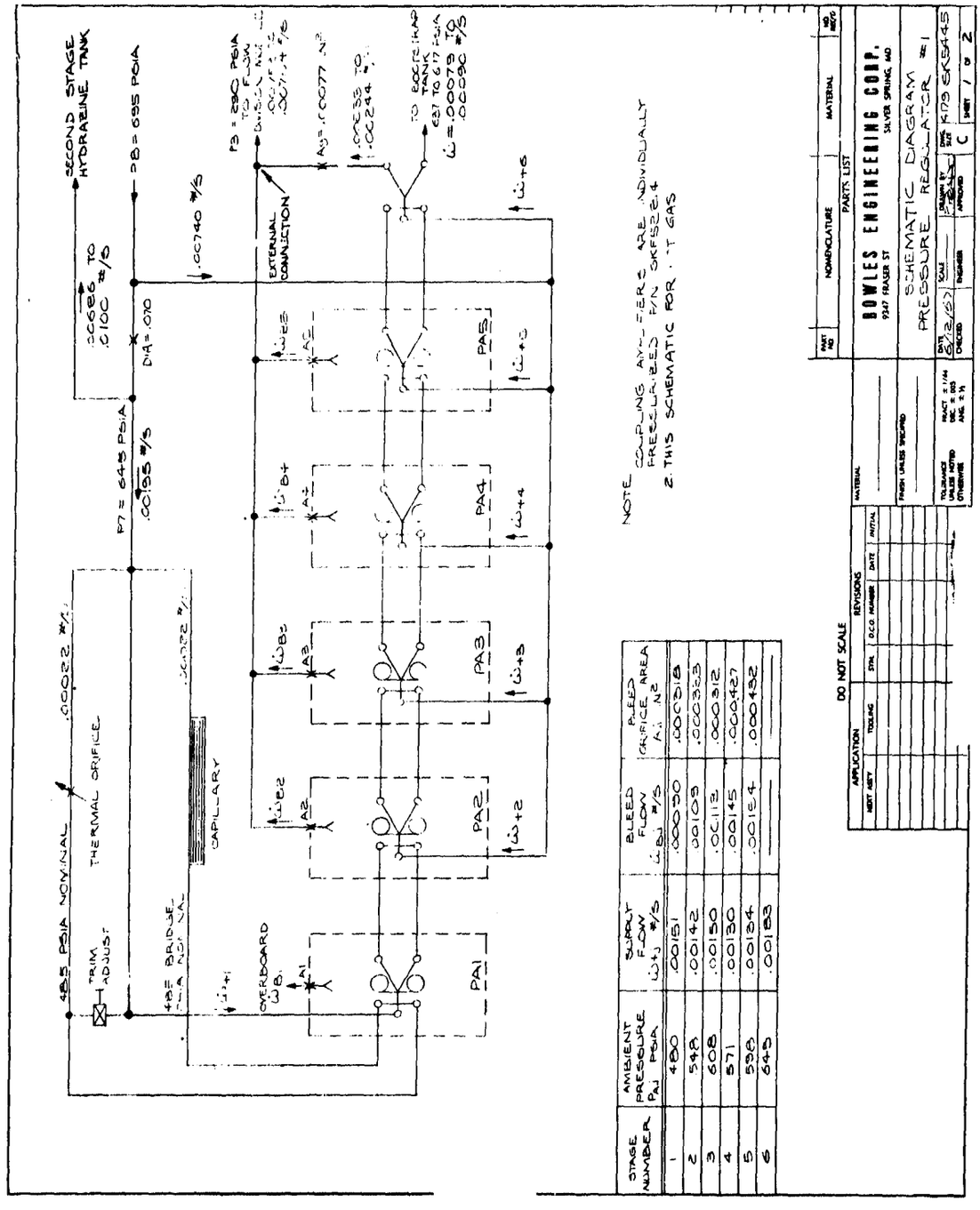

STAGE NUMBER	AMBIENT PRESSURE Pai PSIA	SUPPLY FLOW $\dot{w}_{si}$ #/S	BLEED FLOW $\dot{w}_{Bi}$ #/S	BLEED ORIFICE AREA Ai IN²
1	480	.00151	.00050	.000518
2	548	.00142	.00109	.000383
3	608	.00150	.00112	.000312
4	571	.00130	.00145	.000427
5	598	.00134	.00164	.000482
6	645	.00183	———	———

Figure 71. Schematic Diagram - Pressure Regulator No. 1

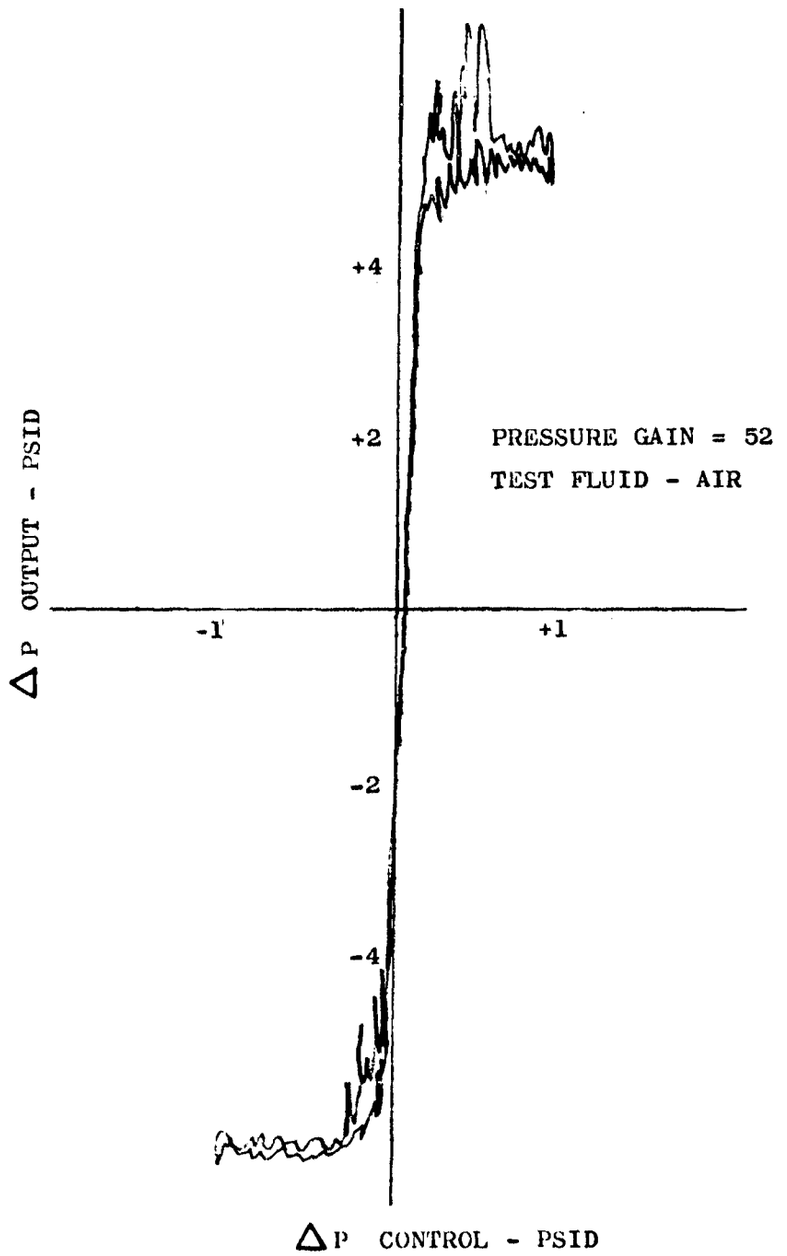

Figure 72. Pressure Gain Test of Five Vented Amplifiers Driving a Non-Vented Diverter Amplifier

IV, C, Fluidic Control Components (cont.)

The basic schematic for regulator testing is shown on Figure No. 73. Photographs of the test component and test set-up are included as Figures No. 74 and No. 75, respectively. Initial testing of the regulator commenced on 8 June 1967. Gaseous nitrogen (GN_2) at ambient temperatures was used as the test fluid during preliminary tests but the test data were inconclusive. All attempts to achieve a null condition of the sensing amplifier, at the specified test conditions, were unsuccessful. However, the use of air or GN_2 resulted in pressure sensor error signals of too small a magnitude to be effectively instrumented. Subsequent testing was conducted using 1300°F N_2H_4 decomposition products gas. Several attempts were made to test the regulator at the designed operating conditions. However, these tests were unsuccessful largely as a result of gasket erosion and subsequent failure, which caused excessive internal and external leakage. Gasket deterioration caused by temperature began at approximately 800°F and became increasingly worse as temperature increased. The gaskets failed during all of the attempts to reach the design temperature. Component skin temperatures in the range of 900°F were recorded.

Additional tests were conducted using N_2H_4 decomposition products gas at lower temperatures (600°F to 800°F). The effect of testing the regulator at a supply gas temperature somewhat lower than the designed condition was to lower the null point of the capillary-orifice bridge sensing unit. Pressure and flow values at this lower null point had not been determined; therefore, approximated values were applied. With nominal pressures set in the supply and output lines of the regulator, the output gas flow in the line which supplies pressurization to the second stage N_2H_4 propellant tank was increased and decreased over a limited range. This was accomplished by adjusting a load simulating valve in the output leg of the regulator. Review of the test data recorded over this operating range disclosed that the diverter output crossover point was not achieved. After further analysis, this indicated that the conditions required to effect a null point were not attained throughout the test range.

In a final attempt to obtain steady state performance data for the first-stage pressure regulator, it was decided that gaseous helium at ambient temperature could effectively be used to evaluate the component. In addition, its use would greatly facilitate the test procedures.

The primary performance variables influencing regulator operation were temperature, and molecular weight and viscosity. An analysis was performed to predict regulator performance using helium. The error signal using helium was calculated to be nearly four times that of air at the same temperature. This is represented on Figure No. 76. Converted nominal flow rates and pressure for the regulator input and output legs, using GHe, are indicated on Figure No. 77. This approach and the results of the analysis were presented to Bowles Engineering for their concurrence and they agreed that the approach was feasible.

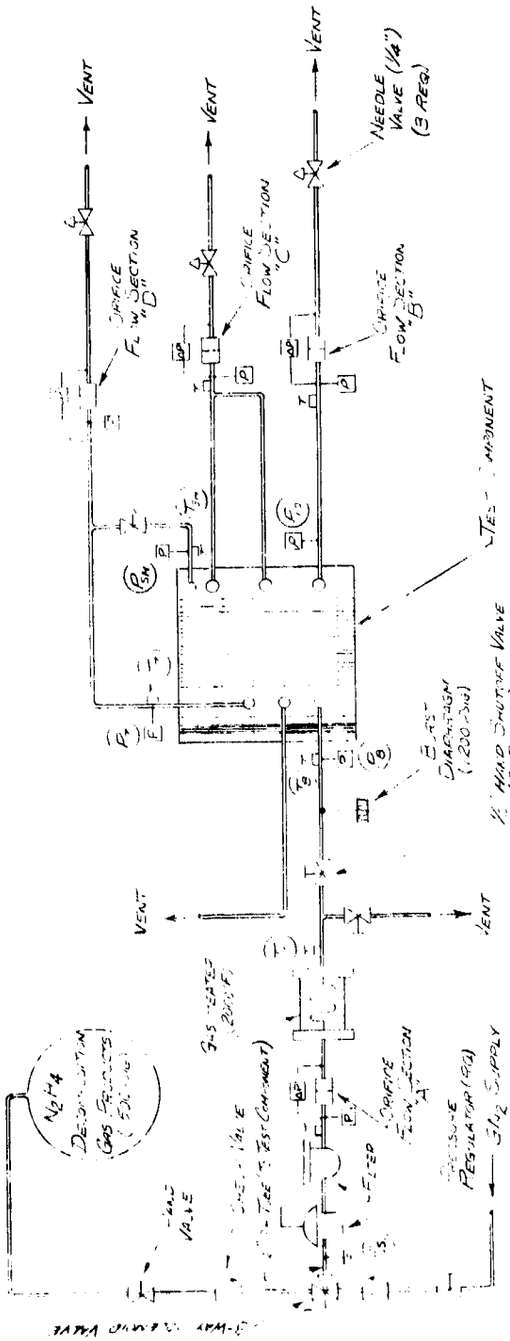

Figure 73. Test Schematic - First-Stage Regulator Sensing and Control Module Assembly

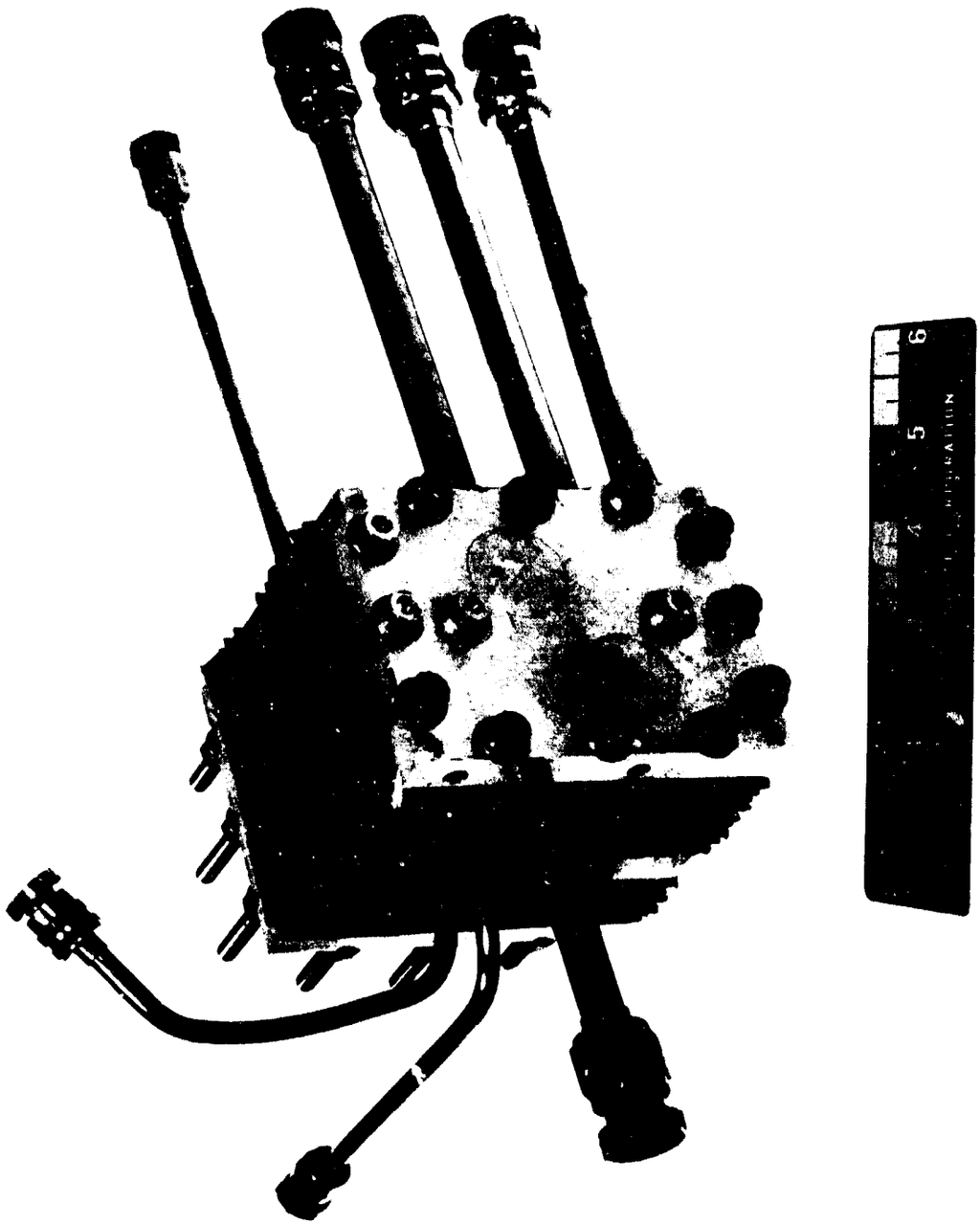

Figure 74. First-Stage Pressure Regulator

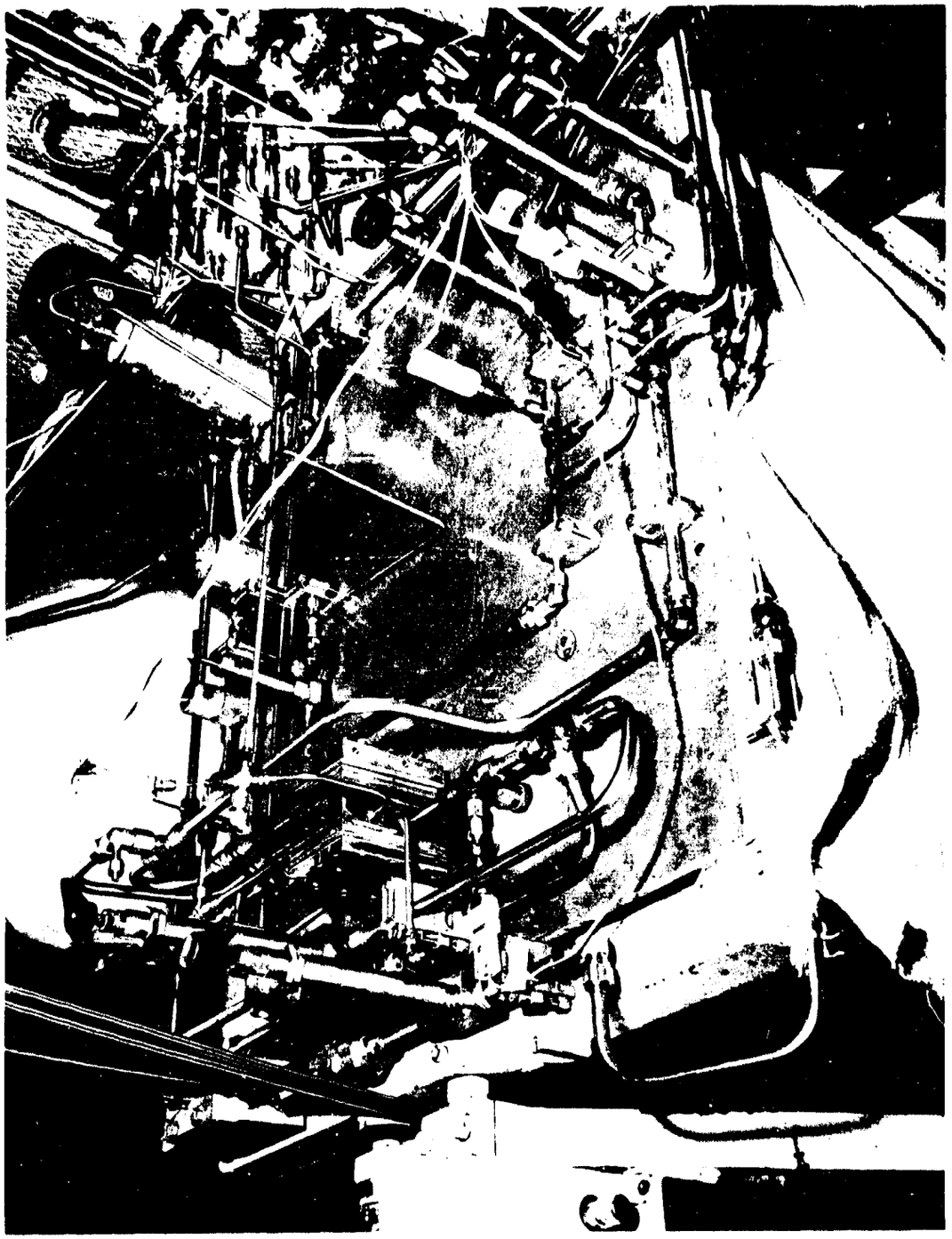

Figure 75. Test Set-Up - First-Stage Regulator Control Module

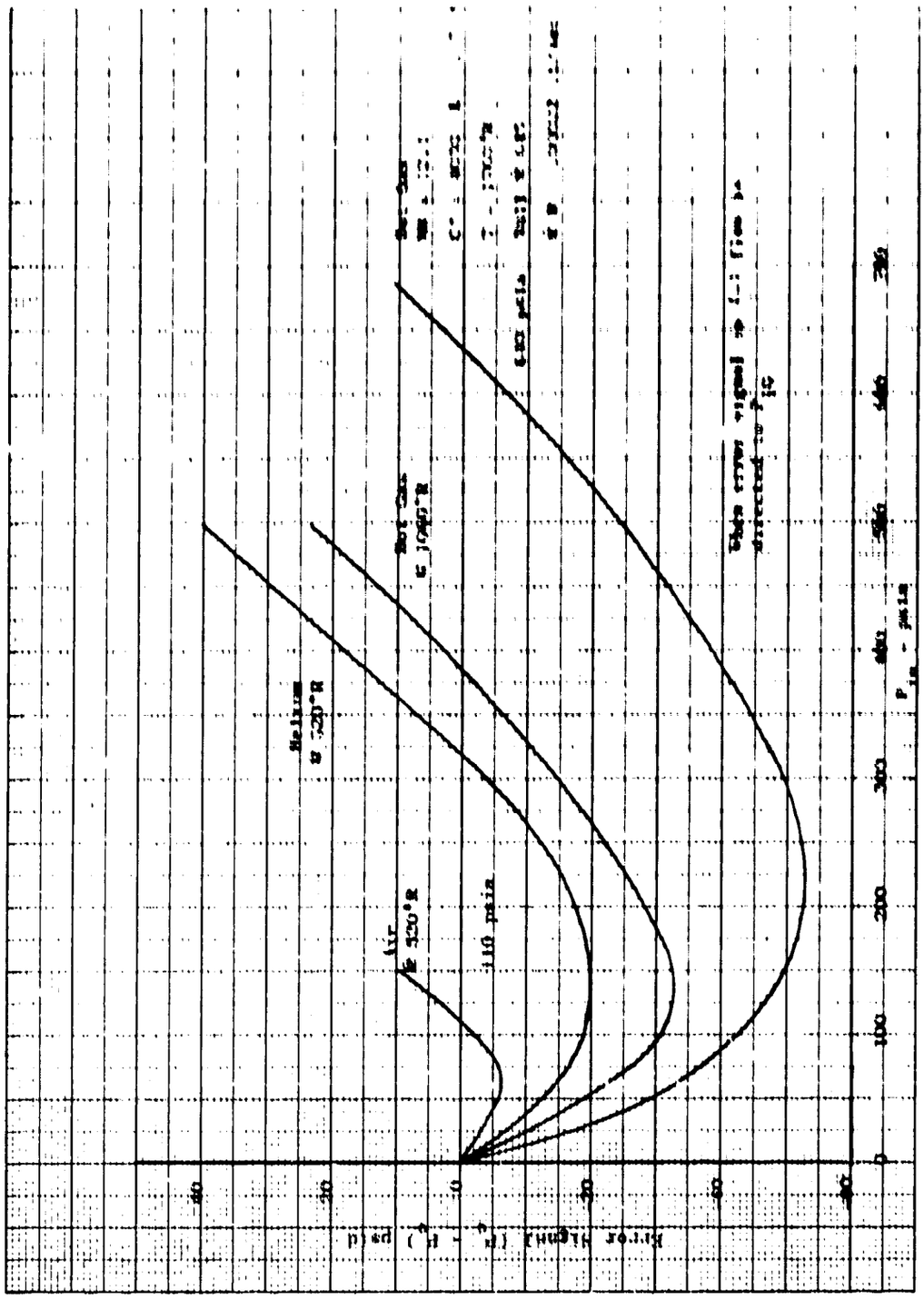

Figure 76. Stage 1 Pressure Regulator Pressure Sensing Module

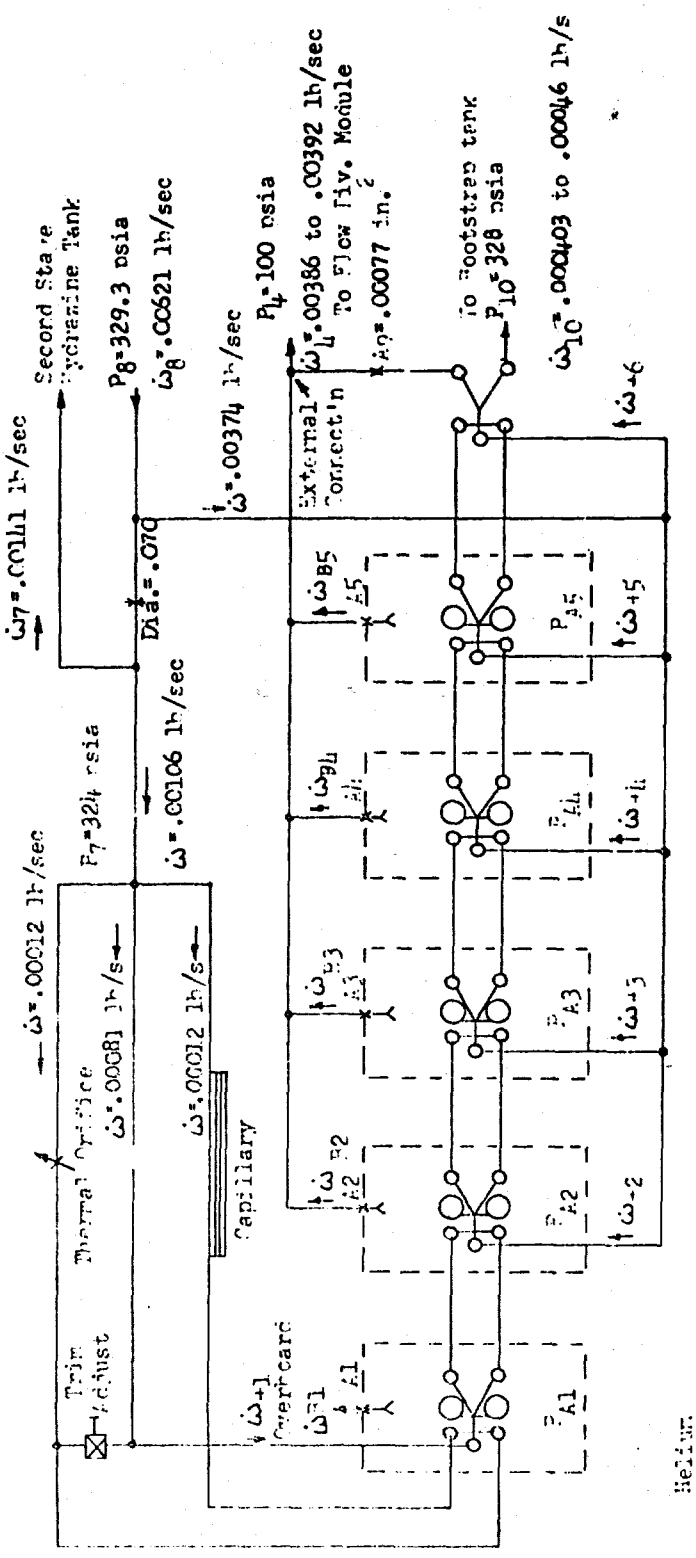

Stage Number	Ambient Pressure P_{Aj} psia	Supply Flow ω_{+j} lb/sec	Bleed Flow ω_{-j} lb/sec	Bleed Orifice Area A_j in.²
1	235	.00081	.000474	.000318
2	246	.000719	.000563	.000323
3	204	.000759	.000582	.000312
4	275	.000658	.000746	.000427
5	264.5	.000678	.000780	.000432
6	-	.000925	-	-

Note:
1) Coupling Amplifiers are Individually Pressurized P/N 882264
2) This Schematic for Helium at 70 °F

Figure 77. First-Stage Pressure Regulator Flow Schematic

modified-test setup and schematic are shown on Figure No. 78. Orifices lled in the output legs of the regulator were sized to provide critical flow at the nominal operating pressures A subsonic orifice flow section was used to measure and control gas supply to the regulator inlet.

The capability of effecting a null point condition of the regulator was of primary importance th oughout these latter tests as it was in previous tests. Several approaches were used without success. In the first approach, the regulator supply and output pressures as well as the flow rates were set at the nominal values. From this point, the supply pressure (P_8) was varied $\pm$ 25% from the nominal setting. Several data points were recorded within this range. However, there was no indication that the regulator was approaching a null condition and the relationship between the simulated outputs to the propellant and bootstrap tanks (P_7 and P_{10}, respectively) remained in direct proportion to each other. In proper operation, a crossover point would occur where P_{10} became inversely proportional to P_7.

A second test approach was used wherein the simulated output to the propellant tank (P_7) was adjusted over a $\pm$ 20% range from nominal setting. To accomplish this, the load valve (1/4-in. needle valve) in that line was set to equal the same nominal pressure and flow values provided by the critical flow orifice. Then, the orifice was removed from the line and the needle valve adjusted to increase and decrease the output flow. The results in this approach were comparable to those previously experienced. Test data showed no relationship of the regulator output pressures and flows to suggest any probability of achieving effective regulator performance.

A thermal analysis of the PBPS first-stage pressure regulator design was performed to investigate regulator performance under system thermal effects and to provide a history of the pertinent temperatures for the entire 800 sec of the anticipated mission.

b. Second-Stage Pressure Regulator Control Module

(1) Function and Basic Operation

The second-stage pressure regulator assembly for PBPS application regulates and controls input propellant (N_2H_4) flow to the Stage II gas generator and pressurization gas to the main propellant tanks. As in the case of the first-stage pressure regulator, the main supply gas to the second-stage pressure regulator is received from the Stage I gas generator combustion process. Excess gas emitted from the second-stage pressure regulator is diverted downstream in the controls subsystem to be used as control fluid for the engine controls.

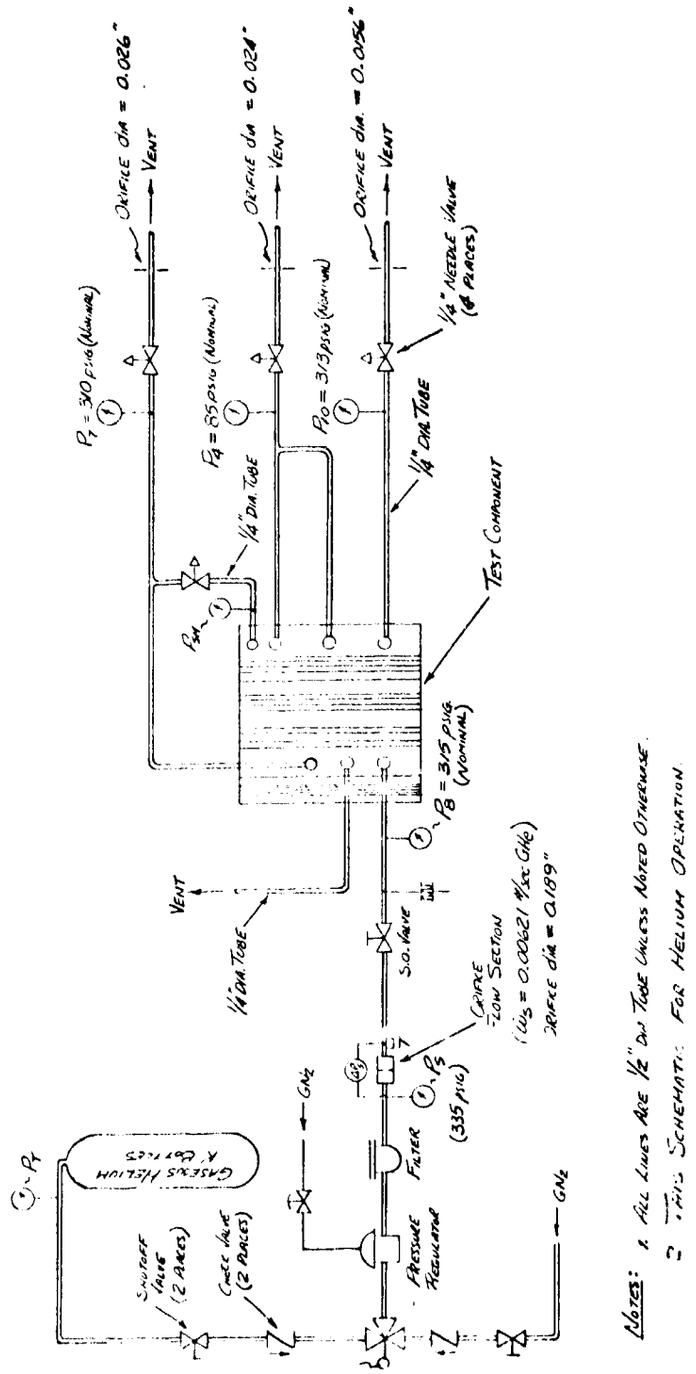

Figure 78. Test Schematic - First-Stage Pressure Regulator and Control Module Assembly

IV, C, Fluidic Control Components (cont.)

The second-stage pressure regulator is similar in operation to the first-stage regulator except that the regulator output amplifier error signal is used to control a gas/liquid vortex throttle which, in turn, regulates input hydrazine flow to the Stage II gas generator. The schematic diagram for the second-stage pressure regulator is included as Figure No. 79. This diagram shows the intended amplifier staging with a tabulation of pressures and flows for each stage. This configuration was proposed after repeated attempts to cascade non-vented diverters were unsuccessful. This approach consisted of using the last vented amplifier stage (Stage 5) to drive a diverter stage (Stage 6); using the diverter stage to drive a large vented amplifier stage (Stage 7); and using the large vented amplifier stage to drive a final diverter stage (Stage 8). The effect of interposing a large vented amplifier stage was to serve as a means of decoupling the interaction region pressures between non-vented diverter stages.

In operation, the two control ports of a diverter amplifier are controlled by regulated Stage I gas generator output flow balanced against the main propellant tank ullage pressure properly orificed to produce equilibrium at the desired tank pressure set point. When tank pressure falls below the desired level, the diverter (Stage 8) directs less gas flow to the vortex throttle which increases hydrazine flow to the Stage II gas generator thereby restoring the main propellant tank pressure. Conversely, high tank pressure acts to decrease hydrazine flow in the same manner. Amplification of the error signal from approximately 0.5 psi delta to approximately 43 psi delta is accomplished by staging of the diverter amplifiers as required.

The second-stage pressure regulator control differs from the first-stage unit in several aspects. The major difference is the absence of a separate pressure sensing device in the second-stage regulator. Because of this, no thermal compensation is required. A second difference is the manner in which the diverter amplifiers are staged. Staging of these units is dependent upon the pressure and flow gains required in the control system. Each separate diverter amplifier was tested and performance rated in these categories. The amplifiers then were individually selected and cascaded as required to obtain the necessary gain requirements.

Thirdly, the second-stage regulator control includes a gas-liquid vortex throttle which controls propellant flow to the Stage II gas generator. The vortex throttle, analogous to a mechanical control valve, is actually a separate component but for the PBPS application, it is classified as part of the second-stage regulator control. The basic operating principles of the vortex throttle will be discussed in more detail in the engine controls technical discussion section of this report.

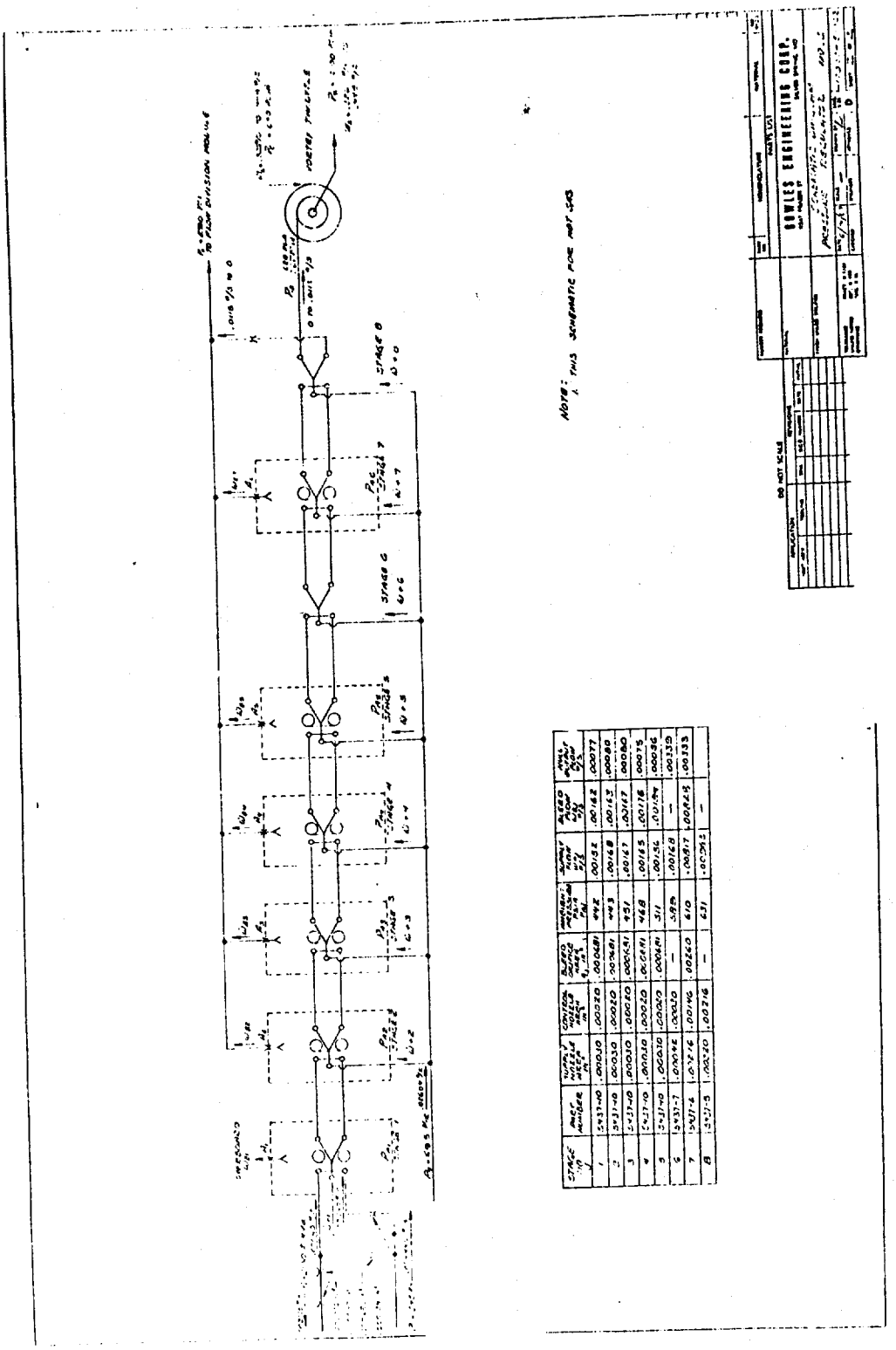

Figure 79. Schematic Diagram - Pressure Regulator No. 2

IV, C, Fluidic Control Components (cont.)

(2) Component Description and Specifications

The experimental model of the second-stage pressure regulator is very similar in appearance to the first-stage pressure regulator assembly. An assembly drawing of the component is included as Figure No. 80. The assembly consists of individual diverter elements and cover plates brazed as a subassembly. The resulting modules than are stacked and sealed with flat plate gaskets held with bolts for easy removal and inspection. Also included are manifold plates and orifice plates which are sized as required to provide the circuit trim and bias functions.

The gas emitting from one output leg (P_{12}) of the final stage (non-vented) diverter is used as the control fluid for the second-stage regulator vortex throttle. A simplified assembly drawing of the second stage regulator throttle is included as Figure No. 81. The assembly consists of a separate liquid and gas chamber with an interchamber crifice plate. Both the liquid and the gas enter the throttle tangentially into separate cylindrical chambers with a 90 degree liquid lead. The vortexing action of the relatively small stream of gas influences the liquid vortex so as to impede or halt the flow of liquid through the device and out the exit.

Basically, the unit operating pressure and temperature requirements are identical to those of the first-stage component. Supply gas to the pressure regulator is 695 $\pm$ 35 psia at a temperature of approximately 1400°F, and a supply flow rate of 0.020 lb/sec. Regulated propellant tank pressure is 290 $\pm$ 15 psia and regulated gas flow to the main propellant tanks is 0.075 lb/sec to 0.090 lb/sec. Bypass gas flow rate to the flow division module is zero to 0.020 lb/sec while that to the engine controls is 0.23 lb/sec to 0.40 lb/sec. N_2H_4 was supplied to the vortex throttle at a pressure of 640 $\pm$ 45 psia and a flow rate of 0.30 lb/sec to 0.45 lb/sec. Control fluid available from the pressure regulator unit and used to throttle propellant flow in the vortex throttle is 0.020 lb/sec maximum.

(3) Amplifier Development

Amplifier development for the second-stage pressure regulator occurred simultaneously with that for the first-stage component because the same basic technology was involved. Like problems were encountered in attempting to stage non-vented diverters. As a result of these major problems, a survey of the industry was initiated in regard to possible accomplishments with staged, non-vented fluid amplifiers in high pressure applications. Fifty-one companies were contacted and 50 of these responded negatively, indicating little work was being done in the field. One replied affirmatively indicating some experience and preliminary evaluation in regard to non-vented, staged amplifiers in the pressure range of 300 psig. However, they envisioned a minimum diverter development program ranging from nine to twelve months for the particular design application.

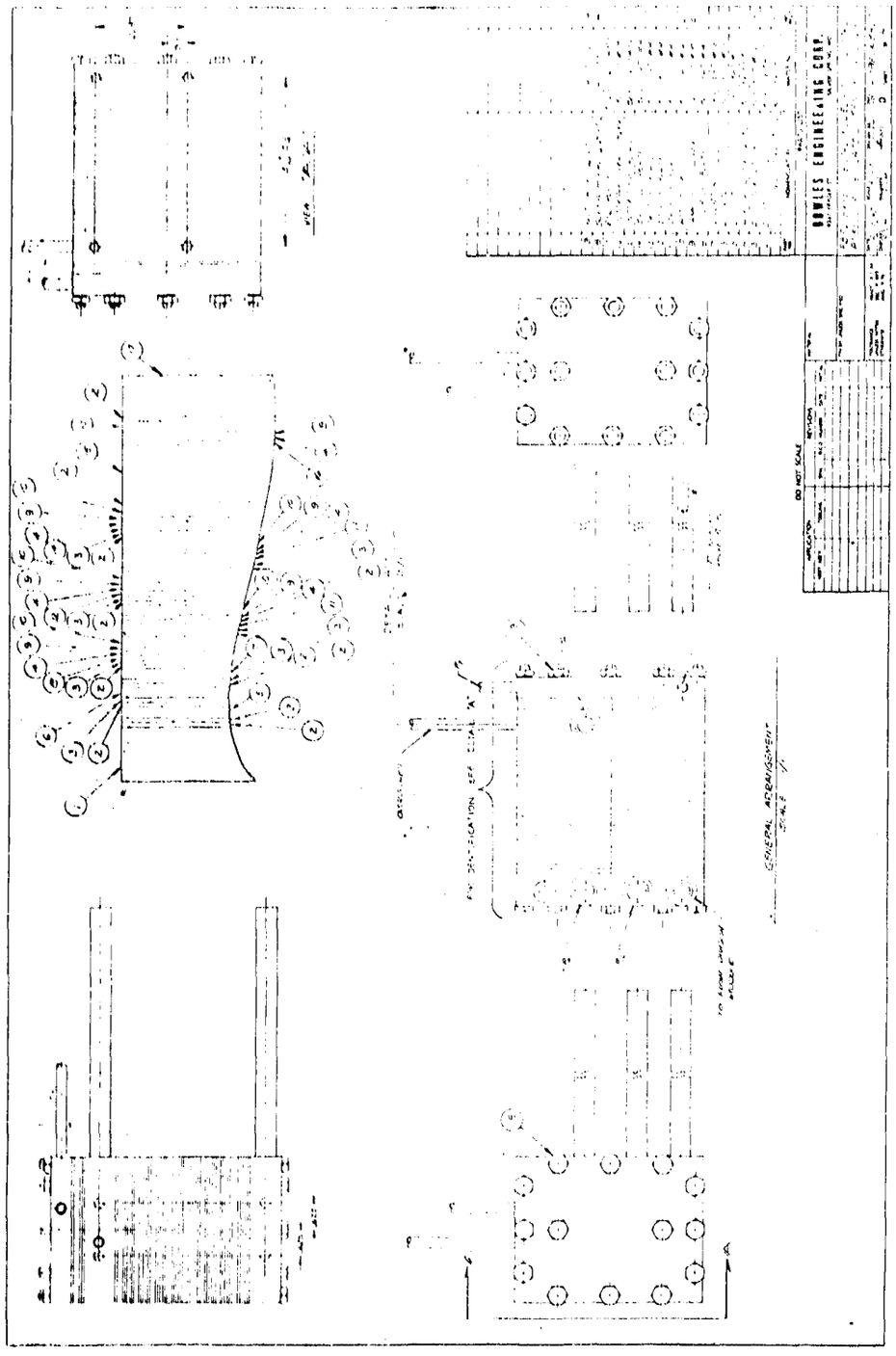

Figure 80. Second-Stage Pressure Regulator Sensing Module

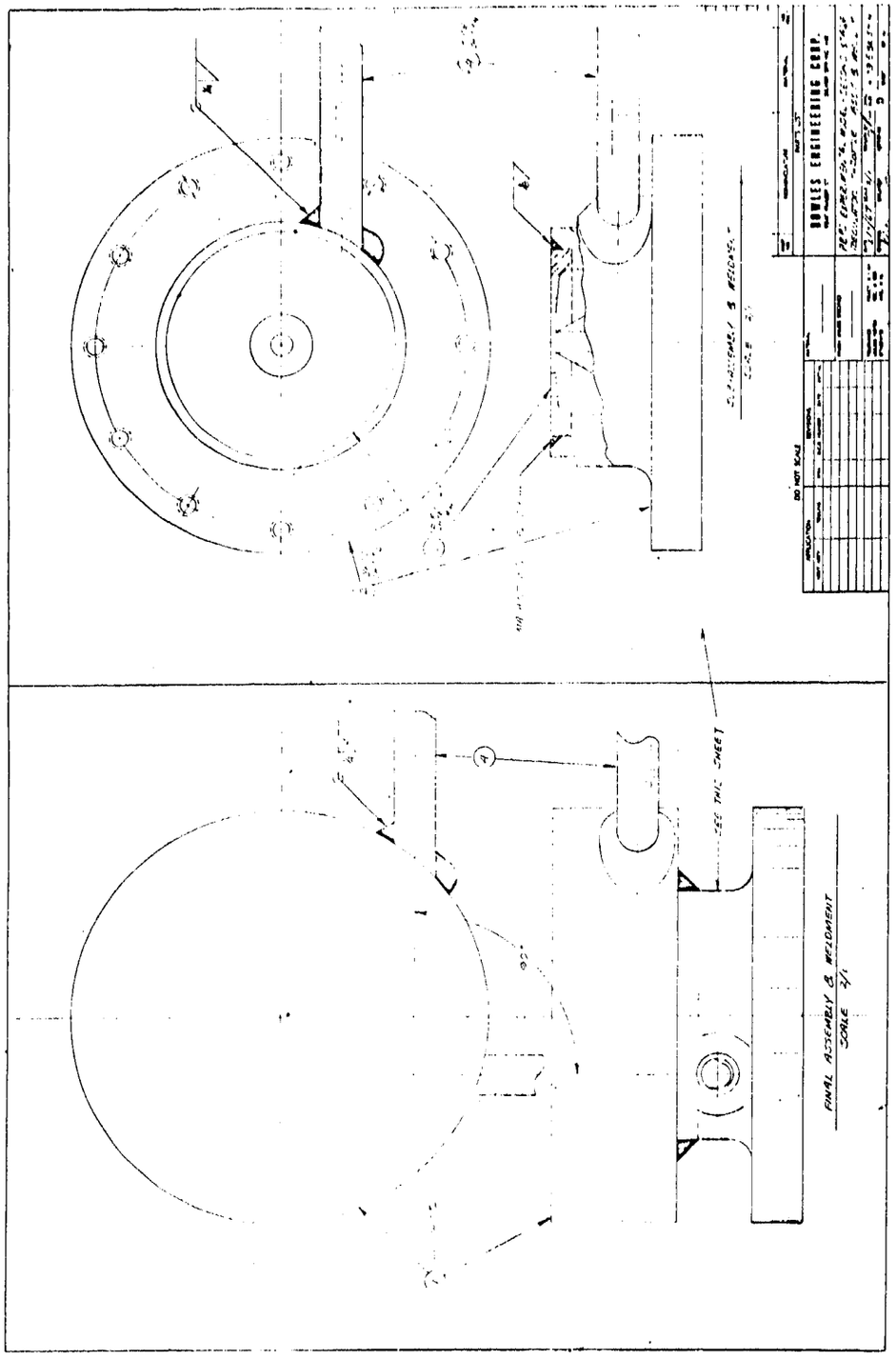

Figure 81. Second-Stage Regulator Throttle Assembly

IV, C, Fluidic Control Components (cont.)

Additional problems were experienced by Bowles Engineering concerning the fabrication of the second-stage amplifiers. The interaction regions of the amplifiers were machined by an "elox" process to maintain the close tolerances required. The copper form tools used in this operation were machined by panamilling and an error was made on the length of the splitter tip, which affected the end result of all amplifier units necessitating re-manufacture of the elements.

The six vented amplifiers and two non-vented diverters were received with all elements in the unbonded condition because it was planned to subsequently braze the cover plates on each amplifier and eliminate the gasket leaking problem. These elements were pressure tested at Bowles Engineering in the unbonded state and an over-all gain of 27 was recorded for the cascade. This was considered as sufficient for regulator operation.

Again, major problems were experienced during the amplifier bonding process. Initially, the plates were inspected and found to be of poor quality as regarded flatness and surface condition. All plates were bright-annealed in dry hydrogen and lapped in an effort to obtain good joint contact. One unit was rejected because of surface conditions. The remaining assemblies were copper-plated to provide the copper braze cycle. A re-braze cycle, using Nioro braze powder, was attempted to seal the edges of the holes around the periphery of the elements. The parts remained discolored and visual inspection showed the edge sealing to be inadequate. Two additional Nioro braze cycles for edge sealing were attempted with little success.

(4) Component Testing and Evaluation

All scheduled testing of the second-stage pressure regulator assembly was suspended because of the difficulties encountered with the amplifier development and fabrication

Limited testing of the second-stage regulator throttle was conducted. The vortex throttle was designed and fabricated in plexiglas, aluminum, and stainless steel. The plexiglas model was flow tested in conjunction with the Hamilton Standard second-stage gas generator injector using air and water as the test fluids. The test revealed that the throttle operation was considerably better than had been expected during system preliminary design. This achievement allowed a reduction of some 50% of the gas flow required from the first-stage pressurization system to the second-stage regulator. The reduction would result in a requirement for less hydrazine in the first-stage bootstrap tank. Figure No. 82 shows the flow test and the configuration of the throttle. Test results are presented in Figure No. 83.

Figure 82. Vortex Throttle Second-Stage Gas Generator Injector Test

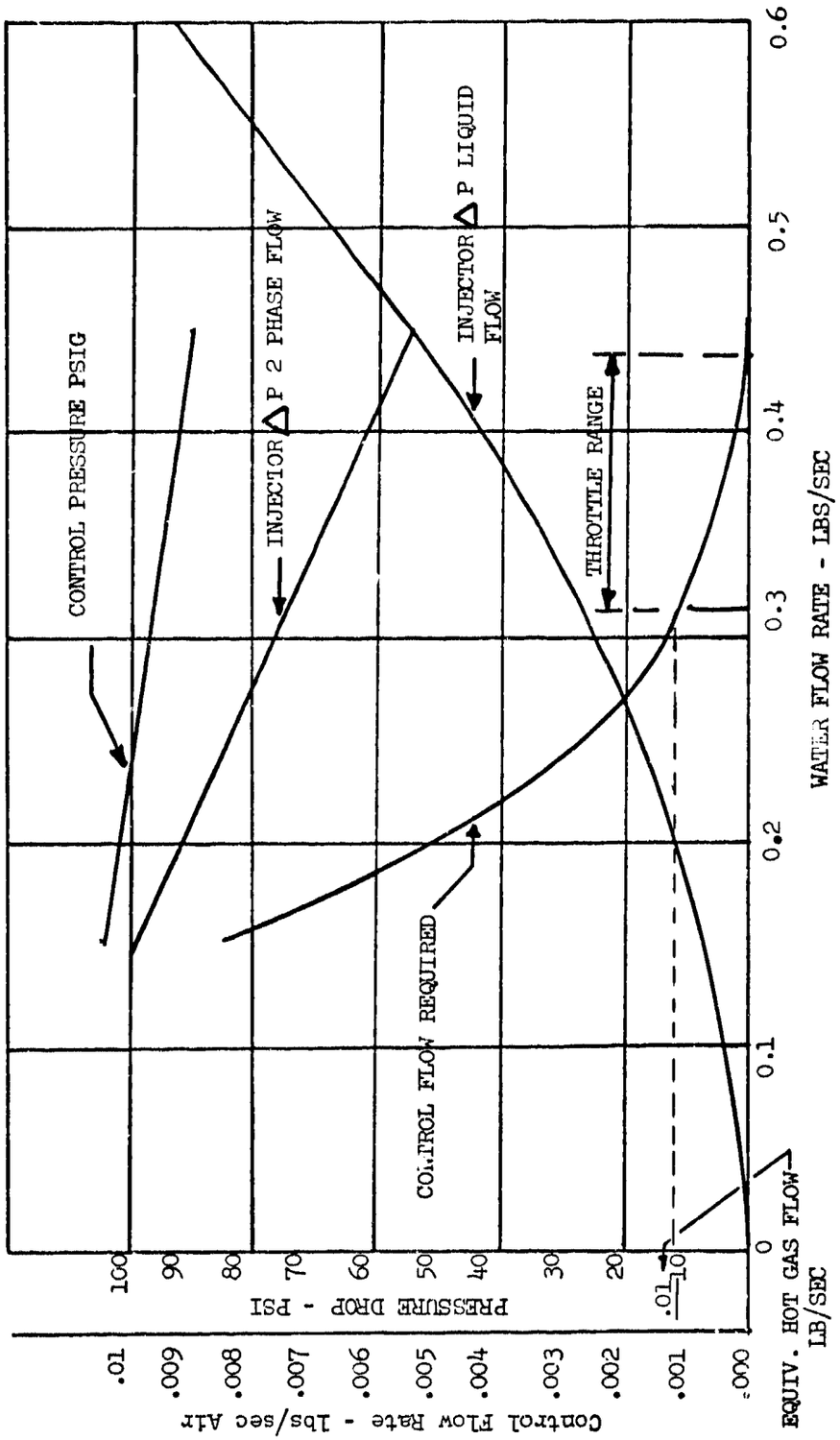

Figure 83. Second-Stage Gas Generator Injector and Vortex Throttle

IV, C. Fluidic Control Components (cont.)

The aluminum model was test fired with the Hamilton Standard second-stage gas generator. The primary objective of this test was to determine the effect of two phase inlet flow upon gas generator stability. Test results showed that throttling by introducing gas into the liquid flow had a stabilizing influence upon the gas generator.

The stainless steel throttle was tested at Bowles Engineering. It was tested with the four final stages of the regulator amplifier cascade which consisted of alternated vented and unvented amplifiers. The assembly performed adequately; water flow was controlled from 0.44 lb/sec to 0.29 lb/sec. The water supply pressure was 620 psig and the air supply pressure to the amplifiers was 680 psig. This testing was accomplished with the amplifiers in the unbonded condition.

c. Flow Division Module and Vent Control Module

The function of the flow division module was to provide for the smooth diversion of gas flow from the Stage II gas generator to the main propellant tanks and to the engine controls. An early proposed design of this module is shown on Figure No. 84.

The vent control module controls the venting of control gas overboard and provides the back pressure required by the engine controls. A basic envelope drawing of this module is shown on Figure No. 85.

Development of the flow division and vent control modules was cancelled during the first quarter of 1967 because of the limited developmental status of the regulator and engine control modulus.

2. Engine Controls

The PBPS controls subsystem engine controls consist of two [illegible] modules; one for the axial engines and the other for the ACS engines. [illegible] module is made up of two vortex throttle valves and shutoff capability, [illegible]ntrol gas diverter valve, and an electro-pneumatic transducer. The axial [illegible]ngine module provides for thrust control between 50% and 100% of full-thrust while the ACS module provides "ON - OFF" operation only.

a. Axial Engine Control Module

(1) Function and Basic Operation

The purpose of the axial engine control module for PBPS application is to direct and control liquid propellants to the rocket engine thrust chamber. It must be capable of starting and stopping the flow of propellants to the rocket engine and throttling the flow to achieve thrust control continuously between 50% and 100% of full-thrust. Figure No. 86 is a layout of the basic unit.

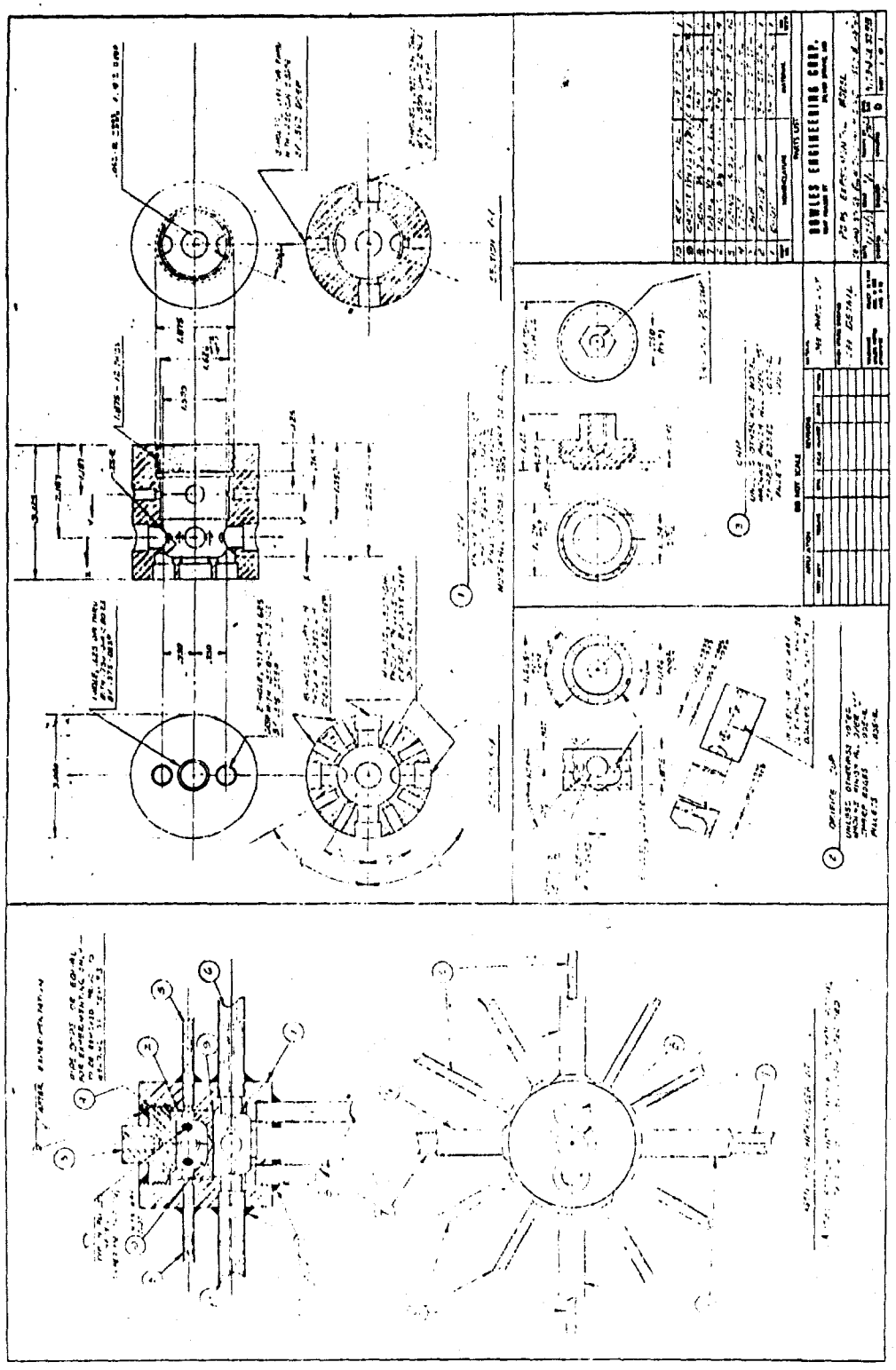

Figure 84. Second-Stage Flow Division Module Assembly

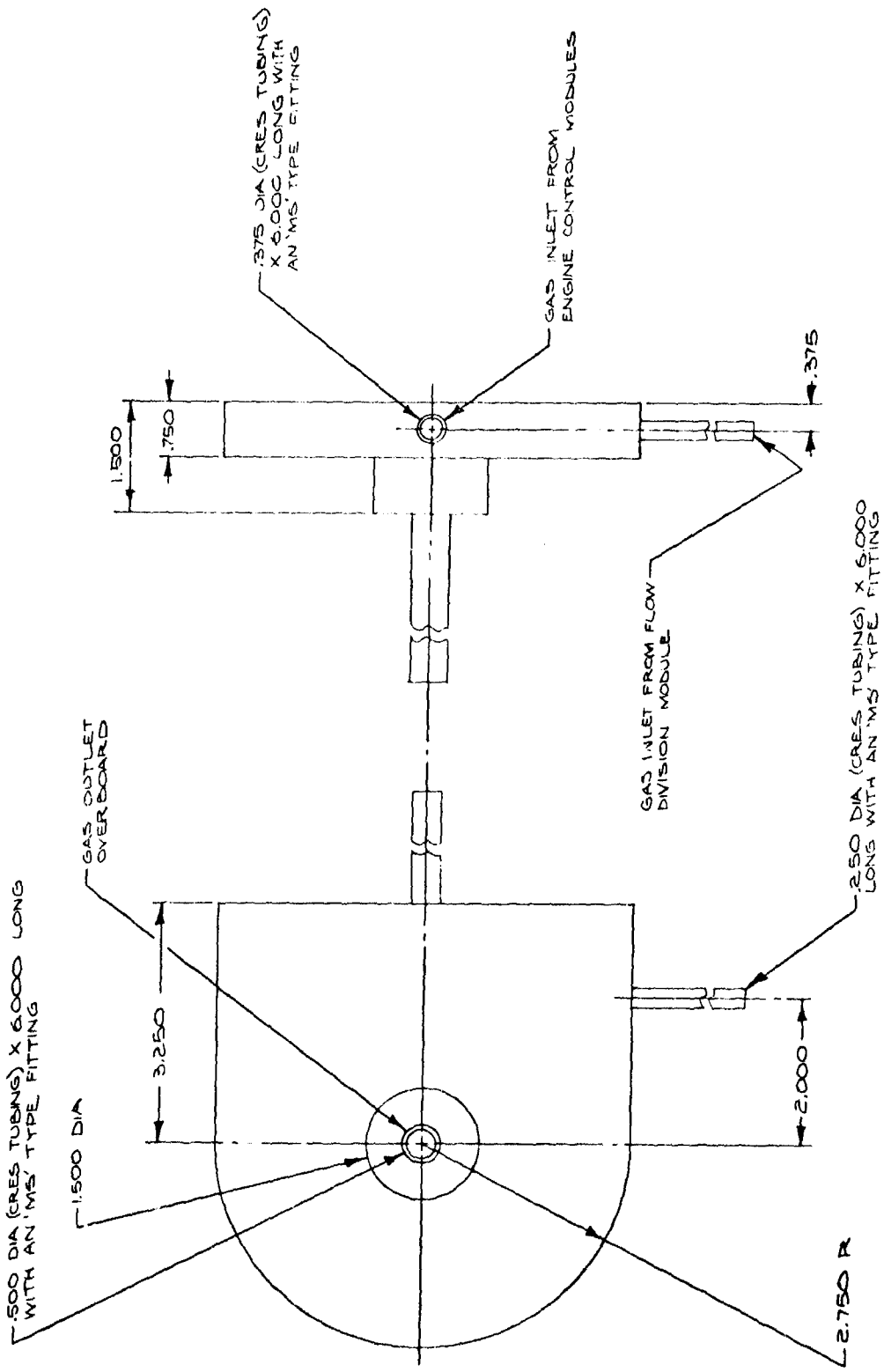

Figure 85. Vent Control Module

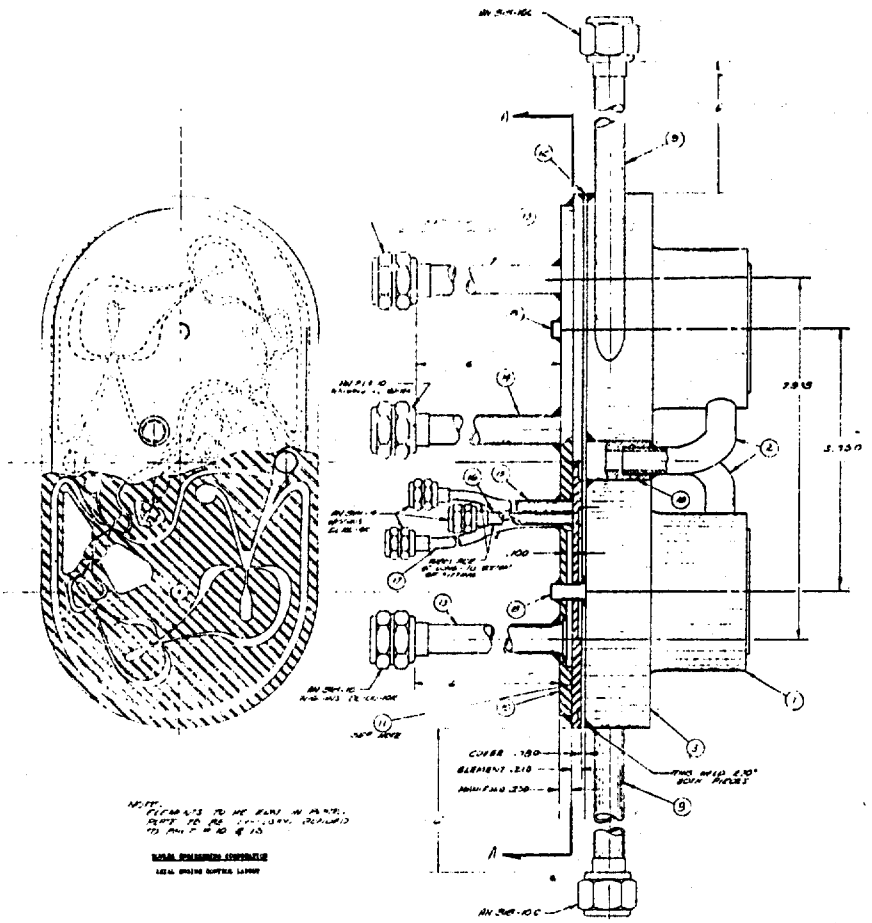

Figure 86. Axial Engine Control Layout

IV, C, Fluidic Control Components (cont.)

Basically, the vortex throttle is a device which utilizes the vortexing action of a small stream of gas injected tangentially in a cylindrical chamber to impede or halt the flow of a liquid or gas flowing through the device. The throttles used in this application are classified as gas-on-liquid units. A simplified representation of a vortex throttle with appropriate nomenclature is included as Figure No. 87. In the full-on condition, a liquid is introduced into the upper chamber and flows out through the discharge port (exit diameter) into the engine injector. The valve is turned off by introducing gas flow into the lower vortex chamber (at the gas inlet) which progressively stops the liquid flow as gas flow increases until complete shutoff is achieved. Varied operating conditions are represented on Figure No. 88.

The gas controlling the throttle is regulated by non-vented diverter valves which direct the gas flow either to the throttle for shutoff or away from the throttle to a vent for full-thrust operation. An electrical interface point, at which signals from a guidance system can be fed into the pneumatic valve control circuit, is provided by means of an electro-pneumatic transducer or small torque motor valve to convert the electrical signal commanding engine operation to a very small differential pressure signal. Then, this small signal is amplified through a series of staged diverter valves, which is similar to the pressure regulator amplifier circuit. This results in a pneumatic signal at the valve capable of regulating liquid flow. Proportional control is provided through the electro-pneumatic transducer to provide thrust control between 50% and 100% full thrust. A feedback loop also is included with chamber pressure being sensed for the feedback signal. The circuit is shown schematically on Figure No. 89.

A D.G. O'Brien Model 102 Torque Motor is used to generate a chamber pressure reference with which the measured chamber pressure is compared in the first-stage of the control amplifier. Approximately 0.002 lb/sec gas flow is used for both generating the reference and for measurement purposes. The latter is to prevent gas at engine temperatures from entering the control circuit.

The reference pressure is generated by a flapper valve in combination with a fixed orifice. The flapper valve motion is determined by the reference current and the generated pressure by feedback action produced as a result of the pressure force acting upon the flapper nozzle area. The nozzle diameter is 0.160-in. while the total stroke of the valve varies from 0.005-in to .001-in. traveling from zero to 100% thrust, respectively.

Vortex throttling performance is expressed in terms of turndown ratio, which is defined as the weight flow rate of the liquid passing through the valve in the full-on condition divided by the weight flow rate of the gas required to completely shut off the liquid flow. Turndown ratio is a

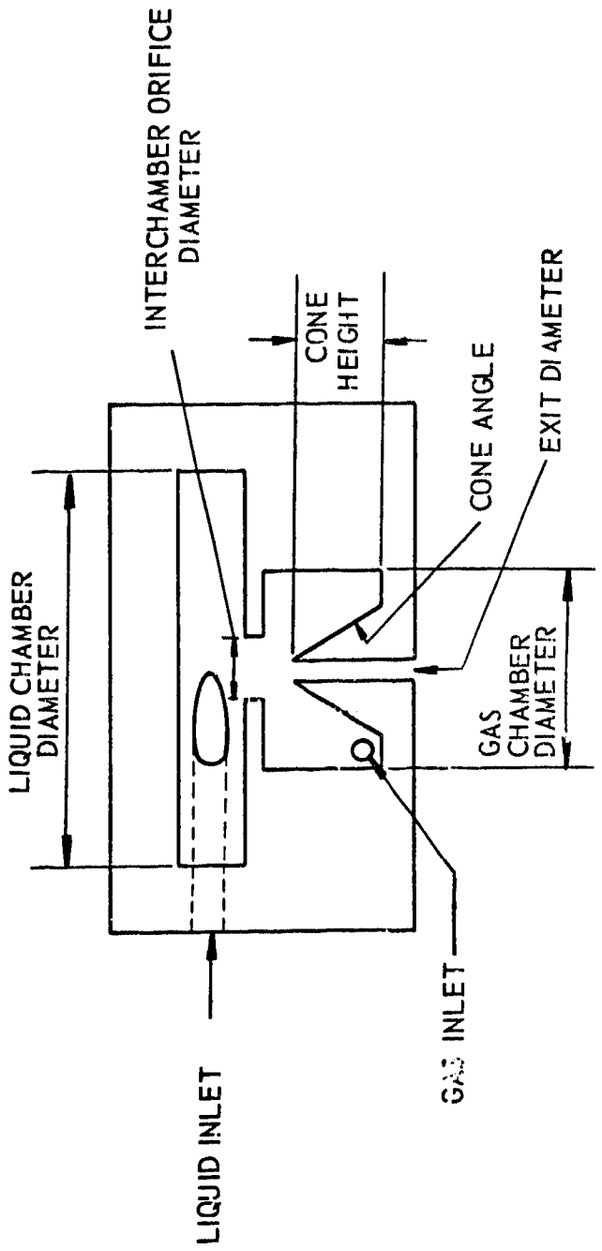

Figure 87. Vortex Throttle Nomenclature

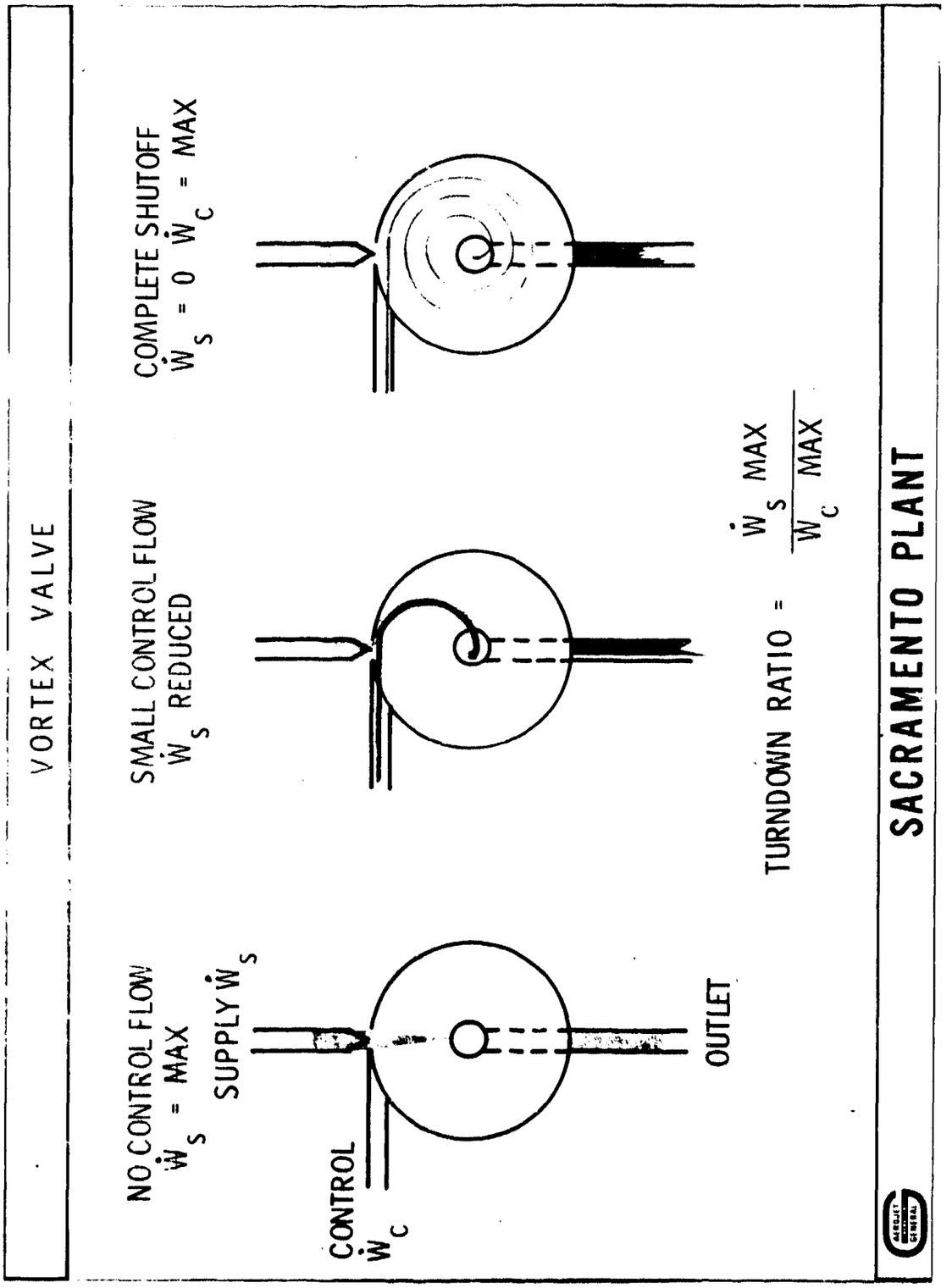

Figure 88. Vortex Valve Control Flow Representation

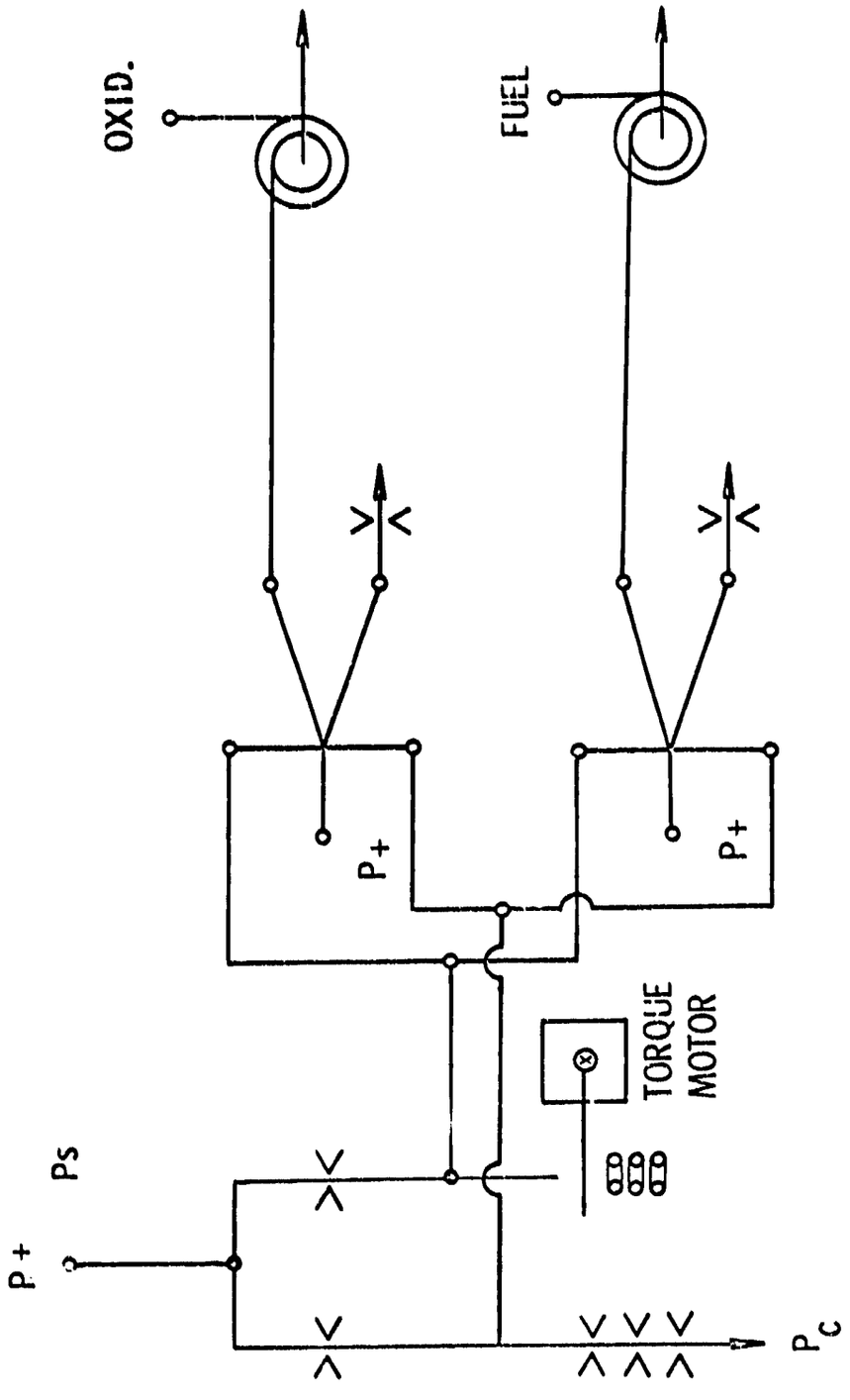

Figure 89. Axial Engine Control Test Schematic

IV, C, Fluidic Control Components (cont.)

function of the type of liquid, type of gas, temperature and pressure; therefore, throttle turndown must be compared upon a figure of merit basis. The unity figure of merit was established at the level of Bowles Engineering capability at the inception of the contracted PBPS effort. It is desirable to raise throttle turndown as high as possible because stored control fluid weight varies directly with throttle gas requirements.

(2) Component Description and Specifications

Figure No. 90 is a photograph of the experimental axial engine control module with the torque motor assembly. As shown, the torque motor assembly is a separate unit that when used is mechanically coupled to the diverter valve cascade by 1/4 in. outside diameter tubing.

The diverter amplifier elements and interconnecting flow passages were machined into 1/8-in. thick steel plates by a pantomilling or eloxing process. The diverter sections for the fuel and oxidizer throttles are separate units. Cover plates, 1/8-in. thick, were assembled adjacent to the diverter platelets. Then, all plates were sandwiched between a 7/16-in. thick, one-piece base plate and two 7/16-in. thick top support plates. Flat gaskets were used between the plates for sealing purposes. The diverter amplifier section was assembled to the vortex throttles using numerous bolts and L-shaped brackets. Figure No. 91 shows the vortex throttle in both the disassembled and assembled configuration.

A cross-sectional view of the vortex throttle is shown on Figure No. 92. Basically, it consists of four separate parts; a liquid chamber, a gas chamber, an interchamber orifice plate, and a cone. The throttle assembly is an all-welded construction with the liquid chamber diameter being exactly double the gas chamber. Extensive testing, subsequently discussed, was accomplished to evolve the sizing of these units.

Basically, the unit is designed with the capability of both pulse mode operation and a continuous throttling mode of operation over the throttling range of full-thrust to 50% of thrust. The response time requirement is 10 millisec which encompasses the time when an electrical signal input to the unit is received to the time the component reaches 90% of rated output flow. The closing or shutdown response requirement also is 10 millisec. Operating pressure and temperature requirements are 500 psig (maximum) and 1400°F (maximum), respectively. Nominal oxidizer and fuel flow rates were specified as 1.23 lb/sec and 0.77 lb/sec, respectively, while nominal control gas flow rate is 0.08 lb/sec. The vortex throttles were designed to provide optimum turndown ratios utilizing available information. However, the specified turndown ratio for each throttle was not to fall below 25 with an assumed propellant inlet pressure of 282 psia and a control gas temperature of 1300°F.

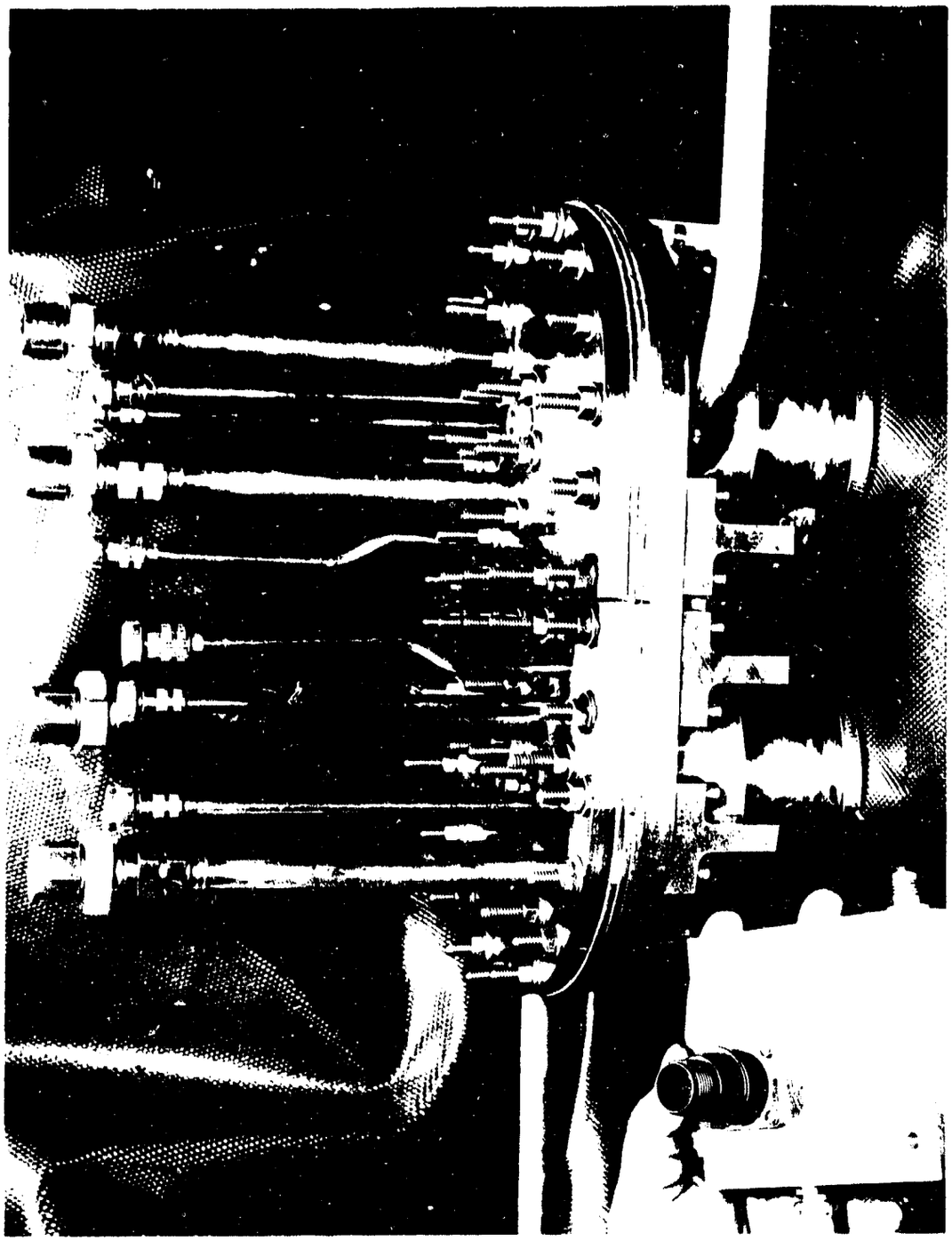

Figure 90. Axial Engine Control Module

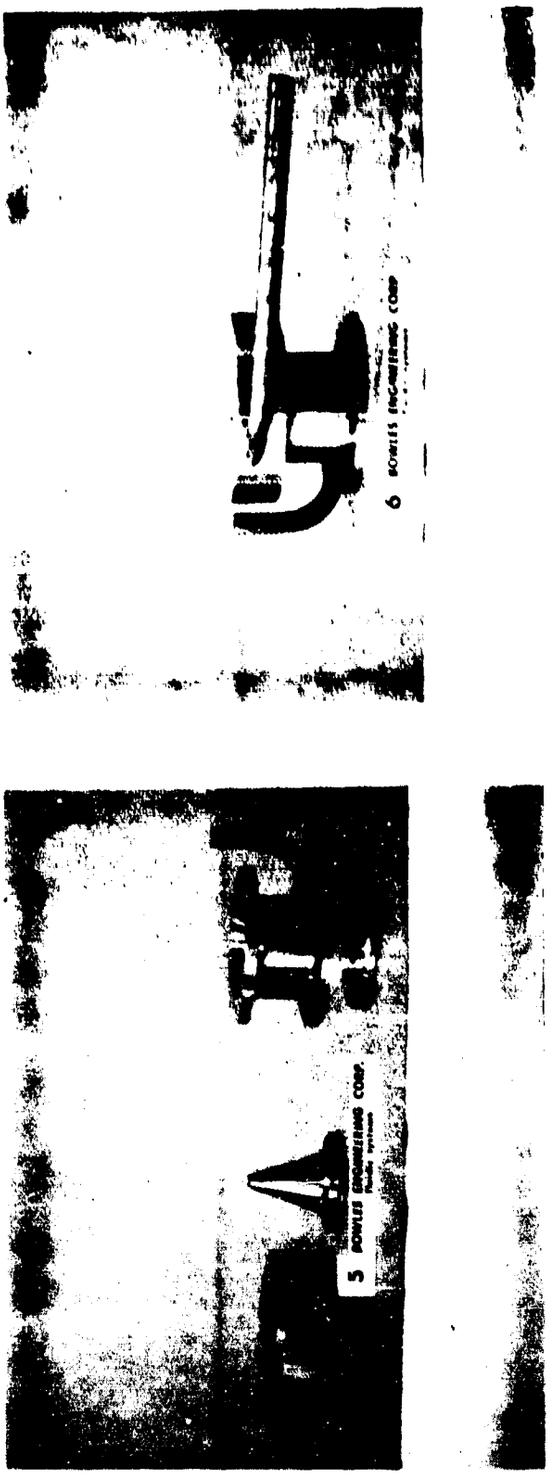

Figure 91. Axial Engine Throttle

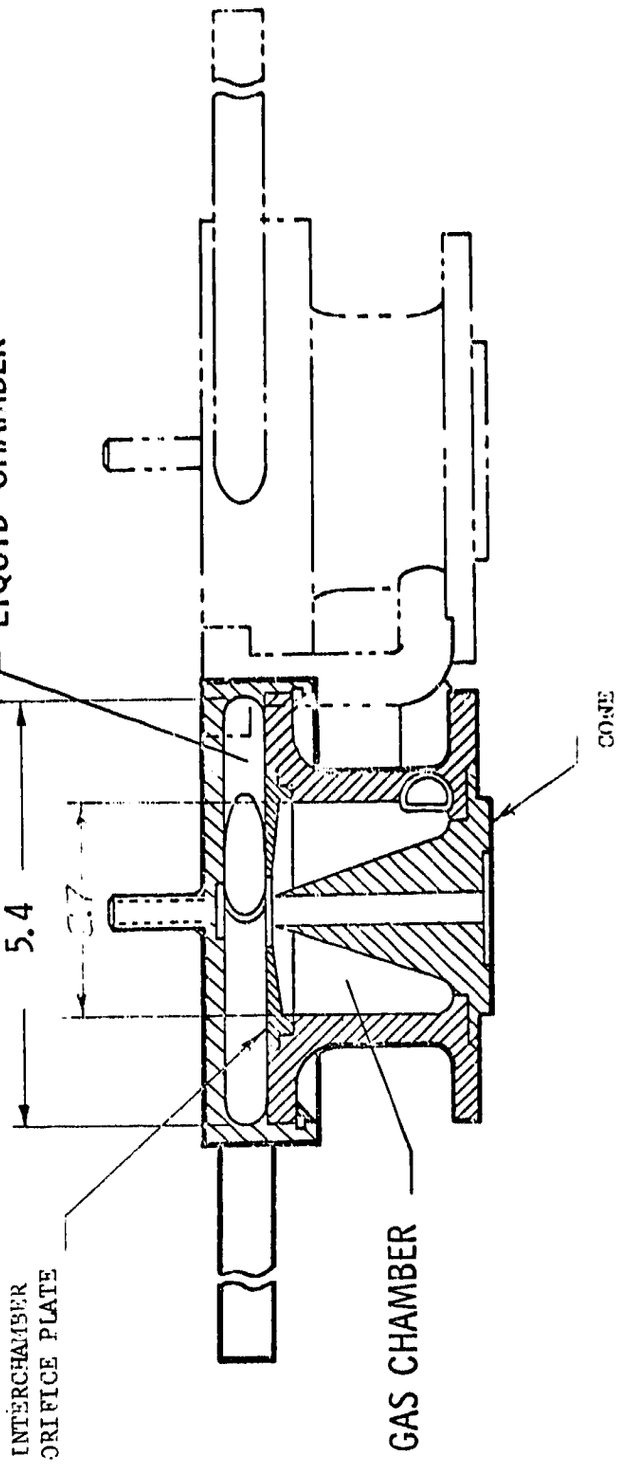

Figure 92. Axial Engine Throttle Configuration

IV, C, Fluidic Control Components (cont.)

(3) Component Development

Development testing of the axial engine control module was very limited because of recurrent delays in scheduled component delivery dates. These difficulties resulted from the development problems encountered by Bowles Engineering early in the program. A major problem in component development was the inability to successfully stage diverter amplifiers. This problem seriously affected the development of all PBPS control components because a basic diverter amplifier configuration was designed for all units.

Tests of plastic model diverters were conducted at low pressures to establish the configuration needed to provide the required pressure and flow gain characteristics for the engine control modules. The configuration selected as a result of these tests demonstrated pressure gains of up to 3.0. However, staging attempts using the same configuration diverters were unsatisfactory. A pressure gain of 3.8 was obtained across two elements whereas this gain should have been in the order of 9. It appears that a pressure gain was obtained only in a very narrow range of operating conditions.

The initial axial engine control module design utilized a seven-stage diverter amplifier control system (see Figure No. 93). However, because of difficulties encountered in staging the diverters, it was decided to evaluate the component using only one diverter to operate each throttle. This operation of the axial throttle with a single-stage diverter was demonstrated by Bowles Engineering. Figure No. 94 is the test schematic and includes the test results. It should be noted that even though these tests were a limited success, throttle turn-on was achieved only by lowering the vent pressure below system specifications.

Considerable vortex throttle testing was completed concurrently with the initial design phase of the axial engine control module. This testing was directed primarily toward evolving an optimum throttle turndown ratio. An Aerojet-General-sponsored parametric test program was undertaken. The necessary test hardware was designed and fabricated. Those factors considered relevant to the influence of throttle turndown ratio were defined and evaluated in the test program based upon a statistical analysis approach. Numerous throttle configurations were evaluated. The resulting information was incorporated into the final axial engine throttle design.

Bowles Engineering tested both vortex throttles (no diverters) for turndown ratio with air and water. The results were satisfactory and the data indicated that a system turndown of at least 31:1 could be anticipated. This figure was converted to system conditions from a turndown of 19:1 using air and water as the test fluids. The test setup and results are

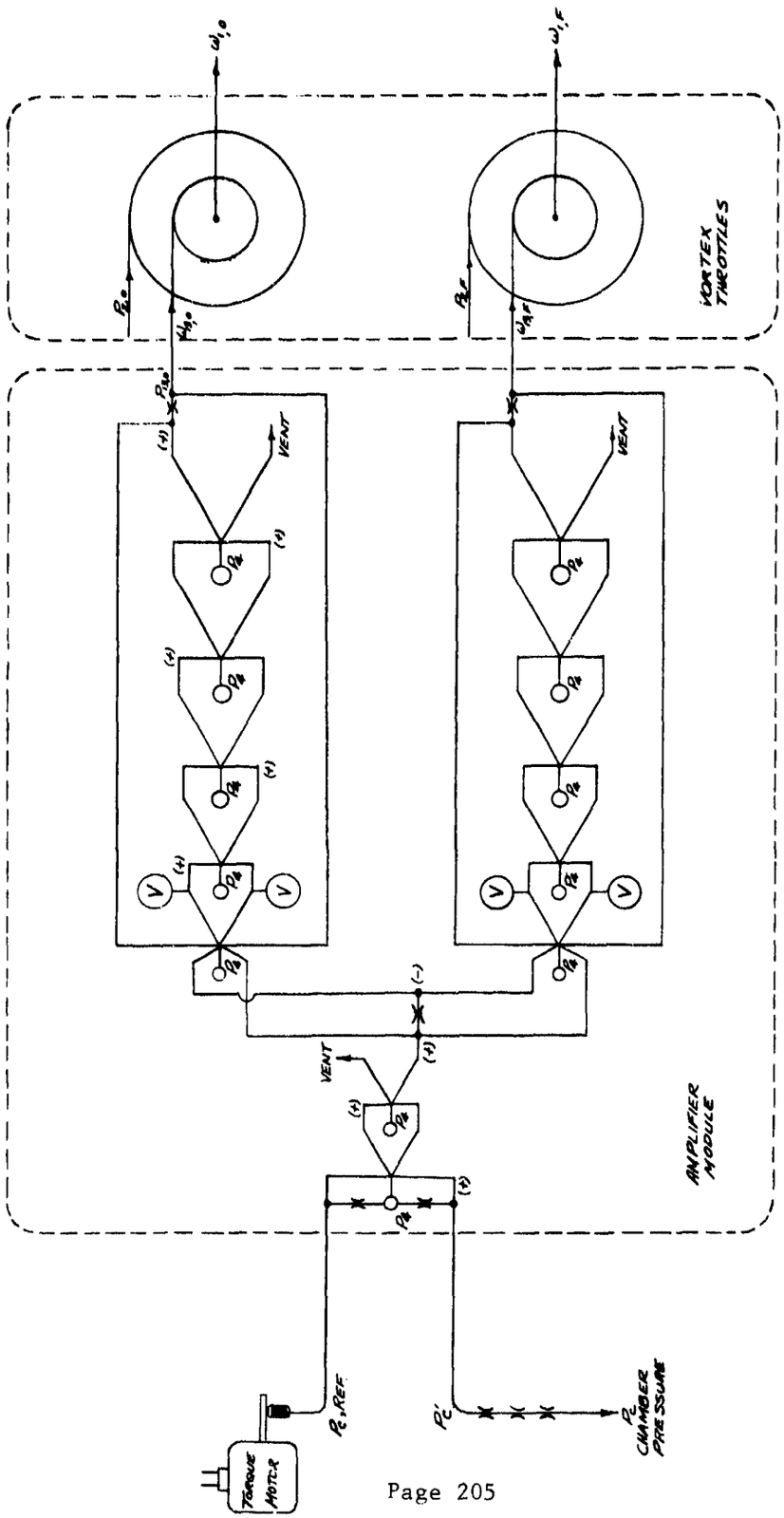

Figure 93. Axial Engine Control Module

OBJECT: .0 DEMONSTRATE THE ABILITY OF THE N5393 (.064 x .128) DIVERTER TO OPERATE THE AXIAL THROTTLE.

TEST SET-UP:

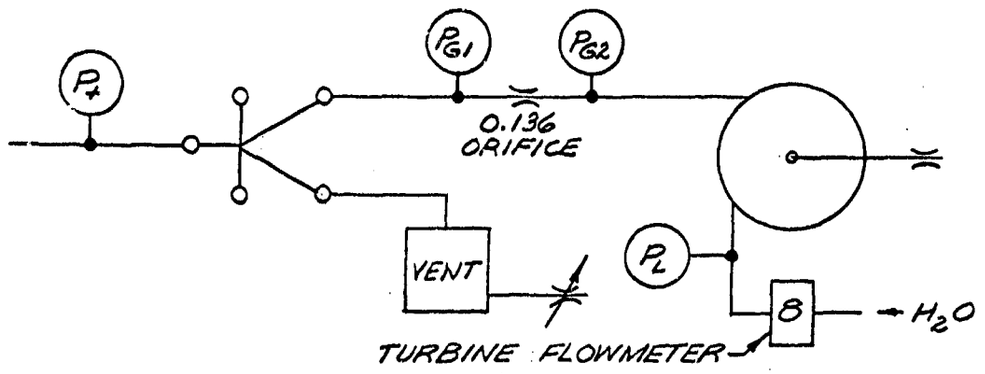

RESULTS:

P_T (psia)	P_L (psia)	P_{G1} (psia)	P_{G2} (psia)	WATER FLOW (FT^3/SEC)	COMMENTS
462	278	293	281	0	
463	275	310	275	0.0011	VENT PRESSURE WAS REDUCED
473	338	337	330	0.0113	BELOW 200 psia
407	263	260	255	0.0137	

CONCLUSION: THE DIVERTER OPERATED THE AXIAL THROTTLE THROUGHOUT ITS ENTIRE RANGE. THROTTLE TURNON HOWEVER, WAS ACHIEVED BY LOWERING THE VENT PRESSURE BELOW SYSTEM SPECIFICATIONS.

Figure 94. Axial Throttle Test Set-Up and Results

IV, C, Fluidic Control Components (cont.)

shown on Figure No. 95. In addition to the throttle tests, the pressure reference assembly, which included the torque motor and the flapper/nozzle unit, was tested and calibrated to provide a curve of torque motor current versus reference pressure. The test results, shown on Figure No. 96, indicated that performance of the torque motor valve was essentially linear over the anticipated operating pressure range.

Some difficulty was encountered by Bowles Engineering in sealing of the diverter assemblies. However, this problem was alleviated by thorough lapping of the diverter plates in conjunction with a modification of the plates to allow space for additional bolts. This increased the effective gasket loading and a subsequent proof and leak test revealed no appreciable GN_2 leakage in pressures up to 750 psig.

The only testing of the axial engine control module was a laboratory evaluation of the unit using ambient temperature GN_2 and water as the test fluids. Figure No. 97 is a schematic of the test set-up and Figures No. 98 and No. 99 are photographs of this set-up. In Figure No. 98, the throttles are shown with the diverters installed, whereas the diverters were removed in Figure No. 99. In both instances, the throttles are mounted on the axial engine injector.

The first tests were attempts to control the unit using the diverters to modulate the control gas flow. However, complete liquid shutoff could not be obtained with the diverters even when the vent leg of each diverter was capped to ensure complete diversion of control gas into the throttles. This was probably caused by the control gas achieving sonic velocity across the diverter power nozzle. As a result, insufficient gas momentum was available to stop the flow of liquid with the gas supply pressure available. Then, the diverters were removed and the throttles tested separately. These throttles exhibited the same stability problem as had been previously identified with the ACS throttles. The tests were conducted using GN_2 as the control gas. Liquid flow rate was measured as a function of control gas flow rate and control port pressure. Control gas flow rate was increased until liquid shutoff occurred to obtain turndown ratio data.

From visual observation of the testing, it appeared that effective throttling control was restricted to the low control gas flow range. As control gas flow increased and the throttle approached the shutoff condition, liquid flow stability and throttling control degenerated.

OBJECT: TO CALCULATE THE TURNDOWN RATIO OF EACH AXIAL THROTTLE.

TEST CONFIGURATION

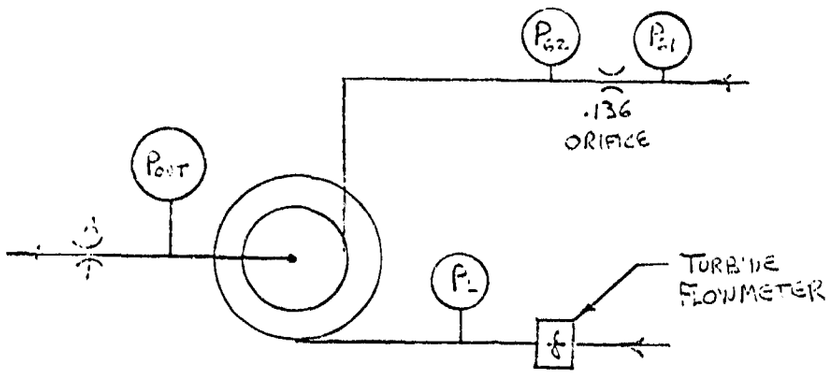

RESULTS:

THROTTLE	CONDITION	P_{g1} (PSIG)	P_{g2} (PSIG)	P_L (PSIG)	P_{out} (PSIG
1	ON	-	-	265	248
1	OFF	325	290	270	265
2	ON	-	-	265	225
2	OFF	320	280	270	260

THE FOLLOWING TURNDOWN RATIOS WERE CALCULATED:

THROTTLE	TURNDOWN RATIO
1	19.4
2	18.4

Figure 95. Axial Throttle Test Set-Up

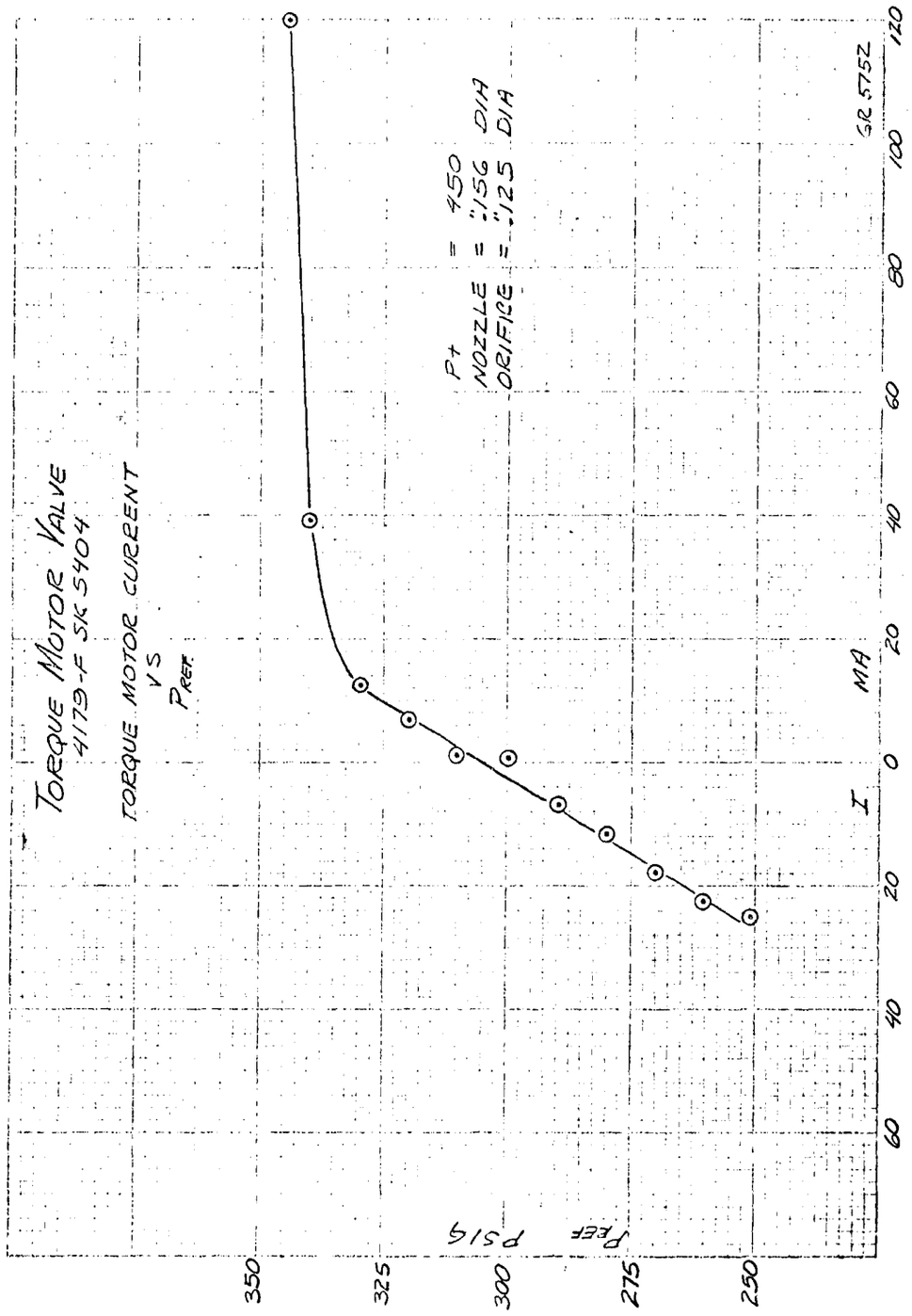

Figure 96. Torque Motor Current vs Pressure

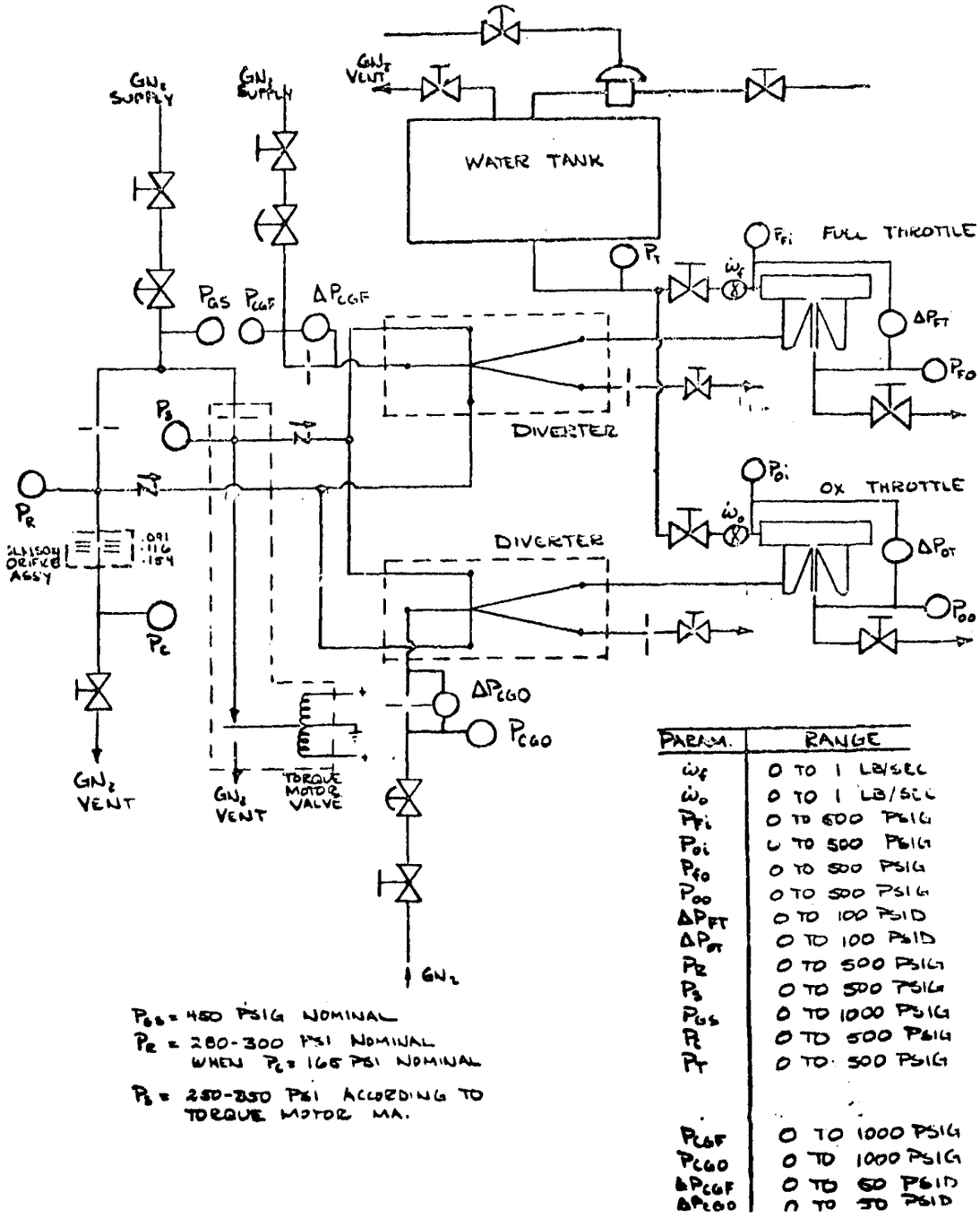

PARAM.	RANGE
$\dot{\omega}_f$	0 TO 1 LB/SEC
$\dot{\omega}_o$	0 TO 1 LB/SEC
P_{fi}	0 TO 600 PSIG
P_{oi}	0 TO 500 PSIG
P_{fo}	0 TO 500 PSIG
P_{oo}	0 TO 500 PSIG
ΔP_{FT}	0 TO 100 PSID
ΔP_{OT}	0 TO 100 PSID
P_R	0 TO 500 PSIG
P_S	0 TO 500 PSIG
P_{GS}	0 TO 1000 PSIG
P_C	0 TO 500 PSIG
P_T	0 TO 500 PSIG
P_{CGF}	0 TO 1000 PSIG
P_{CGO}	0 TO 1000 PSIG
ΔP_{CGF}	0 TO 50 PSID
ΔP_{CGO}	0 TO 50 PSID

Figure 97. Axial Engine Control Module Test Schematic

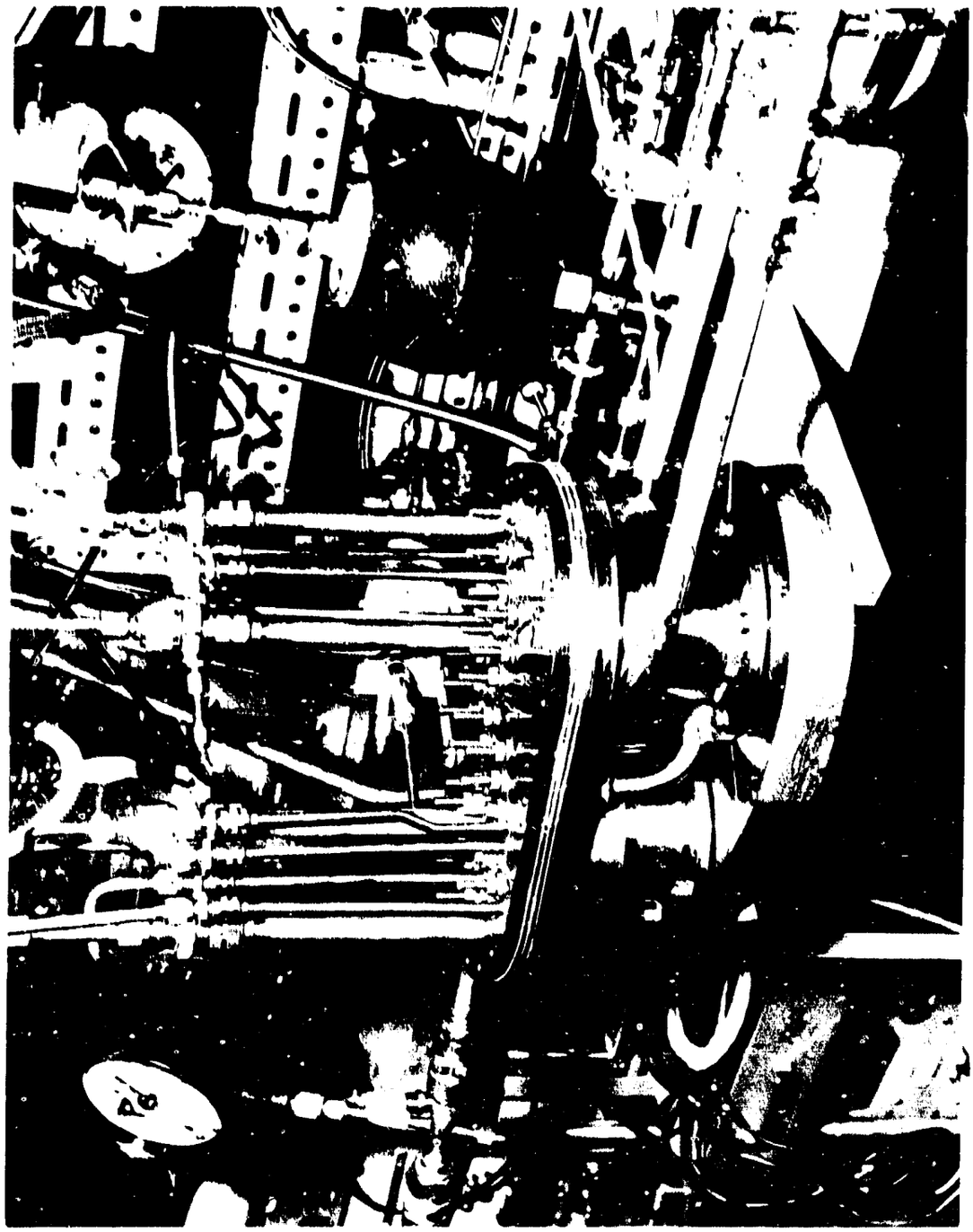

Figure 98. Vortex Throttle with Diverters Installed

With the injector installed on the throttle, it was noted that the fuel circuit was first affected when control gas flow increased, especially the fuel film cooling supply. Complete shutoff of the fuel circuit resulted at a slightly lower gas flow rate than that required for the oxidizer circuit.

Several development problems with the axial engine control module were evident as a result of the tests performed. The first problem was related to diverter performance. Liquid shutoff could not be obtained when controlling the vortex throttles through the diverters. As previously mentioned, this problem appeared to result from insufficient gas flow or momentum. Increasing the power and receiver nozzle sizes in the diverter was a possible solution of this problem.

A second problem was flow stability or the ability to maintain a constant flow rate for any set condition throughout the range from on-to-off. Flow oscillations were evident to some degree even during steady-state operating conditions. These oscillations could have easily resulted in engine combustion instabilities.

A third problem closely related to flow stability was throttling ability. Both throttles tested showed unsatisfactory throttling ability. It was discovered that liquid flow was extremely sensitive to a small change in control gas flow. As a result, the desired operating band for the component was very narrow and allowed no tolerance for system pressure variations. The axial engine control module had to be capable of throttling propellant flow over the 50% to 100% flow range; therefore, this was a significant problem.

A final development problem encountered was throttle response time. The extent of this problem was realized during testing of the ACS engine controls. In the engine application, the control gas was approximately 1300°F and with extended off-times, the vortex throttle became hot as a result of heat transfer effects. When liquid flow was initiated after an extended off period, the heat transfer from the throttle to the liquid produced propellant vaporization. This vaporization affected response time in that the period it took to reach full liquid flow became a function of the temperature, mass, and surface area of the vortex throttle.

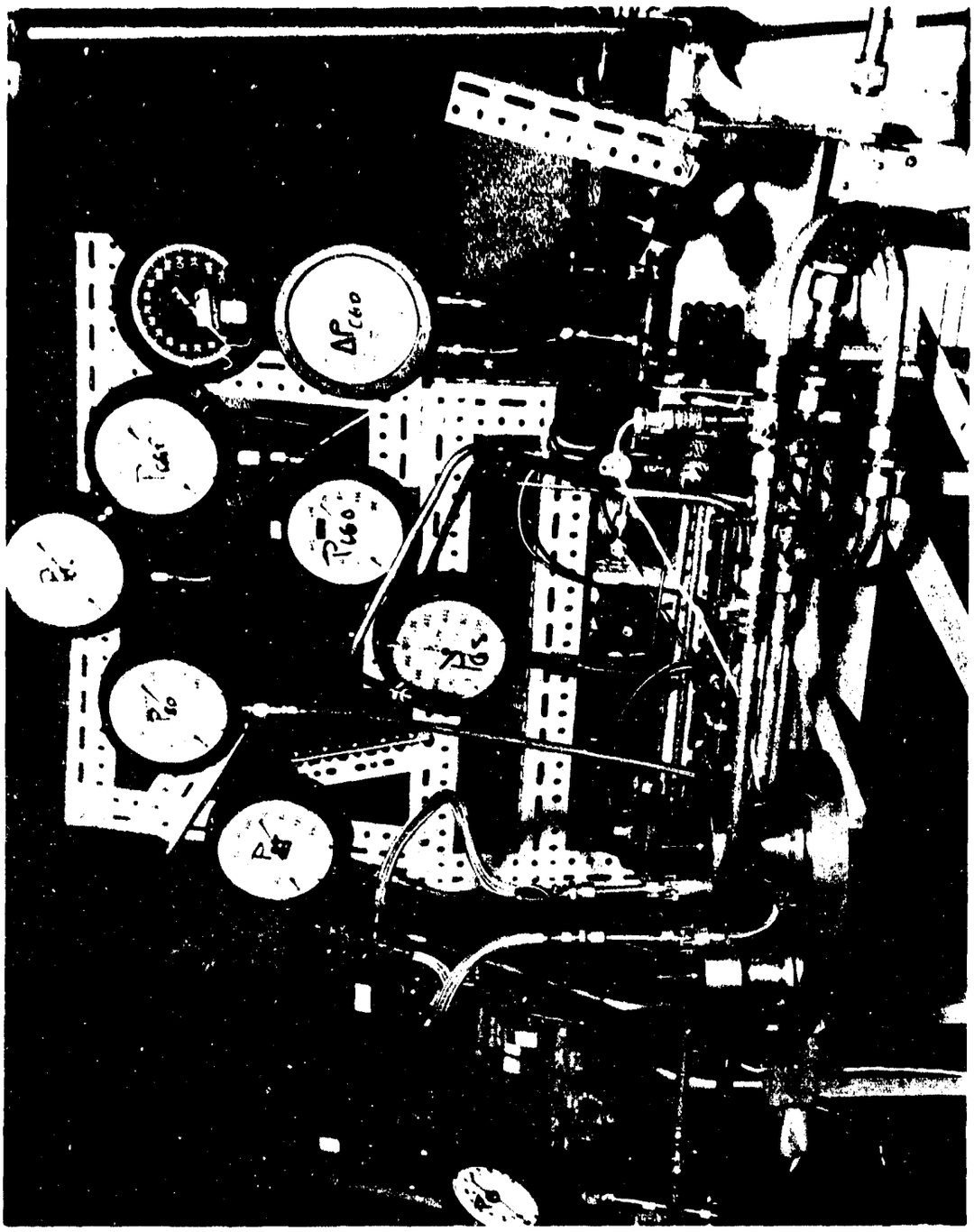

Figure 99. Axial Engine Vortex Throttle Test

IV, C, Fluidic Control Components (cont.)

b. ACS Engine Control Module

(1) Function and Basic Operation

The function of the Attitude Control System (ACS) engine control module for PBPS application is to direct and control liquid propellants to the rocket engine thrust chamber. It must be capable of starting and stopping the flow of propellants to the rocket engine upon initiation of an electrical signal from the guidance system.

The operation of the ACS engine control module is basically the same as that of the axial engine control module with one major exception. The ACS unit is simply an "ON-OFF" control device with no capability for propellant throttling. It was designed to operate in a pulse mode operation where the duration of pulses can vary from 0.030 sec to 800 sec. The component consists of two vortex throttles (one for oxidizer and one for fuel) and a separate diverter amplifier section for each throttle. The electrical interface point, at which signals from a guidance system are fed into the pneumatic valve control circuit, remained undefined for the ACS control module. A flapper valve/torque motor device, such as the one used in the axial engine control module, could be adapted for the ACS application.

The vortex throttles for the ACS control component are of the same basic design as those used in the axial unit. Acutally, early development data related to vortex valve technology was instrumental in defining the basic configuration for both units. A standard development component was used by Bowles Engineering in all of the early tests and a scaling technique was applied in the sizing of vortex throttles to achieve desired flow and pressure requirements for each PBPS application.

Gas flows continuously through the vortex throttle when the engine is not operating; therefore, the use of these devices is most attractive in controlling the small attitude control system engines where the engine liquid flow rates are relatively low. As a result, the gas required to prevent liquid from flowing also is low. For a 100 lb thrust bipropellant ACS engine requiring approximately 0.35 lb/sec liquid flow, it takes approximately 0.011 lb/sec of hot gas to prevent the propellants from flowing. A very small residual thrust from the expending control gas will result when the engine is in the off condition because the gas exhausting from the valve passes through the engine injector and nozzle.

The diverter valve design for the ACS engine control module also is the basic design used for the axial unit. Similarly, only one diverter amplifier was utilized for the oxidizer circuit and another for the fuel circuit because of the diverter staging problems encountered. Throttle

IV, C, Fluidic Control Components (cont.)

operation was regulated by the non-vented diverters. Control gas flow was directed to the throttles for propellant shutoff and away from the throttles to an overboard vent for full-thrust engine operation.

(2) Component Description and Specifications

One-half of the ACS engine control module is shown on Figure No. 100 and includes the oxidizer circuit control (i.e., vortex throttle with attached diverter amplifier section). Various stages of assembly are shown on Figure No. 101. The fuel and oxidizer subassemblies are actually separate units fastened together by a cross-member bolting directly to the top of the vortex throttles. Then, the complete module is assembled to the ACS engine injector.

The diverter amplifier elements for the ACS control module were machined in 0.049-in. thick steel plates. These elements were then assembled between adjoining support plates. Flat gaskets of an asbestos material were sandwiched between the plates for sealing the hot gas used as the control fluid. Following this, the diverter sections were joined to the vortex throttles by welding. In the experimental test module, an external supply port and an internal manifold connection from one leg of the diverter output provided the gas inlet flow channel to the vortex throttle. This allowed testing of the module both with or without the diverter amplifier section. In actual use with the diverters, the alternate gas inlet port is used for instrumentation purposes.

Figure No. 102 is a cross-sectional view of the ACS vortex throttle configuration. There are two basic design differences between the ACS and the axial throttle. The ACS model has a conical liquid chamber and flow straightening vanes, which were incorporated in an attempt to improve flow characteristics and throttle turndown ratio. The function of the flow straightening vanes was to remove the rotational motion of the liquid before it passed through the throttle exit. This reduced the liquid pressure losses in the exit passage and permitted the use of a smaller exit. The smaller exit should have decreased the flow rate of gas required because the rotational motion of the gas was not affected by the vanes. Subsequent test results to evaluate these modifications were not completely satisfactory. It appeared that gas flow was affected by the straightening vanes and the anticipated results were not realized. A relocation of the straightening vanes was considered as one possible correction.

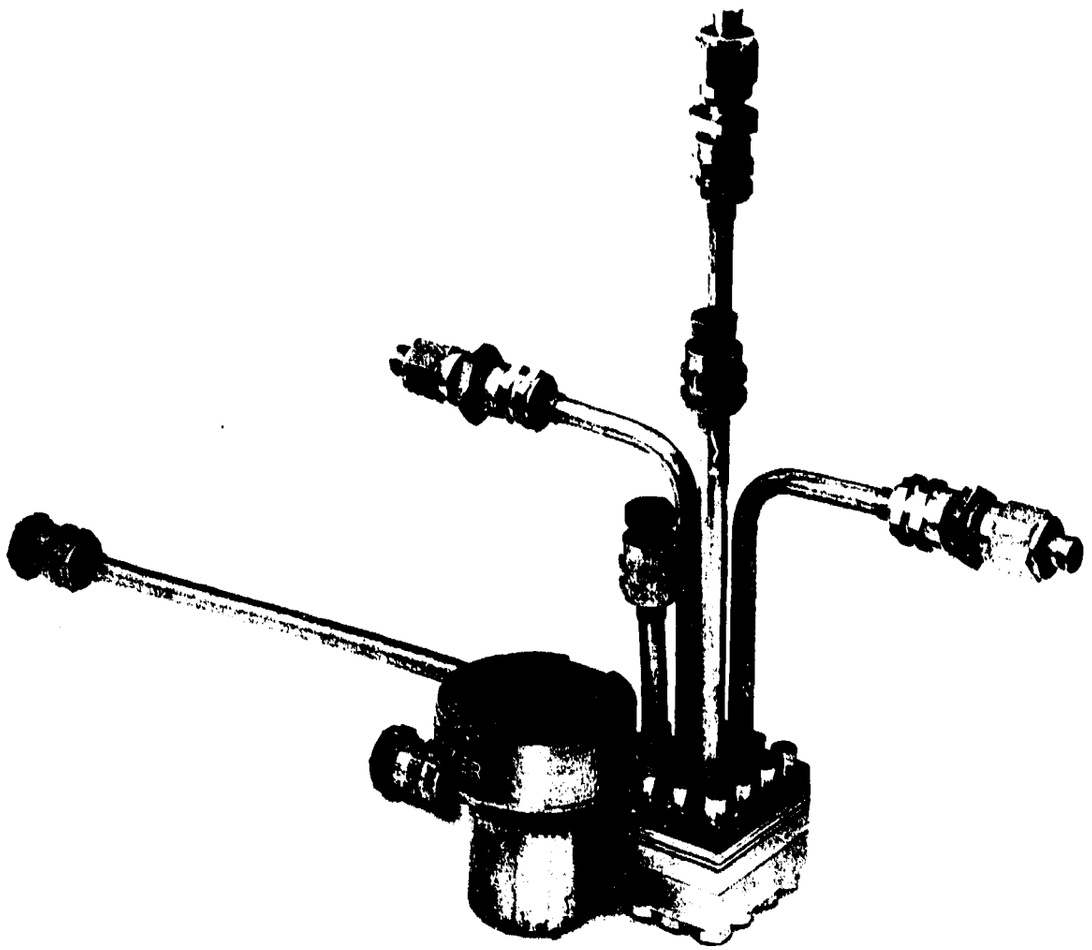

Figure 100. ACS Oxidizer Vortex Throttle

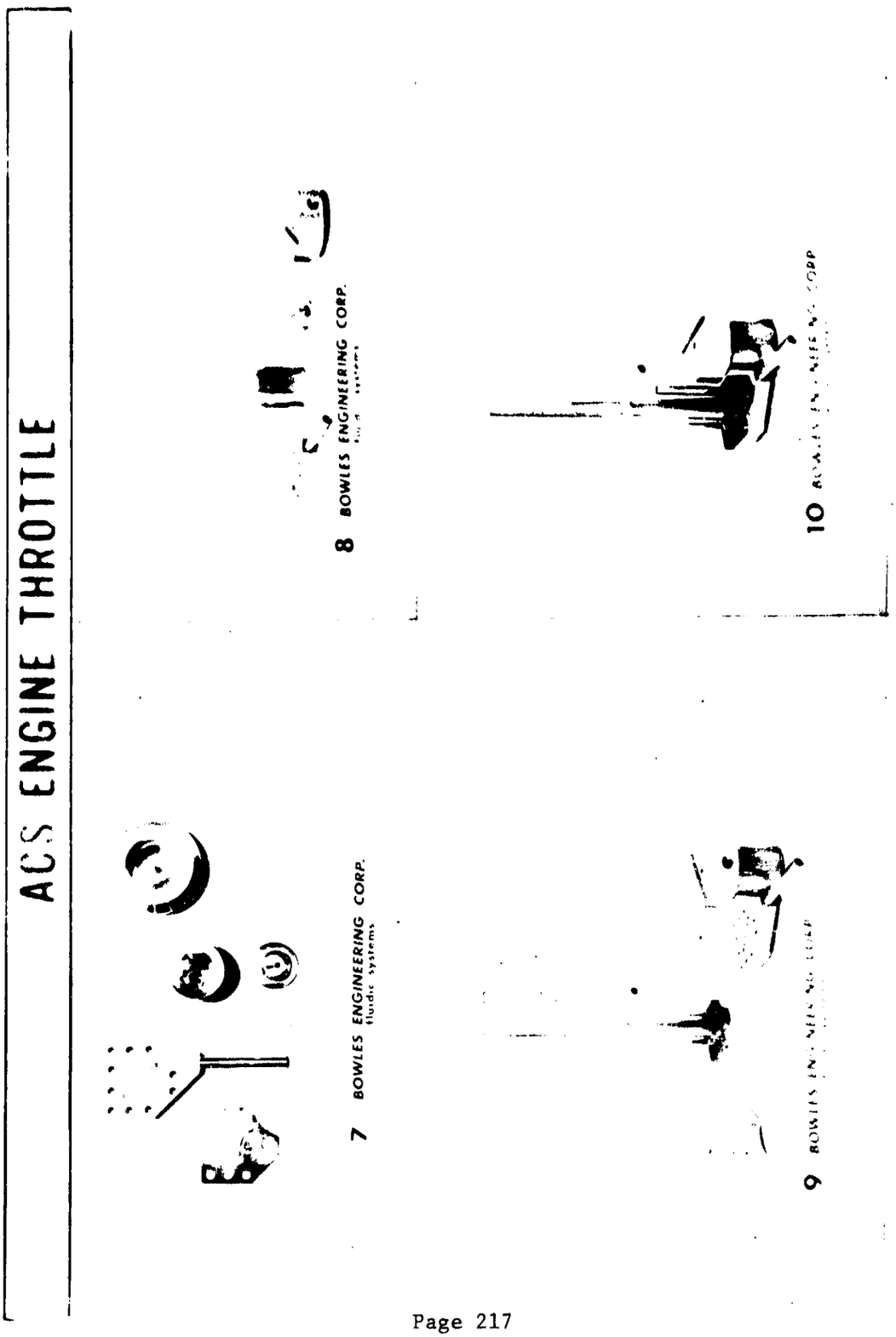

Figure 101. ACS Engine Control Module

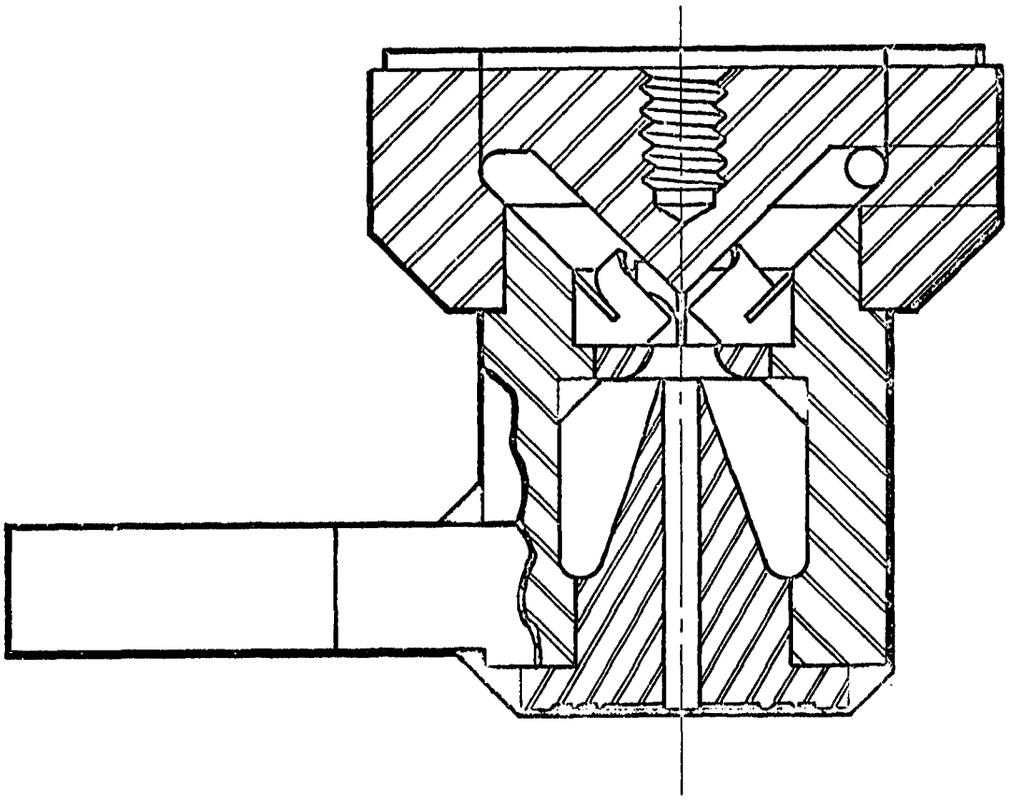

Figure 102. ACS Vortex Throttle Configuration

IV, C, Fluidic Control Components (cont.)

The component was designed to operate strictly in an on-off, open-loop mode with no proportional control. The operating response requirement was 10 millisec for both starting and shutdown. Operating pressure and temperature requirements were 500 psia (maximum) and 1400°F (maximum), respectively. Nominal flow rates were 0.162 lb/sec (oxidizer), 0.101 lb/sec (fuel), and 0.010 lb/sec (control gas). Throttle turndown ratios were set at a minimum of 25 under system operating conditions.

(3) Component Development

A number of tests were conducted at Bowles Engineering using various diverter amplifier configurations to control a full-size model of an ACS vortex throttle. These tests were performed at actual system pressures using air and water as the working fluids. The test set-up is shown on Figure No. 103. The test objectives were to determine the diverter size and configuration that would operate the throttle as well as to establish the required inputs to this diverter. The configuration was selected and the test results for two sizes of this diverter are presented on Table XIX.

TABLE XIX

ACS THROTTLE AND DIVERTER TEST RESULTS

Item No.	Diverter Type and Size	P_T psia	P_{CL} psia	P_{CR} psia	P_{CL} psia	P_{CR} psia	P_V psia	P_1 psia	P_2 psia	P_3 psia	P_{AMB} psia	Throttle Condition
1	N5393 A_T = 0.018-in. x 0.036-in.	515.	277.	405.	291.	283.	276.	285.	298.	247.	15.	Off
2	Same as Item 1	519.	320.	250.	277.	277.	273.	278.	279.	183.	15.	Full On
3	N5393 A_T = 0.020-in. x 0.040-in.	423.	248.	335.	293.	265.	257.	287.	299.	249.	15.	Off
4	Same as Item 3	422.	324.	316.	277.	267.	261.	284.	285.	189.	15.	Full On

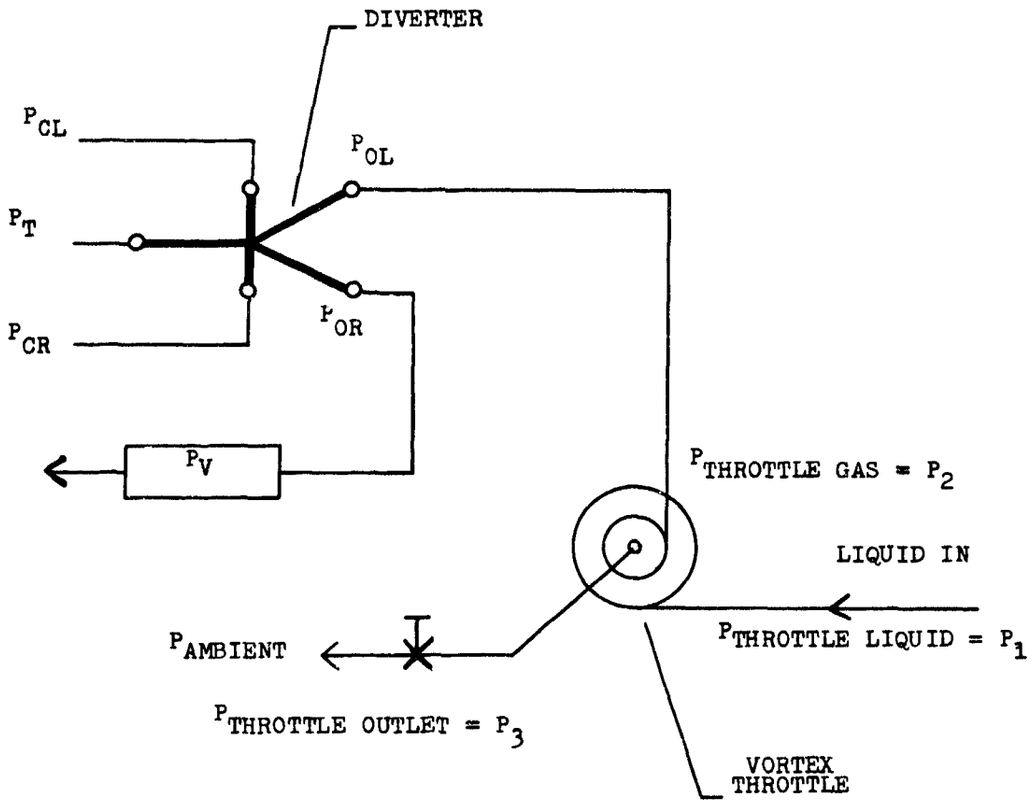

Figure 103. ACS Throttle and Diverter Test Set-Up

IV, C, Fluidic Control Components (cont.)

After the ACS Engine Control Module was delivered to Aerojet-General, preliminary checkout and evaluation testing of the unit were initiated using water and ambient temperature nitrogen. Considerable difficulty was encountered in controlling the throttles with the diverters. In each instance, re-adjustment of the diverter supply and vent line pressures was required to switch from the "on" to the "off" throttle condition. The oxidizer throttle was tested separately, without the diverter amplifier, to determine its effectiveness and turndown ratio performance. These data are shown on Table XX.

TABLE XX

ACS OXIDIZER THROTTLE TESTS WITHOUT DIVERTER

CONTROLS SUBSYSTEM

Test	Cond	P_{FI} Psig	P_{FD} Psig	$\dot{W}_w$ lb/sec	P_{cp} Psig	Tg °F	$\dot{W}_g$ lb/sec	TDR
1	ON	209	279	0.1002	-	-	-0-	
	OFF	305	299	-0-	322	52	0.00963	10.40
2	ON	301	281	0.0972	-	-	-0-	
	OFF	308	302	-0-	322	52	0.00898	10.82
3	ON	305	285	0.0972	295	-	-0-	
	OFF	312	305	-0-	326	52	0.0092	10.82
4	ON	305	288	0.0928	296	-	-0-	
	OFF	312	307	-0-	326	50	0.0092	10.10

IV, C, Fluidic Control Components (cont.)

The resulting turndown ratio of 10.4:1 for GN_2 and water indicated an approximate system turndown ratio of 33:1 for the unit when operated with hot gas and propellant. The fuel throttle and diverter were tested using 1000°F mixed gas (N_2H_4 decomposition) and water as the test fluids. The throttle outlet flange seal ruptured causing a test shutdown before sufficient data could be obtained. External leakage from the diverter elements was experienced. Investigation revealed that the gasket material used in this experimental design was inadequate for operating at temperatures exceeding 800°F for any prolonged period of time. The problem was alleviated by substituting a more suitable gasket material.

The diverter amplifier elements from both control modules were reworked by Bowles Engineering. Then, the reworked oxidizer module was tested for the primary purpose of achieving dynamic test data. Several tests were conducted to evaluate component transient response for the valve off-to-on and on-to-off operating conditions. The test fluids used were gaseous nitrogen and water at ambient conditions. Only the input control port pressure and the output pressure were monitored during the initial test. The time responses were recorded with a polaroid camera mounted on an oscilloscope (see Figure No. 104). The first test run resulted in a full-off to full-on time response of 1.5 sec. This long response time was attributed to the time required to fill the downstream volume. Consequently, another test was made with the downstream volume reduced to simulate the injector manifold volume. The results of this test are shown on Figures No. 105 and No. 106. The nomenclature is defined on Figure No. 107. These time response tests resulted in "opening" times of 175 millisec, a considerable improvement over the initial tests. Moreover, it is important to note that the valve was never completely turned off. This was partially attributed to defective operation of the attached diverter amplifiers. To achieve a valid time response test, stable operation of the component is required.

A subsequent series of tests involving the ACS fuel throttle only was initiated using N_2H_4 decomposed gas and monomethylhydrazine (MMH) at system pressures and temperatures. A major reason for these tests was to determine the compatibility of the test fluids. The diverter control element was not used in these tests because of the erratic performance results they exhibited in previous tests. Also, previous plans to test the oxidizer and fuel modules simultaneously were cancelled for the same reason. A schematic of the test set-up is shown on Figure No. 108.

A series of on-off operations and a throttling test was conducted. In the on-off test, the duty cycle followed was 10 sec of throttle on, 30 sec of throttle off, 15 sec of throttle on, 300 sec of throttle off, and 20 sec of throttle on. The transients for each of these operations are shown on Figures No. 109 through No. 116. The response from off-to-on varied considerably depending upon the off time to actuation. After the 30 sec off period, the throttle response was

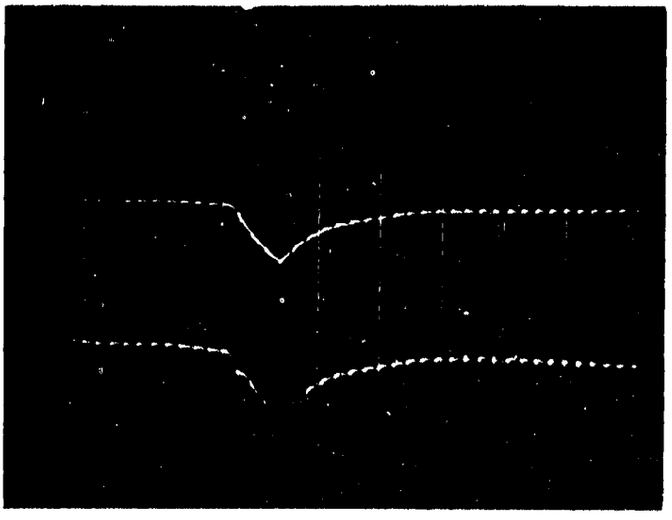

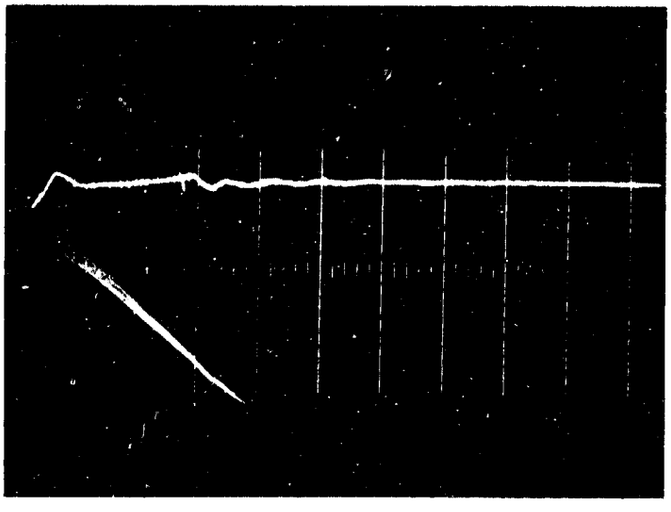

Figure 104. Oxidizer Vortex Valve (Large Downstream Volume)

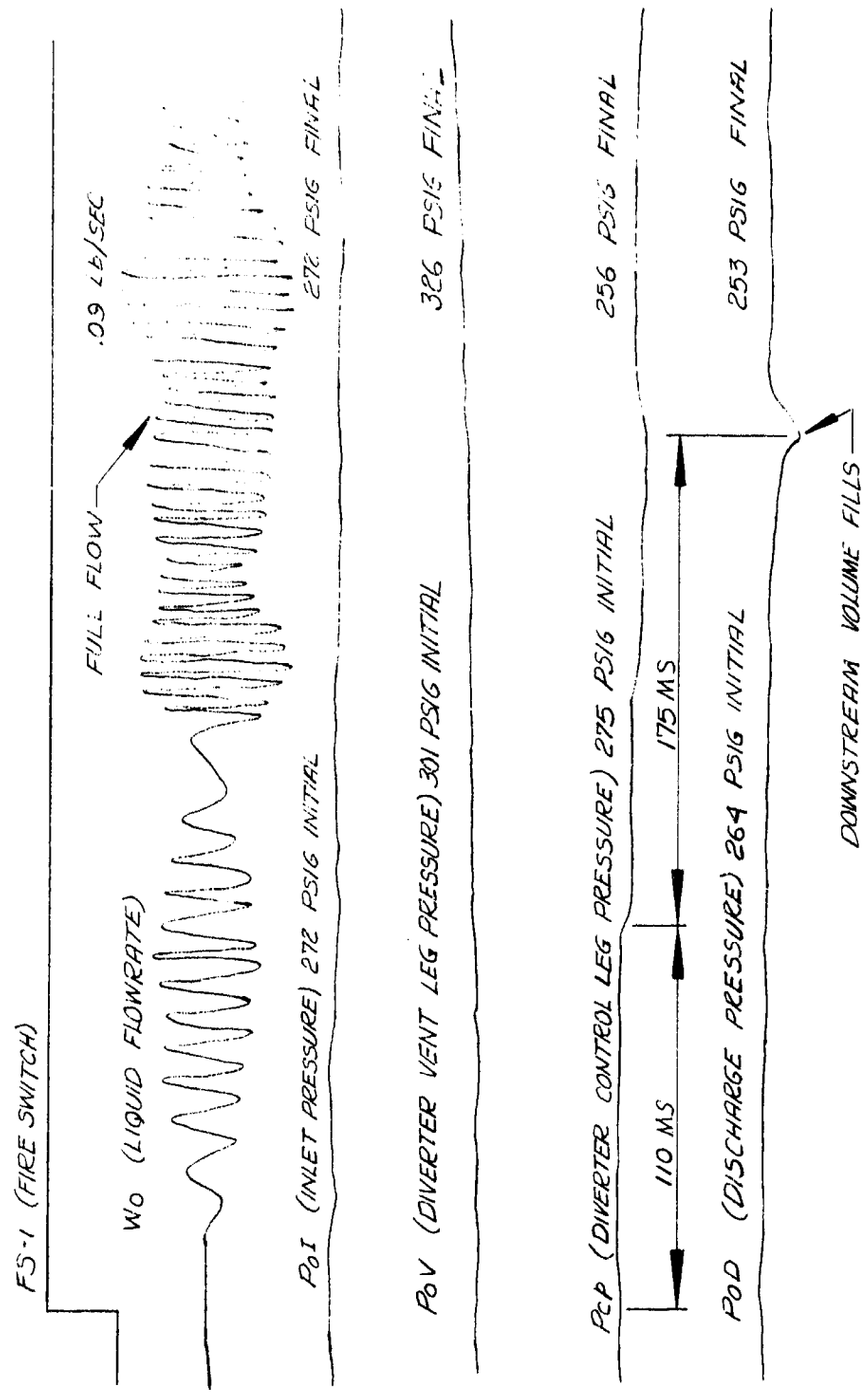

Figure 105. Oxidizer ACS Vortex Valve

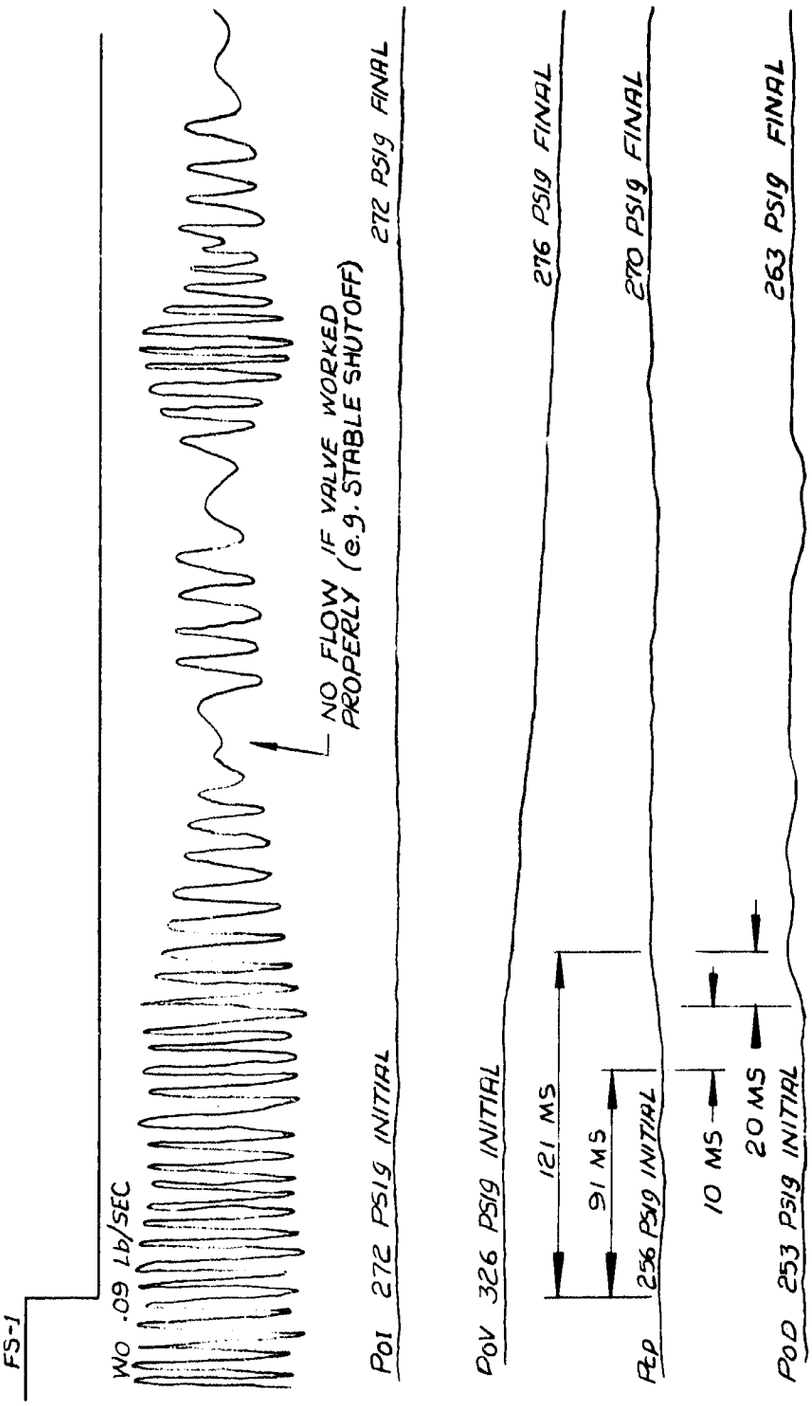

Figure 106. Oxidizer ACS Vortex Valve

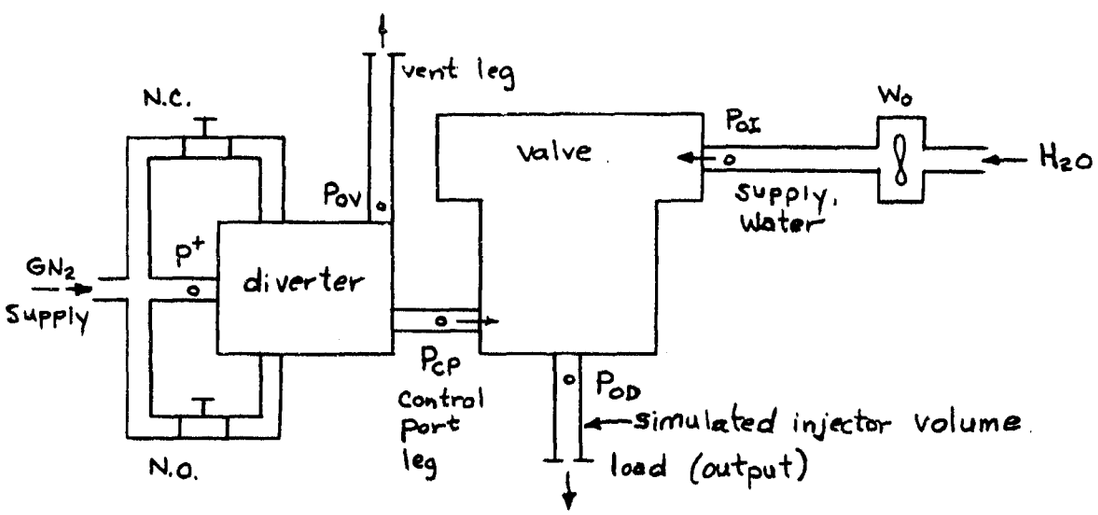

Figure 107. Location of Transducers, ACS Vortex Valve Tests

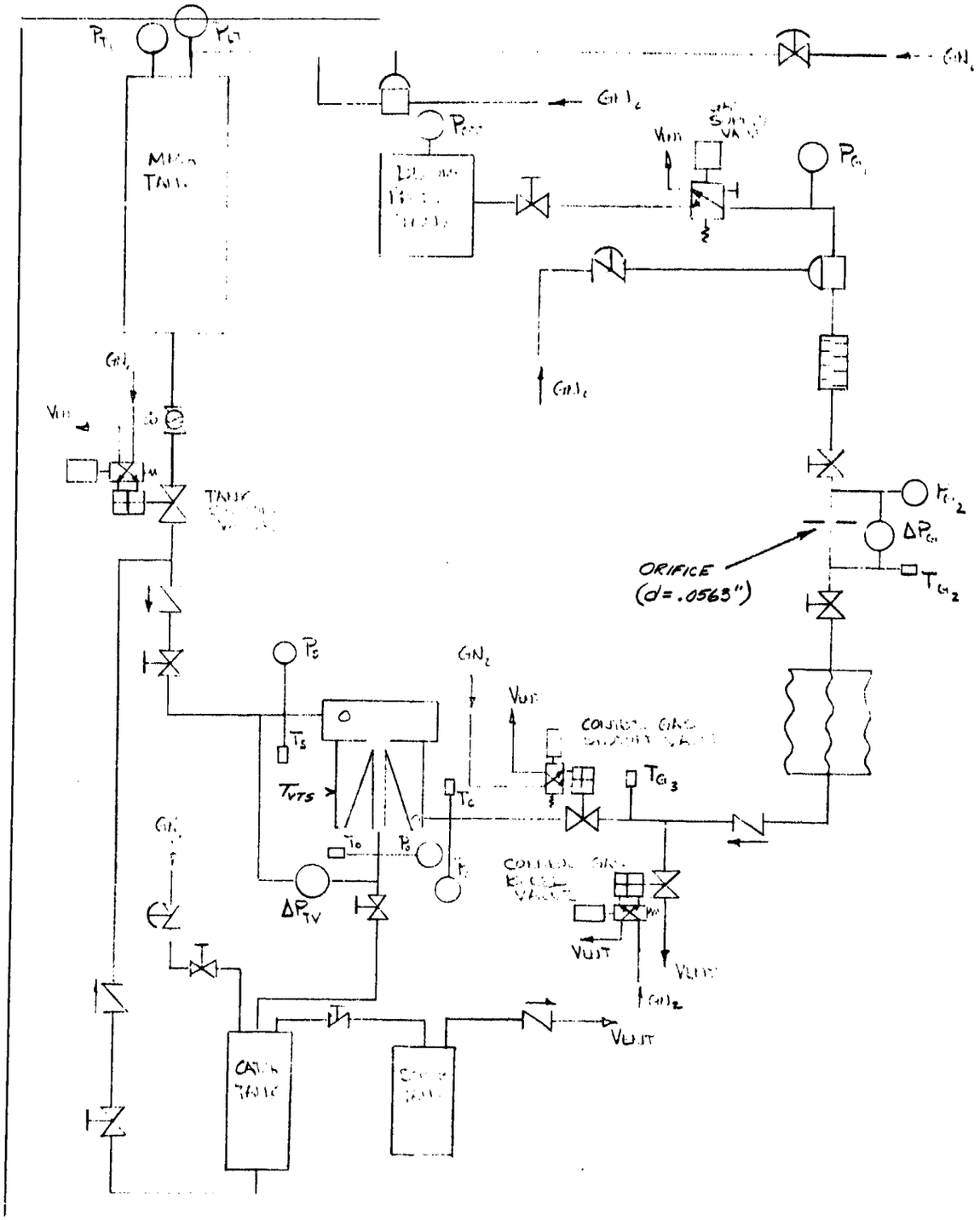

Figure 108. ACS Vortex Throttle Test Schematic

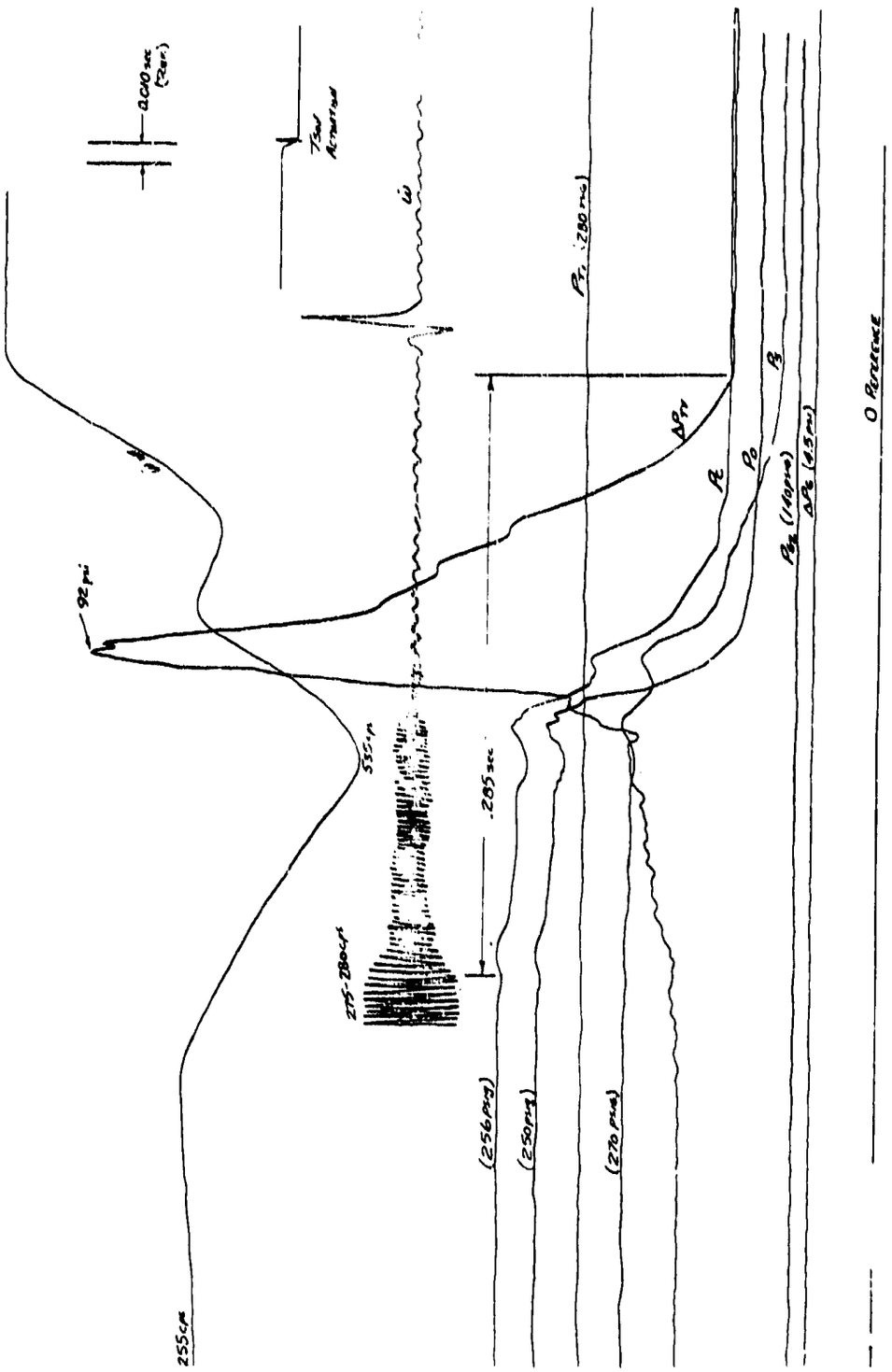

Figure 109. Initial Actuation, ACS Fuel Throttle Test

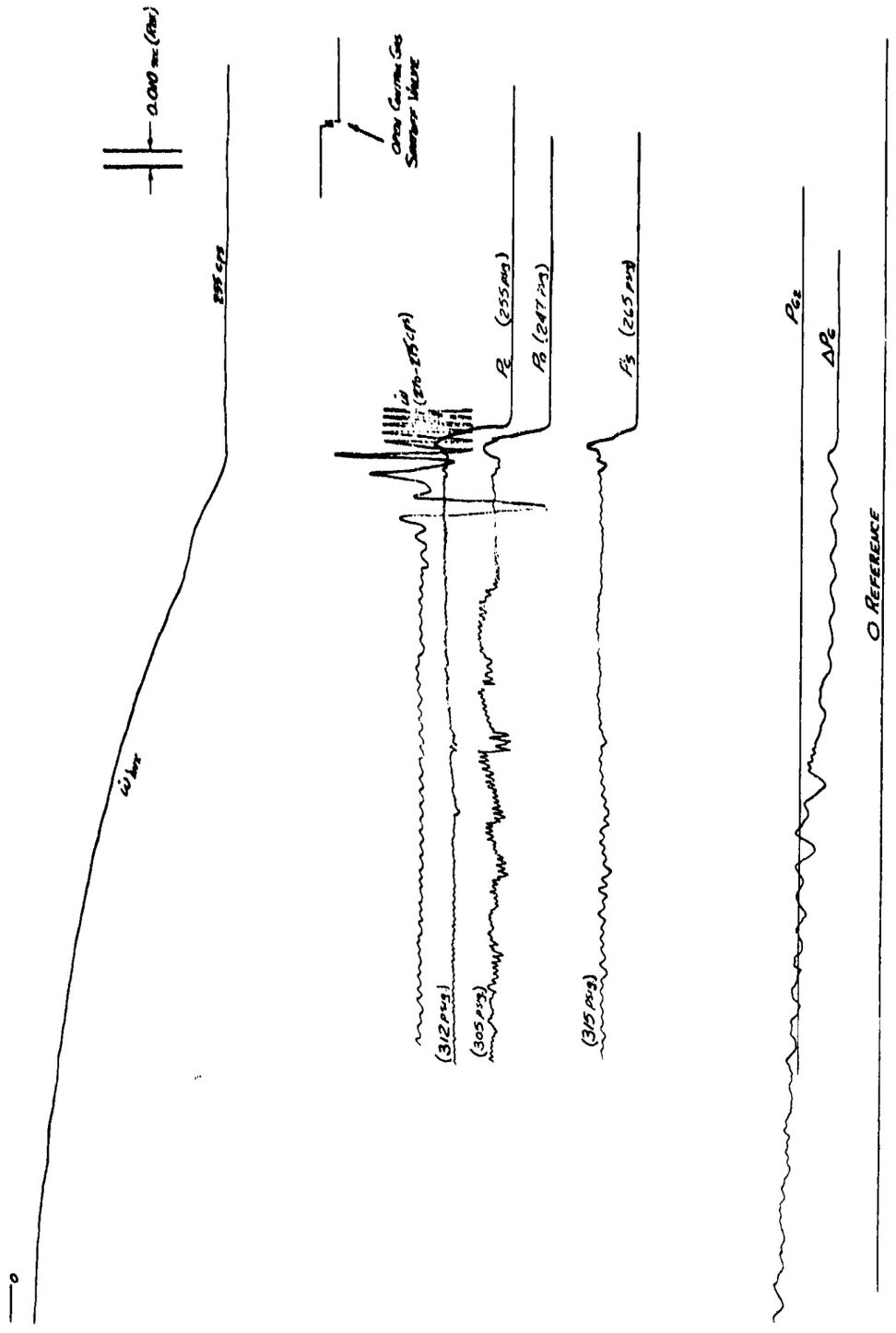

Figure 110. First Throttle Shut-Off

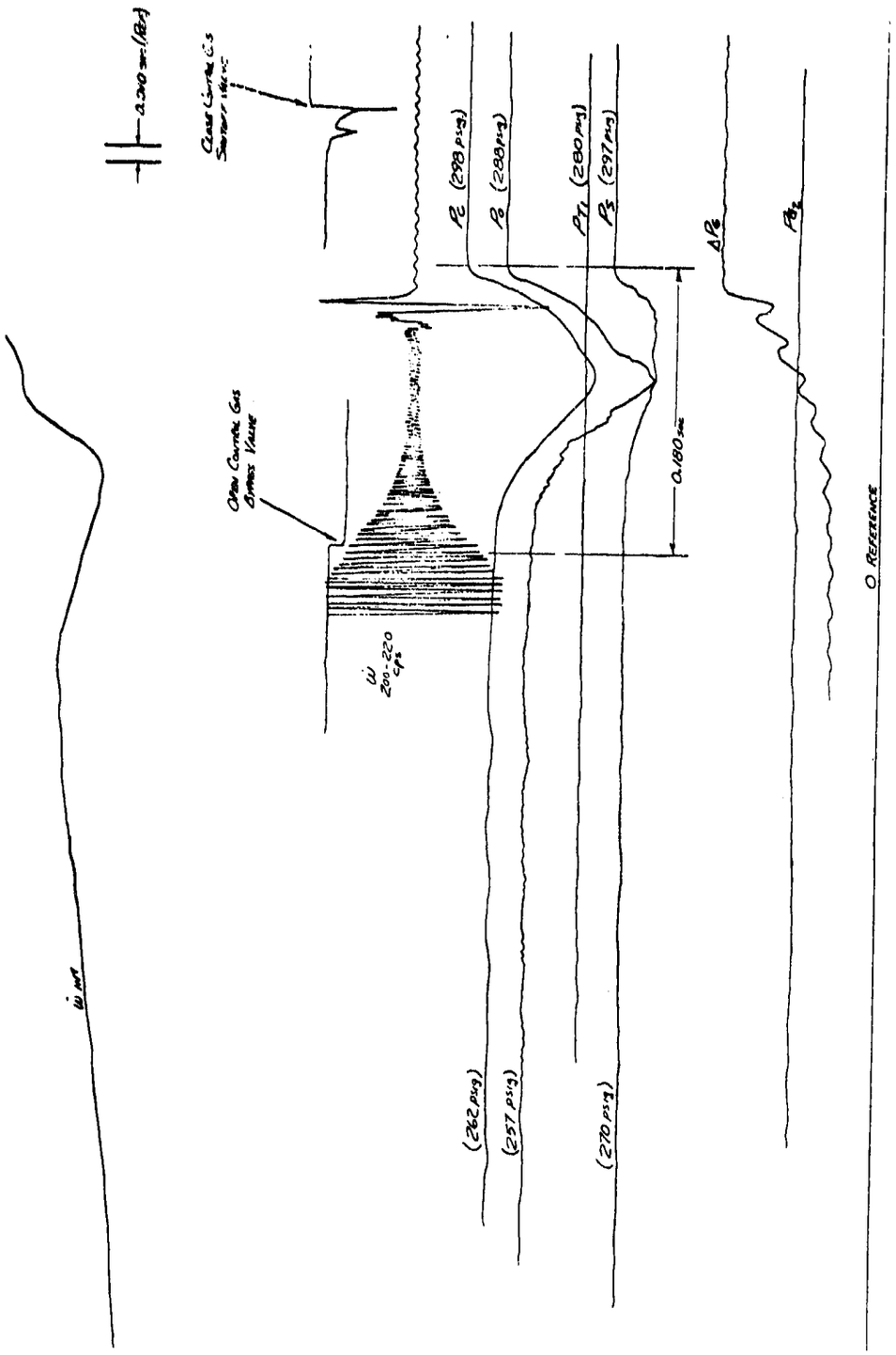

Figure 111. Second Throttle Actuation

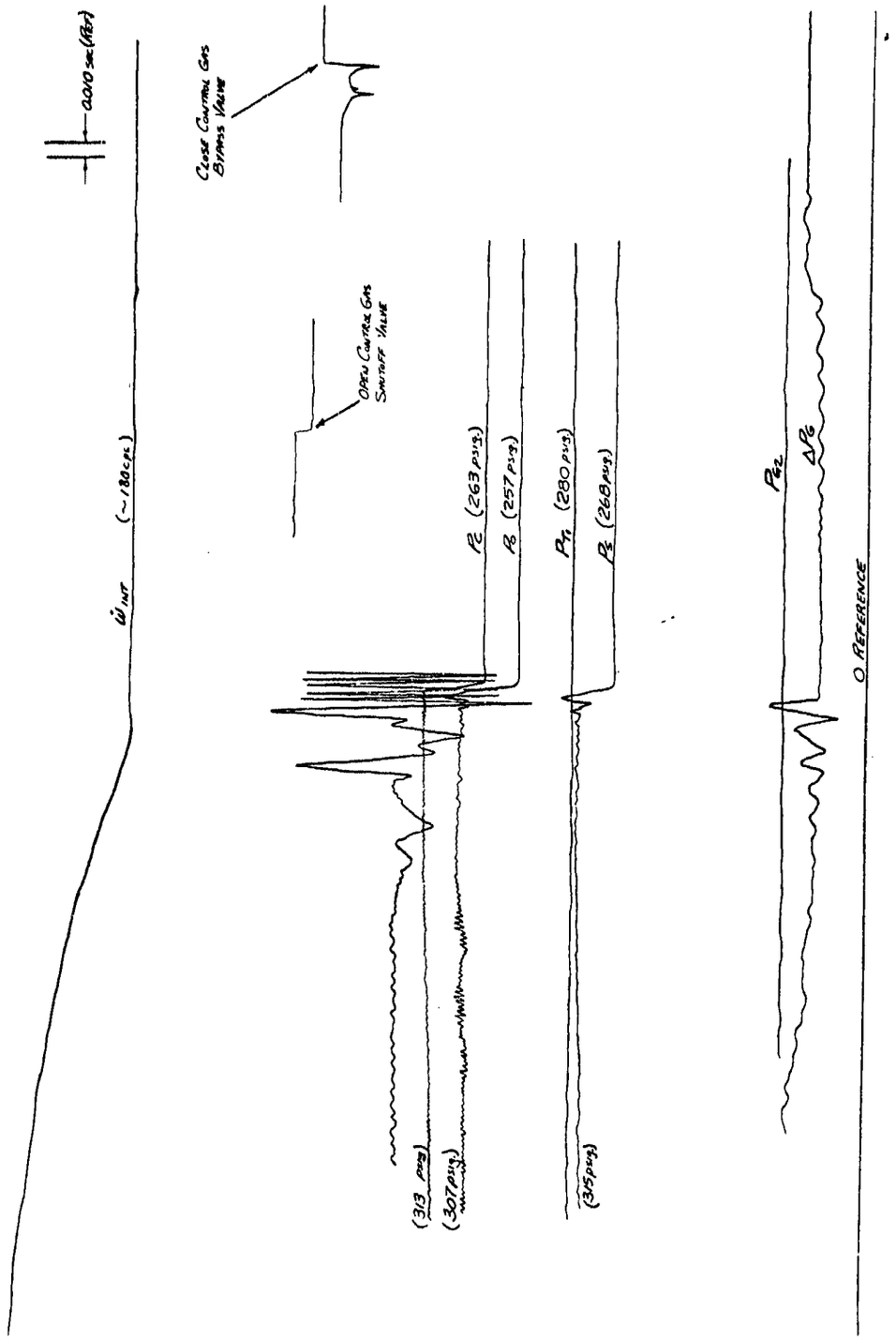

Figure 112. Second Shut-Off - ACS Fuel Throttle

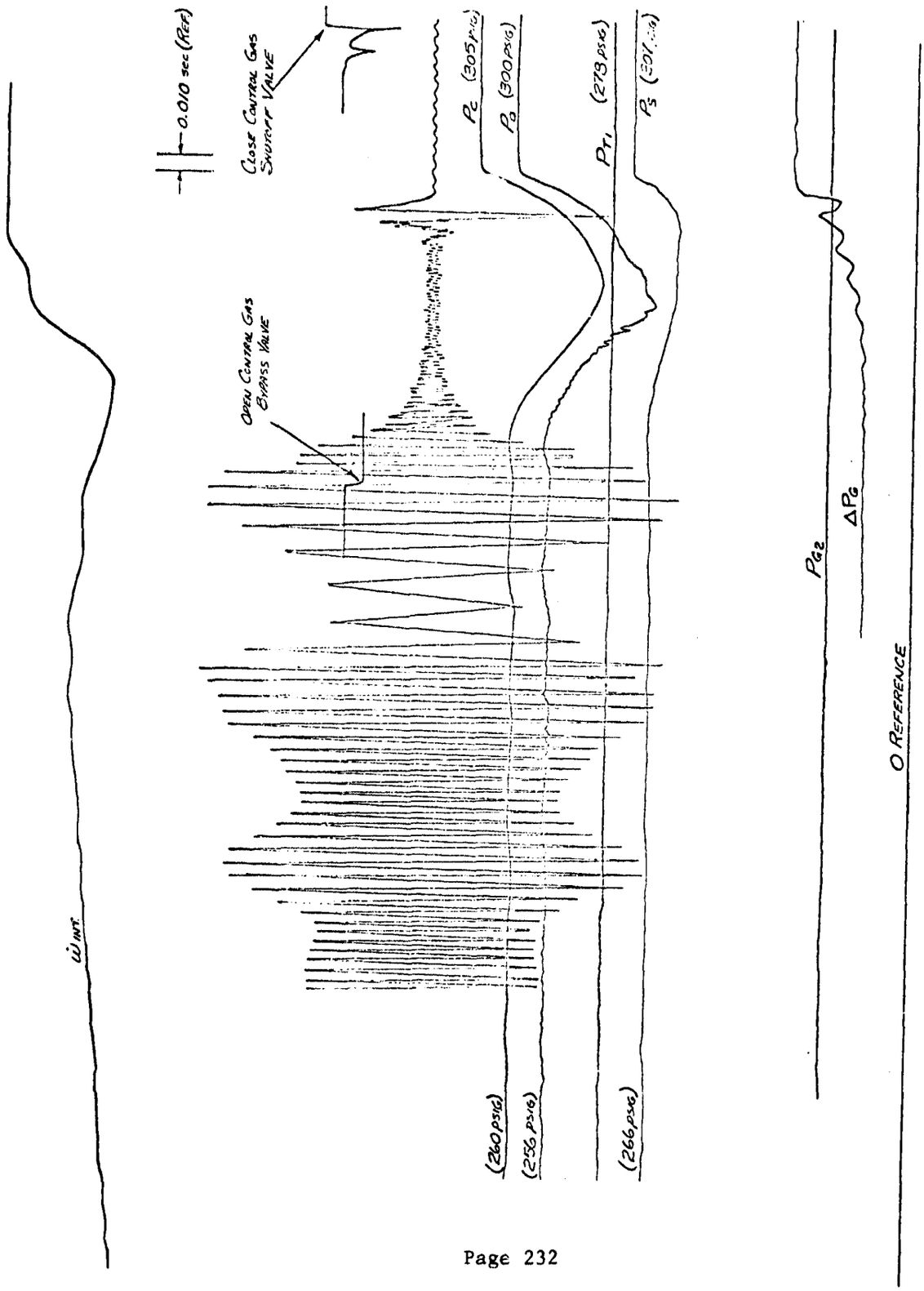

Figure 113. Third Throttle Actuation

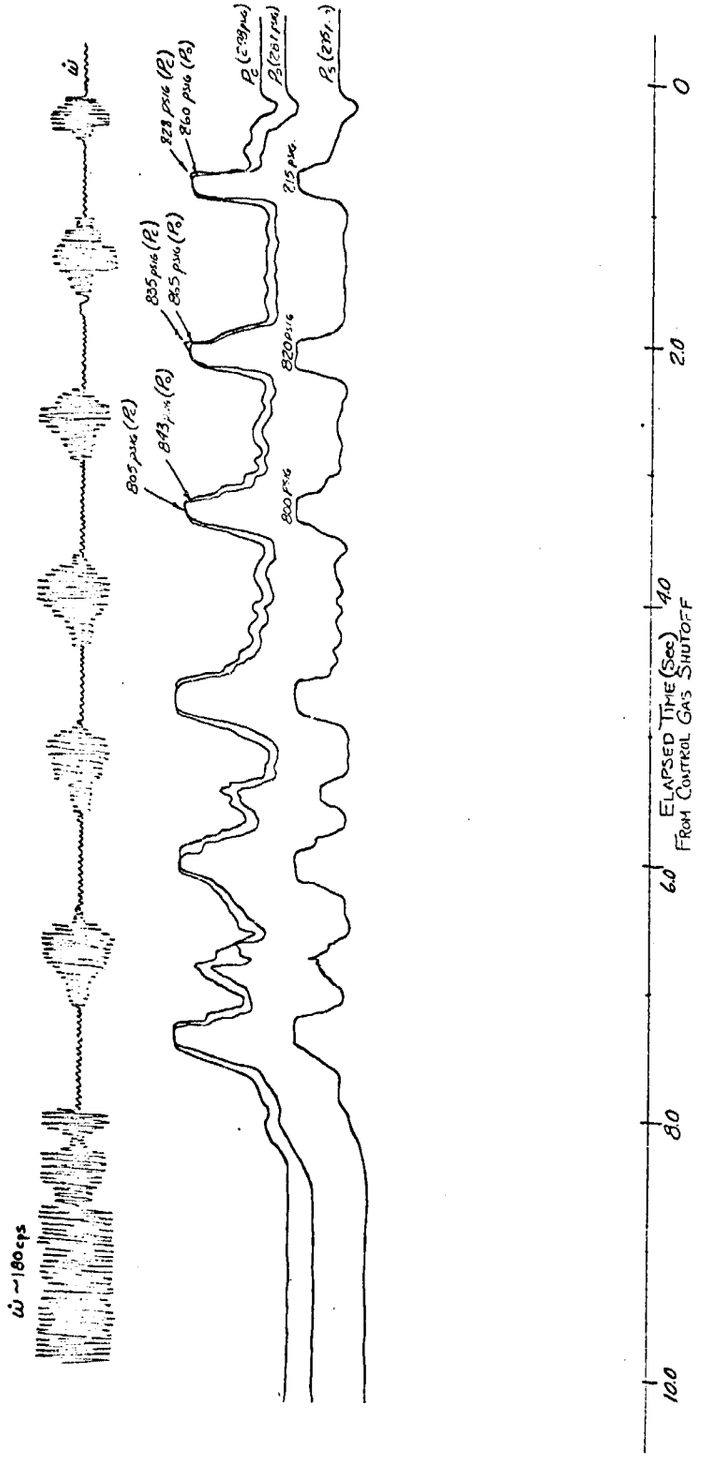

Figure 114. Fourth Throttle Actuation

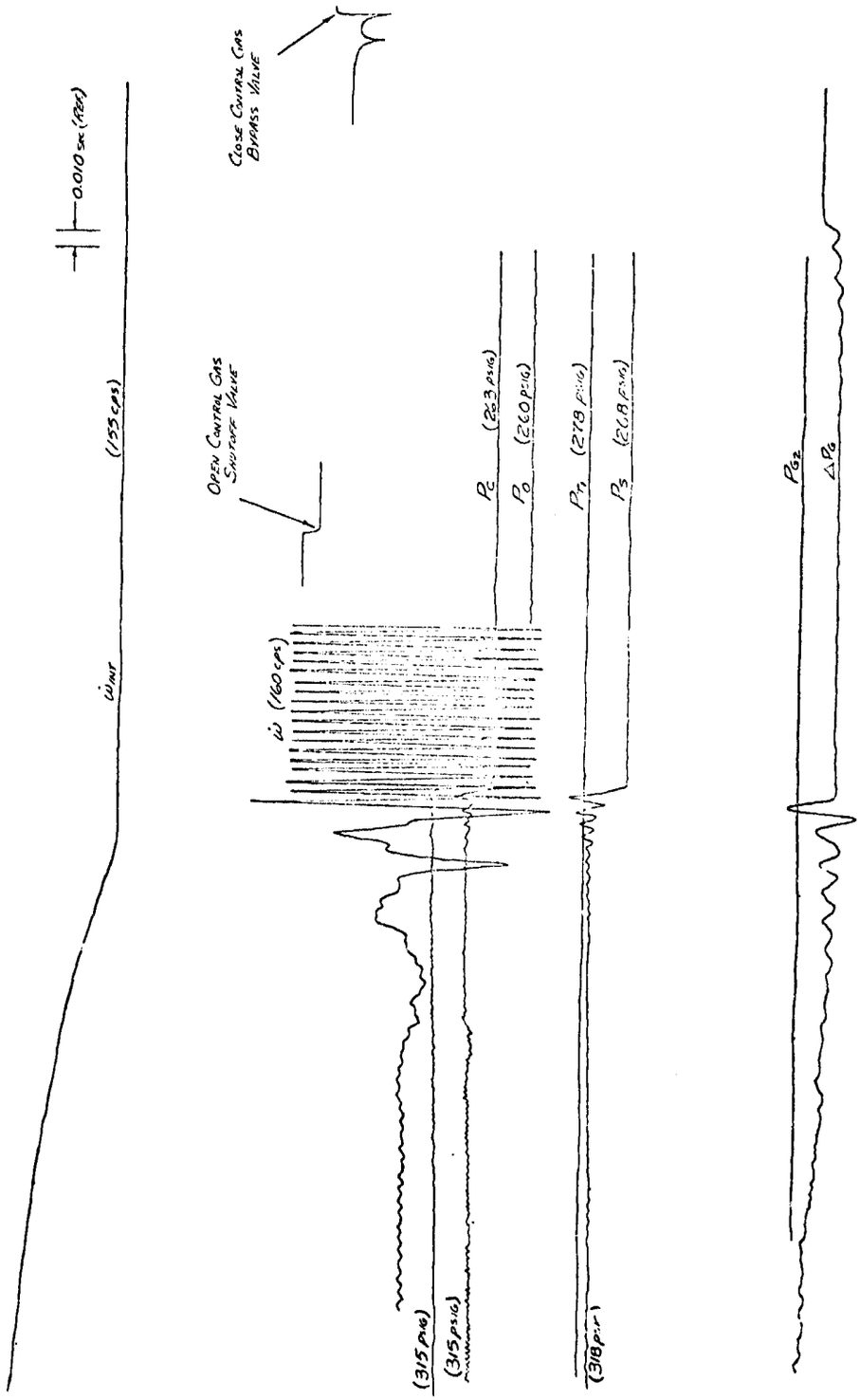

Figure 115. Third Shut-Off - ACS Fuel Throttle

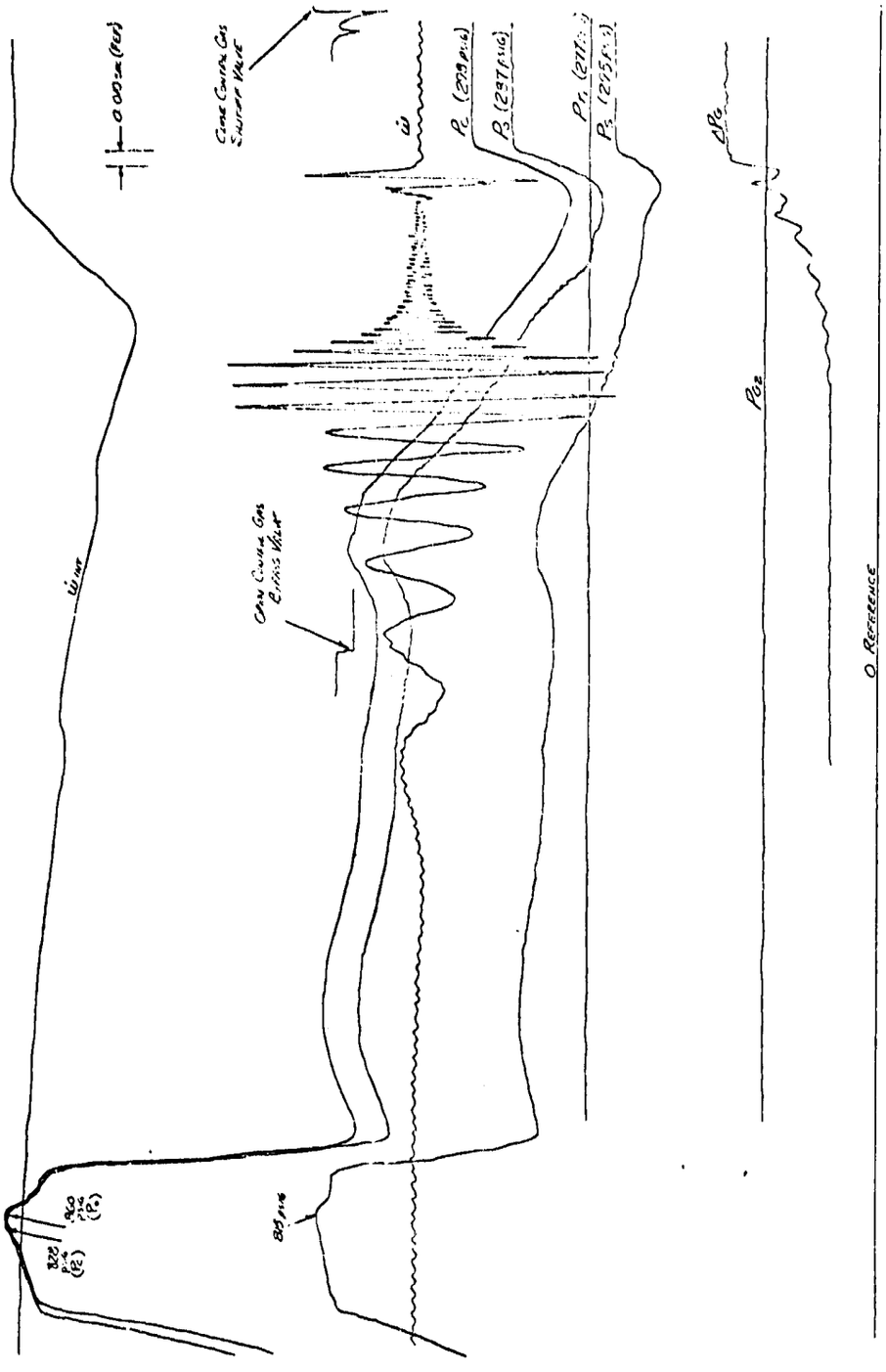

Figure 116. Fourth Throttle Actuation

IV, C, Fluidic Control Components (cont.)

0.180 sec. AFter the 5 min off period, the response was 8.0 sec. The increase in response time attributable to thermal effects was expected. A thermal analysis, which was applicable to the ACS experimental component design but to an unknown extent, was conducted.

In the throttling test, the unit exhibited the same unstable performance during throttling that was apparent in the GN_2/water tests. However, at no time throughout these tests was there any indication of a reaction between the N_2H_4 decomposed gas and the fuel.

Similar tests of the oxidizer half of the ACS control module were not conducted for two reasons. First, the compatibility of the mixed gas and N_2O_4 had been previously verified in development tests conducted early in the PBPS program. Secondly, the ACS oxidizer throttle was being utilized for supplemental testing in connection with the PBPS Engine Development Program and System Design (Contract FO4611-67-C-0095).

IV, Phase II - Subsystem Development (cont.)

D. WORKHORSE ENGINE SUBSYSTEM

The workhorse engine subsystem was provided to verify the integration of the fluidic controls with a bipropellant engine. The engine subsystem identified in Phase I included four axial engines of nominal 600 lb thrust. Each of these engines was to be throttled 2:1 to provide center-of-gravity control and steering. The throttling would be accomplished by the fluidic control vortex throttles. This had a major impact upon the axial engine because a special injector was required to operate at a sustained throttled level with the two-phase flow provided by the gas entrainment in the propellant from the vortex throttled.

1. Axial Engine

a. Injector

An injector was designed and fabricated for use in testing the axial fluidic control module. This unit, a 16-element unlike doublet, was designed to distribute the two-phase gas-liquid from the vortex throttle to the injection elements at a constant gas/liquid ratio over a 2:1 throttling range.

The design consisted of an injector head with stainless-steel distribution plates brazed to it. These plates contained feed channels milled and drilled in a pattern to uniformly split the gas-liquid without separating the constituents.

Two types of flow splitting devices were used in this design. A vortex chamber divider, similar to the design tested in the fuel circuit of the ACS flow model, was used to make the initial division of the gas-liquid constituents into 8 oxidizer and 10 fuel chambers. The second split involved a simple channel division by forming a Y with the milled slots.

Fuel for combustion chamber cooling was introduced into the combustion chamber from an annular plenum, which was similar in design to the oxidizer circuit of the ACS flow model. This plenum was fed by two of the 10 initial fuel passages to give 20% coolant flow.

b. Workhorse Chamber

A copper heat sink combustion chamber was designed and fabricated for the two-phase flow injector. This chamber provided ≈ 20 sec of sustained run duration for checkout of the vortex throttles.

IV, D, Workhorse Engine Subsystem (cont.)

2. ACS Engine

a. ACS Flow Model

A seven-element F-O-F triplet injector model was designed, fabricated, and flow tested with an ACS vortex throttle at the Bowles Engineering facility. This test series successfully demonstrated two concepts of dividing the multi-phase gas-liquid propellants without separating the constituents overflow rates ranging from full-thrust to 30% thrust. A uniform flow pattern was observed down to flow rates equivalent to 30% thrust in the fuel circuit. Similar results were noted for the oxidizer circuit wherein a swirl chamber was used to distribute the multi-phase liquid-gas. Gaseous nitrogen and water were used to simulate the propellants and the control gas for these tests.

The flow passage designs used in this model performed satisfactorily over the 2:1 throttling range required for the axial engine. These designs, in addition to the manifold configurations recommended earlier by Bowles Engineering, were evaluated for application to the axial engine injector design.

b. ACS Workhorse Engine

An existing aluminum injector and a previously-tested beryllium thrust chamber were to be used to test the ACS fluidic control module. An adapter was designed to mate the control module to the injector. The injector and chamber were to be used without any changes. This hardware would permit testing using a control gas within the temperature limits of the aluminum injector. The existing injector, a 15-element F-O-F triplet, was acceptable for the vortex throttle integration firings because no sustained throttling was required with the ACS engine. The two-phase flow condition, which occurs during throttling, would take place only during the start and shutdown transients.

An adapter plate was required to increase the spacing of the propellant inlet ports on the injector, to mate with the interface on the control module, and to provide a method for attaching the valve to the injector. This beryllium chamber would operate as a heat-sink for durations that are satisfactory for evaluating the fluidic control modules.

E. SUBSYSTEM INTEGRATION

The preparation for hot gas expulsion of the Arde ring-stabilized bladder propellant tank was initiated with the re-calibration of the first stage gas generator of the monopropellant gas generator subsystem. The first

IV, E, Subsystem Integration (cont.)

stage of the gas generator subsystem was designed to provide an outlet pressure of 700 psia when operated as a two-stage subsystem. The first stage bootstrap circuit was re-calibrated to incorporate the prototype AM355 stainless-steel tank and provide an outlet pressure of 400 psi for direct expulsion of a propellant tank. The differential area of the prototype bootstrap tank has a pressure ratio of 1.56 as compared to the 1.4 ratio of the workhorse aluminum tank previously tested. The re-calibration was achieved by disassembling and resetting the pressure switch controls of the gas generator subsystem provided by Hamilton Standard. The integrated test set-up is shown on Figure No. 117.

Six gas generator subsystem tests were conducted to demonstrate the satisfactory gas generator operation for tank hot gas expulsion. The final test demonstrated the displacement of water from a flanged Arde tank without a bladder to evaluate the tank wall thermodynamics. Water was displaced over a 425 sec limited duty cycle demonstration of alternate flow rates of 80 sec of 2.42 lb/sec and 10 sec of 0.07 lb/sec. The maximum tank wall temperature achieved was 480°F adjacent to the hot gas inlet flange.

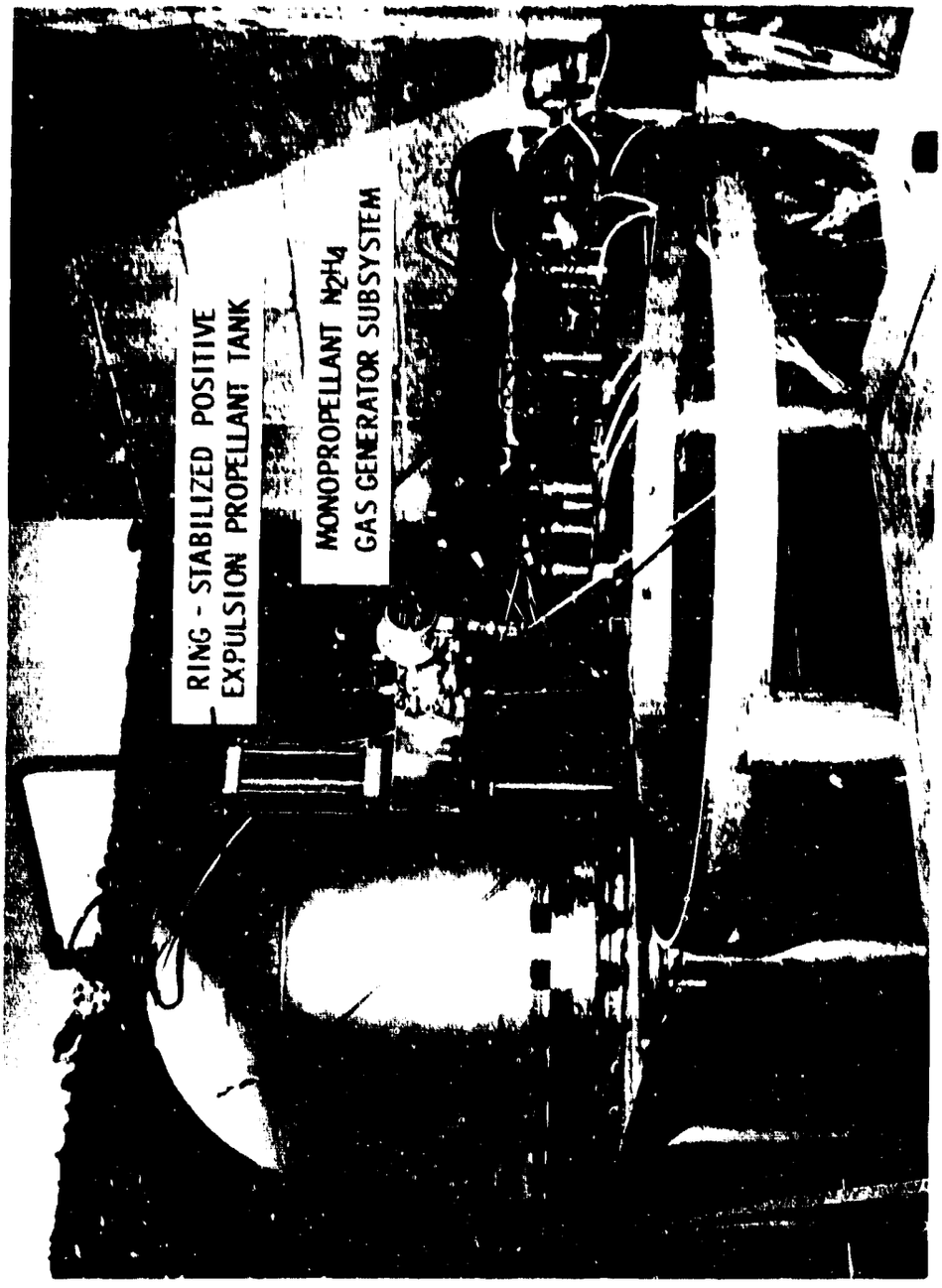

Figure 117. Integrated Test Set-Up

V. FOLLOW-ON EFFORT

The Advanced PBPS Subsystems Development contract effort, AF 04(611)-11614 served to satisfactorily demonstrate the concept of the ring-stabilized propellant expulsion tank and resulted in the development of a gas generator subsystem which is capable of providing hot gas for the expulsion process. The integration of these two subsystems to demonstrate hot gas expulsion of the propellants, N_2O_4 and MMH, from flightweight tank assemblies is being accomplished by the Air Force Rocket Propulsion Laboratory under Contract F04611-67-C-0095.

In this demonstration, the components fabricated and developed under Contract AF 04(611)-11614 are being utilized. The bootstrap gas generator subsystem using the workhorse pressure switch and solenoid valve controls provides the hot gas supply. The preparation and checkout of this subsystem were outlined in Section IV, E.

The ring-stabilized diaphragm propellant tanks of a flightweight configuration will be provided by the subcontractor, Arde, Inc., for the subsystem integration testing under the F04611-67-C-0095 contract. These propellant tanks will be fabricated from expulsion diaphragm shells and tank components that are residual from the AF 04(611)-11614 contract.

Confidential
Security Classification

DOCUMENT CONTROL DATA - R&D

(Security classification of title, body of abstract and indexing annotation must be entered when the overall report is classified)

1 ORIGINATING ACTIVITY *(Corporate author)*

Aerojet-General Corporation
P.O. Box 15847
Sacramento, California 95813

2a REPORT SECURITY CLASSIFICATION
Confidential

2b GROUP
4

3 REPORT TITLE
Demonstration of Advanced Post-Boost Propulsion Subsystems (U)
Final Report

4 DESCRIPTIVE NOTES *(Type of report and inclusive dates)*
Technical Report AFRPL-TR-68-126 1 July 1966 through 30 April 1968

5 AUTHOR(S) *(Last name, first name, initial)*
Jones, Roy E.
Lemke, Donald E.
Goodman, Owen D.

6 REPORT DATE	7a TOTAL NO. OF PAGES	7b NO. OF REFS
August 1968	248	0

8a CONTRACT OR GRANT NO.	9a ORIGINATOR'S REPORT NUMBER(S)
AF 04(611)-11614	None
b. PROJECT NO.	
c.	9b OTHER REPORT NO(S) *(Any other numbers that may be assigned this report)*
d.	None

10 AVAILABILITY/LIMITATION NOTICES
In addition to security requirements which must be met, this document is subject to special export controls and each transmittal to foreign governments or foreign nationals may be made only with prior approval of AFRPL (RPPR/STINFO), Edwards, California 93523.

12 SPONSORING MILITARY ACTIVITY
Air Force Rocket Propulsion Laboratory
Air Force Systems Command
Edwards, California

13 ABSTRACT

See Attached.

DD FORM 1 JAN 64 1473

Confidential
Security Classification

ABSTRACT

The Demonstration of Advanced Post-Boost Propulsion Subsystems Program, Contract AF 04(611)-11614, had as its objective the development of improved technology for advanced, post-boost liquid propulsion subsystems having a ten-year storage life and which would be maintenance-free, inherently reliable, and offer minimal production costs. Although originally planned as a three-phase program, it was subsequently modified into two phases; a Preliminary Design effort (Phase I) and a Subsystem Development effort (Phase II). In Phase I, primary subsystem concepts were identified and evaluated for Phase II development. The latter effort was devoted to providing technological improvements in the primary subsystems selected which would permit their ready incorporation into an Advanced Post-Boost Propulsion System for the next generation of ICBM weapon systems. The Aerojet-General Corporation, as prime contractor, utilized specialized subcontractor experience for the development effort associated with three of the primary subsystems. The Hamilton Standard Division of United Aircraft development activity concerned a staged, monopropellant gas generator for pressurization. Arde, Inc. was responsible for the propellant tanks and positive expulsion. They utilized all-welded steel conospheroid tanks with wire-reinforced, controlled collapse, steel diaphragms. Controls were the concern of the Bowles Engineering Corporation. All-fluidic controls were applied for both the regulation of pressurization and controlling the engine. Hot gas from the pressurization subsystem is used to perform these control functions. Aerojet-General accomplished the necessary engine development which was limited to workhorse hardware solely intended for use in testing the controls subsystem components. Development culminated in gas pressurization and propellant tank/expulsion subsystem demonstrations that indicate these subsystems are ready for final weapon system development as well as application. In connection with the fluidic controls components, the feasibility of the concept was demonstrated; however, further basic component technology research will be required for any selected application.

14 KEY WORDS	LINK A		LINK B		LINK C	
	ROLE	WT	ROLE	WT	ROLE	WT
PRELIMINARY DESIGN						
PRESSURIZATION SUBSYSTEM DEVELOPMENT						
PROPELLANT TANK/EXPULSION SUBSYSTEM DEVELOP.						
FLUIDIC CONTROL COMPONENTS DEVELOPMENT						
Pressurization Controls						
Axial Engine Control Module						
ACS Engine Control Module						
WORKHORSE ENGINE SUBSYSTEM						
Axial Engine						
ACS Engine						
SUBSYSTEM INTEGRATION						

INSTRUCTIONS

1. ORIGINATING ACTIVITY: Enter the name and address of the contractor, subcontractor, grantee, Department of Defense activity or other organization *(corporate author)* issuing the report.

2a. REPORT SECURITY CLASSIFICATION: Enter the overall security classification of the report. Indicate whether "Restricted Data" is included. Marking is to be in accordance with appropriate security regulations.

2b. GROUP: Automatic downgrading is specified in DoD Directive 5200.10 and Armed Forces Industrial Manual. Enter the group number. Also, when applicable, show that optional markings have been used for Group 3 and Group 4 as authorized.

3. REPORT TITLE: Enter the complete report title in all capital letters. Titles in all cases should be unclassified. If a meaningful title cannot be selected without classification, show title classification in all capitals in parenthesis immediately following the title.

4. DESCRIPTIVE NOTES: If appropriate, enter the type of report, e.g., interim, progress, summary, annual, or final. Give the inclusive dates when a specific reporting period is covered.

5. AUTHOR(S): Enter the name(s) of author(s) as shown on or in the report. Enter last name, first name, middle initial. If military, show rank and branch of service. The name of the principal author is an absolute minimum requirement.

6. REPORT DATE: Enter the date of the report as day, month, year; or month, year. If more than one date appears on the report, use date of publication.

7a. TOTAL NUMBER OF PAGES: The total page count should follow normal pagination procedures, i.e., enter the number of pages containing information.

7b. NUMBER OF REFERENCES: Enter the total number of references cited in the report.

8a. CONTRACT OR GRANT NUMBER: If appropriate, enter the applicable number of the contract or grant under which the report was written.

8b, 8c, & 8d. PROJECT NUMBER: Enter the appropriate military department identification, such as project number, subproject number, system numbers, task number, etc.

9a. ORIGINATOR'S REPORT NUMBER(S): Enter the official report number by which the document will be identified and controlled by the originating activity. This number must be unique to this report.

9b. OTHER REPORT NUMBER(S): If the report has been assigned any other report numbers *(either by the originator or by the sponsor)*, also enter this number(s).

10. AVAILABILITY/LIMITATION NOTICES: Enter any limitations on further dissemination of the report, other than those imposed by security classification, using standard statements such as:

(1) "Qualified requesters may obtain copies of this report from DDC."

(2) "Foreign announcement and dissemination of this report by DDC is not authorized."

(3) "U. S. Government agencies may obtain copies of this report directly from DDC. Other qualified DDC users shall request through _____."

(4) "U. S. military agencies may obtain copies of this report directly from DDC. Other qualified users shall request through _____."

(5) "All distribution of this report is controlled. Qualified DDC users shall request through _____."

If the report has been furnished to the Office of Technical Services, Department of Commerce, for sale to the public, indicate this fact and enter the price, if known.

11. SUPPLEMENTARY NOTES: Use for additional explanatory notes.

12. SPONSORING MILITARY ACTIVITY: Enter the name of the departmental project office or laboratory sponsoring *(paying for)* the research and development. Include address.

13. ABSTRACT: Enter an abstract giving a brief and factual summary of the document indicative of the report, even though it may also appear elsewhere in the body of the technical report. If additional space is required, a continuation sheet shall be attached.

It is highly desirable that the abstract of classified reports be unclassified. Each paragraph of the abstract shall end with an indication of the military security classification of the information in the paragraph, represented as *(TS), (S), (C), or (U)*

There is no limitation on the length of the abstract. However, the suggested length is from 150 to 225 words.

14. KEY WORDS: Key words are technically meaningful terms or short phrases that characterize a report and may be used as index entries for cataloging the report. Key words must be selected so that no security classification is required. Identifiers, such as equipment model designation, trade name, military project code name, geographic location, may be used as key words but will be followed by an indication of technical context. The assignment of links, rules, and weights is optional

GPO 886-551